Résistance à la cavitation: Des mécanismes physiologies à la génétique évolutive

Jean-Baptiste J.-B. Lamy

N° 4499

THÈSE

Présentée à

L'UNIVERSITÉ de BORDEAUX 1

ÉCOLE DOCTORALE « SCIENCES ET ENVIRONNEMENTS »

Par Jean-Baptiste LAMY

Pour obtenir le grade de **DOCTEUR**

SPÉCIALITÉ :

Écologie évolutive, fonctionnelle et des communautés

Résistance à la cavitation :
Des mécanismes physiologiques à la génétique évolutive

De la bulle aux gènes…

Resistance to cavitation:
From physiological mechanisms to evolutionary quantitative genetic

From the bubble to genes…

Soutenue le 13 mars 2012

Antoine KREMER (DR, INRA Bordeaux)	Président
Jean-Christophe DOMEC (Pr. Bordeaux Science Agro)	Rapporteur
Santiago C. GONZÁLEZ-MARTÍNEZ (CR, INIA Madrid)	Rapporteur
Thierry SIMMONNEAU (DR, INRA Montpellier)	Examinateur
Ophélie RONCE (CR, ISEM Montpellier)	Examinatrice
Sylvain DELZON (CR, INRA Bordeaux)	co-Directeur de thèse
Hervé COCHARD (DR, INRA Clermont-Ferrand)	co-Directeur de thèse
Christophe PLOMION (DR, INRA Bordeaux)	Directeur de thèse

Laboratoire BIOGECO Équipe Ecologie et génomique fonctionnelle Bâtiment B2, Avenue des Facultés

33405 Talence

Mes remerciements :

Tout d'abord, rendons à César ce qui est à César, merci à Sylvain Delzon, Christophe Plomion et Hervé Cochard, vous formez une belle équipe de directeurs de thèse, un joyeux triptyque qui se complète à merveille. J'ai été (et je suis encore) un thésard heureux ! J'ai grandement apprécié la confiance, la très grande liberté, le soutien financier et scientifique que vous m'avez accordé pendant ces trois années. J'essayerais de rendre à la pareille à mon échelle.

Je n'oublie pas Régis Burlett, Annabel Porté, Yann Guengant, Frédo Lagane, Emilie Chancerel et Laurent Bouffier qui turbinent dans l'ombre et qui font avancer furieusement le Schmilblick.

Merci à Laurent Salera, et Frédéric Bernier pour l'accès aux ressources génétiques et au défunt TREESNIP. Je remercie aussi l'ensemble de l'unité expérimentale car j'ai eu dans les mains des jeux de données monstrueux qui doivent valoir leurs pesant de sueur.

J'ai beaucoup aimé et j'aime toujours l'ambiance du laboratoire, tout est furieusement enthousiaste, les baignades dans la Leyre, les déconnades improvisées avec l'équipe Euca, les discussions scientifiques et statistiques avec Antoine Kremer, JP Soularue, Luc Barbaro et Jean-Marc Gion. Je dois aussi rendre justice à Monsieur Brice Giffard (Claudio). Combien d'heures avons-nous débattu sur nos utilisations respectives des modèles mixtes et sur l'orthodoxie statistique de nos démarches. Je résumerais ces discussions en disant « Gardons un esprit critique et du bon sens… une grosse dose de tout ça ». Longue vie à BIOGECO !

Merci aux stagiaires que j'ai tenté d'encadrer, et qui en revanche, m'ont toujours beaucoup aidés : Mathieu Réveillas, Andres Plaza, Pierre Ouallet, Pauline Bouche, Maximilien Larcher. Soyez pugnace, la recherche n'est pas un monde bisnours…

Vielen Dank an das Team von Institut für Systematische Botanik und Ökologie for inviting me for the weistwrust & bretzel party all the Friday morning! Thank Hans for reparing my internet connection every week. Thank to Helen for your great patience, I am not sure that you have improved your English with me, I am sure it was other way, I improved my English with you! Thank to Steven for your help during my intership and for the scientific discussion about phylogeny, Glühwein and wood anatomy.

Pour la suite, je dégoupille :
Mes ziziments :

Autant je me suis escrimé à essayer de pondre un truc chiadé, ficelé, statistiqué ! Autant là… C'est du à brûle-pourpoint ! Un bon pétard mammouth tenu en pleine main… Ne chercher pas… un fil conducteur ? Ben hey ! y en a pas… Ce poulet-là, je ne le relirais pas, y en aura des fautes, pour sûr cousin !... Le texte est généré par des processus markoviens… Salmigondis verbeux, allons y !

La fin, on la tient, JP, on y est [presque] arrivé…
« Une thèse, mes loufiats c'est dure et ça dure ! » qu'on nous avait dit…
- Héhé, je dirais qu'une thèse ça laboure, et profond, la cervelle, le corps, les sentiments… La vie dans son ensemble. Ca étrille l'échine comme un blizzard descendu du Vignemale, et ruine les gambettes comme les aoûtâts en autonome. Faut dire que je n'ai pas épargné ma sueur… Que surgira des ces sillons cérébraux abreuvés de musique classique, de soupe aux champignons du campus et à la водка ? La question est ouverte, la page de nouveau vierge…

Merci JP d'avoir été mon acolyte… d'avoir fait si souvent la boustifaille pour tout le monde à la colocation… d'avoir planter des fèves cet hiver… de ne pas râler plus de 10 secondes quand tu te rends compte que la cuistance s'approchait d'une porcherie… d'avoir rigolé quand on pété le canapé qui devait remplacer celui qu'on avait déjà pété… d'accepter de faire du canoë pendant les nuits d'hivers sur le lac de Lacanau. Merci à Pithivier et à Sir Aliaksandr Kolbas avec qui rien n'est triste ! Eux aussi étaient dans le coup du canapé ! Ils n'ont jamais été en reste, eux aussi ont été d'excellents alcooliques… L'ambiance me manquera c'est sûr.
N'oublions pas les meubles : La table de Saint Michel et aux chaises survivantes qui ont bu au moins autant que nous. Merci aux deux générations de canapés (pas les mêmes que les précités) qui ont hantés nos bureaux.
Merci, à mon frérot Pierre, à qui la surenchère ne fait jamais peur, une nuit dans un canyon en novembre, un tour en hélico avec les gendarmes, au canoë coulé dans les passes du bassin d'Arcachon, et les trois canoës de bois, qui finalement, ont eu une fin moins violente. Aux ours qu'on a jamais vu au canada, aux myrtilles et aux framboises, à Bécu en béret basque.

إلى ليتيسيا، التي وضعتني على هذا الدرب.
أنا مدين لها بهذا الشيء على الأقل.

A mes deux jeunes neveux et à ses parents… A mon frère aux cheveux longs, à ma sœur qui grandit et aux géniteurs de la tribu Lamy qui ont dû en baver. A Sophie, qui a fait les frais de la dizaine de « dernières lignes droites » et qui me supporte encore. Finalement ce méchant monde capitaliste est presque bon… On écrira ensemble la prochaine eschatologie, en attendant, bonne apocalypse. Je fête la mienne !

Avant propos

Cette thèse porte sur le mécanisme physiologique de la resistance à la cavitation et la variabilité intraspécifique de ce caractère. Elle a été réalisée en cotutelle entre les UMR BIOGECO et PIAF et a fait l'objet d'un co-financement entre la Région Auvergne et le département d'écologie des forêts, des prairies et des milieux aquatiques de l'INRA. J'ai également bénéficié de l'appui du projet Européen NOVELTREE pour réaliser le phénotypage des différentes populations étudiées, d'une bourse de mobilité de l'INRA, de l'EGIDE et d'un projet innovant INRA.

J'ai choisi de présenter les résultats et de les discuter dans une première partie rédigée en français[1] (voir Synthèse), suivie d'une seconde partie (Annexes) qui regroupe l'ensemble des articles ou manuscrits d'articles rédigés en anglais soumis à des revues internationales.

La synthèse peut être lu indépendamment des articles. Cependant, par soucis de concision, aucun détail méthodologique n'y est reporté. J'ai utilisé des figures issues de la littérature scientifique internationale dont je cite les références et dont les légendes ont été traduites en français afin de conserver l'homogénéité du texte. Les chapitres débutent sur des parties intitulées « rappels généraux », elles peuvent être sautés sans nuire à la compréhension globale de la synthèse.

[1] Autant que faire ce peut, j'ai évité les anglicismes.

Sommaire

Synthèse

1- Introduction

La sécheresse n'est peut être pas le danger le plus fréquent pour les plantations de Pins ! Observations personnelles au cours de la thèse… janvier 2009.

1.1 Capacité adaptative des arbres forestiers face à la sécheresse

Les événements climatiques extrêmes, actuels comme passées, retiennent de plus en plus l'attention des climatologues et des modélisateurs de l'IPCC (Alexander et al., 2006; Beniston et al., 2007; Granier et al., 2007; Parey, 2008) en raison de l'impact qu'ils ont sur les activités humaines mais aussi sur l'évolution des écosystèmes[2] (Gould & Eldredge, 1977; Lewontin, 2008). Les climatologues ont établi que la moyenne des températures terrestres augmente, mais, plus dommageable, la variance associée aussi (Beniston et al., 2007; Della-Marta & Beniston, 2008). Les écosystèmes forestiers naturels et plantés subissent d'ores et déjà les effets directs et indirects de l'augmentation de sécheresses extrêmes (Breshears et al., 2005; Bréda, 2006; Bréda et al., 2006; Bréda & Badeau, 2008; Allen et al., 2010). La prévention et la gestion de ces risques naturels passent par l'évaluation précise de la capacité adaptative des espèces d'arbres (espèces clé de voûte) de ces écosystèmes afin de pérenniser la qualité et la quantité des services écologiques (Lindner et al., 2007, 2010). Plusieurs champs d'activités économiques sont intéressés par ces questions : Quel est le seuil de sécheresse pour lequel la plantation sera détruite (effets directs de la sécheresse ou indirects par les ravageurs) ? Quels caractères sont pertinents pour améliorer la survie des individus face à la sécheresse ? Comment créer et/ou sélectionner des génotypes adaptés aux conditions climatiques de demain ? Comment adapter les pratiques forestières pour acclimater les arbres ?

Evaluer la capacité adaptative d'une espèce d'arbre passe par : i/ l'identification et la compréhension des mécanismes clés impliqués dans la tolérance et/ou la résistance à la sécheresse, ii/ la quantification de la variation phénotypique de ces mécanismes et iii/ le déterminisme génétique de cette variation (Figure 1) (Lindner et al., 2010; Scotti, 2010).

[2] La biologie a toujours été déchirée entre des visions continue et discontinue. En science de l'évolution, ce débat est illustré par la polémique entre Lamarck et Cuvier, le premier soutient une vision graduelle de l'évolution, le second pense qu'au contraire, l'évolution passe par des grandes révolutions des plans d'organisations. Ici, ayons une position intermédiaire, l'évolution graduelle est possible (microévolution) mais il existe des radiations brutale d'espèces après des extinctions massives (c.f. la crise crétacé tertiaire).

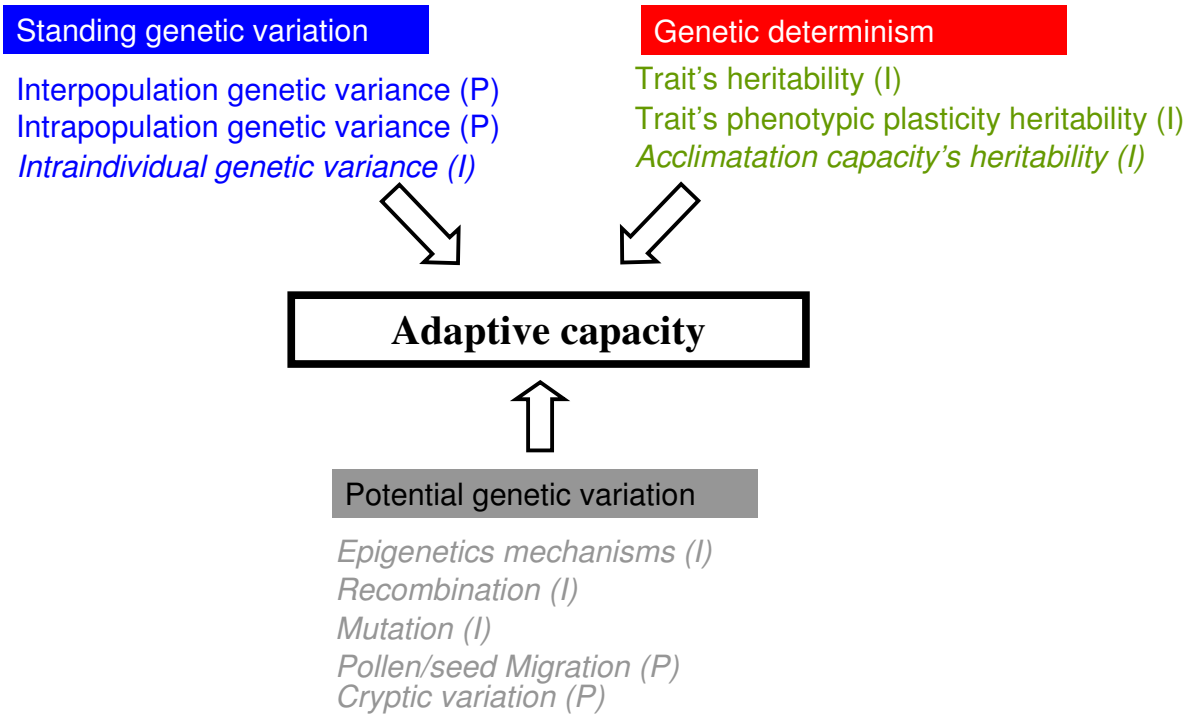

Figure 1 : Définition opérationnelle de la notion de capacités adaptative. La capacité adaptative d'une espèce se conçoit face à un danger précis (la sécheresse, le froid) afin d'identifier les caractères limitant l'adaptation (réduire les dimensions du phénotype). Les lettres entre parenthèses précisent le niveau hiérarchique : « P » population, « I » individu impliqué dans l'adaptation. Dans cette thèse ne seront pas abordés les items en italique. Une capacité adaptative (*adaptive capacity*) dépend de la variation (non nécessairement génétique) du(des) caractère(s) ainsi que de la variation dite potentielle, qui peut apparaître *de novo* (mutation, recombinaison) ou être révélée (mécanismes épistatiques et/ou épigénétiques). Cette variation sera d'autant plus efficace si elle est héritée (heritability) ou si la capacité à exprimer de la variation est héritable (phenotypic plasticity and/or acclimatation capacity). Modifié d'après Le Rouzic & Carlborg, (2008), Lindner et al., (2010) et Scotti, (2010)**.**

Notre objectif principal était d'identifier des variables physiologiques causales de la survie d'une espèce à la sécheresse. Ceci nous a amenés à choisir un caractère physiologique très corrélé à la fitness afin d'estimer au mieux la capacité adaptative de l'espèce face à la sécheresse. Lors d'une sécheresse, l'eau disponible pour les tissus vivants est limitée, ainsi l'ensemble des mécanismes de régulation situés sur le trajet de la sève brute est susceptible d'être impliqué dans la survie lors d'un tel stress.

1.2 Mourir de la sécheresse : Périr par la soif ou la faim ?

« I would fain die a dry death » W. Shakespeare The Tempest (I.1)

La mortalité des plantes due à la sécheresse est une variable difficile à mesurer, plusieurs mois d'observation sont nécessaires. Seules des études menées sur le long terme ou des sécheresses expérimentales proposent des hypothèses claires sur les processus menant à la mort d'une plante. Par conséquent ces hypothèses sont âprement débattues dans la littérature scientifique (Figure 2).

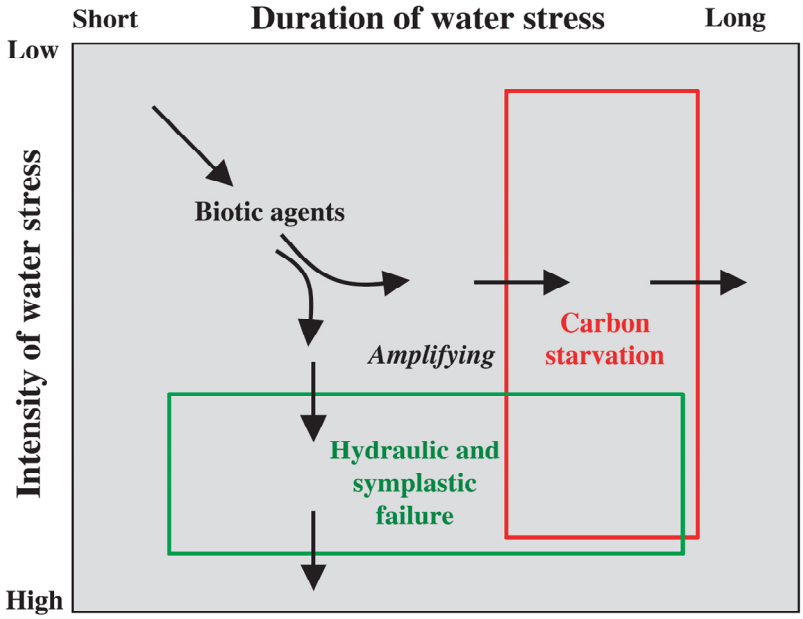

Figure 2 : Deux hypothèses sur les mécanismes menant à la mort pendant une sécheresse. La mort par la faim *(Carbon starvation)* et la mort par la soif *(Hydraulic and symplastic failure)* en fonction de l'intensité du stress (*Intensity of water stress*, en x) et la durée du stress hydrique (*Duration of water stress,* en y). Les agents biotiques (*Biotic agents,* flèches noires) amplifient les dégâts dus au stress hydrique. D'après McDowell et al., (2008)**.**

La polémique est articulée autour de deux hypothèses (McDowell et al., 2008; McDowell, 2010): (i) Mort par la faim (« *Carbon starvation* »), les cambiums et méristèmes cessent de fonctionner par manque de ressources carbonées disponibles. La sécheresse va induire la fermeture stomatique, donc l'assimilation carbonée va chuter. Afin de maintenir ces cellules en vie (respiration de maintenance et défense), la plante épuise ses métabolites carbonés issus des réserves ou de l'autophagie. (ii) Mort par la soif (« *Hydraulic and symplastic failure* »), les cambiums et les méristèmes vont se dessécher à cause de l'évaporation trop élevée et/ou d'un apport en eau insuffisant. La déconnexion hydraulique entre le sol et le système racinaire et/ou l'embolie du xylème empêche d'acheminer l'eau du sol aux tissus vivants. Traditionnellement, la première hypothèse a toujours été en odeur de sainteté comparée à la seconde, mais de nombreuses expériences soutiennent la seconde (Brodribb & Cochard, 2009; Brodribb et al., 2010). Les processus liés au métabolisme du carbone sont imbriqués dans

ceux impliqués dans la circulation de l'eau. Ils sont couplés par des rétroactions réciproques (chargement et déchargement du phloème, régulation de la température foliaire et homéostasie des photosystèmes, contrôle stomatique, la résorption de l'embolie). Aussi un consensus actuel se dégage ; la dégradation d'un processus entamerait inévitablement la dégradation de l'autre (McDowell, 2010, 2011). Lors d'une sécheresse, plusieurs études montrent l'importance des caractères hydrauliques dans la survie ou non des plantes.

1.3 Les caractères physiologiques clés pour survivre à la sécheresse

Breshears et al., (2005) et Adams et al., (2009) rapporte un dépérissement forestier important dans la région de Los Alamos (*Los Alamos National Laboratory, New Mexico, USA*). Dans les années 2000, les forêts de la région étaient composées d'un mélange de *Pinus edulis* et *Juniperus monosperma*. En 2004, après deux années d'un événement el niño de grande intensité, 99% de la population *Pinus edulis* disparaît, tandis que la population *Juniperus monosperma* a survécu (Figure 3).

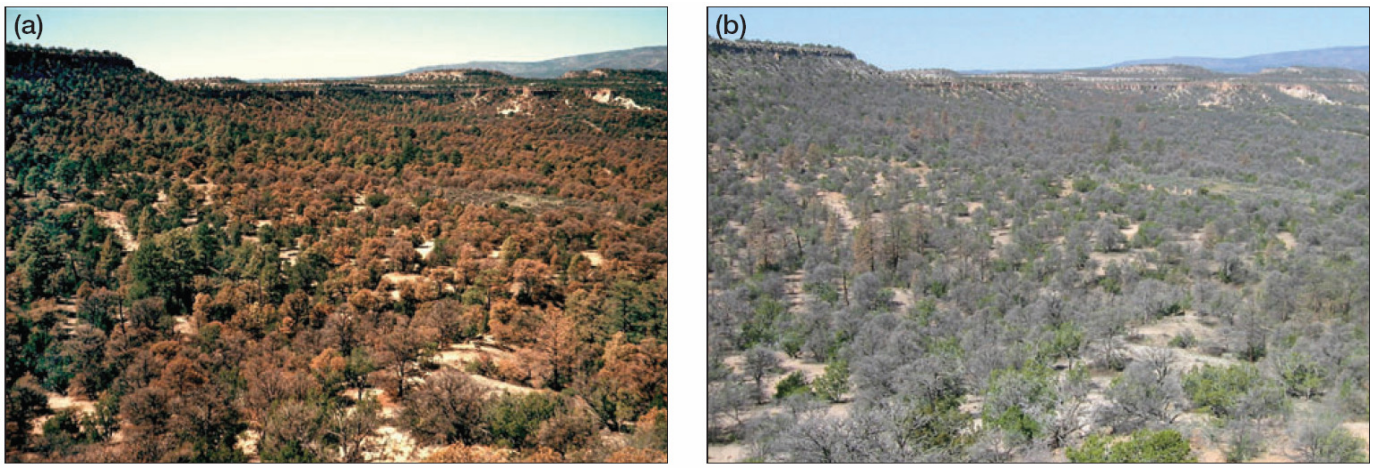

Figure 3 : Transformation du paysage associé au dépérissement de *Pinus edulis* après un événement el niño. (a) en octobre 2002, les aiguilles des pins sont brunies (b) deux années plus tard (mai 2004), les pins ont perdu leurs aiguilles et les troncs sont gris, la mortalité est proche de 99%, les individus encore verts sont les *Juniperus monosperma*. D'après (Breshears et al., 2009)**.**

La mort des individus de *Pinus edulis* était précédée d'une période de 10 mois durant laquelle l'assimilation carbonée était nulle et le potentiel hydrique foliaire diminuait. Les deux espèces co-occurrentes ont des différences marquées pour deux paramètres physiologiques essentiels : (i) la valeur de potentiel hydrique foliaire à laquelle les stomates sont complètement fermés ($P_{100}^{stomata}$), l'assimilation carbonée est, alors, nulle ; (ii) la résistance à la cavitation (P_{50}) qui est la valeur de potentiel hydrique pour laquelle le xylème a perdu 50% de sa conductivité initiale.

Cette perte de conductivité est due à l'embolie issue de la cavitation de la sève (formation de bulles d'air et de vapeur d'eau lors de forte transpiration). *Juniperus monosperma* possède un seuil de résistance à la cavitation (P_{50}) plus bas que *Pinus edulis* (-8.9 versus -4.1 MPa). *Juniperus* est donc plus résistant à la cavitation que *Pinus*. Imagions le cas suivant, ces deux espèces ont le même potentiel hydrique foliaire est de -5.5 MPa. A cette valeur, le système conducteur de sève de *Juniperus* reste intact alors que celui de *Pinus* aura perdu 100% de sa conductivité initiale. De la même manière, *Juniperus* fermera complètement ses stomates ($P_{100}^{stomata}$) pour une intensité (et/ou durée) de sécheresse beaucoup plus forte que *Pinus* (-4 MPa versus -2MPa). Les caractéristiques hydrauliques sont déterminantes pour la survie à la sécheresse que l'espèce meurt de « faim » ou de « soif ».

L'autre source d'information provient de sécheresses expérimentales suivies de périodes de réhydratation. Brodribb & Cochard, (2009) et Brodribb et al., (2010) mettent en évidence la bonne corrélation qui existe entre un potentiel hydrique létal (potentiel hydrique pour lequel la plante meurt) et la résistance à la cavitation (P_{50}) sur 4 espèces du genre *Callitris* (Figure 4).

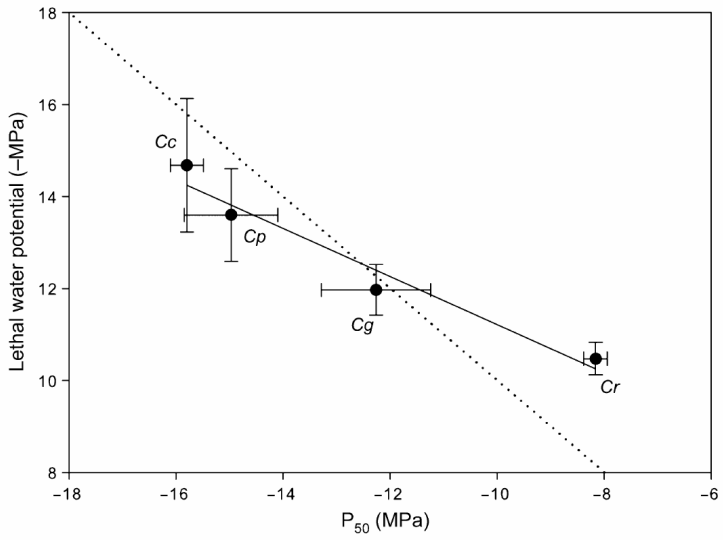

Figure 4 : Le potentiel hydrique létal (*lethal water potential*, en y) et la résistance à la cavitation du xylème (P_{50} en x, MPa) du tronc sont fortement positivement corrélés (R^2 = 0.95 ; P < 0.05). *Cc* : *Callitris columellaris*, *Cg* : *Callitris gracilis*, *Cp* : *Callitris preissii*, *Cr* : *Callitris rhomboidea*. D'après (Brodribb et al., 2010)**.**

D'autres arguments renforcent l'idée que la résistance à la cavitation est un estimateur fiable de la survie à une sécheresse extrême. Dans une méta-analyse sur 167 espèces, Maherali et al., (2008) montre une bonne adéquation entre les précipitations annuelles moyennes et la résistance à la cavitation pour les conifères et les angiospermes sempervirents après une correction pour tenir compte de la phylogénie (voir la Figure 5). Cette corrélation est aussi

retrouvé entre des indices écologiques et la resistance à la cavitation (Brendel & Cochard, 2011). L'ensemble de ces études montre qu'en moyenne les conifères ont une meilleure resistance à la cavitation, qui serait due à l'anatomie du xylème (Brodribb & Hill, 1999).

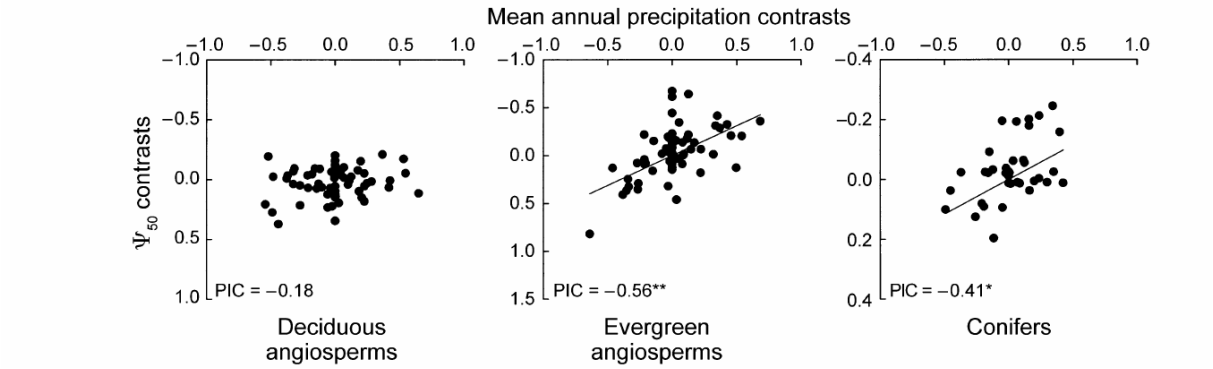

Figure 5 : Corrélation entre la résistance à la cavitation (ψ_{50} *contrasts* en y) et les précipitations annuelles moyennes (*mean annual precipitation contrasts,* en x) pour différents groupes écologiques après correction pour tenir compte de la phylogénie. Les données résistance à la cavitation ont été logarithmisées. D'après Maherali et al., (2004)**.**

D'un point de vue théorique et empirique, la résistance à la cavitation serait donc un estimateur fiable de la survie à une sécheresse extrême. La résistance à la cavitation est une mesure longue et fastidieuse, existe-il des caractères plus faciles à mesurer et bien corrélés à la résistance à la cavitation ?

1.4 Relation entre résistance à la cavitation et anatomie du bois

Certains auteurs montrent que la densité du bois pourrait être un bon estimateur de la résistance à la cavitation (Hacke & Sperry, 2001) tant au niveau interspécifique qu'intraspécifique (Rosner et al., 2007; Dalla-Salda et al., 2009, 2011). En effet, Martinez-Meier et al., (2008) a mis en évidence que les survivants à la canicule de 2003 avaient un bois plus dense que les individus morts chez *Pseudotsuga menziesii*. Rosner et al., (2007) et Dalla-Salda et al., (2011) montre sur 6-7 clones de la même espèce une corrélation entre la densité du bois initiale et la résistance à la cavitation. Cependant, ces études sont rares et faiblement répétées, il convient de tester la robustesse de la relation entre résistance à la cavitation et la densité du bois sur un grand nombre d'individus non apparentés (fond génétique large). L'étude des corrélations entre les caractères ne saurait suffire, il est crucial de comprendre quelles variables anatomiques expliquent la variation de résistance à la cavitation.

Les conifères montrent en moyenne une résistance à la cavitation plus importante que les angiospermes (-4.78 ± 0.44 [3] versus -2.65 ± 0.18 MPa, (Maherali et al., 2004)), cette différence peut être expliquée par d'anatomie du bois (Brodribb & R.S. Hill, 1999; Maherali et al., 2004).

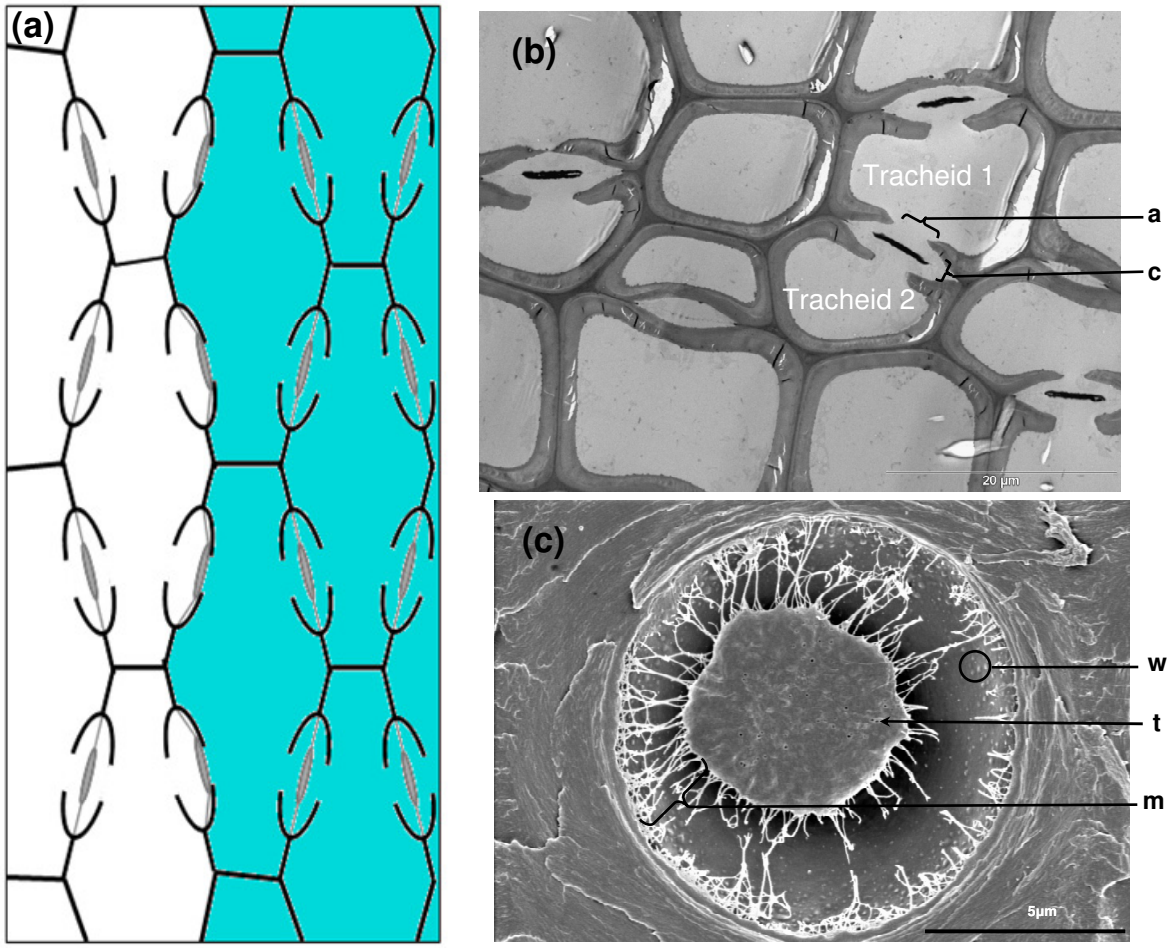

Figure 6 : Réseau de trachéides et ponctuation aréolée des gymnospermes. (a) Schéma d'un réseau de trachéides (vue longitudinale tangentielle). En blanc les trachéides embolisées (remplies d'air et de vapeur d'eau) et en bleu les trachéides fonctionnelles, entre les deux, les torus des ponctuations aréolées séparent l'air de la sève. Ils sont aspirés (coté sève, car la pression est décroissante du coté air vers le coté sève) et donc plaqués contre l'ouverture. (b) image de microscopie électronique à transmission montrant, en coupe transversale, un réseau de trachéides avec des ponctuations aréolées non aspirées. (c) image de microscopie électronique à balayage montrant une ponctuation aréolée non aspirée, une partie de la chambre a été enlevée pour permettre de voir le torus et les microfibrilles. Légendes : *a* ouverture de la ponctuation aréolée (*pit aperture*), *c* chambre de la ponctuation aréolée (*pit chamber*), *w* verrues sur les parois de la chambre (*warts*), *t* torus de la ponctuation aréolée (*torus*), *m* microfibrilles suspendant le torus (*pit margo*), pour désigner toutes les microfibrilles on utilisera de terme de treillis.

3 Erreur standard.

L'appareil vasculaire des gymnospermes est essentiellement constitué de trachéides (bois homoxylé). Une trachéide est le segment unitaire de l'appareil vasculaire des gymnospermes, elle provient d'une cellule cambiale qui ne s'abouchera pas à sa voisine comme c'est le cas chez les angiospermes (formation de vaisseaux). La sève brute passe d'une trachéide à l'autre via des interruptions dans la paroi cellulaire de la trachéide appelées ponctuations aréolées (*circular bordered pit*). Chacune des ces interruptions est constituée d'un volume (*pit chamber*) dans lequel le torus (épaississement issu de la paroi primaire) flotte suspendu par des microfibrilles. Lors de différences de tensions[4] (condition favorable à l'apparition de cavitation) entre deux trachéides, il joue le rôle de valve. Il vient se plaquer sur l'ouverture de la chambre pour éviter la propagation de l'embolie (Figure 6a). Les angiospermes n'ont pas ce système de valve (ponctuation simple). De plus, chez les gymnospermes la segmentation hydraulique est beaucoup plus élevée du fait de la faible dimension des trachéides en comparaison avec les longs vaisseaux des angiospermes. Malgré tout, ce système de valve est imparfait, car les gymnospermes subissent des phénomènes d'embolie due à la cavitation.

Il existe quatre hypothèses pour expliquer la propagation de la cavitation dans l'appareil vasculaire des gymnospermes.

[4] Nous utiliserons le terme de tension pour parler de pression négative. Aussi écriais-je que la tension *A* est plus forte que la tension *B* si la valeur absolue de la pression négative de *A* = -5 MPa est plus forte que *B*=-2 MPa. De plus, le terme tension est plus proche de la force que les molécules subissent dans l'appareil vasculaire des arbres, il s'agit d'une tension au sens mécanique du terme.

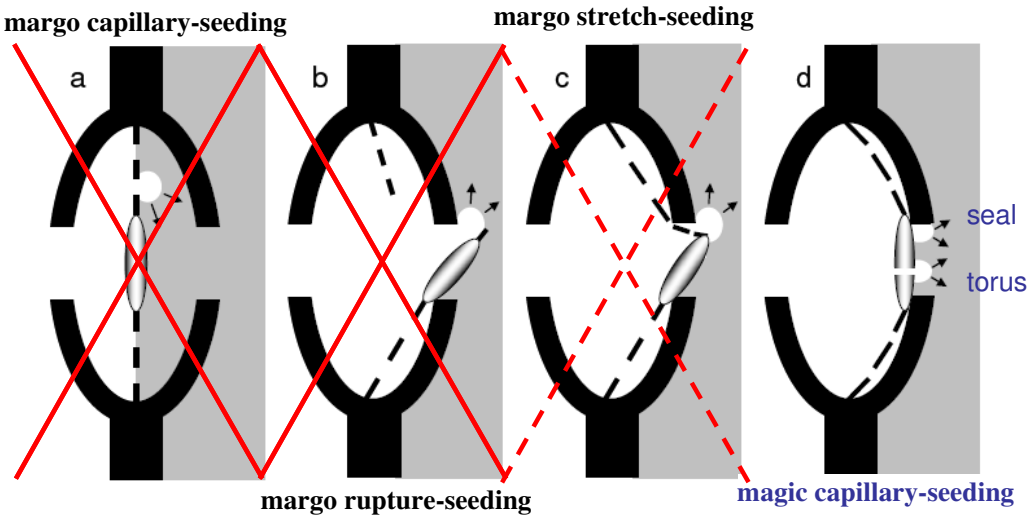

Figure 7 : Illustration des hypothèses expliquant la propagation de l'embolie chez les coniferes. (a) Pour des tensions induisant des phénomènes de cavitation, le torus n'est pas aspiré et le germe d'air apparaît sur les pores délimités par les microfibrilles du treillis. C'est l'hypothèse du germe d'air sur le treillis de microfibrilles ; (b) Les microfibrilles se brisent et le torus passe à travers l'ouverture de la ponctuation et laisse passer un germe d'air. C'est l'hypothèse du germe d'air par rupture des microfibrilles. (c) Les microfibrilles sont suffisament élastiques pour que le torus passe à travers l'ouverture et laisse apparaître un pore du treillis. C'est l'hypothèse du germe d'air par étirement du treillis. (d) Le torus joue son rôle de valve mais le germe d'air passe quand même, a travers le torus ou sur les bords de l'ouverture. C'est l'hypothèse du germe d'air « magique ». Les traits rouges pleins indiquent si les hypothèses ont été invalidées par de la modélisation et/ou des études experimentales. Les traits rouges en tireté montrent que ces hypothèses sont peu probables mais elles ne sont pas complèment exclues.

La première hypothèse, celle de l'apparition d'un germe d'air sur le treillis de microfibrilles (*margo capillary-seeding*), a été repoussée par des arguments issus de la modélisation car la tension nécessaire à l'aspiration du torus contre l'ouverture est en deçà des mesures de P_{50} (Domec et al., 2006). De plus, la loi de Laplace-Young prédit une rupture d'un ménisque air-eau au niveau d'un pore du treillis à une tension bien plus faible que celle induisant de la cavitation (Delzon et al., 2010). Donc le torus joue son rôle de valve à des tensions plus faibles que celles qui provoquent la cavitation. La seconde hypothèse, celle du germe d'air par rupture des microfibrilles (*margo rupture-seeding*), a été écartée par des expériences. De l'eau a été injectée sous pression dans une branche afin d'induire, dans un premier temps, le plaquage des torus sur l'ouverture de la chambre ; et dans un second temps, la pression a été augmentée pour rompre les microfibrilles. La conductance de la branche n'a jamais augmenté, au contraire elle diminue tout le long de l'expérience (Cochard et al., 2009). Donc la rupture des microfibrilles ne paraît pas être une hypothèse probable pour expliquer la cavitation. La

troisième hypothèse, celle de l'apparition d'un germe d'air par étirement du treillis, a été aussi infirmée par des mesures anatomiques de la flexibilité des microfibrilles, un estimateur de leur élasticité. Plus une espèce a des microfibrilles flexibles plus cette espèce est résistante à la cavitation ((Delzon et al., 2010) mais voir (Sperry & Tyree, 1990)). Reste à tester la dernière hypothèse qui prévoit une rupture capillaire et le passage d'une bulle d'air malgré la fermeture l'ouverture par le torus. Il s'agit d'observer la microanatomie du torus et de vérifier qu'il est bien imperméable à l'air comme supposé dans les trois modèles précédents. Ce point a fait l'objet d'une étude spécifique dans le cadre de cette thèse.

1.5 La variation de la résistance à la cavitation, le moteur de l'adaptation face à la sécheresse.

Les événements climatiques extrêmes fonctionnent comme des filtres, ne passent au travers que les individus possédant une combinaison de valeurs de caractères (souvent des valeurs extrêmes) permettant leur survie et leur reproduction (fitness élevée). Ainsi plus une population a une variation importante, plus elle aura une capacité adaptative importante. La variation est donc le moteur de l'évolution. Dans un premier temps, nous nous intéresserons à la variation interspécifique de la résistance à la cavitation et au rôle de la sélection naturelle dans la genèse de celle-ci. Dans une seconde partie, nous ferons un état de l'art sur la variation intraspécifique de la résistance à la cavitation et les déterminismes connus de cette variation.

1.5.1 La variation interspécifique de la résistance à la cavitation a-t-elle été façonnée, en partie, par la sélection naturelle ?

La variation de la résistance à la cavitation a surtout été caractérisée au niveau interspécifique (Maherali et al., 2004; Delzon et al., 2010) (Figure 8). Au sein des gymnospermes, ce caractère varie de –2.2 pour *Taxodium distichum* (espèces qui vit dans les marais à l'ouest des Etats-Unis d'Amérique) à –16 MPa pour *Callitris columellaris* (espèce du désert Australien).

Figure 8 : Phylogramme illustrant la variation interspécifique de la densité du bois (D_{mean}, à gauche) de la résistance à la cavitation (P_{50}, à droite). Les couleurs chaudes indiquent une forte résistance à la cavitation et une densité du bois importante. La variation est importante au sein des gymnospermes pour la P_{50}, en revanche beaucoup plus limité au sein du genre *Pinus*. D'après (Larcher et al., 2011)**.**

Dans une méta-analyse, Maherali et al., (2004) montre que des espèces éloignées phylogénétiquement peuvent avoir une P_{50} similaire et cela dans une proportion plus importante que celle due simplement au hasard (simulée par un modèle brownien[5]). Des travaux préliminaires au laboratoire sur un large panel d'espèces de gymnospermes montrent les mêmes tendances (Figure 8). Cette convergence évolutive est interprétée comme une trace de l'action de la sélection naturelle (homoplasie). Cependant, dans une étude similaire limitée au seul genre botanique *Juniperus*, un conservatisme phylogénétique est détecté, c'est-à-dire que des espèces phylogénétiquement proches se ressemblent plus que sous l'attendu du modèle brownien (Willson et al., 2008).

1.5.2 La variation intraspécifique et ses déterminismes, les grandes inconnues

Dans cette thèse, nous n'aborderons pas la variation intra-individu, cette question a été abordée par les physiologistes et écophysiologistes (voir (Cochard et al., 1999; Domec & Gartner, 2001; Mayr & Cochard, 2003; Holste et al., 2006; Beikircher & Mayr, 2008)). A cause de la difficulté de l'estimation de la P_{50}, l'exploration de la variation intraspécifique a longtemps été limitée à quelques populations sur des effectifs faibles par population (Table 1). De plus la diversité des dispositifs et des espèces (ou sous-espèces) étudiées ne permet pas de tirer des conclusions générales.

[5] Modèle simplifié d'une évolution neutre, ces modèles sont utilisé en physique pour simuler la diffusion de molécule dans un liquide. Ces modèles appartiennent aux modèles markoviens (de marche aléatoire), ils n'utilisent aucune des hypothèses de dérive génétique habituellement utilisées en génétique des populations.

Table 1 : Etat de l'art des études intraspécifiques sur la résistance à la cavitation. *Npop* : nombre de population, *Nind* : nombre d'individus par population utilisés pour mesurer la résistance à la cavitation. La table est divisée en deux parties, la première partie correspond aux études conduites en test de population (ou de provenances) et/ou de descendance, la seconde aux études « *in situ* ». *Differentiation* : si les auteurs ont conclu à de la différenciation entre populations ou pas. Lorsqu'il y a deux items dans la ligne, cela se rapporte aux différents organes étudiés. Il est important de noter que les méthodes statistiques ont toutes été très différentes pour inférer de la différenciation entre les populations.

Population trial	Npop	Nind	Traits	Organ	Differentiation	References
Pseudotsuga menziesii	4	10	P50	Stem/root	yes/yes	(Kavanagh et al., 1999)
Quercus wislizenii	3	6	P50	Stem	no	(Matzner et al., 2001)
Pinus contorta var latifolia	4	15	P50/Slope	Stem	yes	(Wang et al., 2003)
Pinus pinaster	4	5	P50 /Slope	Stem	no	unpublished
Saccharum sp	0	4	P10/P50/P88	Leaf	yes	(Neufeld et al., 1992)
Olea europaea	2	2	P50	Stem	yes	(Ennajeh et al., 2008)
Populus trichocarpa	4	5	P12/Slope	Stem	yes	(Sparks & A.R. Black, 1999)
Ambrosia dumosa	3	6	P50	Stem	yes	(Mencuccini & J. Comstock, 1997)
Hymenoclea salsola	3	6	P50	Stem	yes	(Kolb & Sperry, 1999a)
Artemisia tridentata	3	10	P50	Stem	yes	(Kolb & Sperry, 1999b)
Fagus sylvatica	17	15	P50	Branch	no	(Wortemann et al., 2011)
Pinus pinaster	6	11	P50	Branch	no	(Corcuera et al., 2011)
In situ						
Pinus sylvestris	12	6.8	P50	Branch	no	(Martinez-Vilalta et al., 2009)
Acer grandidentatum	2	9	P50	Stem/root	no/yes	(Alder et al., 1996)
Pinus sylvestris	2	10	P50/Slope	Branch	no	(Martinez-Vilalta & Pinol, 2002)
Pinus ponderosa	2	6	P50/Slope	Branch	no	(Maherali et al., 2002)
Cordia alliodora	3	3	P50	Branch	yes	(Choat et al., 2007)
Artemisia tridentata	3	10	P50	Stem	yes	(Kolb & Sperry, 1999a)
Juniperus scopulorum	2	12	P50/Slope	Stem/root	no/no	(Ogle et al., 2009)
Fagus sylvatica	5	25	P50	Branch	yes	(Herbette et al., 2010)

Dans l'étude la plus puissante sur le plan statistique, (Martinez-Vilalta et al., 2009) montre, pour 12 populations réparties dans l'ensemble de l'aire de distribution de *Pinus sylvestris,* que la variance phénotypique de la résistance à la cavitation est faible (coefficient de variation phénotypique, $CV_P < 10\%$). Cependant, cette étude ne fait pas la part entre la variance génétique, la variance environnementale et les interactions éventuelles qui peuvent masquer ou augmenter les deux premières composantes. Très récemment, Wortemann et al., (2011); Corcuera et al., (2011) montrent qu'il y a une variation génétique et une plasticité phénotypique pour la résistance à la cavitation mais leur stratégie d'échantillonnage ne permet pas de dériver des paramètres génétiques. L'ensemble des travaux réalisés avant les trois auteurs précités (2009) ne permettait pas d'avoir une conclusion tranchée sur l'existence ou non de variation génétique pour la résistance à la cavitation. En conséquence, aucune

estimation de la variance additive de ce caractère n'a été publiée, et seule une étude a fait une détection QTL (infructueuse) pour ce caractère (Lauri et al., 2011). Ces étapes sont des préalables cruciaux pour l'exploration du déterminisme de la résistance à la cavitation et éventuellement son intégration dans un programme d'amélioration.

1.6 Objectif de la thèse : Mécanismes physiologiques impliqués dans la résistance à la cavitation et déterminisme de la variation phénotypique chez *Pinus pinaster*.

Cette thèse s'inscrit dans la problématique de la réponse des populations d'arbres au réchauffement climatique, notamment face aux sécheresses intenses. Les espèces arborées sont les espèces clé de voûte ou espèces fondatrices pour les écosystèmes forestiers. Elles représentent la majeure partie de la biomasse des terres émergées, conditionnent la majorité des flux d'énergies et de matières (90% du stock de carbone des écosystèmes continentaux) et structurent fortement l'espace (Potter, 2008). Les réponses des écosystèmes forestiers sont majoritairement fonction de la réponse de ces espèces.

L'objectif de cette thèse est double :

(i) il s'agit de mieux comprendre le mécanisme physiologique de la résistance à la cavitation grâce à une étude comparée de la résistance à la cavitation et de l'anatomie des ponctuations aréolées à l'échelle interspécifique chez les conifères,

(ii) d'explorer l'étendue et la structuration de la variation phénotypique de la résistance à la cavitation et, grâce aux modèles de génétique quantitative, d'en comprendre les déterminismes.

Pour chacun de ces objectifs, nous avons dégagé les questions de recherche et les hypothèses associées suivantes :

I) Mécanismes de résistance à la cavitation chez les gymnospermes :

- Où se situe la rupture capillaire (le germe d'air) dans la ponctuation aréolée des gymnospermes ?

Hypothèse : Le torus n'est pas aussi imperméable à l'air que les physiologistes le présupposent.

II) Variation intraspécifique et son déterminisme génétique :

- Quelle est l'étendue de la variation phénotypique de la résistance à la cavitation entre populations naturelles de climats contrastés ?

Hypothèse : Etant donnée l'importance du caractère dans la physiologie hydrique de l'arbre, de la variation à l'échelle interspécifique et de la variation climatique des populations choisies,

on s'attend à observer des différences fortes entre populations en terme de résistance à la cavitation et donc en terme de résistance à la sécheresse.

- *Quelle est la part génétique de cette variation ?*

Hypothèse : Comme les autres caractères liés à la morphologie du bois (densité, composition chimique) ce caractère doit être fortement héritable.

- *Quelle la part de la plasticité phénotypique dans cette variation ?*

Hypothèse : Pas d'hypothèse *a priori*. La littérature en discute beaucoup mais n'apporte pas de réelles estimations de cette plasticité phénotypique.

- *Quelle est l'architecture génétique de la résistance à la cavitation ?*

Hypothèse : Il est attendu que les QTL (*quantitative trait loci)* de la résistance à la cavitation colocalisent avec des QTL précédemment cartographiés pour la densité du bois. Vraisemblablement les gènes (ou groupe de gènes) impliqués dans la mise en place des parois cellulaires sont aussi impliqués dans la mise en place des ponctuations.

2- Fonctionnement hydraulique de l'arbre et mécanisme de résistance à la cavitation

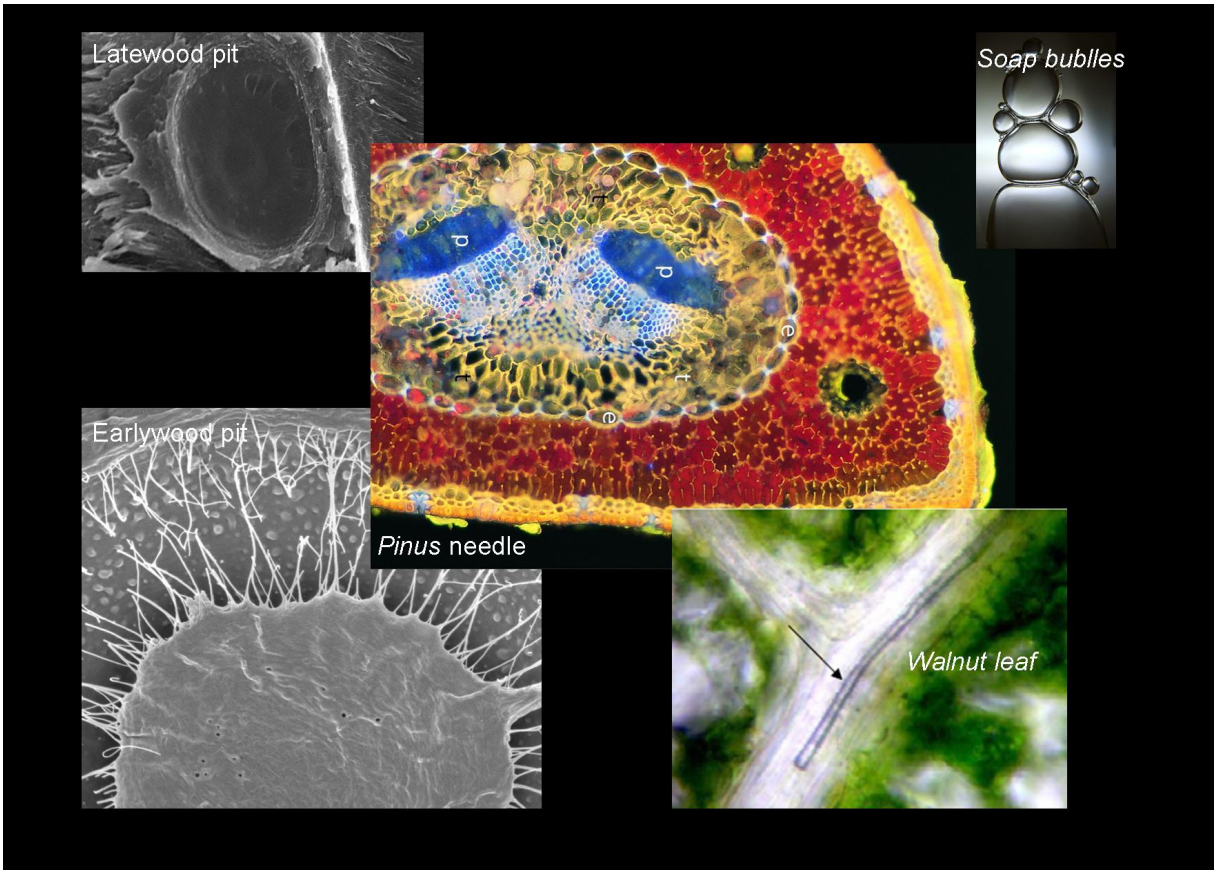

Les objectifs de cette partie sont de replacer la problématique de la cavitation dans le fonctionnement hydraulique de l'arbre, faire un état de l'art des modèles expliquant la propagation de la cavitation chez les conifères et de vérifier l'une des hypothèses sous-jacentes des modèles précédents, c'est-à-dire que le torus est imperméable à l'air (l'hypothèse n°4 : germe d'air magique). Pour cela des mesures de microanatomie de la ponctuation aréolée et particulièrement du torus ont été effectuées.

2.1 Le continuum hydrique sol-plante-atmosphère, rappels généraux

Dans la majorité des espèces, la circulation de l'eau dans la plante est un phénomène physique passif. Il existe quelques exceptions comme les poussées racinaires ou de branches, ces processus dit actifs (nécessitant de l'énergie) co-existent avec un transport passif et ne prévalent qu'une partie de l'année souvent lors de la mise en place des feuilles. La théorie tension-cohésion (*Cohesion-tension theory*, voir (Sperry et al., 1996; Wei et al., 1999; Cochard, 2002a; Tyree & Zimmermann, 2002; Angeles et al., 2004)) est le paradigme actuel qui explique la circulation à longue distance de l'eau (sève brute) dans les plantes.

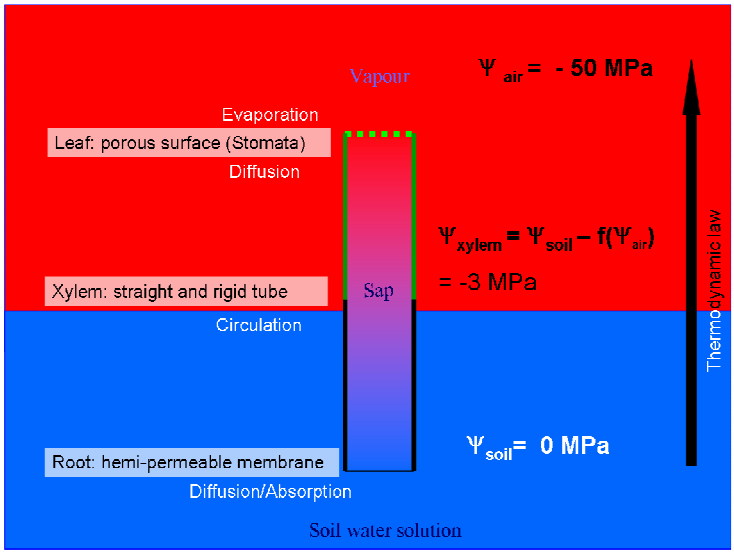

Figure 9 : Illustration de la théorie adhésion-cohésion-tension. La couleur bleue représente un sol saturé en eau avec un potentiel hydrique (ψ_{soil}) égal à zéro. La couleur rouge représente un air pauvre en vapeur d'eau avec un potentiel hydrique faible (ψ_{air}). La plante est représentée comme un tube ayant une extrémité fixée dans le sol, la sève est séparée de la solution du sol par une membrane hémiperméable (les racines). L'extrémité à l'air est une surface transpirante, l'eau s'évapore des pores appelés stomates.

La thermodynamique montre que l'eau circule des potentiels hydriques élevés vers les potentiels hydriques faibles. La plante fonctionne comme une pompe aspirante mue par l'énergie solaire. L'air ayant le potentiel hydrique le plus bas, les molécules d'eau s'évaporent au niveau de la chambre sous-stomatique et d'autres molécules d'eau vont les remplacer en entraînant leur voisines grâce aux liaisons hydrogènes. Grâce au continuum hydraulique que forme en phase liquide les molécules d'eau, la dépression créée par l'évaporation au niveau des feuilles va se propager jusqu'aux racines de proche en proche. Par cette force aspirante l'eau va être extraite du sol. La sève dans l'arbre est donc tirée par le haut, elle est sous tension (pression négative) et non poussée par le bas. D'autres forces soutiennent la colonne de sève : i/ les molécules d'eau adhèrent aux parois du xylème via les liaisons hydrogènes, ii/ les ménisques au niveau de la paroi cellulaires des cellules de la chambre sous-stomatique ont des rayons faibles, ils peuvent supporter des colonnes d'eau de plusieurs centaines de mètres (forces capillaires).

2.2 Quand les bulles s'en mêlent

La cavitation est un phénomène bien connu en physique, il s'agit d'apparition de cavités, issues de vaporisations locales, au sein d'un liquide. On peut imaginer des variations de pression très locales qui amènent un petit volume de liquide à franchir la limite liquide-gaz (chemin isotherme, flèche noire sur la figure 10). Dans le cas d'eau pure et dégazée, la vaporisation du liquide est due à la rupture spontanée des liaisons hydrogènes entre les molécules d'eau, la nucléation de la vapeur se fait au sein de la colonne d'eau, on qualifie cette nucléation d'homogène (cavitation homogène). La nucléation peut être activée (se dérouler à plus faibles tensions) par différents supports comme des bulles d'air préexistantes, sur une interface eau/air, sur une surface hydrophobe, et/ou une eau non pure. On parlera de cavitation hétérogène.

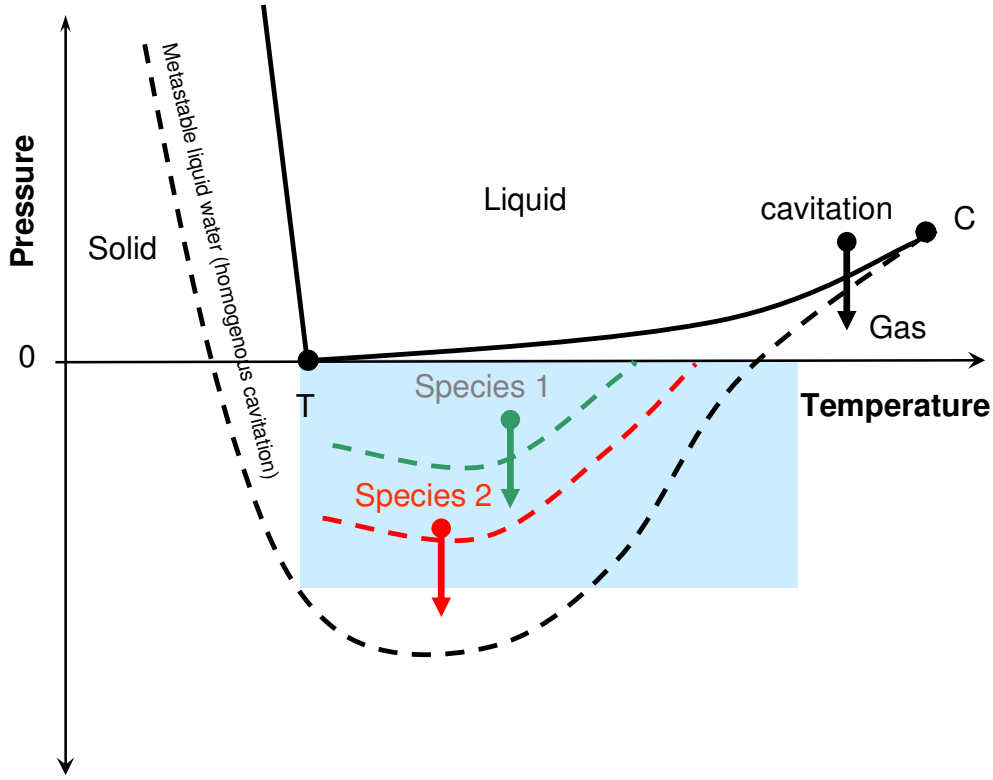

Figure 10 : Diagramme de phase de l'eau. Les lignes pleines délimitent les états de l'eau en fonction de la pression (*Pressure,* en y) et de la température (*Temperature,* en x). Les lignes en pointillé montrent l'extension possible du domaine liquide (lignes spinoïdales de Speedy). L'espace compris entre les lignes en pointillé et pleines est un domaine thermodynamiquement métastable (ψ_{crit}). La flèche noire montre un chemin isotherme d'un volume d'eau liquide qui franchit la limite liquide-gaz amenant à la vaporisation locale de l'eau par cavitation dite homogène. La partie en couleur du graphique délimite schématiquement le domaine de pression et de température qui existe dans la sève. Les limites en pointillé et en couleurs correspondent à l'extension possible du domaine liquide de l'eau dans le xylème (ψ_{crit_1} et ψ_{crit_2}) de l'espèce 1 (en vert) et 2 (en rouge). L'espèce 1 (en vert) est peu résistante à la cavitation, l'espèce 2 (en rouge) est très résistante à la cavitation. Les domaines d'extension de l'eau liquide chez les plantes sont réduits par rapport à l'eau pure car l'irrégularité des parois, la présence d'ions et de bulle d'air augmente les probabilités de cavitation (cavitation hétérogènes). Modifié d'après Caupin & Herbert, (2006), Cochard, (2006) et Herbert & Balibar (2006)**.**

Comme vu précédemment, l'eau contenue dans la sève est généralement sous pression négative aussi appelée tension ($\psi_{xylem} < 0$). Les molécules d'eau de sève sont étirées. Si l'on regarde un diagramme de phase de l'eau, pour des pressions négatives (tension) l'eau devrait être sous forme de gaz. Or l'eau n'est pas un liquide parfait, les liaisons hydrogènes étendent le domaine liquide. Aussi, l'eau de la sève est dans un état thermodynamiquement métastable lorsqu'elle est sous tension et encore liquide. En cas de tension forte (par exemple transpiration importante et peu d'eau dans le sol) ou de bulle d'air favorisant la nucléation

(décongélation de la sève), l'eau de la sève passera la limite de métastabilité (ψ_{crit}) de l'eau liquide en tension (Figure 10) et elle se vaporisera ($\psi_{xylem} < \psi_{crit}$) (Cochard, 2006). La limite de métastabilité de l'eau liquide en tension (ψ_{crit}) est dépendante de l'anatomie du xylème, on estime ψ_{crit} par P_{50}. L'estimation de P_{50} et les mécanismes précis de cavitation dans les gymnospermes seront abordés plus tard.

Les conséquences de la cavitation dans l'appareil vasculaire des plantes pourraient être dramatique si les plantes ne régulaient pas leur transpiration grâce aux stomates. Une demande évaporatoire de l'air très forte (ψ_{air}) va augmenter la tension sur le xylème, si jamais $\psi_{xylem} < \psi_{crit}$ la cavitation dans la sève démarre. L'embolie, créée par cavitation, bloque la circulation de la sève, ψ_{xylem} chute, entraînant d'autant plus de cavitation, et ainsi de suite. Le seuil de tension déclenchant de la cavitation (ψ_{crit}) est déterminé par l'anatomie du xylème. Ce seuil biophysique contraint la capacité de transpiration maximale. La régulation des flux hydriques est donc capitale pour les plantes afin d'éviter le cercle vicieux de l'embolie (*Runaway Embolism*).

2.3 La régulation des interfaces du continuum sol-plante-atmosphère

En cas de forte transpiration et/ou de faible teneur en eau du sol, la cavitation menace l'intégrité du système de transport à longue distance de la sève brute. En effet, les plantes exploitent les propriétés particulières de l'eau (liaisons hydrogènes) pour extraire l'eau du sol et l'apporter jusqu'en haut des cimes grâce à l'énergie solaire (d'après (Koch et al., 2004) la hauteur limite pour un arbre serait de 122m). Oui, les plantes sont des fainéantes ! Tout déséquilibre entre les entrées et les sorties d'eau va induire un surcroît de tension dans le xylème qui peut conduire à la cavitation. Aussi les plantes régulent strictement les flux d'eau entrants et surtout sortants.

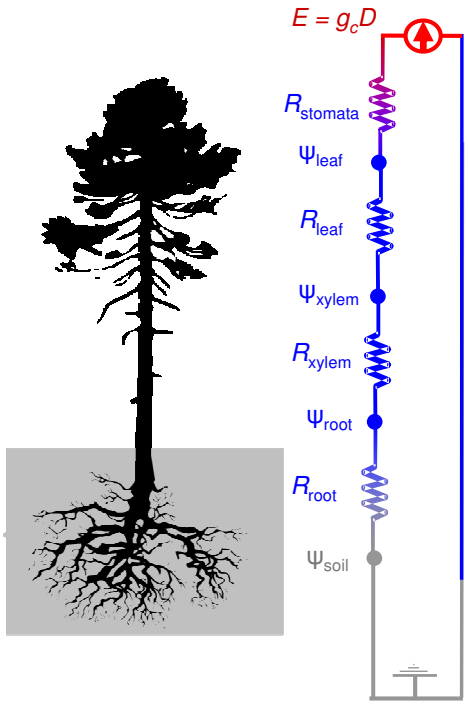

Figure 11 : Représentation du circuit hydraulique d'un arbre grâce à l'analogie d'un circuit électrique. Ici, la plupart des résistances ont été représentées par un potentiomètre car la plante, à long terme, peut agir sur chacune d'elles. Le sol est représenté comme la masse et l'atmosphère (et l'énergie solaire incidente) comme un moteur. Modifié d'après Jones (1992)**.**

Comme le montre la Figure 11, les physiologistes (et écophysiologistes) représentent le circuit hydraulique d'une plante comme un circuit électrique. Le long des potentiels décroissants, il existe plusieurs résistances que la plante contrôle (potentiomètre) ou subit. L'eau rencontre une première résistance au passage de la matrice du sol à la racine. L'eau entre ensuite dans la plante, traverse le cortex racinaire et l'endoderme qui entoure le xylème racinaire. La résistance de ce compartiment est, en partie, sous contrôle de la plante, qui peut l'augmenter (transpiration forte) ou la diminuer (face à des afflux de sel ou de polluants) via des aquaporines (Martínez-Ballesta et al., 2003; Ehlert et al., 2009). Ensuite vient la résistance du xylème, qui, chez les gymnospermes, est partagée à part égale entre le passage des ponctuations et le lumen des trachéides (Hacke et al., 2004; Pittermann et al., 2006, 2010). Puis vient la résistance mésophyllienne, plus complexe, dans laquelle intervient la perméabilité des plasmalemmes, des parois cellulaires, le collapse éventuelle du xylème des nervures, et encore les aquaporines. La régulation de cette résistance est multifactorielle (lumière, conductivité des nervures, phytohormones) et méconnue (Cochard et al., 2004, 2007). La plante contrôle les résistances en phase liquide et aussi une résistance en phase gazeuse qui va réguler les pertes d'eau vers l'atmosphère. La régulation stomatique du flux

hydrique de la plante est le Saint Graal des écophysiologistes, le mécanisme de contrôle est encore âprement débattu dans la littérature (Cochard et al., 2002; Cochard, 2002b; Buckley, 2005; Brodribb, 2009; Brodribb & S.A.M. McAdam, 2011; Brodribb & S. a M. McAdam, 2011). Des dizaines de modèles existent sans qu'aucun ne fasse l'unanimité (Damour et al., 2010).

Ainsi, on peut formaliser le fonctionnement hydrique d'une plante (Sperry et al., 1998) par l'équation :

(1) $$\Psi_{leaf} = \Psi_{soil} - \Psi_{grav} - R_{tot} E_{tot}$$

Avec Ψ_{leaf} le potentiel hydrique foliaire, Ψ_{soil} le potentiel hydrique du sol, Ψ_{grav} le potentiel hydrique dû à la gravité (que l'on peut écrire $hg\rho_{water}$). E_{tot} est la transpiration à travers la cuticule et surtout les stomates, il s'exprime comme étant le produit de la conductance stomatique moyenne de la canopée (g_{c}), du déficit en vapeur d'eau de l'air (D) et de la surface foliaire (A_{L}).

(2) $$\Psi_{leaf} = \Psi_{soil} - hg\rho_{water} - \left(R_{soil} + R_{root} + R_{xylem} + R_{leaf}\right) g_C D A_L$$

La grande difficulté pour établir un modèle hydrique fiable vient surtout de la méconnaissance du contrôle de plusieurs résistances (R_{root}, R_{leaf} et g_C). Pour combler ce manque de connaissance, les modélisateurs ont souvent recours à des relations plus ou moins empiriques entre la résistance et une variable environnementale. En revanche, pour la résistance xylémienne, il est existe un modèle bien établi avec la tension de la sève.

(3) $$R_{xylem} = \frac{1}{K_{\max}} \left(1 - \frac{1}{1 + e^{S_{50}/25(\Psi_{xylem} - P_{50})}} \right)^{-1}$$

Avec $K_{\max}$ la conductivité de la branche sans embolie native. Le reste de la formule est une fonction sigmoïde qui modélise l'apparition et l'extension de l'embolie dans la branche en fonction du potentiel hydrique du xylème. Cette fonction dépend de deux paramètres P_{50} et S_{50} qui représentent respectivement la tension à laquelle le xylème a perdu 50% de sa conductivité initiale et la vitesse à laquelle le xylème perd sa conductivité par unité de tension.

2.4 La cavitation hétérogène, une histoire de passoire ?

La cavitation homogène est une vaporisation spontanée d'un liquide métastable par rupture des liaisons hydrogènes entre les molécules d'eau (Caupin & Herbert, 2006; Herbert & Balibar, 2006; Herbert et al., 2006). En théorie, il existe une tension limite à laquelle l'eau cavite avec une probabilité égale à 1. Seulement la valeur de cette tension limite diffère fortement selon le type de modèle : les modèles thermodynamiques montrent que l'eau cavite quand la tension ≤ -22 MPa, alors que les modèles de nucléation homogène ou de simulation moléculaire montrent que la tension limite serait ≤ -140 MPa (Wheeler & Stroock, 2009). Jusqu'à présent, les valeurs de résistance à la cavitation (P_{50}) mesurées chez les plantes sont inférieures à ces tensions limites théoriques (le champion du monde actuel est un *Callitris columellaris* , P_{50} = -15.8 MPa, vivant dans le désert australien). Par conséquent, ceci implique que le mécanisme de cavitation est hétérogène (Cochard, 2006). Ce n'est pas la rupture mécanique des liaisons hydrogènes qui doit être envisagée mais la présence d'un agent catalyseur (nucléus) qui va inciter la rupture des liaisons des hydrogènes (nucléation).

Plusieurs expériences laissent penser que les bulles d'air préexistantes (anciennes blessures, contact entre l'aubier fonctionnel et non fonctionnel) seraient les agents de nucléation majoritaires (Cochard et al., 1992) chez les plantes. De plus la cavitation chez les angiospermes est du à la rupture d'un ménisque air-sève au niveau d'un pore du treillis de la ponctuation (Sperry & Hacke, 2004). La ponctuation aréolée des gymnospermes évite la propagation de l'embolie en séparant ces trachéides fonctionnelles des trachéides embolisées grâce à l'effet valve du torus. L'examen de la microanatomie du torus révèle une grande diversité comme montré à la figure 12.

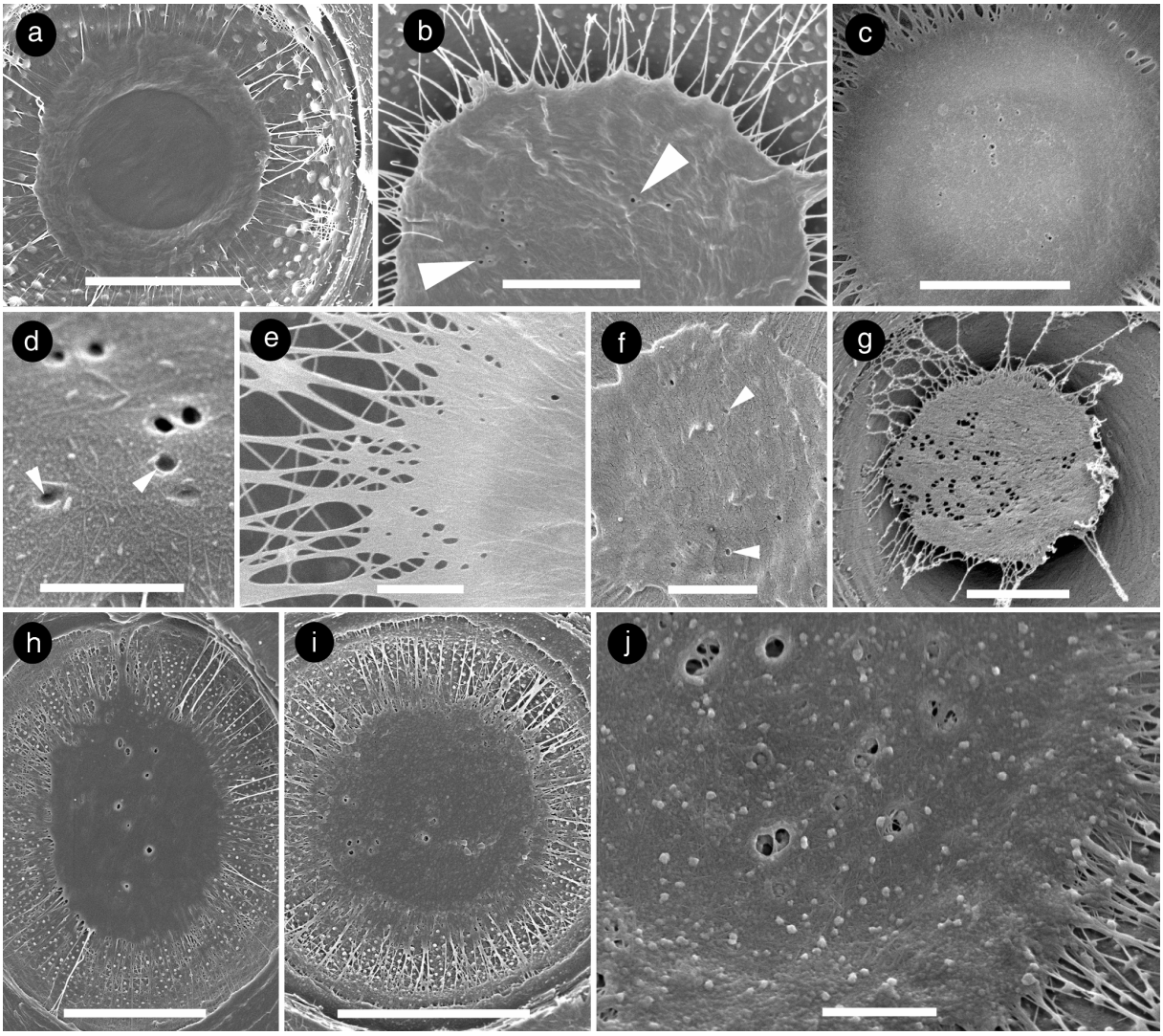

Figure 12 : Images en microscopie électronique à balayage de la ponctuation aréolée des conifères montrant l'ultrastructure du torus. (a) *Pinus radiata*, le torus est aspiré contre l'ouverture que l'on devine par transparence. L'ouverture de la ponctuation aréolée a un diamètre plus faible que le torus lui-même. Echelle = 5 µm. (b) *Pinus pinaster*, les ardillons montrent plusieurs nanopores à la surface du torus. Echelle = 2 µm. (c) *Cephalotaxus harringtonii*, détails sur les nanopores. Echelle = 2 µm. (d) *Picea mariana*, les ardillons montrent encore des nanopores. Echelle = 500 nm (e) *Torreya californica*, détail du torus et du treillis de microfibrilles, les pores à la jonction entre le torus et le treillis ne sont pas interprétés comme d'anciens plasmodesmes. Echelle = 500 nm (f) *Pinus wallichiana*, détail sur les nanopores, certains apparaissent remplis de matière (données TEM, non montrées) d'autres sont au contraire profonds. Echelle = 2 µm (g) *Pinus wallichiana*, cet échantillon est traité avec 100% éthanol ce qui agrandit artificiellement les nanopores. Echelle = 2.5 µm. (h) *Sequoia sempervirens*, le torus est criblé et aspiré. Echelle = 5 µm. (i) *Sequoiadendron giganteum*, vue d'ensemble de torus criblés. Echelle = 5 µm. (j) *Sequoiadendron giganteum*, détail des nanopores. Echelle = 1 µm.

Les torus ne sont pas tous lisses et imperméables. Sur les 33 espèces examinées appartenant à des familles botaniques éloignées (Cupressaceae, Pinaceae, Cephalotaxaceae, Taxaceae,

Sciadopityaceae) 12 espèces ont des petites perforations (*punctured torus*), que l'on dénommera nanopore (*pore in tori*) dans la suite du manuscrit. Ces nanopores apparaissent souvent groupés avec un diamètre moyen de 61 nm±27, leur origine est attribuée à d'anciens plasmodesmes (canaux intercellulaires à moindre sélectivité). Ils ne sont pas systématiques présent sur tous les torus d'un échantillon et ne sont détectés que dans le bois initial.

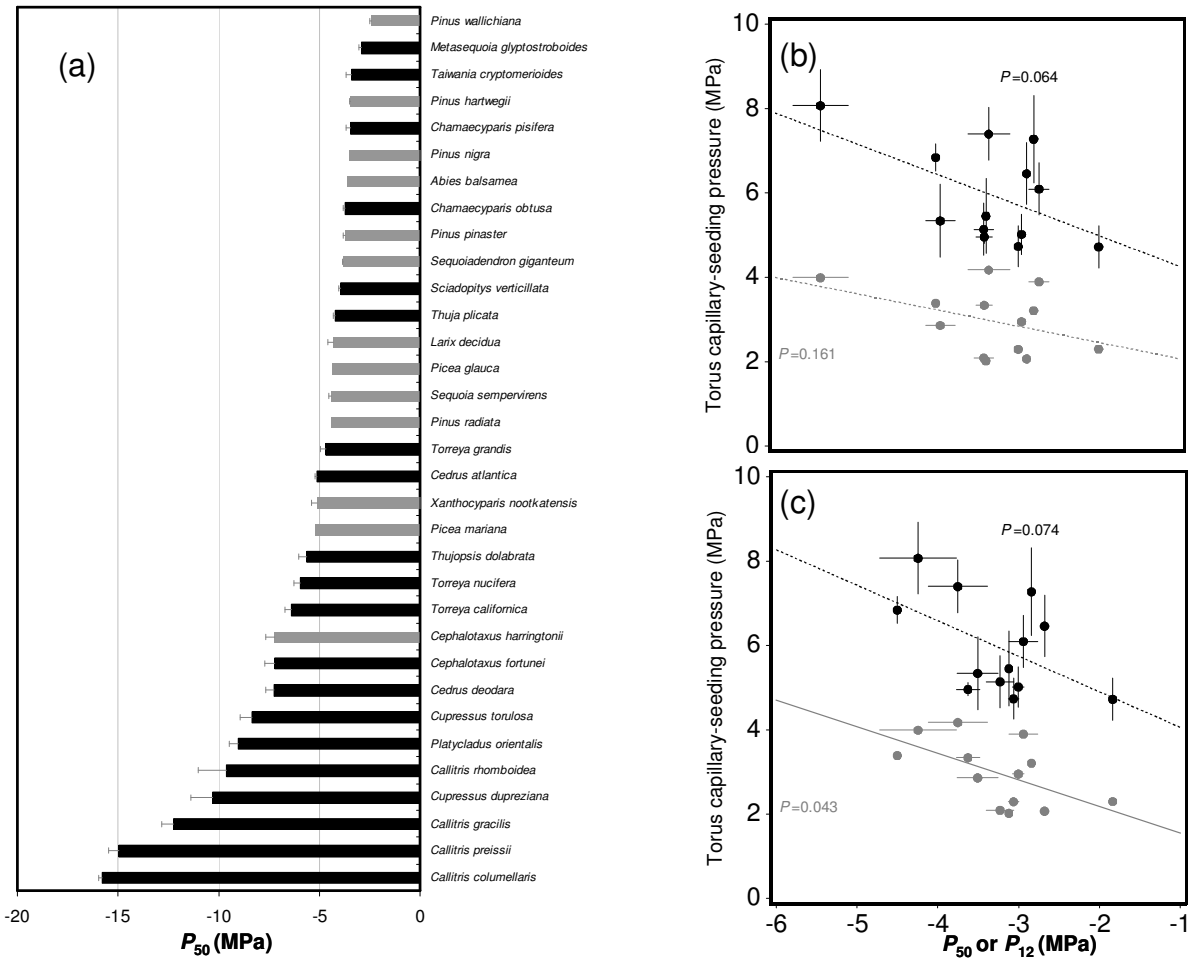

Figure 13 : (a) Diagramme représentant la résistance à la cavitation des espèces étudiées en microanatomie. Les espèces en gris possèdent un torus criblé. (b) Corrélation entre la P_{50}^{xylem} et la tension nécessaire à la rupture d'un ménisque dans un nanopore (« *torus capillary-seeding pressure* »). En noir, tension calculée en prenant en compte le diamètre moyen des nanopores ; en gris tension calculée en prenant en compte le diamètre maximum des nanopores). (c) Corrélation entre la P_{12}^{xylem} et la tension nécessaire à la rupture d'un ménisque dans un nanopore (en noir, tension calculée en prenant en compte le diamètre moyen des nanopores ; en gris tension calculée en prenant en compte le diamètre maximum des nanopores). Les barres d'erreur correspondent aux erreurs standard (n=5 pour chaque espèce).

2.5 Diamètre des nanopores et P_{50}.

Les nanopores ne semblent pas propres à un taxon précis, bien qu'au sein des espèces échantillonnées les *Pinaceae* présentent presque tous des ponctuations à nanopores excepté le genre *Cedrus* qui est aussi le genre le plus résistant à la cavitation. En moyenne, les espèces possédant des nanopores sont moins résistantes à la cavitation que les espèces sans nanopore (régression linéaire *P*-value = 0.02). A partir du diamètre (maximal ou moyen) des nanopores, il possible de calculer quelle sera la tension nécessaire à la rupture d'un ménisque air-eau (*T,* MPa) (grâce à la loi de Laplace-Young). Ainsi, nous avons détecté une corrélation entre P_{12} et *T* calculé sur le diamètre maximum des nanopores. Cette corrélation n'est pas détectée avec P_{50} ou si *T* est calculé sur le diamètre moyen des nanopores. D'un point de vue physiologique, il est plus logique de calculer *T* sur le diamètre maximal car ces ménisques sont les plus fragiles et donc ceux qui provoqueront de la cavitation. De manière identique P_{12} est un estimateur de « début d'entrée de l'air » dans le xylème (*air entry*), donc la tension pour laquelle les ménisques les plus fragiles lâchent correspond aux premiers signes de cavitation détectable.

Traditionnellement, les dimensions du torus, de l'ouverture de la ponctuation et la morphologie des microfibrilles étaient utilisées pour expliquer la variation de la résistance à la cavitation au sein des conifères (Hacke et al., 2004; Choat et al., 2008; Delzon et al., 2010). L'hypothèse du germe d'air qui passerait à travers le torus via les nanopores pourrait être une hypothèse vraisemblable chez les conifères moins résistant à la cavitation.

3- La génétique quantitative évolutive et la variation intraspécifique de la résistance à la cavitation

Cette partie poursuit plusieurs objectifs. Dans un premier temps, je présente les modèles d'analyses issues de la génétique quantitative et les méthodes utilisés dans la suite de l'exposé. Dans un second temps, nous quantifions (i) la variation phénotypique, génétique et la plasticité phénotypique de la résistance à la cavitation, (ii) nous étudions les corrélations avec d'autres caractères ainsi qu'avec des indices climatiques, et (iii) faisons des inférences sur les mécanismes évolutifs qui ont façonné cette variation phénotypique.

3.1 La variation phénotypique et ses déterminants : Acquis et Inné, rappels généraux.

Un des principaux freins épistémologiques à la théorie de l'évolution, à l'époque de Charles Darwin, fut le manque d'un modèle solide qui explique comment la variation passe d'une génération à l'autre, autrement dit : un modèle génétique pour les caractères à variation continue (*quantitative traits*). Les lois de Mendel pourtant déjà découvertes à l'époque ne suffisaient pas car, outre le fait qu'elles étaient méconnues, elles ne modélisaient que la transmission de caractères dits discrets (couleur de fruit, aspect du fruit). La généralisation des lois mendéliennes aux caractères continus a été permise par les progrès des statistiques (formalisation des plans expériences et de l'analyse de variance) et de la génétique mendélienne. Cette théorie, essentielle en biologie moderne, qui fait la synthèse entre la variation phénotypique et la génétique des populations porte le nom abstrus, dissonant de génétique quantitative (*quantitative genetics*). Cette théorie infère l'architecture génétique d'un caractère à partir de la variation phénotypique à travers des modèles statistiques (estimateurs des modèles génétiques) associés à des plans expérimentaux adaptés. La génétique quantitative est une approche descendante (*top-down*).

Dans un premier temps, décomposons la variance phénotypique avec le modèle suivant :

(4) $$P = G + E$$

P est la valeur (variable continue) du caractère phénotypique, elle est fonction, d'une grandeur G qui est la part génétiquement déterminée (l'innée) et d'une autre grandeur E, non héréditaire car due à l'environnement (l'acquis). En génétique, c'est la variation qui nous intéresse, elle est mesurée en variance qui est la moyenne des écarts à la moyenne au carré. Dans la suite de ce travail, je parlerais aussi bien de variation[6] que de son l'estimateur la

[6] La variabilité est la variation potentielle. C'est une propriété théorique.

variance. Si maintenant on passe à l'estimation statistique de ce modèle via une analyse de variance (Falconer & Mackay, 1996) :

(5) $$\sigma_P^2 = \sigma_G^2 + \sigma_E^2 + 2\mathrm{cov}_{GE}$$

Avec σ_P la variance phénotypique, σ_G^2 la variance génétique, σ_E^2 la variance environnementale, et pour des raisons mathématiques il faut ajouter deux fois la covariance entre la variance génétique et environnementale ($2\mathrm{cov}_{GE}$). La covariance est interprétée comme le fait que les génotypes [7] les plus performants se trouvent toujours dans les environnements plus favorables, ce qui est toujours le cas chez les animaux (ils se déplacent) et rarement le cas chez les plantes. De plus, le terme de covariance peut être supprimé en randomisant le dispositif expérimental, c'est-à-dire en allouant de manière aléatoire les génotypes dans les environnements (Falconer & Mackay, 1996).

Le terme σ_G^2 se réfère à la valeur génotypique des individus. Or les individus ne transmettent pas leurs génotypes mais leurs allèles. Les génotypes se reforment à chaque génération par le biais de la méiose (brassage intra (recombinaison) et inter chromosomique (ségrégation chromosomique)) et de la fécondation (fusion des gamètes). Le terme σ_G^2 peut se décomposer selon le modèle infinitésimale de Fisher (le fondement théorique peut être trouvé dans n'importe quel ouvrage de référence de génétique quantitative (Falconer & Mackay, 1996; Lynch & Walsh, 1998)). Selon ce modèle, σ_G^2 est codé par un grand nombre de locus qui ont chacun un effet propre donc additif (A), un effet de dominance (D) et des effets d'interaction inter-locus (I) aussi appelé épistasie.

(6) $$\sigma_G^2 = \sigma_A^2 + \sigma_D^2 + \sigma_I^2$$

L'estimation de ces termes repose sur l'observation que les membres d'une même famille se ressemblent plus que deux individus pris au hasard dans une population. Cette ressemblance est due au fait qu'ils partagent un certain nombre d'allèles en commun, en moyenne 50% pour des pleins frères (covariance entre apparentés). Selon les apparentements du plan d'expérience, on pourra estimer σ_A^2 , σ_D^2 et σ_I^2 . Par exemple, σ_A^2 , aussi appelée variance additive (celle transmise à la descendance) est le cœfficient directeur d'une droite de régression entre la moyenne des valeurs parentales pour un caractère donné et la moyenne des valeurs de la descendance pour le même caractère.

---

[7] Génotypes : Un génotype est l'association de deux allèles d'un même gène. Considérons un locus A, un individu *i* diploïde homozygote sera A_1A_1 ou encore A_2A_2 l'individu *j* hétérozygote sera A_1A_2, le chiffre en indice correspondant à l'allèle. On peut employer le terme génotype pour désigner l'ensemble des allèles sur l'ensemble des locus. Le concept de génotype inclut l'effet indépendant des allèles mais aussi l'effet que l'association entre les allèles peut avoir (voire l'effet de l'association des allèles entre les locus). En d'autres mots, le terme génotype se réfère à la présence d'allèles et aussi à l'association des allèles entre eux.

On quantifie ainsi la part de la variance du caractère qui passe dans la génération suivante grâce à un ratio qu'on appelle l'héritabilité au sens strict (*narrow sense heritability*) :

(7) $$h^2_{ns} = \frac{\sigma^2_A}{\sigma^2_P}$$

On utilise aussi des indices standardisés car la variance est exprimée dans l'unité du caractère, et comme toujours en biologie, il y a une corrélation entre la moyenne et la variance, on utilise des coefficients de variation :

(8) $$CV_A = \frac{\sigma_A}{\overline{X}}$$

Le coefficient de variation additif CV_A est adimensionnel car il correspond au ratio entre l'écart-type additif et la moyenne du caractère. On peut dériver des coefficients de variation pour l'ensemble des variances estimées.

3.2 Le dispositif expérimental ultime en génétique quantitative évolutive : Test de population-descendance

Pour commencer déminons la sémantique ! En effet le test de population-descendances est la version élaborée du *test de provenances* (jargon de généticien quantitatif) ou du *jardin commun* (jargon d'écologue). Ces dispositifs sont anciens en biologie, Henri Louis Duhamel du Monceau assembla des collections de *Pinus sylvestris* qu'il planta en différents sites et de la même façon Gaston Bonnier a utilisé ce dispositif expérimental sur les plantes alpines (Bonnier, 1890).

Le principe du test de provenance est simple : (i) On observe une population naturelle dans son milieu d'origine, par exemple en A, puis l'on fait de même avec une population naturelle en B. (ii) Si on observe que la population de B est plus grande que A, alors on peut faire l'hypothèse que B est constitutivement (innée) plus grande que A ; ou (iii) que l'environnement en B est plus favorable (acquis). Si l'on prend des graines sur les populations A et B que l'on plante dans un nouvel environnement alors on annule les effets de l'environnement ($E= 0$, d'où $P= G$). Et l'on pourra conclure sur l'origine des variances : génétique versus environnementale.

En foresterie, traditionnellement les entités comparées sont des provenances (tests de provenances) c'est-à-dire des individus provenant d'une région plus ou moins bien délimitée (critères climatiques, géomorphologiques, etc). Dans ce travail, nous utiliserons le terme de population plutôt que celui provenance car grâce aux marqueurs moléculaires, il est possible de regrouper les individus qui s'accouplent entre eux, c'est-à-dire de définir des populations.

En génétique quantitative, beaucoup de paramètres dérivent de l'analyse de covariance entre apparentés. En foresterie, toutes les graines issues du même cône, partagent la même mère et forment une famille. Si l'espèce est strictement allogame (comme c'est le cas de *Pinus pinaster*), en faisant l'hypothèse que tous les pères sont différents (nuage pollinique panmictique) alors les graines constituent une famille de demi-frères.

Dans cette étude, nous utiliserons un test de populations-descendances (TPD), c'est-à-dire qu'au sein des populations, nous connaissons les relations généalogiques entre individus. Cela permet d'estimer des paramètres génétiques à deux niveaux (les populations et les familles).

3.3 Dépasser la vision manichéenne (Acquis versus Innée) de la variation phénotypique : Les interactions génotypes × environnements et la plasticité phenotypique.

Nous pouvons écrire $\sigma_P^2 = \sigma_G^2 + \sigma_E^2 + 2\mathrm{cov}_{GE}$. La majorité des plans d'expériences (avec les plantes surtout) peuvent se concevoir pour annuler $2\mathrm{cov}_{GE}$. En revanche, il faut apporter une précision sur ce que l'on entend par environnement. L'environnement se divise en macroenvironnement et en microenvironnement. La distinction n'est pas facile, le macroenvironnement est choisi par l'expérimentateur. Par exemple, si *n* tests de populations sont sciemment placés, à intervalles réguliers, le long de gradients environnementaux (géographique ou climatique), alors l'effet du site quantifiera la variance dite macroenvironementale (σ_E^2). La variance microenvironementale est au contraire la variance qui n'est pas contrôlée par l'expérimentateur, la variation du sol, le microclimat, l'histoire du développement de la plante. Elle est estimée par la variance résiduelle (σ_ε^2).

Malgré le fait que l'on ait alloué de manière aléatoire les génotypes aux environnements (c'est-à-dire que $2\mathrm{cov}_{GE} = 0$) il se peut que les génotypes n'aient pas les mêmes performances dans chaque milieux, dit de manière statistique, qu'il y ait une interaction

génotype*environnement (σ^2_{GE}). Aussi nous écrivons à nouveau, (Falconer & Mackay, 1996; Lynch & Walsh, 1998) :

(9) $$\sigma^2_P = \sigma^2_G + \sigma^2_E + \sigma^2_{GE} + \sigma^2_\varepsilon$$

Où σ^2_P est la variance phénotypique, σ^2_G est la variance génétique, σ^2_E est la variance macroenvironementale, σ^2_{GE} signifie que les génotypes réagissent de manière différente aux environnements. σ^2_ε est la variance résiduelle qui est aussi une mesure de la variance microenvironnementale. Cette formule est illustrée par la Figure 14.

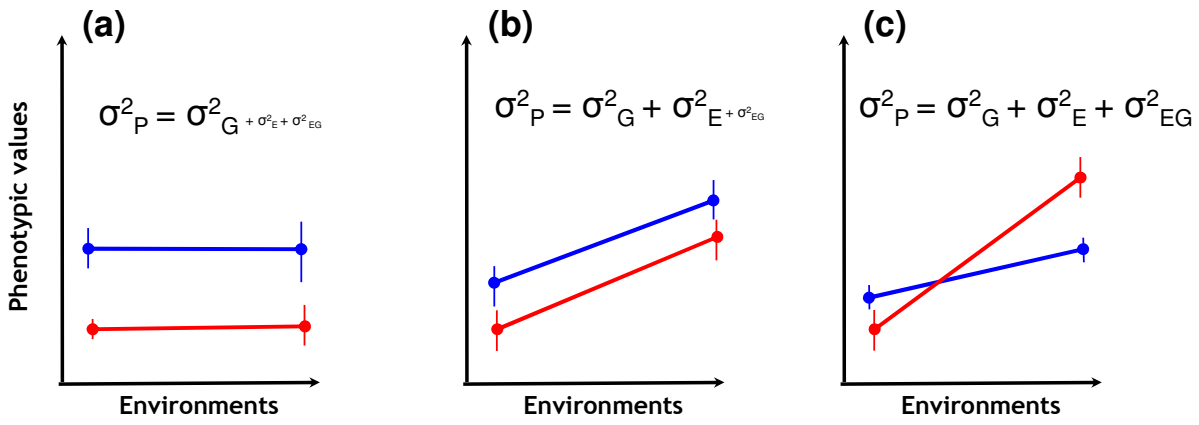

Figure 14 : Variance du caractère phénotypique en fonction de son déterminisme. En bleu et rouge deux entités biologiques pouvant être une collection du même génotype (clones), d'apparentés (descendance d'une même famille), d'individus d'une même population (ancêtres communs) vivant dans deux milieux très différents (points). Ici estimons que les points représentent des moyennes de deux populations différentes (rouge et bleue). Nous faisons l'hypothèse que $2\mathrm{cov}_{GE} = 0$. Au sein d'un même environnement, si les entités n'ont pas la même valeur de caractère alors il y a une variance génétique non nulle, de plus la variation au sein d'une entité biologique est due à de la variance microenvironementale (voir les barres d'erreur sur les points). (a) Dans chacun des environnements les populations montrent des différences ($\sigma^2_G \neq 0$) mais pas de différence entre environnements. La variance phénotypique est seulement génétique et microenvironementale. (b) En plus de la variance génétique et microenvironementale, il y des différences de moyennes entre les environnements ($\sigma^2_G \neq 0$ et $\sigma^2_E \neq 0$). En revanche les populations ont la même valeur de pente (ou la même différence de moyenne entre les environnements). (c) ici les populations, dans les deux environnements, présentent des différences de pentes, il y a donc une interaction entre la population et l'environnement ($\sigma^2_G \neq 0, \sigma^2_E \neq 0$ et $\sigma^2_{GE} \neq 0$).

Classiquement la plasticité phénotypique (σ^2_{PP}) est définie comme la somme de variance environnementale et de l'interaction génotype*environnement : $\sigma^2_{PP} = \sigma^2_E + \sigma^2_{GE}$ (Scheiner & Lyman, 1989; Scheiner, 1993). Il existe beaucoup d'estimateur de la plasticité phénotypique, par exemple en génétique quantitative ces estimateurs accordent plus d'importance à σ^2_{GE} qu'à σ^2_E car le premier est génétiquement héritable, pas le second[8] ; alors que les écologues ne distinguent pas forcément les deux termes. Dans cette thèse, nous utiliserons l'indice de Scheiner (adapté de (Scheiner & Lyman, 1989)) $S = (\sigma^2_E + \sigma^2_{GE}) / \left(\sigma^2_{GE} + \sigma^2_G + \sigma^2_E + \sigma^2_\varepsilon\right)$, cet indice est sensible aux deux termes de la plasticité. Les généticiens quantitatifs utilisent la corrélation génétique pour estimer l'interaction génotype*environnement, ils considèrent qu'un caractère dans deux environnements peut être considéré comme deux caractères et ils calculent une corrélation génétique entre ces deux caractères. Si la corrélation génétique (*r*) est égale à 1 alors il n'y a pas d'interaction génotype*environnement. L'indice *C* est la corrélation génétique moins 1 (*C = 1-r),* varie de manière intuitive : plus *C* est élevé plus le caractère est plastique. Le dernier indice utilisé, *RDPI* (c'est la différence entre individus du même génotype dans des environnements différents divisée par l'une des valeurs phénotypiques), est issu de l'écologie et est sensible à la fois à la variance environnementale et à l'interaction génotype*environnement (Valladares et al., 2006).

3.4 Défi de la mesure de la plasticité phénotypique

La mesure de la plasticité phénotypique est avant tout un défi : (i) expérimentale, il faut disposer de tests de populations-descendances répartis sur l'ensemble de la variance de l'espèce afin d'avoir une bonne image de la plasticité phénotypique et classiquement on obtient une norme de réaction par génotype ou population en fonction (souvent quadratique) d'un paramètre climatique (Rehfeldt et al., 2002). Comme la taille des effectifs nécessaire à ce genre de dispositif est prohibitive, ils ne sont réalisables que pour des caractères faciles à mesurer (liés à la croissance et à la phénologie par exemple), (ii) le second problème est moins essentiel, il est statistique. Les analyses de variances (souvent utilisées dans les analyses de plasticité) reposent sur une hypothèse d'homogénéité des variances des

[8] Il est possible que σ^2_E soit héritable mais non-génétiquement, si par exemple la dissémination est barochorique alors la descendance bénéficiera du même environnement que la mère. Pour une discussion plus avancée sur la notion d'héritabilité non-génétique voir (Danchin & W.H. Wagner, 2010)

différentes modalités au sein d'un facteur. Or, s'il y a plasticité cette hypothèse est systématiquement violée.

L'autre type de problématique que nous détectons dans l'analyse de la plasticité phénotypique (et plus généralement en biologie) est le fait qu'un chiffre ne signifie rien *per se*. Cela est d'autant plus vrai que la plasticité est souvent un terme d'interaction issue d'une analyse de variance plus ou moins obscure. Le terme d'interaction sera rapporté sous forme de probabilité de risque α (*P-value)*, en valeur du test de Fisher (*F-value*), ou dans le meilleur des cas en variance. Les statistiques ne sont pas aussi absolues que les gens[9] le croient. Elles ont, certes, des références internes (les modèles nuls) mais souvent éloignées des objets biologiques qui nous intéressent. Aussi, il est nécessaire d'introduire dans les plans d'expérience des caractères dont on connaît par avance le comportement (plastique ou non plastique) afin de faciliter l'interprétation par une approche comparative.

Dans cette thèse, nous étudierons une partie limitée de la variance totale de l'espèce car nous travaillerons avec au maximum deux tests de population-descendance dotés des mêmes populations et mêmes familles. On parlera de tests de population-descendance jumeaux (TPDJ).

3.5 Le saint Graal en génétique quantitative évolutive.

Le saint Graal en génétique quantitative évolutive est bien sûr de pouvoir faire des inférences rétrospectives de l'action ou la non action de la sélection naturelle sur un caractère. A bien y réfléchir, la sélection naturelle reste une force évolutive assez élusive et peut-être moins courante qu'on ne le croit. En génétique évolutive, une bonne partie de l'effort de recherche est consacrée à la construction de modèles dit nuls, c'est-à-dire que tout y est mis (c'est-à-dire assez peu) sauf la sélection naturelle. Ensuite les données réelles et le modèle nul sont comparés, et si les données réelles sont suffisamment éloignées du modèle nul alors on conclus à l'effet de la sélection naturelle.
Le test classique utilisé pour inférer la sélection naturelle en génétique quantitative (sur espèces non modèles) est la comparaison des valeurs de Q_{ST} et de F_{ST}. Ces deux grandeurs sont des ratios de variances, la variance entre populations divisée par la variance totale (c'est-

[9] les étudiants et moi

à-dire la variance intrapopulation plus la variance interpopulation). Le Q_{ST} est calculé sur les caractères phénotypiques (Spitze, 1993) :

(10) $$Q_{ST} = \frac{\sigma^2_{bp}}{2\sigma^2_A + \sigma^2_{bp}}$$

Avec σ^2_A la variance additive (le facteur 2 est pour les organismes diploïdes), et σ^2_{bp} la variance interpopulation. Le F_{ST} est calculé sur des caractères moléculaires que l'on suppose neutres (n'étant pas la cible directe de la sélection naturelle) par exemple les fréquences alléliques de microsatellites (Michalakis & Excoffier, 1996; Weir & Hill, 2002).

(11) $$F_{ST} = \frac{\sigma^2_{ap}}{\sigma^2_{ip} + \sigma^2_{ap}}$$

Avec σ^2_{ip} la variance intrapopulation, σ^2_{ap} la variance interpopulation[10].

Si les gènes sous-jacents ont un déterminisme purement additif (Goudet & Buchi, 2006; Santure & J. Wang, 2009) et que le caractère phénotypique est sélectivement neutre alors $Q_{ST} = F_{ST}$. Le voila notre modèle nul, c'est le F_{ST} calculé sur les marqueurs neutres. Il n'est pas simulé mais mesuré et donc il faut y associer un intervalle de confiance. La construction de cet intervalle de confiance n'est pas simple, car il y a une erreur due à l'échantillonnage (les populations choisies) et due à la stochastique (dérive génétique et démographie de l'espèce). Les méthodes choisies dans ce travail passent par un double reéchantillonnage (*bootstrap*) : un premier reéchantillonnage non-paramétrique entre les locus suivi d'un second paramétrique en utilisant une distribution de Lewontin-Krahauer (Lewontin & Krakauer, 1973; Whitlock, 2008). Cette distribution permet de modéliser la dérive génétique et les effets dus à la démographie des populations (Figure 15).

De l'autre côté, Q_{ST} est aussi une mesure, elle doit être assortie d'un intervalle de confiance. A la lumière des travaux de O'Hara & Merilä, (2005), nous avons opté pour un reéchantillonnage paramétrique en utilisant la distribution de Satterthwhaite (Satterthwaite, 1946). La comparaison entre ces deux distributions Q_{ST}^* et F_{ST}^*, s'appuie alors, sur un test non paramétrique de comparaison des quantiles 2.5 et 97.5 (Kosorok, 1999), nous fournissons aussi l'intégration de la distribution de Q_{ST}^*-F_{ST} de part et d'autre de zéro (Figure 15).

[10] C'est intentionnellement que je n'ai pas utilisé des symboles identiques pour la variance inter et intra population car elle est calculé sur des objets différents : caractère phénotypique contre marqueurs moléculaires.

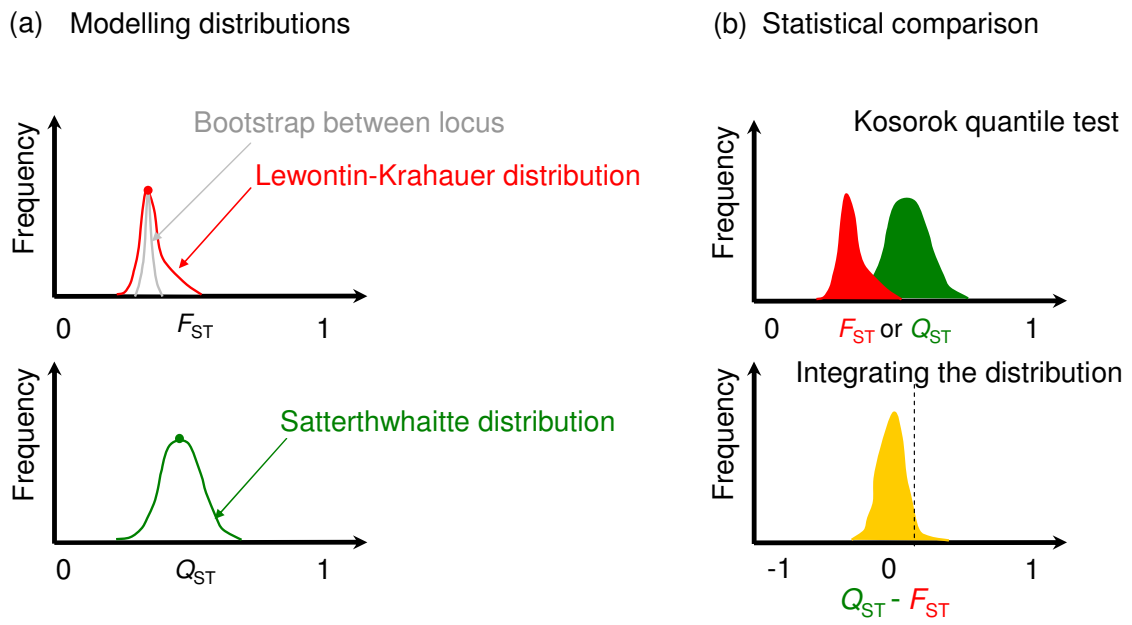

Figure 15: méthodologie de la construction d'intervalles de confiance et de la comparaison de Q_{ST} et F_{ST}. (a) Construction des intervalles de confiance pour le F_{ST} en utilisant un double reéchantillonnage. En gris bootstrap non paramétrique entre locus, en rouge bootstrap paramétrique basé sur une distribution de Lewontin-Krahauer. Le Point en rouge représente la valeur de F_{ST} mesurée sur les locus neutres utilisés. En vert est symbolisée la distribution construite par un bootstrap paramétrique en utilisant la distribution de Satterthwhaitte, le point en vert est la mesure de Q_{ST}. (b) Les deux distributions sont comparées à l'aide d'un test de Kosorok. Une autre statistique est fournie, il s'agit de l'intégration de la distribution en jaune de part et d'autre de zéro. Cette distribution est la différence entre la distribution du Q_{ST}^* et du F_{ST}^*.

La comparaison entre Q_{ST}^* et F_{ST}^* amène à trois cas, un premier cas où $Q_{ST} = F_{ST}$, c'est-à-dire que la variance entre les populations pour le caractère phénotypique étudié est du même ordre de grandeur que celle observée pour les marqueurs moléculaires neutres. Ensuite vient le cas où la variance entre les populations est plus grande que celle observée pour les marqueurs neutres (estimateur de l'effet de la dérive génétique). Classiquement quand $Q_{ST} > F_{ST}$, nous en déduisons que les populations sont sous sélection dite diversifiante, c'est-à-dire que les optimums de sélection sont différents dans chacune des populations. Cette inférence semble robuste même si les gènes sous-jacents ont un déterminisme génétique non additif. Enfin vient le cas ou $Q_{ST} < F_{ST}$, en théorie, cette situation est possible lorsque la sélection est dite uniformisante, c'est-à-dire que les populations ont le même optimum de sélection.

La comparaison entre Q_{ST} et F_{ST} présent beaucoup de limitations : (i) limites expérimentales : estimer un Q_{ST} nécessite 20 populations au moins avec une dizaine de famille, comprenant elles-mêmes un minimum de 5 descendants (soit 1000 individus). La mesure du F_{ST} a des

exigences d'échantillonnage moins fortes (30 individus par population et une dizaine de locus polymorphes semblent suffire). En revanche, il semblerait que les microsatellites ne soient pas les marqueurs idéaux en raison de leurs taux de mutations probablement trop élevés par rapport aux taux de mutations des gènes sous-jacents aux caractères quantitatifs (Kronholm et al., 2010; Meirmans & Philip, 2011; Whitlock, 2011; Edelaar & Björklund, 2011; Edelaar et al., 2011). Ces auteurs recommandent donc de travailler avec des SNP (*single nucléotide polymorphism*). (ii) limites théoriques : il est certain qu'un Q_{ST} contient beaucoup plus d'informations qu'un F_{ST} calculé sur 10 locus. Il est avéré que l'architecture génétique (le nombre de gènes, le déséquilibre d'association entre les effets alléliques, présence d'épistasie) a un impact décisif sur le Q_{ST}. Il existe des situations de découplage entre le Q_{ST} et le F_{ST} bien documentées par Le Corre & Kremer, (2003) et Kremer & Le Corre, (2011). Ces situations apparaissent quand la covariance (négative comme positive) entre effets alléliques est favorisée (combinaison favorable d'allèles) plutôt que le résultat du changement des fréquences alléliques.

3.6 Phénomique et la plus grande essoreuse au monde

Le génotypage est de moins en moins un obstacle technique en génétique, à tel point que les scientifiques peinent à suivre la cadence. A titre d'exemple, chez une espèce non modèle comme *Pinus pinaster*, des puces de génotypage de plusieurs milliers de polymorphismes ont été mises au point et utilisées dans des programmes de recherche (Chancerel et al., 2011). Le phénotypage est désormais le principal frein à l'exploration des facteurs moléculaires sous-jacents à la variance phénotypique[11] (Houle, 2010; Houle et al., 2010). La mesure de la résistance à la cavitation n'échappe pas à cette règle. Aussi nous avons opté pour l'utilisation du Cavitron (Cochard, 2002a; Cochard et al., 2005). Utilisée rigoureusement (Beikircher et al 2010) c'est une méthode fiable pour la mesure de la vulnérabilité à la cavitation chez les conifères. Elle a permis d'augmenter le débit de phénotypage de façon considérable par rapport à d'autres méthodes traditionnelles (Sperry & Donnelly, 1988). Le Cavitron est constitué d'une centrifugeuse[12] modifiée avec un système hydraulique qui permet de mesurer une conductivité. Un segment de branche parfaitement hydraté est centré sur un plateau spécialement conçu au laboratoire (Precis 2000, Bordeaux, France). La vitesse de rotation

[11] Je cite pour le plaisir, une revue intitulée « Dénombrer les cheveux des nos têtes : Défis et promesses de la phénomique »
[12] D'où le titre, la plus grande essoreuse au monde, car nous essorons littéralement les branches à plus de 10000 tours par minute.

engendre des forces centrifuges qui génèrent des tensions (pressions négatives) dans le

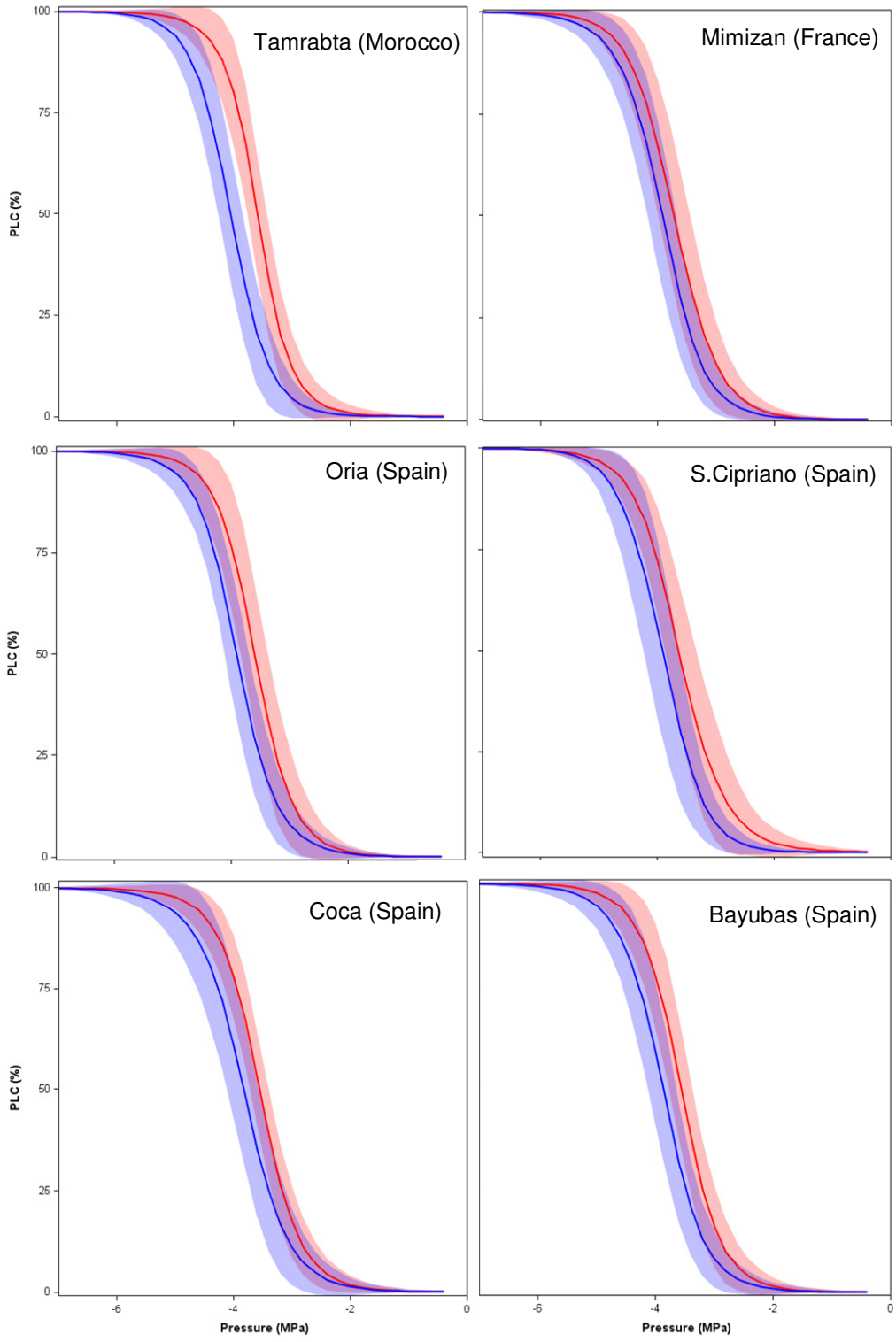

Figure 16 : Courbe de vulnérabilité moyenne pour chacune des 6 populations dans deux sites. En rouge, le site sec et en bleu le site humide (n =33 et 40 respectivement). Le trait plein représente la moyenne et la bande colorée représente l'écart-type par rapport à la moyenne.

segment, simulant ainsi l'effet d'une sécheresse sur le xylème. En parallèle, un circuit hydraulique permet la mesure de la conductivité hydraulique pendant la rotation du segment et de suivre l'évolution de cette conductivité lorsque la vitesse de rotation augmente (des tensions croissantes). La résistance à la cavitation est alors dérivée de la variation de perte de conductance hydraulique d'une branche soumise à une tension croissante (Figure 16). Cette relation est appelée la « courbe de vulnérabilité ». Chaque courbe de vulnérabilité nécessite plus de 30 mesures de conductances hydrauliques, sur lesquelles on ajuste le modèle suivant (Pammenter & Vander Willigen, 1998) :

$$PLC = \frac{100}{1 + e^{\frac{S_{50}^{xylem}}{25}\left(P - P_{50}^{xylem}\right)}}$$

Où *PLC*, est la perte de conductance hydraulique de la branche mesurée (%) et *P* la tension qu'exerce le Cavitron (MPa) au centre du segment. L'attrait principal de ce modèle est que ces 2 paramètres ont des significations biologiques: P_{50}, l'abscisse du point d'inflexion de la courbe, correspondant à la valeur de tension pour laquelle la branche a perdue 50% de sa conductivité initiale ; S_{50} la pente d'une tangente au point d'inflexion (P_{50}) mesure la vitesse à laquelle la cavitation progresse dans la branche (% MPa^{-1}). Ainsi, en début thèse, j'ai participé à la mise en place du *Cavitplace* qui fait partie du réseau de « Phénotypage haut débit en écophysiologie » (http://sylvain-delzon.com/caviplace/cavit-place et http://herve.cochard.free.fr/Techniques.htm)

3.7 Echantillonner la variance d'une espèce : *Pinus pinaster*

Pinus pinaster est l'espèce utiliser de cette thèse, elle a été choisie pour l'importance des ressources en terme de dispositifs expérimentaux (test de population-descendance (TPD), test de descendance), des données génétiques (marqueurs neutres, cartes génétiques), pour l'intérêt économique dans la sylviculture du bassin méditerranéen et à cause de l'extension future de son bioclimat en France (Badeau & Dupouey, 2004). Cette espèce a une aire de distribution discontinue (isolation génétique des populations élevées $F_{ST} = 0.1$) qui s'étend du moyen atlas marocain jusqu'à la pointe de la Bretagne (Hamrick, 2004). Il pousse donc dans des endroits contrastés en terme climatique.

Pour les raisons évoquées auparavant le phénotypage de la résistance à la cavitation reste limité, nous avons choisi de maximiser la variation climatique et évolutive de l'espèce dans l'échantillonnage des populations. En croisant les données géographiques (extractions des

cordonnées spatiales de l'ensemble (769) des populations uniformément réparties sur l'aire de distribution) et les données climatiques associées, nous avons représenté l'enveloppe bioclimatique de *Pinus pinaster* grâce à une analyse en composante principale (ACP). Comme la Figure 17 l'indique, les deux premiers axes (PC1 : 47% et PC2 :23%) expliquent 70% de la variance totale, le premier axe est corrélé avec le déficit hydrique et l'évapotranspiration, et anti-corrélé avec le nombre de jours de pluie et le vent, il servira d'indice d'aridité. Le second axe est plutôt corrélé aux températures (maximum, minimum, moyenne) et au contenu en vapeur d'eau de l'air, et anti-corrélé avec l'amplitude thermique journalière, c'est un axe décrivant la continentalité. Le gradient de couleur provient d'une analyse de densité non paramétrique (*kernel density analysis*). Cette analyse permet de savoir dans quelle partie de la niche bioclimatique (espace bidimensionnel décrit par l'ACP) les populations se trouvent en majorité. On repère deux groupes (tache rouge), l'une rassemblant des populations issues du Nord de l'aire de répartition recevant beaucoup de pluie (Espagne du Nord et la côte Française atlantique) et un autre groupe composé de populations plus continentales souvent plus arides (Centre et Sud de l'Espagne avec les populations du Moyen Atlas marocain). Nous avons sélectionné 6 populations présentes dans deux TPDs [13] et couvrant toute la variation de l'axe 1.

[13] Je rappelle que TDP veut dire test de population-descendance.

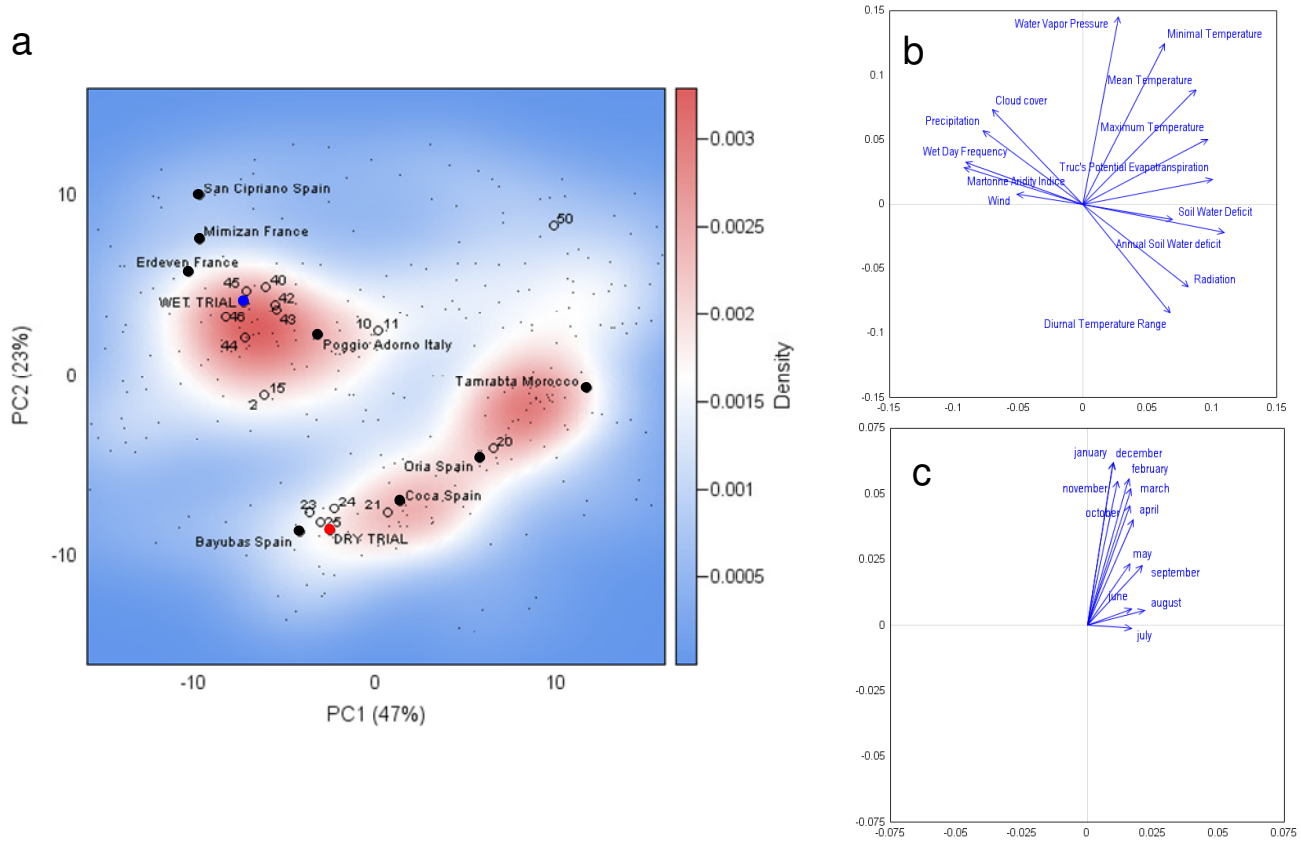

Figure 17 : Analyse en composantes principales (ACP) sur 769 populations x 168 variables climatiques mensuelles. (a) Premier plan (*PC1, PC2*) avec en superposition un gradient de couleur indiquant la probabilité de trouver une population de *Pinus pinaster* (petit points noirs) dans l'enveloppe climatique (plan décrit par les deux axes). Le rouge et le bleu représentant la haute et faible probabilité de trouver une population de *Pinus pinaster* vivant dans le bioclimat décrit par la composante principale (CP en français) 1 et 2 de la ACP. CP1 et CP2 représentant 47% et 23% respectivement de la variance totale. CP1 peut être interprété comme un indice d'aridité et CP2 comme un indice de continentalité.

- **Les cercles correspondent aux populations suivies pour la hauteur des arbres dans les tests de population-descendances jumeaux (TDPJ): #2: Restonica, Corse; #10: Aullène, Corse; #11: Pineta, Corse; #15: Pinia, Corse; #21: Arenas de San Pedro, Espagne; #23: Cuellar, Espagne; #24: Valdemaqueda, Espagne; #25: San Leonardo de Yagüe, Espagne; #40: Petrock, France ; #42: Hourtin, France; #43: Le Verdon, France; #44: Olonne sur mer, France; #45: Saint Jean de Monts, France; #46: Pleucadec, France; #50, Tabarka, Tunisie.**
- **Les points noirs légendés en minuscule correspondent (i) aux populations suivies pour la résistance à la cavitation et la hauteurs dans les TDPJ et (ii) aux populations naturelles *in situ*.**
- **Les points de couleurs sont les TDPJ, rouge pour le test de population-descendance (TDP) « sec » (Calcena, Espagne) et bleu pour le TDP « humide » (Pierroton, France). Pour plus de renseignements sur les variables climatiques et leur source voir les annexes. A cause du nombre de variables important (168), nous proposons deux cercles de corrélations, (b) montre les vecteurs propres moyennés pour chaque variables climatiques et (c) illustre les vecteurs propres moyennés pour chaque mois.**

3.8 Dispositif expérimental : Tests de populations-descendances jumeaux (TPDJ) et population naturelles in situ

Comme l'indique la Figure 17, les TPDJ sont situés dans des zones différentes du bioclimat de *Pinus pinaster*. Le TPD Espagnol (point rouge, Figure 17) a un indice d'aridité (coordonnées du premier axe, -7.3) plus élevé que le TPD Français (-2.5), cependant, il faut noter que la différence entre les deux TPD est plus importante sur le second axe de l'ACP (-8.5 versus 4.1 respectivement). En conséquence, la comparaison entre les deux TPDs n'explorera qu'une partie de la plasticité du caractère au sein de l'espèce. Chacune des populations sélectionnées pour la P_{50} sera, aussi, échantillonnée directement sur le terrain, en populations naturelles.

Au delà de la résistance à la cavitation (P_{50}), plusieurs caractères ont été mesurés, notamment des caractères liées à la croissance, à la composition isotopique en carbone des aiguilles et à la densité du bois (Table 2). Les caractères liés à la croissance ont été très étudiés dans la littérature, et leurs patrons de variation sont bien connus. Ils serviront de reference pour les caractères moins connus comme P_{50}.

Table 2 : Bilan des caractères disponibles et le nombre populations en fonction des TPD et de la campagne d'échantillonnage *in situ*.

traits	unit	Wet trial	Dry trial	*in situ*	N. of pop
h	cm	yes	yes	yes	24-6[a]
P_{50}	MPa	yes	yes	yes	6
D_{mean}	g cm^{-3}	yes	no	no	6
$\varnothing_{2007}$	mm	yes	no	no	6
B_{tot}	g	yes	no	no	6
A_{Leaf}	m^2	yes	no	no	6
A_L/A_S	m^{2}cm^{-2}	yes	no	no	6
$\delta^{13}C$	‰	yes	no	no	6
Δ_h	cm	yes	no	no	6

[a]Le premier chiffre indique le nombre de populations phenotypée en TPD et le deuxième chiffre indique le nombre de populations phénotypé in situ.

3.9 Méthodologie pour quantifier les mécanismes impliqués dans la variance phénotypique.

Cette partie sera articulée autour de la formule suivante $\sigma_P^2 = \sigma_G^2 + \sigma_E^2 + \sigma_{GE}^2 + \sigma_\varepsilon^2$. Cette formule lie la variance phénotypique à des variances causales :

- σ_P^2 est la variance phénotypique, estimée à partir des mesures de caractères (résistance à la cavitation et croissance en hauteur) en retranchant les effets dus a l'environnement expérimental (dispositif en bloc). Dans notre cas, il y aura, un $\sigma_{P\_in\_situ}^2$ (associé à $CV_P^{in-situ}$) calculé sur les populations *in situ*. C'est la somme des variances génétiques, des variances macroenvironnementales, microenvironnementales et des interactions résultantes. Il s'agit de l'estimateur le plus grossier de la variance intraspécifique. Il y aura également un $\sigma_{P\_ppt}^2$ (associé à CV_P^{tpd}) calculé sur les populations en TPD. C'est la somme des variances génétiques, microenvironnementales et des interactions respectives. C'est un estimateur plus fin de la variance intraspécifique, débarrassé des effets macroenvironnementaux qui sont souvent importants.
- σ_G^2 est la variance génétique estimée à partir des mesures de caractères réalisés dans les deux tests de populations-descendances (TDP), et comme ces tests sont hiérarchisés [14], ils permettent de décomposer la variance génétique en deux composantes ($\sigma_G^2 = \sigma_{bp}^2 + \sigma_{f(pop)}^2$) la variance génétique entre les populations (σ_{bp}^2, estimée à partir des performances des populations) et la variance génétique à l'intérieur des populations (ou entre les familles, $\sigma_{f(pop)}^2$, estimée à partir des performances des familles de chacune des populations). Dans le cas présent, nous disposons de deux tests de populations-descendances jumeaux (TDPJ) disposés dans deux sites différents, nous aurons donc deux estimations de σ_{bp}^2 et $\sigma_{f(pop)}^2$ indépendantes dans deux macroenvrionnements différents.
- σ_E^2 est la variance macroenvironnementale, le seul moyen de l'estimer dans notre cas est de soustraire les moyennes pour un même caractère entre les deux TDP. Un test situé dans le Sud-Ouest de la France[15] (Cestas, Aquitaine) sera considéré comme le

[14] Un TDP est un test de population-descendance, cela signifie qu'il est composé de *n* population dans laquelle il y a, emboîtée, *m* familles. Les familles sont dites emboîtées dans les populations car la famille1 de la population 1 n'existe pas dans la population 2. On écrira famille emboîtée dans la population : *f(pop)*.

[15] Le plus beau coin de France, *Lou pais de fetjat…* et pour se faire plaisir, un proverbe graveleux *: Tala testo, talas ancas.* Celui qui trouve la traduction, qu'il me l'envoie à jblamy@free.fr et la récompense est prévue (rien que pour le mérite d'avoir lu la thèse jusqu'ici et d'avoir fait l'effort de chercher la traduction). Relecteurs officiels exclus de fait de cette compétition.

test « humide », l'autre test situé dans le centre de l'Espagne (Calcena, Argon) sera par conséquent le test « sec » (voir Table 3 et Figure 18).

- σ^2_{GE} est la comparaison entre les TDP des différences de performances entre les populations ou les familles. La somme des deux termes ($\sigma^2_E + \sigma^2_{GE}$) est définie comme la plasticité phénotypique (σ^2_{PP}).
- σ^2_ε est la variance résiduelle que l'on peut interpréter comme une variance microenvironnementale lorsqu'elle est calculée sur un TPD.

L'ensemble de ces variances sera estimé statistiquement grâce à des modèles mixtes dont le détail est décrit dans les annexes.

3.10 Hypothèses de travail

Notre échantillonnage maximise la variance attendue et compte tenu des arguments développés en introduction sur l'importance du caractère en physiologie et sa variation interspécifique, nous prévoyons que : (i) la variance phénotypique pour la résistance à la cavitation sera importante (ii) et corrélée l'axe 1 de l'ACP (variation clinale, i.e. plus l'aridité augmente plus la résistance à la cavitation augmente), (iii) une part importante de la variance génétique sera due à la variance entre les populations, (iv) résultant d'une sélection diversifiante entre les populations.

Table 3 : Coordonnées géographiques, variables climatiques (et pédologiques), altitude des populations de *Pinus pinaster*, ainsi que des tests de populations-descendances.

Populations	Longitude (°)	Latitude (°)	*n*	Elevation (m)	P_i (mm)	T_m (°C)	VPD_{max} (hPa)	*ETP* (mm)	*Mito*	*Chloro*
Bayubas de Abajo (Spain)	-2.87	41.52	37- 182	955	561	10.5	11.42	882.9	*W*	a
Coca (Spain)	-4.08	41.37	37- 122	788	452	11.9	14.23	718.7	*W*	a
Mimizan (France)	-1.30	44.13	38- 154.5	37	1176	13.2	7.26	751.59	*W*	a
Oria (Spain)	-2.62	37.87	32- 155.5	1232	451	13.4	14.29	922.59	*W*	j
San Cipriano (Spain)	-8.70	42.13	35- 114	310	1625	13.8	8.54	721.91	*W*	g
Tamrabta (Morocco)	-5.02	33.66	38- 113	1760	550	15.1	18.56	976.54	*M*	k

Trials	Longitude (°)	Latitude (°)	*n*	Elevation (m)	P_i (mm)	T_m (°C)	VPD_{max} (hPa)	*ETP* (mm)	Soil
Dry, Calcena (Spain)	-1.72	41.62	196-1857	997	452	11.1	11.1	778.2	Shaly sandstone
Wet, Cestas (France)	-0.78	44.74	240-5569	61	800	12.7	6.70	743.8	Sandy podzol

N, nombre d'individus (moyenné sur les TPDs) échantillonnés pour la résistance à la cavitation et la croissance respectivement dans l'ensemble du dispositif; Pi , moyenne annuelle des précipitations; Tm, moyenne annuelle des températures atmosphériques ; VPDmax, maximum du déficit en vapeur d'eau de l'air (en Juillet pour toutes les populations); ETP, évapotranspiration potentielle annuelle cumulée. Mito : W pour mitotype caractérisant des populations de l'ouest européen, M pour mitotype caractérisant des populations africaines seulement ; Chloro, seules sont reportées les plus majoritaires, voir Burban & Petit, (2003).

3.11 Quantifier la variance phénotypique : populations naturelles *in situ*

Pour la resistance à la cavitation, les coefficients de variation phénotypiques pour les populations naturelles *in situ* ($CV_P^{in-situ}$) sont de même ordre de grandeur que les coefficient de variation phénotypique en TPD (CV_P^{tpd}), 6.97 versus 6.5 (moyennée sur les deux TPDs). La plasticité phénotypique est probablement faible pour ce caractère. En revanche, pour *h*, nous trouvons 47.2 versus 28, ce qui annonce que la croissance est probablement très plastique.

3.12 Quantifier la variance génotypique : Variance interpopulation, test de population

La variance génétique σ_G^2 peut être décomposée en variance génétique entre les populations (σ_{bp}^2) et en variance génétique à l'intérieur des populations ($\sigma_{f(pop)}^2$). Arrêtons-nous un instant sur la significativité biologique de σ_{bp}^2, la seule variance qui nous intéressera dans ce paragraphe. L'évolution est faite de phénomènes aléatoires (dérive génétique) ou déterministes (sélection naturelle) et les populations sont l'unité fondamentale d'une espèce[16], donc on considère que chaque population est une expérience[17] indépendante de l'évolution de l'espèce. En d'autres termes, au cours de l'évolution, la moyenne pour un caractère donné, dans une population donnée va varier de manière plus ou moins aléatoire au cours du temps et indépendamment de ce qui se passe dans une population lointaine. C'est la variance entre les moyennes de plusieurs populations (σ_{bp}^2) qui va renseigner sur l'importance des processus déterminismes versus stochastiques.

La contribution relative de σ_{bp}^2 à la variance totale (Table 4) est supérieure pour *h* que pour la P_{50}, 8.07 versus 0.86 % respectivement. Ainsi il n'y a pas de différences entre les populations pour la P_{50}. Une autre manière de mesurer la différence entre les populations est d'utiliser le

[16] C'est pour cela qu'on parle de génétique des populations plutôt que de génétique des individus.
[17] Je pourrais écrire réalisation, répétition au sens statistique du terme.

Q_{ST} qui est un ratio de la variance entre les populations divisé par la variance génétique totale ($\frac{\sigma^2_{pop}}{\sigma^2_{pop} + 2\sigma^2_A}$) ainsi *h* a un Q_{ST} plus élevé que la P_{50} (Q_{ST} moyen : 0.23 vs. 0.02).

Les caractères liés à la croissance ont des Q_{ST} élevés, diamètre au collet ($ø_{2007}$), la surface des feuilles (A_{leaf}) et l'accroissement moyen en hauteur (Δ_h). La littérature fourmille de résultats identiques pour des caractères liés à la croissance (Yang et al., 1996; Navarro et al., 2005; Steane et al., 2006; Tripiana et al., 2007; Ramirez-Valiente et al., 2010). De manière opposée, il existe des caractères avec des Q_{ST} faible proches de ceux mesurés pour P_{50} tels que densité moyenne du bois, densité minimale, densité maximale (D_{mean}, D_{min} et D_{max}). Ce type de patron est rare dans littérature, d'ailleurs Leinonen et al., (2008) suspecte un biais de publication. Néanmoins, il existe quelques publications (Lee & Frost, 2002; Edmands & Harrison, 2003; E Chapuis et al., 2007; Elodie Chapuis et al., 2008; Yoshida et al., 2008; Chun et al., 2009; Scheepens et al., 2010) qui démontrent l'existence de caractères variant très peu. Les autres caractères ont un comportement intermédiaires entre ces deux extrêmes comme le ratio surface transpirante sur surface conductrice, la biomasse totale et la composition isotopique en carbone des aiguilles (A_L/A_S, B_{tot} et $\delta^{13}C$).

3.13 Quantifier la variance génotypique : Variance intrapopulation, test de population-descendance

La variance à l'intérieur des populations résulte de la variance entre les familles ($\sigma^2_{f(pop)}$) et de la variance résiduelle (σ^2_ε). Pour *h* et P_{50}, la contribution relative, en pourcentage, de $\sigma^2_{f(pop)}$ à la variance totale est sensiblement identique, 10.47% versus 13.91% respectivement (Table 4). Mais ces indices de variances en % cachent une autre réalité biologique, la valeur absolue de la variance entre ces deux caractères est très différente. Raisonnons sur la quantité de variance dite additive (σ^2_A), c'est-à-dire la quantité de variance qui est directement transmise à la descendance et qui est nécessaire à l'évolution par sélection naturelle ou artificielle. Comme la valeur absolue de la variance est exprimée dans l'unité du caractère (la variance est donc corrélée à l'unité), il convient de standardiser les mesures de variance par la moyenne du caractère, on obtient donc un coefficient de variation qui est sans dimension. Ainsi les CV_A de P_{50} montre une valeur bien inférieure au CV_A de *h*, (4.9 contre 13.6), aussi l'évolution de la P_{50} par sélection naturelle ou artificielle sera plus faible.

Les variances estimées permettent aussi de calculer une héritabilité, c'est-à-dire la proportion de variance présente dans une population qui passera dans la génération suivante. Ainsi les caractères liés à l'anatomie du bois (P_{50} et D_{mean}) présentent des héritabilités supérieures aux caractères liés à la croissance (h, $\varnothing_{2007}$ et Δ_h) (cf Table 4). Nos estimations sont cohérentes avec les valeurs d'héritabilités mesurées dans la littérature (Louzada & Fonseca, 2002; Aguiar et al., 2003), malgré le nombre restreint de génotypes pour les caractères liés au bois (Lynch & Walsh, 1998).

Table 4 : Composantes de la variance mesurée en TDP (σ_P^2 , σ_{bp}^2 , σ_A^2 , σ_ε^2), héritabilité (h^2_{ns}±SE), coefficients de variation (CV_P, CV_A, CV_{BP}, CV_R) et différenciation des populations (Q_{ST}).

Site	Traits	σ_P^2	σ_{bp}^2	σ_A^2	σ_ε^2	h^2_{ns}	CV_P	CV_A	CV_{BP}	CV_R	Q_{ST}
Sec	*h*	151.2	8.043	27.13	144.4	0.17 ± 0.07	34.96	14.8	8.0	34.1	0.12
Sec	P_{50}	0.053	0.0004	0.034	0.045	0.61 ± 0.27	6.43	5.06	0.4	5.9	0.005
Humide	*h*	570.8	204.1	190.0	523.3	0.33 ± 0.03	21.7	12.5	13	20.8	0.34
Humide	P_{50}	0.067	0.0027	0.035	0.058	0.51 ± 0.23	6.60	4.75	1	6.1	0.04
Humide	D_{mean}	0.001	$1.9\ 10^{-5}$	$0.5\ 10^{-3}$	0.001	0.38 ± 0.20	10	7	1	10	0.02
Humide	$ø_{2007}$	50.63	31.92	17.55*	46.24	0.34±0.12	37	22	29	36	0.47
Humide	B_{tot}	16124	3246	9207	13822	0.57±0.08	43	32	19	40	0.14
Humide	A_{Leaf}	0.427	0.104	0.1817	0.382	0.425±0.14	37	24	35	35	0.22
Humide	$\delta^{13}C$	0.284	0.030	0.059	0.269	0.213 ± 0.10	1.7[a]	0.8[a]	0.6[a]	1.7[a]	0.19
Humide	Δ_h	112.7	55.0	40.96	102.5	0.363 ± 0.06	26.9	16.2	18.8	25.7	0.18
Humide	A_L/A_S	0.01	0.0008	0.002	0.014	0.38 ± 0.11	26.3	16.2	6.8	25.0	0.08
%	*h*	42.04	8.07	10.47 [c]	39.40	na	na	na	na	na	na
%	P_{50}	25.52	0.86	13.91 [c]	59.69	na	na	na	na	na	na
4											
In situ	*h*	2514	1789	na	724.9	na	47.2		39.8	25.3	na
In situ	P_{50}	0.064	0.010	na	0.053	na	6.97		2.83	9.64	na

Les variances estimées proviennent d'un modèle mixte adapté à chaque TDP (modèle statistique voir en annexe). $\mathbf{h^2_{ns}}$ est l'héritabilité au sens strict (erreur standard). σ_P^2 est la variance phénotypique, σ_{bp}^2 est la variance génétique entre les populations, σ_A^2 est la variance génétique additive ($\sigma_A^2 = 4\sigma_{f(pop)}^2$), σ_ε^2 est la variance résiduelle. CV_P est le coefficient de variance phénotypique après avoir été ajusté aux effets des blocs, CV_{BP} est le coefficient de variation entre les populations, CV_A est le coefficient de variation additif, CV_R est le coefficient de variation résiduelle. Q_{ST} est l'indice de différenciation génétique des populations (Spitze, 1993). "[a]" indique les *CVs* de $\delta^{13}C$ ne peuvent pas être comparés aux autres *CVs* des autres caractères car le standard utilisé pour le $\delta^{13}C$ n'est pas absolu mais relatif (Brendel et al., 2002, 2008). Le clair fond grisé indique la valeur standardisée des variances après les avoir moyennées entre les TDP et les avoir ramenées en %. "[c]" indique que la variance utilisée dans le calcul n'est pas directement la σ_A^2 mais bien $\sigma_{f(pop)}^2$. Le fond grisé foncé indique les valeurs de variance *in situ* issues d'un modèle mixte n'ayant que l'effet population en aléatoire.

3.14 Quantifier la Plasticité phénotypique, tests de populations-descendances jumeaux.

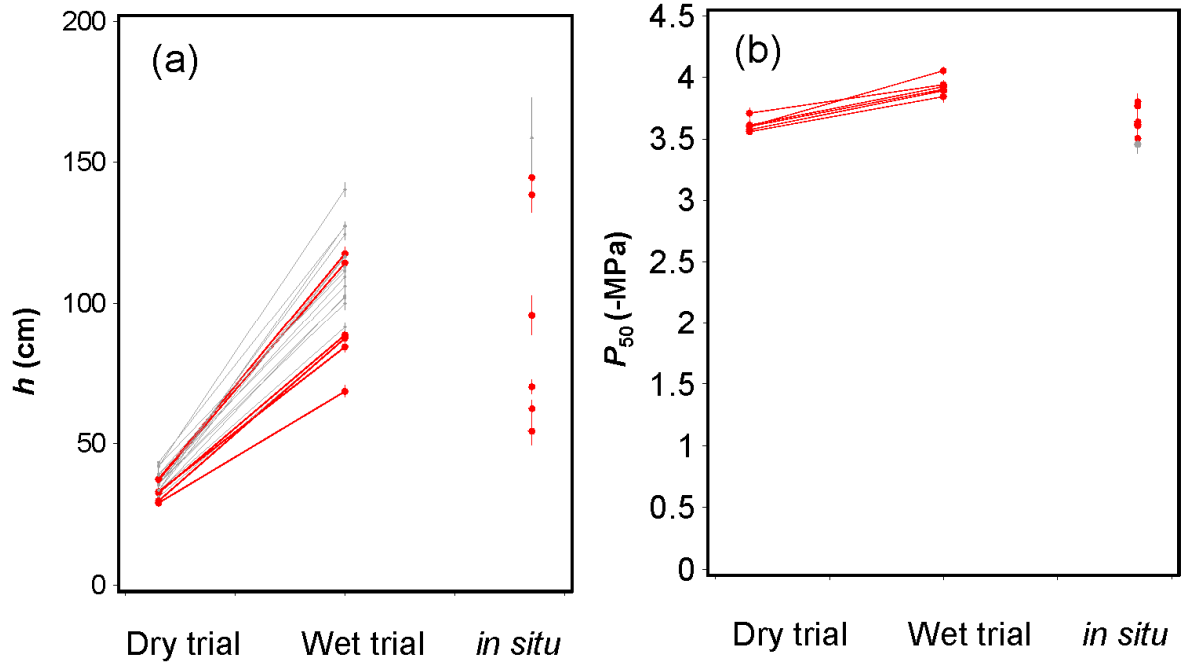

Figure 18 : Moyenne des populations pour (a) la croissance en hauteur à quatre ans (âge cambiale, pour chaque population n= 163 ± 14) (b) la résistance à la cavitation (n= 36 ± 1). Pour les mesures sur populations naturelles *in situ* (n = 11). En rouge les populations sélectionnées, en gris populations supplémentaires présentent dans le jeu de données. Les barres d'erreurs sont les erreurs standard. *Dry trial* : test sec, *Wet trial* : test humide.

La plasticité phénotypique peut se comprendre de manière intuitive avec la Figure 18, par exemple *h* montre une pente importante entre les deux TDP, ce qui suggère une plasticité phénotypique importante. En revanche, la P_{50} présente une pente faible entre les TDP. La plasticité phénotypique ne s'estime jamais graphiquement, mais statistiquement via des analyses de variance.

La plasticité phénotypique peut s'écrire $\sigma^2_{PP} = \sigma^2_E + \sigma^2_{GE}$, le second terme est génétiquement héritable et peut être la cible de la sélection naturelle alors que le premier non. Notre étude permet de décomposer σ^2_{GE} en deux niveaux, un niveau σ^2_{popE} dû à la population, et un niveau σ^2_{fE} dû à la famille. On utilisera trois indices de plasticité phénotypiques : *C, S* et *RDPI* (détail de calcul voir annexe). L'indice *C* est une estimation directe de σ^2_{GE} (Lynch & Walsh, 1998), en revanche *S* estime directement σ^2_{PP} (Scheiner & Lyman, 1989) et pour finir l'indice

RDPI estime lui aussi σ^2_{PP} mais sans passer par une analyse de variances (Valladares et al., 2006), c'est l'indice le plus robuste qui intègre la plasticité au niveau de la famille et de la population. L'interprétation de ces indices est intuitive, plus un indice est élevé, plus le caractère est plastique.

Pour les deux caractères, *h* et P_{50} la contribution de la variance macroenvironnementale (σ^2_E exprimée en %) à la variance totale domine l'ensemble des autres variances (81% pour *h* et 54% pour P_{50}). Pour *h*, la plasticité au niveau de la population est importante alors qu'elle est très faible pour P_{50}. Les deux caractères ont une interaction génotype*environnement due à la famille (σ^2_{fE}) du même ordre de grandeur (Table 4). Sur la base de *RDPI*, nous résumerons en disant que *h* est un caractère bien plus plastique que P_{50}. P_{50} a un *RDPI* parmi les plus faibles croisés dans la littérature, en revanche, la plasticité phénotypique de la croissance a été bien documentée pour *Pinus pinaster* et nos résultats sont cohérents avec ces études (Alia et al., 1995, 1997; Correia et al., 2008; Aranda et al., 2010).

Table 4. Estimateurs de la plasticité phénotypique pour la résistance à la cavitation (P_{50}) et la croissance en hauteur (*h*).

	Population		Famille		Total	
	P_{50}^{xylem}	*h*	P_{50}^{xylem}	*h*	P_{50}^{xylem}	*h*
C	0	0.15	0.88	0.78	na	na
S	0.51	0.90	0.90	0.98	na	na
RDPI	na	na	na	na	0.08	0.65

3.15 Corrélation entre les caractères

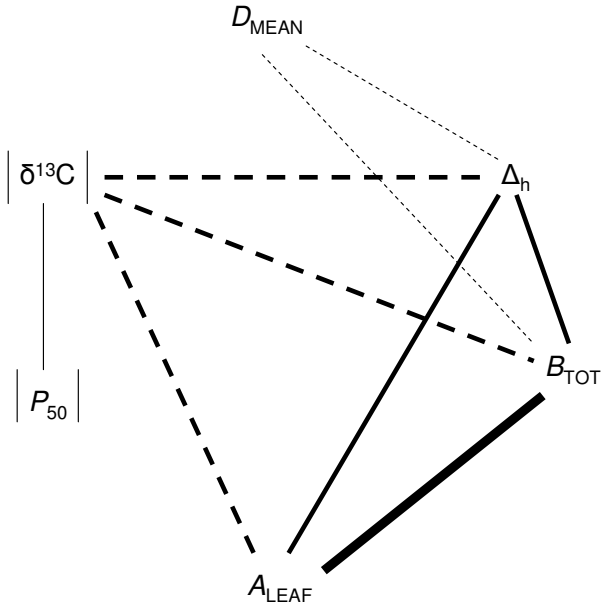

Figure 19 : Structure des corrélations génétiques de Pearson entre caractères (moyennes familiales ajustées aux effets de l'environnement). Les segments en tiré indiquent une corrélation négative entre les caractères alors que les segments pleins indiquent une corrélation positive. P_{50} et δ13C ont été passées en valeur positive. De plus la largeur du segment renseigne sur la *P-value* : 0.05> segment fin > 0.01, 0.01> segment moyen > 0.001, 0.001> segment large, pour chaque corrélation (n=48).

La valeur absolue de P_{50} est corrélée à la valeur absolue $\delta^{13}C$, en d'autres termes, plus un génotype est résistant à la cavitation moins il utilise l'eau de manière efficiente. Ladjal et al., (2007) met en évidence cette même relation chez *Cedrus*. On peut supputer que la sélection naturelle a retenu, en environnement sec, les génotypes allouant plus de carbone à la construction d'un bois plus résistant à la cavitation. Ces génotypes évitent le cercle vicieux de l'embolie en maintenant une conductivité stomatique élevée et une conductance hydraulique à faibles potentiels hydriques foliaires (activité photosynthétique), d'où une diminution de l'efficience d'utilisation de l'eau pour les génotypes issus de régions arides (Guehl et al., 1996; Picon et al., 1996). En revanche, il existe d'autres études où une relation inverse est mise en évidence ou pas de relation du tout (Fichot et al., 2009; Maherali et al., 2009; Martinez-Vilalta et al., 2009).

Ensuite la densité du bois (D_{mean}) est faiblement et négativement corrélée à B_{tot} et à Δ_h. Ainsi plus un génotype croît vite et met de la biomasse en place, moins son bois sera dense en moyenne. De la même façon, plus un génotype croît vite (en terme de hauteur, de biomasse

ou de surface de feuille) plus il sera efficient. Les caractères liés à la croissance sont fortement et positivement corrélés entre eux. La faible corrélation des caractères liés aux propriétés anatomiques du bois (P_{50} et D_{mean}) avec les autres caractères est aussi due à leur faible variance.

3.16 Corrélation avec le climat

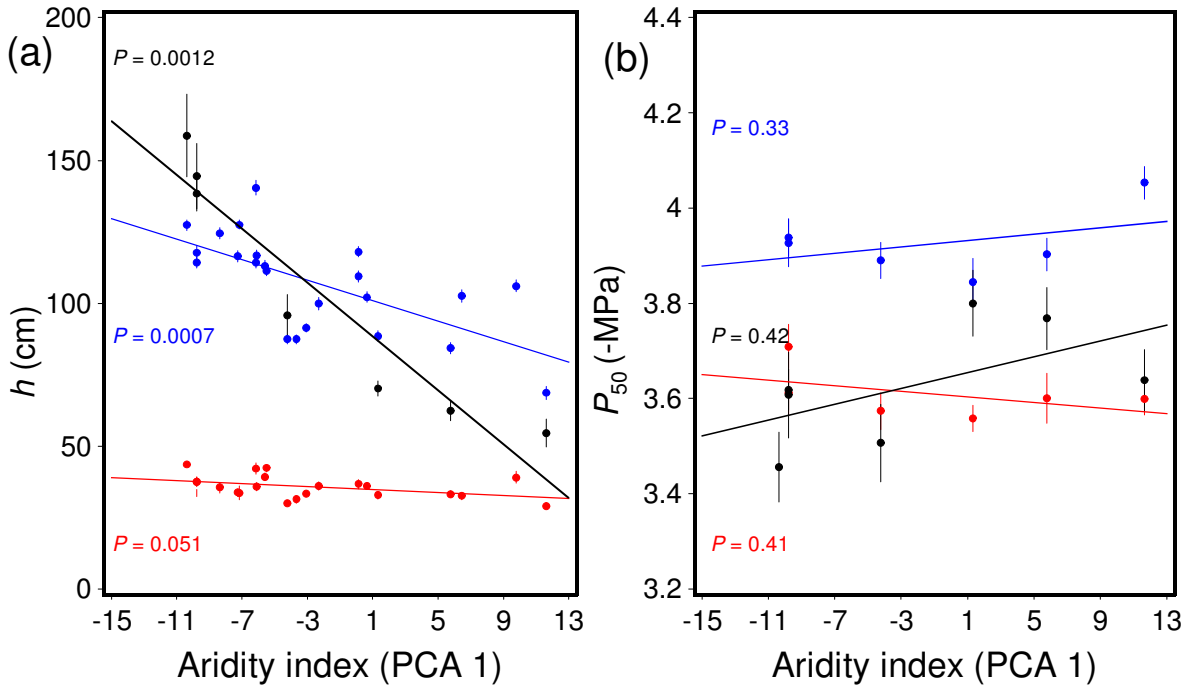

Figure 20 : La valeur moyenne des populations pour (a) *h* et (b) P_{50} en fonction l'indice d'aridité calculé sur les données climatiques de l'aire d'origine des populations. En Bleu valeur mesurée dans le test humide (Cestas, France) et en rouge dans le test sec (Calcena, Espagne) et en noire sur les populations naturelles *in situ*. La *P-value* associée est issue d'une régression linéaire. Les barres d'erreur représentent l'erreur standard.

La croissance en hauteur (*h*) des populations varie de manière clinale avec l'aridité du climat d'origine dans les deux tests de populations-descendances (Figure 20). En revanche, la variation clinale est amoindrie dans le test sec ce qui signifie qu'il y a de la plasticité phénotypique. On ne détecte pas de variation significative clinale de la P_{50} au climat dans les deux TPDs. De plus suivant le test de population, la pente de la régression change. D'autres auteurs ont déjà observé des variations contre-clinale de la P_{50} par rapport au climat d'origine (Martinez-Vilalta et al., 2009; Herbette et al., 2010; Corcuera et al., 2011). Les auteurs des articles sus-cités invoquent une batterie d'hypothèses : (i) utilisation de variables climatiques liées à la sécheresse, or il existe de la cavitation liée à des gels hivernaux. Cette hypothèse

nous paraît peu crédible car *Pinus pinaster* vit dans des environnements peu soumis au gel et les conifères sont protégés du gel grâce au faible diamètre des trachéides (Hacke & Sperry, 2001; Pittermann & Sperry, 2003) (ii) Les variables climatiques utilisées caractérisent le compartiment atmosphérique et non le sol qui est déterminant lors d'une sécheresse. Cependant les variables climatiques utilisées sont moyennées sur 30 ans, nous ne pensons pas que la dynamique hydrique du sol a une inertie qui dépasse ces 30 ans. Pour nous, les relations complexes entre la P_{50} et le climat sont avant tout dues à la faible variance entre les populations.

3.17 Inférences évolutives

La variance entre les populations (Q_{ST}) pour un caractère phénotypique a été comparée à la variance (entre les populations) des fréquences alléliques des marqueurs neutres (F_{ST}). Pour *h*, dans les deux TPD, la variance observée entre les populations est toujours plus élevée que la variance attendue sous l'effet de la dérive ($Q_{ST} > F_{ST}$). Ce signal est moins fort dans le TPD sec à cause de la forte plasticité phénotypique de ce caractère à l'échelle de la population. Ce patron de variation peut être interprété comme une trace de sélection diversifiante, c'est-à-dire que des populations ont des optimums de sélection différents et la variance de ces optimums est plus grande que la variance neutre.

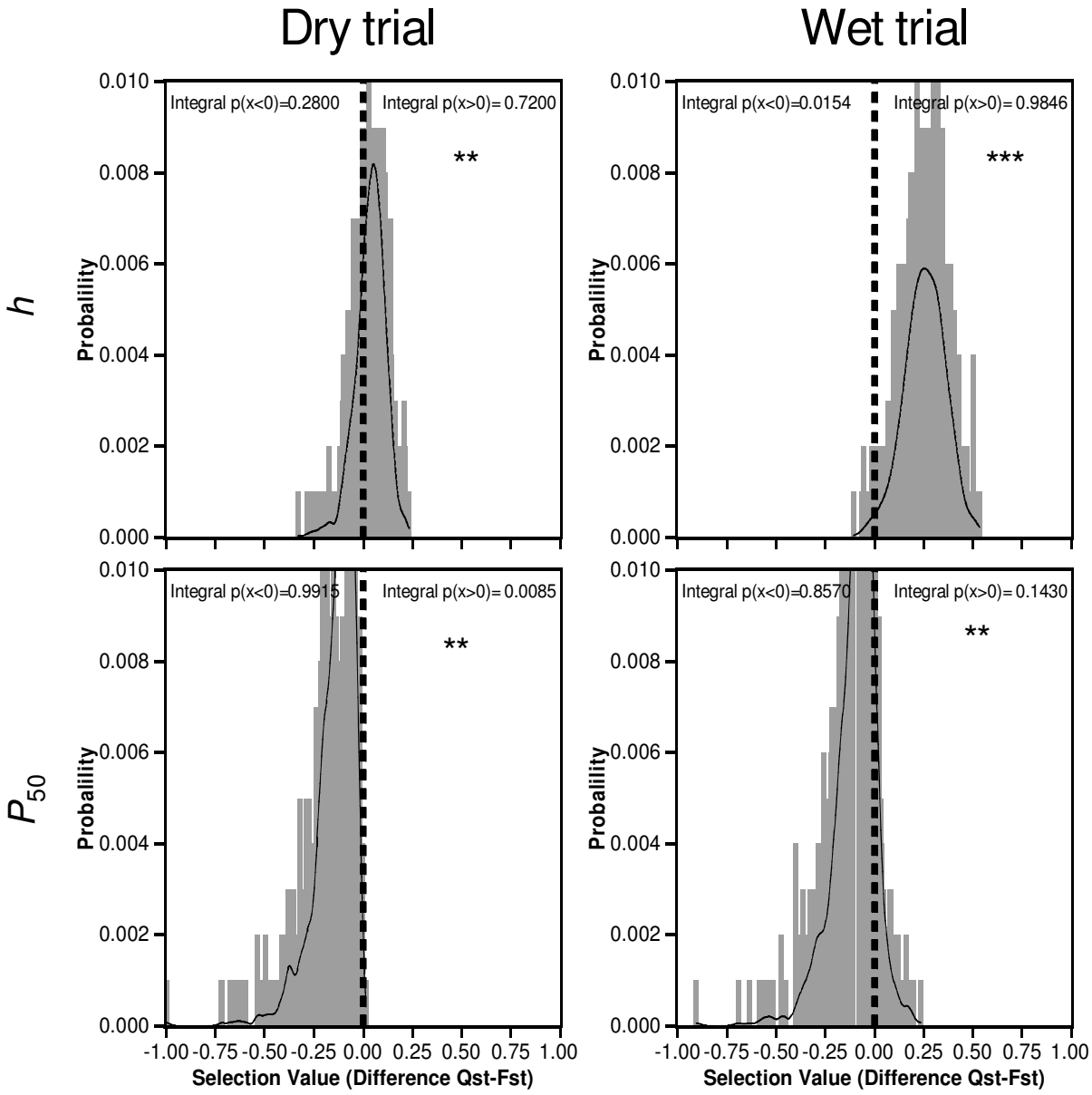

Figure 21 : Distribution de la différence Q_{ST}-F_{ST} pour *h* et P_{50}^{xylem} dans chacun des TPD. Une distribution centrée sur zéro montre que le Q_{ST} et le F_{ST} ne sont pas différents l'un de l'autre. Une distribution intégralement répartie entre 0 et 1 signifie que le Q_{ST} est plus grand que le F_{ST}, une distribution intégralement répartie entre -1 et 0 signifie que le Q_{ST} est plus petit que le F_{ST}. Les étoiles correspondent à la significativité du test de Kosorok sur les quantiles 2.5 et 97.5 (Kosorok, 1999). « ns » ***P-value* > 0.05,** « * » **0.05> *P-value*>0.01,** « ** » **0.01> *P-value*>0.001,** « *** » **0.0001> *P-value*.**

Pour P_{50}, on observe aussi le même signal dans les TPD, à savoir que la variance observée entre les populations (Q_{ST}) est moins importante que celle attendue sous le modèle nul (F_{ST}). Classiquement ce patron de variation est interprété comme de la sélection uniformisante, c'est-à-dire que les populations ont le même optimum de sélection, bien qu'elles proviennent

des zones climatiques contrastées, les populations ont convergées vers la même valeur de caractère (Figure 21). Cette inférence n'est pas aussi facile à démontrer que la précédente, et ce pour plusieurs raisons : (i) il existe des cas particuliers où l'isolation des populations associées à de faibles tailles effectives (d'un point de vue de la reproduction) induit une variance neutre importante qui sera supérieure à la variance des optimum de sélections pour les caractères phénotypiques. Il est donc possible d'avoir des cas, où $Q_{ST} < F_{ST}$ même si le caractère est sous (faible) sélection divergente (Le Corre & Kremer, 2003, 2012; Kremer & Le Corre, 2011). (ii) Dans ces comparaisons Q_{ST} et F_{ST}, il est supposé que les gènes codant pour un caractères phénotypique ont un comportement additif, c'est-à-dire qu'en faisant simplement la somme des effets des gènes (sur le caractère phénotypique), on obtient la valeur du caractère réellement mesuré. Or il est fortement probable que la plupart des gènes aient des comportements non additifs. Plusieurs auteurs ont modélisé (et dérivé analytiquement) les effets de relations de dominance entre deux allèles d'un même locus (Lopez-Fanjul et al., 2003; Goudet & Buchi, 2006; Goudet & G. Martin, 2007; Miller et al., 2008; Santure & J. Wang, 2009), et montrent qu'en moyenne $Q_{ST} < F_{ST}$ sauf pour certaines fréquences alléliques et selon certains modèles démographiques. De la même façon, les relations épistatiques (interaction des allèles à différents locus) montrent qu'en moyenne $Q_{ST} < F_{ST}$ (Whitlock, 1999; Lopez-Fanjul et al., 2003). L'architecture génétique aurait un rôle important dans les cas où $Q_{ST} < F_{ST}$, et elle pourrait mimer les effets de la sélection uniformisante. (iii) L'hypothèse de la sélection naturelle pour expliquer la variance entre populations ($Q_{ST}>F_{ST}$) tout comme l'absence de variance ($Q_{ST}<F_{ST}$) entre populations ressemble fort à *« l'adaptationiste »* dénoncé par Gould & Lewontin, (1979). A aucun moment les adaptationistes n'envisagent pas (ou peu) que la sélection puisse être limité dans son action et qu'une partie du phénotype est figé par une architecture génétique robuste (plan d'organisation) héritée de l'histoire évolutive (ne pouvant pas être modifié à vau-l'eau). D'un point de vue épistémologique, il est plus judicieux et parcimonieux de penser que $Q_{ST} < F_{ST}$ résultent d'une architecture génétique particulière (issue de l'histoire évolutive) qui réduit la variation d'un caractère (canalisation), plutôt que d'une sélection dont les optimums varient peu ou pas (sans hypothèse sur la faible variance des optimums sélectifs).

3.18 Architecture génétique du caractère

Nous avons aussi réalisé une détection QTL (*Quantitative traits loci*) pour P_{50} dans deux fonds génétiques différents. Cette analyse statistique consiste à rechercher des associations

robustes entre un marqueur génétique, positionné sur une carte génétique et la variation d'un caractère quantitatif (nécessité d'avoir des mesures phénotypiques sur une collection d'individus apparentés).

Le premier fond génétique exploré correspond à une descendance de plein frère (118 individus de 15 ans, 3^{ieme} générations d'amélioration) issu d'un croisement d'individus landais de vigueur contrastée (fond génétique étroit). La carte génétique a été établie à partir de AFLP (amplified fragment length polymorphism) par Chagné et al., (002). Aucun QTL n'a été détecté sur ce fond génétique. Un second fond génétique a été alors exploré, il s'agit d'une descendance F2 (103 individus de 10 ans) issue de l'autofécondation d'un hybride Corse*Landais (fond génétique large, voir Figure 22). Un QTL a été détecté avec seulement l'algorithme bayesien (Hu & Xu, 2009, 2010; Che & Xu, 2010) sur le chromosome 11 pour P_{50}. Le faible effectif de la population de détection qui entraîne une surestimation du QTL à cause de l'effet Beavis, conjugué au fait que seul l'algorithme (le plus sensible), détecte ce QTL nous incite à être prudent. Ce QTL ne colocalise pas avec d'autres QTL connus pour des caractères liés au bois. En guise de vérification, il est prévu de mesurer la P50 sur 500 arbres que compte ce pedigree. Par ailleurs, d'autres détections QTL doivent être entreprises sur des fonds génétiques plus larges (par exemple hybrides interspécifiques) et avec des tailles d'effectifs plus importantes pour limiter les faux positifs (Xu, 2003).

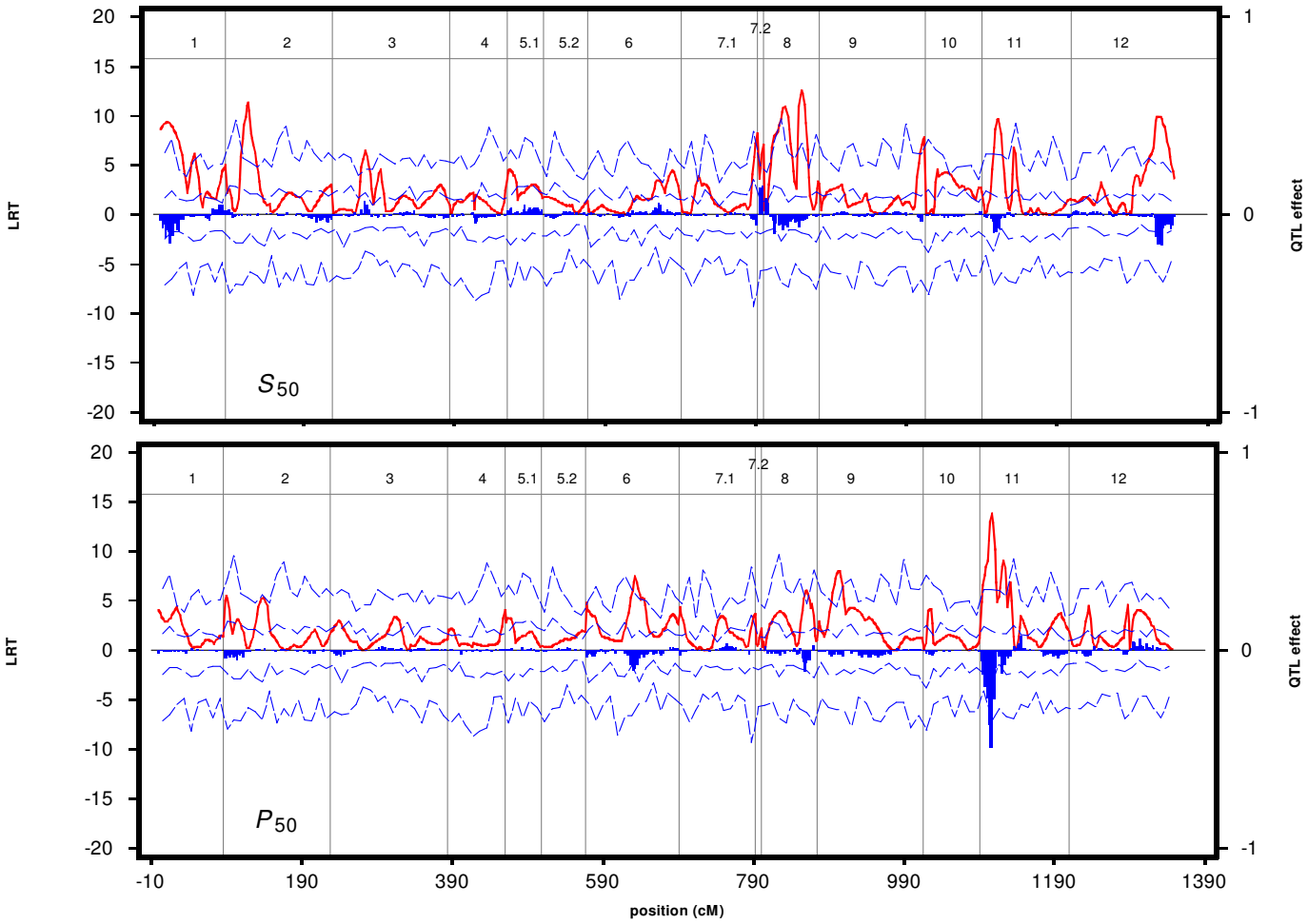

Figure 22 : Detection de QTL pour P_{50} et S_{50} sur une descendance F2 (n=103). Deux algorithmes de détection QTL ont été utilisés : En rouge, le profil du ratio du log de la vraisemblance (log-likelihood ratio test, i.e. LRT) obtenu grâce au *fisher scoring algorithm* et en gris le seuil critique (α = 0.05 au niveau génome) calculé grâce à la formule de Piepho (Piepho, 2001)**. L'histogramme en bleu correspond à l'effet de substitution allélique du QTL calculé grâce à l'algorithme Bayesien (*bayesian shinkage algorithm*), les lignes discontinues en bleu correspondent au modèle nul, α = 0.1 (proche de l'axe des abscisses) et α = 0.05 (loin de l'axe des abscisses) au niveau génome. Les chiffres en entête de 1 à 12 correspondent aux groupes de liaisons de la carte génétique de l'hybride corse*landais.**

4 Conclusions et Perspectives

4.1 Le mécanisme de cavitation est-il universel chez les conifères ?

Les nanopores trouvés dans les torus de l'ensemble des *Pinaceae* et les ex-*Taxodiaceae* examinés (maintenant incorporé dans les *Cupressaceae*), à l'exception du plus résistant d'entre eux *Cedrus*, et la compatibilité entre les ordres de grandeurs calculés entre les P_{50} et les seuils de rupture des ménisques montrent que l'hypothèse de la rupture capillaire au niveau du torus (*torus capillary-seeding*) est crédible. Les caractères fonctionnels anatomiques tels que la flexibilité du torus et le recouvrement (ou leur produit : l'effet valve, (Delzon et al., 2010)) n'expliquent pas plus de variation que le diamètre des nanopores pour les espèces à torus percés. Cela renforce la vraisemblance de cette hypothèse. En revanche, contrairement à ce qui était suggéré par la littérature, il n'y a pas forcément un mécanisme universel de propagation de la cavitation (Cochard et al., 2009; Delzon et al., 2010), il est certainement dépendant de l'anatomie du taxon étudié. Les nanopores expliqueraient la cavitation pour des espèces de conifères peu résistantes (*Pinaceae* ou ex-*Taxodiaceae*) mais pour les espèces résistantes, le joint torus-paroi pourrait être l'élément clé. La bulle d'air passerait entre la paroi et le torus car leurs bordures ne sont pas parfaitement planes, il existe des verrues (*wartz*) (Figure 24). Cependant certains auteurs montrent que ces verrues augment l'adhésion entre l'eau et les parois (Kohonen & Helland, 2009). On peut imaginer la formation de ménisques entre le torus, les verrues et plus les verrues sont en densité importantes plus les ménisques créés ont des rayons petits et donc résistant aux tensions. Cela nécessiterait de mesurer la hauteur des verrues (TEM), leur densités (SEM) et calculer la tension de rupture avec la loi de Laplace-Young.

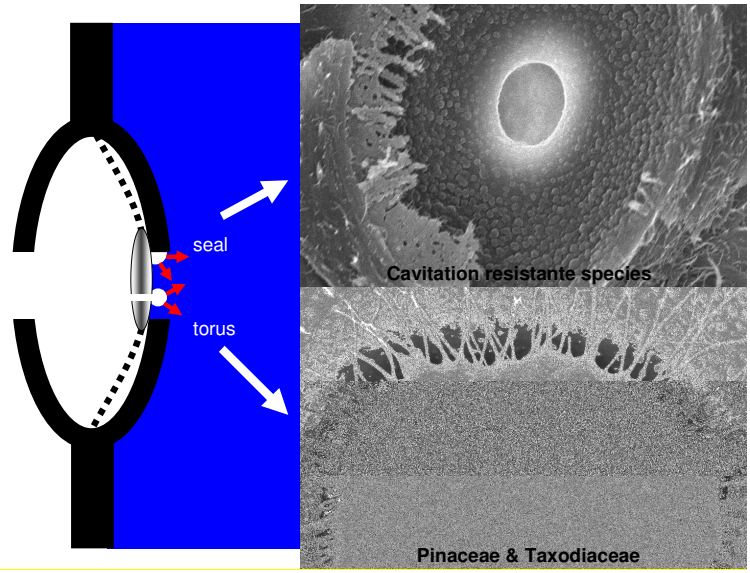

Figure 23 : Description des hypothèse probables de la propagation du germe d'air chez les conifères. Chez les espèces peu résistantes (*Pinaceae* et ex-*Taxodiaceae*) le germe d'air passe à travers les nanopores. Pour les espèces résistantes, des études ciblées sur la zone de contact entre le torus et les arches de la chambre sont nécessaires. Cette zone de contact n'est pas lisse mais souvent recouverte de verrues (*wartz*) ayant des propriétés biochimiques différentes du reste de la paroi.

4.2 Espèces à nanopores : où est passée la rustine ?

Notre étude micro-anatomique conforte l'hypothèse que ces nanopores sont issus de plasmodesmes secondaires. Ils en partagent les caractéristiques morphologiques, diamètres proches (68 nm pour les nanopores et 40 nm pour les plasmodesmes dans des tissus encore vivants), apparaissent en agrégats de paires ou de tirades comme les plasmodesmes dit secondaires. Les plasmodesmes ont un rôle (information positionnelle) dans la transformation drastique des parois cellulaires au niveau des plaques criblées des vaisseaux du phloème. De même, il est suspecté que les motifs des performations scalariformes sont guidés en partie par la position des plasmodesmes (Bell & Oparka, 2011; Brecknock et al., 2011). Plus directement, Dute et al., (2008) montre que des plasmodesmes secondaires semblent avoir un rôle dans la signalisation positionnelle du centre du torus lors de la formation de la ponctuation chez *Abies sp.* et *Metasequoia sp*. Si les plasmodesmes jouent aussi un rôle dans la formation des ponctuations dans les espèces ne présentant pas de nanopore, il sera important de comprendre, chez ces espèces, quels sont les enzymes, et les gènes régulateurs qui permettent de boucher les nanopores pendant l'ontogénie de la ponctuation ; et si cette fonction nouvelle est apparue chez ces espèces ou une fonction perdue secondairement chez les espèces à nanopores (*Pinaceae* et ex-*Taxodiaceae).*

4.3 Patron de variation intraspécifique

Sur la base des variances, phénotypiques (σ_P^2), intrapopulationnelles (σ_A^2 , σ_ε^2) et interpopulationnelles (σ_{bp}^2), nous pouvons distinguer deux groupes de caractères.

4.3.1 Caractères ne présentant pas de variance interpopulationnelle et non corrélés au climat

Les caractères liés aux propriétés anatomiques du bois (P_{50} et D_{mean}). Ils ont généralement une variance phénotypique et additive faible (CV_{P} et $CV_{\text{A}} \leq 10\%$) mais statistiquement significative. En revanche la variance interpopulationnelle est très faible ($CV_{\text{BP}} < 1\%$) et non significative. Plusieurs études récentes ont estimé la variance intraspécifique de la résistance à la cavitation de *Pinus sylvestris*, *Fagus sylvatica* et *Pinus pinaster* (Table 5). Les CV_{P} estimés en tests de population (CV_P^{tpd}) ou en populations *in situ* ($CV_P^{in-situ}$) sont du même ordre de grandeur. Les $CV_P^{in-situ}$ sont plus élevés que CV_P^{tpd} car la variance génétique et la plasticité phénotypique sont confondues. Il est à noter une plus grande variation de la résistance à la cavitation pour *Fagus sylvatica*, elle peut s'expliquer par une diversité cellulaire plus grande au sein du xylème à laquelle doit être associée une plus grande variation de la dimension des ponctuations. Malgré ce surcroît de variation, Wortemann et al., (2011) n'observe pas de variance significative entre les populations pour la résistance à la cavitation.

Table 5 Synthèse des estimations de la variance phénotypique pour la résistance à la cavitation.

Genre	*Espéce*	CV_{P} (%)[a]	design[b]	Auteurs[c]
Fagus	*sylvatica*	9.94	TP	(Wortemann, 2011)
Fagus	*sylvatica*	13.17	TP	(Wortemann, 2011)
Fagus	*sylvatica*	11.26	TP	(Wortemann, 2011)
Fagus	*sylvatica*	10.7	TP	(Wortemann, 2011)
Pinus	*pinaster*	4.87	TP	(Corcuera et al., 2011)
Pinus	*pinaster*	6.60	TPD	(Lamy et al., 2011)
Pinus	*pinaster*	6.43	TPD	Cette thèse
Pinus	*pinaster*	6.36	*In situ*	Cette thèse
Pinus	*sylvestris*	8.15	*In situ*	(Martinez-Vilalta et al., 2009)

« a » Les CV_{P} sont issus soit de la publication elle-même soit recalculé *a posteriori* grâce aux données de l'article. « b » TP =test de populations, TPD = test de populations-descendances. « c » Nous avons reporté les CV_{P} pour chacun des tests de population retrouvé dans la littérature, ainsi il y a 5 chez *Fagus sylvatica*, 3 chez *Pinus pinaster*.

Nous ne trouvons pas de corrélation entre la moyenne de la résistance à la cavitation des populations et les variables climatiques du site d'origine comme des études précédentes (Martinez-Vilalta et al., 2009; Corcuera et al., 2011; Wortemann et al., 2011). Les populations *Pinus pinaster* ne présentent pas de variance génétique ou phénotypique clinale ou contre-clinale pour la resistance à la cavitation (Figure 20).

4.3.2 Caractères variables entre les populations et corrélés au climat

Les caractères liés à la croissance (h, Δ_h, A_{Leaf} et $\emptyset_{2007}$) présentent des patrons bien différents, avec des variances phénotypiques et additives plus élevées (CV_P et CV_A > 12%) mais surtout une variance entre les populations beaucoup plus importante (CV_{BP} > 12%). La valeur moyenne des populations est négativement corrélée avec l'aridité du climat de la provenance. Les populations xériques poussent moins vites et allouent plus de carbone à leurs appareils racinaire que leurs homologues mésiques. Ces populations présentent des clines génétiques faible à important (suivant le TPD) avec le climat d'origine et des clines phénotypiques encore plus prononcé.

4.4 Plasticité phénotypique de la résistance à la cavitation

La plasticité phénotypique a été approchée de plusieurs manières dans cette thèse. La première est qualitative. Elle peut être vue comme la différence entre la variance phénotypique estimée sur des populations naturelles *in situ* ($CV_P^{in-situ}$) qui est la somme de σ_G^2, σ_E^2 et I_{GE} et des populations ayant poussées en test de population CV_P^{tpd} qui est σ_G^2. Ainsi *Pinus pinaster* et *Fagus sylvatica* ont un $CV_P^{in-situ}$ et CV_P^{tpd} sont sensiblement égaux pour la resistance à la cavitation, cela démontre que la plasticité phénotypique pour ce caractère est faible (Corcuera et al., 2011; Wortemann et al., 2011 et nos travaux, Table 5). La seconde est quantitative. Elle consiste à utiliser plusieurs tests de populations ayant des entités biologiques communes (des génotypes clonés, des individus appartenant à la même famille, des individus de mêmes populations) mais poussant dans des sites différents. Cette approche permet la quantification de la plasticité phénotypique, mais cette quantification doit être comparée à des caractères ayant une plasticité connue afin d'avoir un référentiel. Notre étude montre que la résistance à la cavitation a une plasticité faible et bien inférieure à celle de la croissance, mais pour les deux caractères cette variation est piloté par le macroenvironnement

(σ_E^2) avant tout (Table 5). Une autre limite de l'étude de la plasticité phénotypique de la résistance à la cavitation est due à la nature même de la mesure du caractère. La résistance à la cavitation est une mesure de perte de conductance relativement à une mesure de conductance initiale supposée sans embolie. Aussi la résistance à la cavitation ne peut pas se mesurer dans des milieux très xériques, ou lors de sécheresses expérimentales (où les individus sont en stress hydrique permanent) car cette quantité d'embolie native est importante.

4.5 Evolution des caractères liés aux propriétés du bois

La comparaison entre Q_{ST} et F_{ST} montre que la variance entre les populations pour les caractères liés aux bois (D_{mean} et P_{50}) est plus faible que sous l'attendu de la dérive génétique ($Q_{ST}<F_{ST}$). En science de l'évolution, l'absence de variance pour un caractère entre populations est difficile à expliquer. En effet, un caractère sous sélection varie entre populations car les optimums de sélection sont rarement les mêmes (sélection diversifiante) et un caractère phénotypique neutre d'un point de vue évolutif (cas assez rare finalement) varie entre populations de manière aléatoire car la fréquence des gènes sous-jacents change par simple effet d'échantillonnage des allèles d'une génération à l'autre (dérive génétique). La construction du test Q_{ST} versus F_{ST} permet d'estimer la variance attendue sous l'effet de la dérive génétique (Le Corre & Kremer, 2003; Whitlock, 2008; Kremer & Le Corre, 2011). Classiquement, l'interprétation $Q_{ST}<F_{ST}$ repose sur une sélection dite uniformisante, c'est la somme des effets de n sélections stabilisatrices avec le même optimum de sélection dans chacune des n populations (provenant de milieux contrastés).

Cette interprétation n'a pas notre faveur pour plusieurs raisons : (i) il existe des arguments théoriques qui montrent que l'architecture génétique (nombre de gènes, relation de dominance entre allèles, pléiotropie, relation épistatique entre locus et la structure des covariances entre l'effet allélique au sein et entre les populations) peut conduire à $Q_{ST} < F_{ST}$ sans intervention de la sélection (Whitlock, 1999; Lopez-Fanjul et al., 2003; Goudet & Buchi, 2006; Goudet & Martin, 2007; Miller et al., 2008; Santure & Wang, 2009; Kremer & Le Corre, 2011). Sachant que la plupart des gènes ont des relations pléiotropiques et épistatique entre eux (Carlborg & Haley, 2004; Segrè et al., 2005; Boone et al., 2007; Le Rouzic et al., 2008), il est plus parcimonieux de qualifier le caractère de « canalisé », c'est-à-dire que l'architecture génétique contraint la variance du caractère contre des perturbations génétiques et/ou environnementales. La canalisation est certainement issue d'un épisode sélectif très ancien qui a façonné une architecture génétique robuste (contraintes génétiques) et qui pourrait se transmettre pendant

plusieurs milliers de générations (spéciation). La température du corps des mammifères, la forme des ailes chez le genre *Drosophila* en sont les exemples les plus probants (Hansen & Houle, 2004), (ii) Expliquer la non variation entre populations avec un modèle de sélection naturelle, n'est pas heuristique. Certes, le modèle de sélection uniformisante est très efficace pour reproduire $Q_{ST}<F_{ST}$, mais il ne fournit aucune hypothèse à tester. Aussi, il nous paraît plus fructueux et exact de faire l'hypothèse que le caractère est contraint génétiquement (iii) L'utilisation récurrente de la sélection pour expliquer la variation comme la non variation laisse croire que tout est optimisé dans un organisme. Or c'est faux, Gould & Lewontin, (1979) ont démontré qu'il y a des limites à l'adaptation. Quelques années plus tard (Bradshaw, 1991) propose de s'intéresser aux cas où l'évolution échoue, il nomme cela la *genostasis*. L'écologie évolutive devrait se saisir de ces concepts peu documentés car peu étudiés.

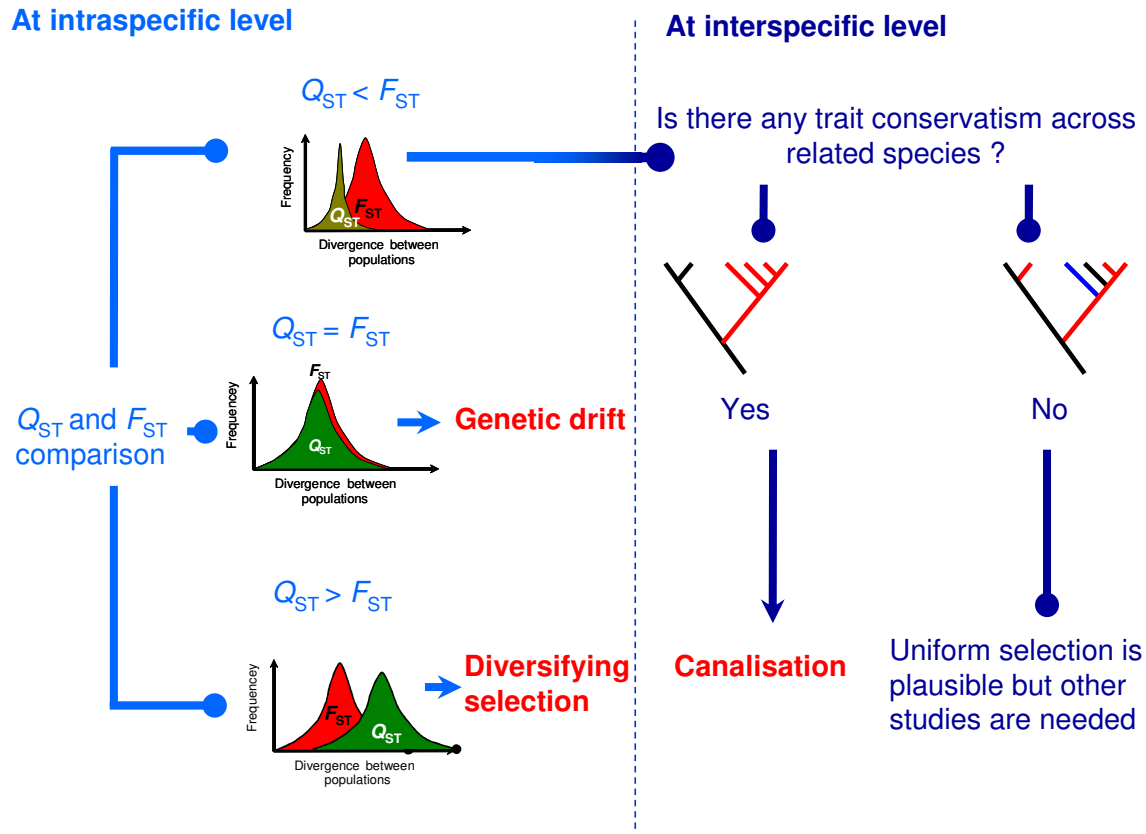

Figure 24 : Arbre de décision pour l'interprétation des comparaisons Q_{ST} et F_{ST}. La comparaison statistique des deux quantités Q_{ST} et F_{ST} mène à trois cas possibles, (i) Q_{ST} = F_{ST}, c'est-à-dire les événements de sélection sont probablement de même intensité que ceux de la dérive génétique. (ii) Le Q_{ST} > F_{ST}, les populations présentent plus de variance que sous l'attendu de la dérive génétique. (iii) Le dernier cas ou $Q_{ST}<F_{ST}$ n'est pas facile à interpréter, il faut faire appel à d'autres informations comme les patrons de variations dans des espèces voisines. Si les espèces voisines présentent les mêmes patrons de variations alors on peut conclure que le caractère est probablement canalisé. Les cercles pleines indiquent

que l'inférence n'est pas robuste et qu'elle nécessite de plus d'information. Une flèche indique que l'inférence est robuste.

Aussi, sur la base des comparaisons entre Q_{ST} et F_{ST} et des arguments développés ci-dessus, nous avons fait l'hypothèse que ces caractères sont canalisés. Cette hypothèse de caractères canalisés est étayée par d'autres éléments (Figure 25). Chez les espèces proches, *Pinus sylvestris* et *Pinus hartewgii* les valeurs de P_{50} sont proches de celle de *Pinus pinaster*, et les différences entre les populations sont faibles (données non publiées). Ces espèces partagent certainement les mêmes architectures génétiques pour ces caractères (d'où les mêmes patrons de variations) plutôt que les mêmes optimums sélectifs (i.e. sélection uniformisante) entre toutes les populations de toutes ces espèces. La canalisation peut être tester de plusieurs manières, (i) l'inactivation ciblé de gènes régulateurs (et codant pour des chaperonines par exemple) impliqués dans l'expression du caractère, et d'observer la variation des phénotypes, s'il y a une augmentation significative de la variation, cela veut dire qu'il y avait de la diversité génétique caché et que donc l'architecture génétique tamponnait la variance génétique (Queitsch et al., 2002; Sangster et al., 2007, 2008). (ii) L'autre stratégie est de comparer la diversité génétique du caractère canalisé (qui devrait être basse) et de la comparer la diversité génétique moyenne du génome (Fu et al., 2009).

4.6 Conséquences pour les programmes d'amélioration génétique

Le patron de variation des caractères liés au bois suggère que la sélection (par troncature par exemple) est possible (héritabilité moyenne des caractères liés au bois) mais le gain à chaque génération sera limité (variance additive faible). L'épuisement de la variance additive est théoriquement possible mais des expériences menées sur le long terme montrent qu'elle est renouvelée par la variance mutationnelle à chaque génération (Carlborg et al., 2006). Si la résistance à la cavitation comme la densité du bois sont des caractères réellement canalisés alors une partie de la diversité génétique est invisible (*cryptic genetic variation*) car tamponnée par l'architecture génétique (covariance négative entre les effets alléliques, épistasie directionnelle négative, pléiotropie) (Le Rouzic & Carlborg, 2008). *A priori,* une sélection par troncature[18] renforcerait la covariance négative entre effets alléliques (Bulmer, 1974; Mueller & James, 1983). En revanche, l'épistasie fournirait à chaque génération de la

[18] Type de sélection la plus courante chez les améliorateurs. Il s'agit de faire se reproduire ensemble les individus au dessus d'un certain seuil (seuil de troncature).

variance en apparence additive (Hansen & G.P. Wagner, 2001; N.H. Barton & Turelli, 2004; Carlborg et al., 2006; Hansen, 2006; Hansen et al., 2006; Turelli & N.H. Barton, 2006). A la lueur des travaux empiriques et de récents modèles théoriques sus-cités, il est essentiel de modéliser l'évolution de caractères à déterminisme complexe (canalisés) sous sélection artificielle.

Pour conclure, autant l'amélioration classique de ces caractères à faible variance additive reste difficile, autant il sera facile de choisir parmi les arbres «élites»[19], des arbres ayant une densité du bois et une résistance à la cavitation importante (ou l'inverse) car les deux caractères ne sont pas corrélés. Il faudra en revanche tenir compte des corrélations entre densité du bois et croissance.

4.7 Conséquences pour la capacité adaptative de *Pinus pinaster* face à la sécheresse

Quantifier la capacité adaptative de *Pinus pinaster* face à la sécheresse revient à faire le bilan de la variation disponible pour chacun des termes déterminant un modèle hydrique de l'arbre. Une partie de cette variation a été mesuré dans cette thèse, cependant il existe une variation cachée ou potentielle (cf Figure 1). Construisons donc un modèle hydrique faisant intervenir quelques uns des caractères mesurés dans cette thèse. Par souci de simplicité, nous négligeons le potentiel hydrique dû à la gravité et en combinant l'équation 2 et 3, on peut écrire :

$$\Psi_{leaf} = \Psi_{soil} - A_L\left(R_{soil} + R_{root} + \frac{1}{K_{\max} f(P_{50}, S_{50}, \Psi_{xylem})} + R_{leaf}\right) g_c D \quad (10)$$

Avec Ψ_{leaf} le potentiel hydrique foliaire, Ψ_{soil} le potentiel hydrique du sol, g_c la conductance stomatique moyenne de la canopée, D le déficit en pression de vapeur d'eau de l'air, avec R_x les résistances des différents organes et R_{xylem} exprimé avec la fonction sigmoïde faisant intervenir la P_{50}. En exprimant g_c sous la forme d'une conductivité (g_c) et en divisant les résistances par les surfaces conductrices de l'arbre (A_S), on peux écrire :

$$\Psi_{leaf} = \Psi_{soil} - \frac{A_L}{A_S}\left(R^s_{soil} + R^s_{root} + \frac{1}{K^s_{\max} f(P_{50}, S_{50}, \Psi_{xylem})} + R^s_{leaf}\right) g_c D \quad (11)$$

Les résistances (ou conductivités) sont en unité de A_S et il s'agit donc de résistances spécifiques symbolisées par R^s. Nous savons que R_{xylem} participe à moins de 30% de la

[19] Parents de la future génération d'amélioration qui présentent une croissance supérieure au seuil de troncature

résistance totale de l'arbre (Cruiziat et al., 2002) et que seul P_{50} est héritable, CV_A[20] de ce caractère est <6 %, en comparaison, le CV_A du rapport A_L/A_S est plus élevé > 12 %. D'un point de vue théorique, *Pinus pinaster* a plus de variation disponible pour la sélection (naturelle et artificielle) sur A_L/A_S que sur P_{50}. De plus, les deux caractères, R_{xylem} et A_L/A_S, ont vraisemblablement une plasticité phénotypique différente, plus forte pour A_L/A_S que pour P_{50}. Donc si la tolérance à la sécheresse de *Pinus pinaster* doit être améliorée, il est plus stratégique de sélectionner des arbres mettant en place beaucoup de bois par rapport à une surface foliaire réduite (A_L/A_S élevé). En écophysiologie il est connu que les populations de Pin font de l'ajustement hydraulique, les populations poussant sur des sites secs mettent en place plus de surfaces conductrices que transpirantes par rapport aux populations vivant en milieu plus humide. Aussi le ratio A_L/A_S est négativement corrélé à l'aridité du climat (Addington et al., 2006; Martinez-Vilalta et al., 2009).

L'amélioration de la résistance à la sécheresse à court terme de *Pinus pinaster* passe certainement par la sélection d'individu ayant une stature adaptée à la sécheresse (rapport A_L/A_S). Cependant cela irait contre les efforts de deux générations d'améliorations. L'amélioration de la sécheresse de *Pinus pinaster* passe par l'amélioration de caractères physiologiques plutôt que morphologiques comme cela été fait pour les plantes céréaliéres. En effet, *Pinus pinaster* a une marge de sécurité étroite, c'est-à-dire qu'il ferme ces stomates lorsque la cavitation démarre. Cette stratégie est efficace pour éviter les sécheresses intenses mais elle semble inefficace pour les sécheresses longues. Les Pins épuisent leurs réserves carbonées sans réussir à la reconstituer (assimilation carbonée nulle) et sont sujet à la mort par la faim (Breshears et al., 2009). La résistance à la cavitation contraint fortement le fonctionnement hydraulique des Pins. Une amélioration durable et profonde de sa resistance à la sécheresse passe par la sélection d'individus plus résistant à la cavitation.

La simulation pourrait aider à développer plusieurs ideotypes. Il faudra écrire un modèle semblable à 11, en utilisant comme paramètres d'entrée P_{50}, A_L/A_S réellement mesurés, et simuler une sécheresse du sol. La performance de la population *in silico* pourrait être le temps qu'il faut pour que 50% des individus de la population meurent (un individu est théoriquement mort lorsque $\Psi_{leaf} = P_{88}$). Il serait possible de simuler *n* individus ayant les valeurs mesurées pour P_{50} et A_L/A_S chez le *Pinus pinaster* (tirage aléatoire dans une

[20] Coefficient de variation additive, c'est-à-dire la variance disponible pour la sélection naturelle ou artificielle normalisé par la moyenne du caractère.

distribution normale $N\sim(\mu, \sigma_G^2)$). Deux scénarios pourraient être envisagés, un premier dans lequel A_L/A_S aura été amélioré de 1% et un second dans lequel P_{50} serait amélioré de 1% et de comparer les performances des populations *in silico*. Ainsi le choix d'amélioration de tel ou tel caractère serait fait sur la base du fonctionnement hydraulique de *Pinus pinaster*.

5 - Bibliographie

Adams HD, Guardiola-Claramonte M, Barron-Gafford GA, Villegas JC, Breshears DD, Zou CB, Troch PA, Huxman TE. **2009**. Temperature sensitivity of drought-induced tree mortality portends increased regional die-off under global-change-type drought. *Proceedings of the National Academy of Sciences of the United States of America* **106**: 7063-6.

Addington RN, Donovan L a., Mitchell RJ, Vose JM, Pecot SD, Jack SB, Hacke UG, Sperry JS, Oren R. **2006**. Adjustments in hydraulic architecture of Pinus palustris maintain similar stomatal conductance in xeric and mesic habitats. *Plant, Cell and Environment* **29**: 535-545.

Aguiar A, Almeida Maria Helena, Borralho N. **2003**. Genetic Control of Growth , Wood Density and Stem Characteristics of Pinus pinaster in Portugal. *Genetica* **11**: 131-139.

Alder NN, Sperry JS, Pockman W T. **1996**. Root and stem xylem embolism, stomatal conductance, and leaf turgor in Acer grandidentatum populations along a soil moisture gradient. *Oecologia* **105**: 293-301.

Alexander LV, Zhang X, Peterson TC, Caesar J, Gleason B, Tank A, Haylock M, Collins D, Trewin B, Rahimzadeh F, et al. 2006. Global observed changes in daily climate extremes of temperature and precipitation. *Journal of Geophysical Research-Atmospheres* **111**.

Alia R, Gil L, Pardos JA. **1995**. Performance of 43 Pinus pinaster provenances on 5 locations in central spain. *Silvae Genetica* **44**: 75-81.

Alia R, Moro J, Denis JB. **1997**. Performance of Pinus pinaster provenances in Spain: interpretation of the genotype by environment interaction. *Canadian Journal of Forest Research-Revue Canadienne De Recherche Forestiere* **27**: 1548-1559.

Allen CD, Macalady AK, Chenchouni H, Bachelet D, McDowell NG, Vennetier M, Kitzberger T, Rigling A, Breshears DD, Hogg EH (Ted). **2010**. A global overview of drought and heat-induced tree mortality reveals emerging climate change risks for forests. *Forest Ecology and Management* **259**: 660-684.

Angeles G, Bond B, Boyer J. S, Brodribb TJ, Brooks JR, Burns MJ, Cavender-Bares J, Clearwater M, Cochard H, Comstock J, et al. 2004. The Cohesion-Tension theory. *New Phytologist* **163**: 451-452.

Aranda I, Alia R, Ortega U, Dantas AK, Majada J. **2010**. Intra-specific variability in biomass partitioning and carbon isotopic discrimination under moderate drought stress in seedlings from four Pinus pinaster populations. *Tree Genetics & Genomes* **6**: 169-178.

Badeau V, Dupouey J-luc. **2004**. *Modélisation et cartographie de l ' aire climatique potentielle des grandes essences forestières françaises - Séquestration de carbone dans les grands écosystèmes forestiers en France Projet CARBOFOR*. Nancy.

Barton NH, Turelli M. **2004**. Effects of genetic drift on variance components under a general model of epistasis. *Evolution; international journal of organic evolution* **58**: 2111-32.

Beikircher B, Mayr S. **2008**. The hydraulic architecture of Juniperus communis L. ssp. communis: shrubs and trees compared. *Plant, cell & environment* **31**: 1545-56.

Bell K, Oparka K. **2011**. Imaging plasmodesmata. *Protoplasma* **248**: 9-25.

Beniston M, Stephenson DB, Christensen OB, Ferro CAT, Frei C, Goyette S, Halsnaes K, Holt T, Jylha K, Koffi B, et al. 2007. Future extreme events in European climate: an exploration of regional climate model projections. *Climatic Change* **81**: 71-95.

Bonnier. **1890**. Cultures expérimentales dans les Alpes et les Pyrénées. *Revue générale de botanique* **2**: 513-546.

Boone C, Bussey H, Andrews BJ. **2007**. Exploring genetic interactions and networks with yeast. *Nature reviews. Genetics* **8**: 437-49.

Bradshaw AD. **1991**. The Croonian Lecture, 1991. Genostasis and the limits to evolution. *Philosophical transactions of the Royal Society of London. Series B, Biological sciences* **333**: 289-305.

Brecknock S, Dibbayawan TP, Vesk M, Vesk P a, Faulkner C, Barton D a, Overall RL. **2011**. High resolution scanning electron microscopy of plasmodesmata. *Planta*: 749-758.

Brendel O, Cochard H. **2011**. How plant species cope with water stress. In: Birot Y, Gracia C, Palahi M, eds. Water for forests and people in the mediterranean region, a challenging balance. European union, 76-80.

Brendel O, Pot D, Plomion C, Rozenberg P, Guehl J-M. **2002**. Genetic parameters and QTL analysis of delta C-13 and ring width in maritime pine. *Plant Cell and Environment* **25**: 945-953.

Brendel O, Le Thiec D, Scotti-Saintagne C, Bodenes C, Kremer A, Guehl J-M. **2008**. Quantitative trait loci controlling water use efficiency and related traits in Quercus robur L. *Tree Genetics & Genomes* **4**: 263-278.

Breshears DD, Cobb NS, Rich PM, Price KP, Allen CD, Balice RG, Romme WH, Kastens JH, Floyd ML, Belnap J, et al. 2005. Regional vegetation die-off in response to global-change-type drought. *Proceedings of the National Academy of Sciences of the United States of America* **102**: 15144-15148.

Breshears DD, Myers OB, Meyer CW, Barnes FJ, Zou CB, Allen CD, McDowell NG, Pockman William T. 2009. Tree die-off in response to global change-type drought: mortality insights from a decade of plant water potential measurements. *Frontiers in Ecology and the Environment* **7**: 185-189.

Brodribb TJ. **2009**. Xylem hydraulic physiology: The functional backbone of terrestrial plant productivity. *Plant Science* **177**: 245-251.

Brodribb TJ, Cochard H. **2009**. Hydraulic failure defines the recovery and point of death in water-stressed conifers. *Plant physiology* **149**: 575-84.

Brodribb TJ, Hill RS. **1999**. The importance of xylem constraints in the distribution of conifer species. *New Phytologist* **143**: 365-372.

Brodribb TJ, McAdam S a M. **2011**. Passive origins of stomatal control in vascular plants. *Science (New York, N.Y.)* **331**: 582-5.

Brodribb TJ, McAdam SAM. **2011**. Stomatal (mis)behaviour. *Tree Physiology* **31**: 1039-1040.

Brodribb TJ, Bowman DJMS, Nichols S, Delzon S, Burlett R. 2010. Xylem function and growth rate interact to determine recovery rates after exposure to extreme water deficit. *New Phytologist* **188**: 533-542.

Bréda N. **2006**. Faut-il adapter la gestion de la forêt aux sécheresses et si oui, comment□? *Euroforest 2006*: 1-6.

Bréda N, Badeau V. **2008**. Forest tree responses to extreme drought and some biotic events: Towards a selection according to hazard tolerance? *Comptes Rendus Geosciences* **340**: 651-662.

Bréda N, Huc R, Granier A, Dreyer E. **2006**. Temperate forest trees and stands under severe drought: a review of ecophysiological responses, adaptation processes and long-term consequences. *Annals of Forest Science* **63**: 625-644.

Buckley TN. **2005**. The control of stomata by water balance. *The New phytologist* **168**: 275-92.

Bulmer MG. **1974**. Linkage desquilibrium and genetic variability. *Genetical Research* **19**.

Burban C, Petit RJ. **2003**. Phylogeography of maritime pine inferred with organelle markers having contrasted inheritance. *Molecular Ecology* **12**: 1487-1495.

Carlborg O, Haley CS. **2004**. Epistasis: too often neglected in complex trait studies? *Nature Reviews Genetics* **5**: 618-U4.

Carlborg O, Jacobsson L, Ahgren P, Siegel P, Andersson L. **2006**. Epistasis and the release of genetic variation during long-term selection. *Nature Genetics* **38**: 418-420.

Caupin F, Herbert EM. **2006**. Cavitation in water: a review. *Comptes Rendus Physique* **7**: 1000-1017.

Chagné D, Lalanne C, Madur D, Kumar S, Frigerio JM, Krier C, Decroocq S, Savoure A, Bou-Dagher-Kharrat M, Bertocchi E, et al. 2002. A high density genetic map of maritime pine based on AFLPs. *Annals of Forest Science* **59**: 627-636.

Chancerel E, Lepoittevin C, Le Provost G, Lin YC, Jaramillo-Correa JP, Eckert AJ, Wegrzyn JL, Zelenika D, Boland A, Frigerio JM, et al. 2011. Development and implementation of a highly-multiplexed SNP array for genetic mapping in maritime pine and comparative mapping with loblolly pine. *Bmc Genomics* **12**.

Chapuis E, Trouve S, Facon B, Degen L, Goudet J. **2007**. High quantitative and no molecular differentiation of a freshwater snail (Galba truncatula) between temporary and permanent water habitats. *Molecular Ecology* **16**: 3484-3496.

Chapuis Elodie, Martin G, Goudet J. **2008**. Effects of Selection and Drift on G Matrix Evolution in a Heterogeneous Environment: A Multivariate QST-FST Test With the Freshwater Snail Galba truncatula. *Genetics* **180**: 2151-2161.

Che X, Xu S. **2010**. Significance Test and Genome Selection in Bayesian Shrinkage Analysis. *International Journal of Plant Genomics* **2010**: 11.

Choat B, Cobb AR, Jansen S. **2008**. Structure and function of bordered pits: new discoveries and impacts on whole-plant hydraulic function. *The New phytologist* **177**: 608-25.

Choat B, Sack Lawren, Holbrook NM. **2007**. Diversity of hydraulic traits in nine Cordia species growing in tropical forests with contrasting precipitation. *The New phytologist* **175**: 686-98.

Chun YJ, Le Corre V, Bretagnolle F. **2009**. Adaptive divergence for a fitness-related trait among invasive Ambrosia artemisiifolia populations in France. *Molecular Ecology* **20**: 1378-1388.

Cochard H. **2002a**. A technique for measuring xylem hydraulic conductance under high negative pressures. *Plant Cell and Environment* **25**: 815-819.

Cochard H. **2002b**. Xylem embolism and drought-induced stomatal closure in maize. *Planta* **215**: 466-471.

Cochard H. **2006**. Cavitation in trees. *Comptes Rendus Physique* **7**: 1018-1026.

Cochard H, Coll L, Le Roux X, Ameglio T. **2002**. Unraveling the effects of plant hydraulics on stomatal closure during water stress in walnut. *Plant Physiology* **128**: 282-290.

Cochard H, Cruiziat P, Tyree MT. **1992**. Use of positive pressures to establish vulnerability curves□: further support for the air-seeding hypothesis and implications for pressure-volume analysis. *Plant physiology* **100**: 205-9.

Cochard H, Damour G, Bodet C, Tharwat I, Poirier M, Ameglio T. **2005**. Evaluation of a new centrifuge technique for rapid generation of xylem vulnerability curves. *Physiologia Plantarum* **124**: 410-418.

Cochard H, Froux F, Mayr S, Coutand C. **2004**. Xylem wall collapse in water-stressed pine needles. *Plant Physiology* **134**: 401-408.

Cochard H, Holtta T, Herbette S, Delzon S, Mencuccini M. **2009**. New Insights into the Mechanisms of Water-Stress-Induced Cavitation in Conifers. *Plant Physiology* **151**: 949-954.

Cochard H, Lemoine D, Dreyer E. **1999**. The effects of acclimation to sunlight on the xylem vulnerability to embolism in Fagus sylvatica L. *Plant Cell and Environment* **22**: 101-108.

Cochard H, Venisse J-S, Barigah Têtè Sévérien, Brunel N, Herbette S, Guilliot A, Tyree MT, Sakr S. **2007**. Putative role of aquaporins in variable hydraulic conductance of leaves in response to light. *Plant physiology* **143**: 122-33.

Corcuera L, Cochard H, Gil-Pelegrin E, Notivol E. **2011**. Phenotypic plasticity in mesic populations of Pinus pinaster improves resistance to xylem embolism (P50) under severe drought. *Trees*.

Le Corre V, Kremer A. **2003**. Genetic variability at neutral markers, quantitative trait loci and trait in a subdivided population under selection. *Genetics* **164**: 1205-1219.

Le Corre V, Kremer A. **2012**. The genetic differentiation at quantitative trait loci under local adaptation.

Correia I, Almeida M. H., Aguiar A, Alia R, David TS, Pereira JS. **2008**. Variations in growth, survival and carbon isotope composition (delta C-13) among Pinus pinaster populations of different geographic origins. *Tree Physiology* **28**: 1545-1552.

Cruiziat P, Cochard H, Ameglio T. **2002**. Hydraulic architecture of trees: main concepts and results. *Annals of Forest Science* **59**: 723-752.

Dalla-Salda G, Martinez-Meier A, Cochard H, Rozenberg P. **2011**. Genetic variation of xylem hydraulic properties shows that wood density is involved in adaptation to drought in Douglas-fir (Pseudotsuga menziesii (Mirb.)). *Annals of Forest Science* **68**: 747-757.

Dalla-Salda G, Martinez-meier A, Cochard H, Rozenberg P. **2009**. Variation of wood density and hydraulic properties of Douglas-fir (Pseudotsuga menziesii (Mirb.) Franco) clones related to a heat and drought wave in France. *Forest Ecology and Management* **257**: 182-189.

Damour G, Simonneau T, Cochard H, Urban L. **2010**. An overview of models of stomatal conductance at the leaf level. *Plant, cell & environment* **33**: 1419-38.

Danchin E, Wagner WH. **2010**. Inclusive heritability: combining genetic and non-genetic information to study animal behavior and culture. *Oikos*.

Della-Marta PM, Beniston M. **2008**. Summer heat waves in western Europe, their past change and future projections. In: Bronnimann S, Luterbacher J, Ewen T, Diaz HF, Stolarski RS, Neu U, eds. Climate Variability and Extremes during the Past 100 Years.235-250.

Delzon S, Douthe C, Sala A, Cochard H. **2010**. Mechanism of water-stress induced cavitation in conifers: bordered pit structure and function support the hypothesis of seal capillary-seeding. *Plant, Cell & Environment* **32**: 1-11.

Domec J-C, Gartner BL. **2001**. Cavitation and water storage capacity in bole xylem segments of mature and young Douglas-fir trees. *Trees-Structure and Function* **15**: 204-214.

Domec J-C, Lachenbruch B, Meinzer Frederick C. 2006. Bordered pit structure and function determine spatial patterns of air-seeding thresholds in xylem of Douglas-fir (Pseudotsuga menziesii; Pinaceae) trees. *American Journal of Botany* **93**: 1588-1600.

Dute RR, Hagler L, Black A. **2008**. Comparative development of intertracheary pit membranes in Abies firma and Metasequoia glyptostroboides. **29**: 277-289.

Edelaar P, Björklund M. **2011**. If FST does not measure neutral genetic differentiation, then comparing it with QST is misleading. Or is it? *Molecular ecology* **20**: 1805-12.

Edelaar P, Burraco P, Gomez-Mestre I. **2011**. Comparisons between QST and FST - how wrong have we been? *Molecular ecology* **20**: 4830-9.

Edmands S, Harrison JS. **2003**. Molecular and qunatitative trait variation within and among populations of the intertidal copedpod Tigropus californicus. *Evolution* **57**: 2277-2285.

Ehlert C, Maurel C, Tardieu F, Simonneau T. **2009**. Aquaporin-mediated reduction in maize root hydraulic conductivity impacts cell turgor and leaf elongation even without changing transpiration. *Plant physiology* **150**: 1093-104.

Ennajeh M, Tounekti T, Vadel AM, Khemira H, Cochard H. **2008**. Water relations and drought-induced embolism in olive (Olea europaea) varieties “Meski” and “Chemlali” during severe drought. *Tree Physiology* **28**: 971-976.

Falconer DS, Mackay TFC. **1996**. Introduction to quantitative genetics. *Introduction to quantitative genetics.*: xv + 464 pp.

Fichot R, Laurans F, Monclus R, Moreau A, Pilate G, Brignolas F. **2009**. Xylem anatomy correlates with gas exchange, water-use efficiency and growth performance under contrasting water regimes: evidence from Populus deltoidesPopulus nigra hybrids. *Tree Physiology* **29**: 1537-1549.

Fu J, Keurentjes JJB, Bouwmeester H, America T, Verstappen FW a, Ward JL, Beale MH, de Vos RCH, Dijkstra M, Scheltema R a, et al. 2009. System-wide molecular evidence for phenotypic buffering in Arabidopsis. *Nature genetics* **41**: 166-7.

Goudet J, Buchi L. **2006**. The effects of dominance, regular inbreeding and sampling design on QST, an estimator of population differentiation for quantitative traits. *Genetics* **172**: 1337-1347.

Goudet J, Martin G. **2007**. Under neutrality, QST <= FST when there is dominance in an island model. *Genetics* **176**: 1371-1374.

Gould SJ, Eldredge N. **1977**. Punctuated Equilibria□: The Tempo and Mode of Evolution Reconsidered. *Paleobiology* **3**: 115-151.

Gould SJ, Lewontin RC. **1979**. Spandrels of San-Marco and the panglossian paradigm - A critique of the adaptationist program. *Proceedings of the Royal Society of London Series B-Biological Sciences* **205**: 581-598.

Granier A, Reichstein M, Bréda N, Janssens IA, Falge E, Ciais P, Grunwald T, Aubinet M, Berbigier P, Bernhofer C, et al. 2007. Evidence for soil water control on carbon and water dynamics in European forests during the extremely dry year: 2003. *Agricultural and Forest Meteorology* **143**: 123-145.

Guehl J-M, Picon C, Sénéquier C. **1996**. Discrimination isotopique du carbone et efficience d'utilisation de l'eau chez les arbres forestiers. : 1-15.

Hacke UG, Sperry JS. **2001**. Functional and ecological xylem anatomy. *Perspectives in Plant Ecology Evolution and Systematics* **4**: 97-115.

Hacke UG, Sperry JS, Pittermann J. **2004**. Analysis of circular bordered pit function - II. Gymnosperm tracheids with torus-margo pit membranes. *American Journal of Botany* **91**: 386-400.

Hamrick JL. **2004**. Response of forest trees to global environmental changes. *Forest Ecology and Management* **197**: 323-335.

Hansen TF. **2006**. The evolution of genetic architecture. *Annual Review of Ecology Evolution and Systematics* **37**: 123-157.

Hansen TF, Houle D. **2004**. Evolvability, stabilizing selection, and the problem of stasis. In: Pigliucci M, Preston K, eds. Evolutionary Biology of Complex Phenotypes. Oxford UK.: Oxford University Press, 130-150.

Hansen TF, Wagner GP. **2001**. Modeling genetic architecture: A multilinear theory of gene interaction. *Theoretical Population Biology* **59**: 61-86.

Hansen TF, Alvarez-Castro J M, Carter AJR, Hermisson J, Wagner GP. **2006**. Evolution of genetic architecture under directional selection. *Evolution* **60**: 1523-1536.

Herbert EM, Balibar S. **2006**. Cavitation acoustique dans l'eau pure. *Physique Macroscopique* **Doctor**: 125.

Herbert EM, Balibar S, Caupin F. **2006**. Cavitation pressure in water. *Physical Review* **74**.

Herbette S, Wortemann R, Awad H, Huc R, Cochard H, Barigah T. S. 2010. Insights into xylem vulnerability to cavitation in Fagus sylvatica L.: phenotypic and environmental sources of variability. *Tree Physiology*.

Holste EK, Jerke MJ, Matzner SL. **2006**. Long-term acclimatization of hydraulic properties, xylem conduit size, wall strength and cavitation resistance in Phaseolus vulgaris in response to different environmental effects. *Plant Cell and Environment* **29**: 836-843.

Houle D. **2010**. Numbering the hairs on our heads: The shared challenge and promise of phenomics. *Proceedings of the National Academy of Sciences of the United States of America* **107**: 1793-1799.

Houle D, Govindaraju DR, Omholt S. **2010**. Phenomics: the next challenge. *Nature Reviews Genetics* **11**: 855-866.

Hu Z, Xu S. **2009**. PROC QTL - A SAS Procedure for mapping quantitative trait loci. *International Journal of Plant Genomics* **2009**: 3.

Hu Z, Xu S. **2010**. Principles and Procedures of QTL Mapping.

Jones HG. **1992**. *Plants and microclimate, a quantitative approach to environmental plant physiology - 2nd ed.* (U of Cambridge, Ed.). Cambridge, New York, USA: University of Cambridge.

Kavanagh KL, Bond BJ, Aitken SN, Gartner BL, Knowe S. **1999**. Shoot and root vulnerability to xylem cavitation in four populations of Douglas-fir seedlings. *Tree Physiology* **19**: 31-37.

Koch GW, Sillett SC, Jennings GM, Davis S D. **2004**. The limits to tree height. *Nature* **428**: 851-854.

Kohonen MM, Helland Å. **2009**. On the Function of Wall Sculpturing in Xylem Conduits. *Journal of Bionic Engineering* **6**: 324-329.

Kolb KJ, Sperry JS. **1999a**. Differences in drought adaptation between subspecies of sagebrush (Artemisia tridentata). *Ecology* **80**: 2373-2384.

Kolb KJ, Sperry JS. **1999b**. Transport constraints on water use by the Great Basin shrub, Artemisia tridentata. *Plant Cell and Environment* **22**: 925-935.

Kosorok MR. **1999**. Two-sample quantile tests under general conditions. *Biometrika* **86**: 909-921.

Kremer A, Le Corre V. **2011**. Decoupling of differentiation between traits and their underlying genes in response to divergent selection. *Heredity* **doi:10.103**.

Kronholm I, Loudet O, de Meaux J. **2010**. Influence of mutation rate on estimators of genetic differentiation - lessons from Arabidopsis thaliana. *Bmc Genetics* **11**.

Ladjal M, Deloche N, Huc R, Ducrey M. **2007**. Effects of soil and air drought on growth, plant water status and leaf gas exchange in three Mediterranean cedar species: Cedrus atlantica, C-brevifolia and C-libani. *Trees-Structure and Function* **21**: 201-213.

Lamy J-B, Bouffier L, Burlett Régis, Plomion C, Cochard H, Delzon S. **2011**. Uniform selection as a primary force reducing population genetic differentiation of cavitation resistance across a species range. *Plos One* **6**: e23476.

Larcher M, Fievet V, Burlett Régis, Delzon S. **2011**. Drought tolerance in conifers shows high levels of homoplasy. : 20.

Lauri P-E, Gorza O, Cochard H, Martinez S, Celton J-M, Ripetti V, Lartaud M, Bry X, Trottier C, Costes E. **2011**. Genetic determinism of anatomical and hydraulic traits within an apple progeny – A contribution to the hydraulic efficiency versus safety debate. *Plant and cell & Environment* **34**: 1276-1290.

Lee CE, Frost BW. **2002**. Morphological stasis in the Eurytemora affinis species complex (Copepoda□: Temoridae). *Hydrobiologia* **480**: 111-128.

Leinonen T, O'Hara RB, Cano JM, Merila J. 2008. Comparative studies of quantitative trait and neutral marker divergence: a meta-analysis. *Journal of Evolutionary Biology* **21**: 1-17.

Lewontin RC. **2008**. Punctuated equilibrium. *New York Review of Books* **55**: 39-41.

Lewontin RC, Krakauer J. **1973**. Distribution of gene frequency as a test of theory of selective neutrality of polymorphisms. *Genetics* **74**: 175-195.

Lindner M, Maroschek M, Netherer S, Kremer A, Barbati A, Garcia-Gonzalo J, Seidl R, Delzon S, Corona P, Kolström M. **2010**. Climate change impacts, adaptive capacity, and vulnerability of European forest ecosystems. *Forest Ecology and Management* **259**: 698-709.

Lindner M, Seidl R, Lexer MJ, Kremer A. **2007**. Impacts of Climate Change on European Forests and Options for Adaptation. *Development*.

Lopez-Fanjul C, Fernandez A, Toro MA. **2003**. The effect of neutral nonadditive gene action on the quantitative index of population divergence. *Genetics* **164**: 1627-1633.

Louzada JLPC, Fonseca FMA. **2002**. The heritability of wood density components in Pinus pinaster Ait . and the implications for tree breeding. **59**: 867-873.

Lynch M, Walsh B. **1998**. Genetics and analysis of quantitative traits. *Genetics and analysis of quantitative traits.*: xvi + 980 pp.

Maherali H, Pockman W T, Jackson RB. **2004**. Adaptive variation in the vulnerability of woody plants to xylem cavitation. *Ecology* **85**: 2184-2199.

Maherali H, Sherrard ME, Clifford MH, Latta RG. **2008**. Leaf hydraulic conductivity and photosynthesis are genetically correlated in an annual grass. *The New phytologist* **180**: 240-7.

Maherali H, Walden AE, Husband BC. **2009**. Genome duplication and the evolution of physiological responses to water stress. *New Phytologist* **184**: 721-731.

Maherali H, Williams BL, Paige KN, Delucia EH. **2002**. Hydraulic differentiation of Ponderosa pine populations along a climate gradient is not associated with ecotypic divergence. *Functional Ecology* **16**: 510-521.

Martinez-Meier A, Sanchez L, Pastorino M, Gallo L, Rozenberg P. **2008**. What is hot in tree rings? The wood density of surviving Douglas-firs to the 2003 drought and heat wave. *Forest Ecology and Management* **256**: 837-843.

Martinez-Vilalta J, Pinol J. **2002**. Drought-induced mortality and hydraulic architecture in pine populations of the NE Iberian Peninsula. *Forest Ecology and Management* **161**: 247-256.

Martinez-Vilalta J, Cochard H, Mencuccini M, Sterck F, Herrero A, Korhonen JFJ, Llorens P, Nikinmaa E, Nole A, Poyatos R, et al. 2009. Hydraulic adjustment of Scots pine across Europe. *New Phytologist* **184**: 353-364.

Martínez-Ballesta MC, Aparicio F, Pallás V, Martínez V, Carvajal M. **2003**. Influence of saline stress on root hydraulic conductance and PIP expression in Arabidopsis. *Journals of Plant physiology* **160**: 689-697.

Matzner SL, Rice KJ, Richards JH. **2001**. Intra-specific variation in xylem cavitation in interior live oak (Quercus wislizenii A. DC.). *Journal of Experimental Botany* **52**: 783-789.

Mayr S, Cochard H. **2003**. A new method for vulnerability analysis of small xylem areas reveals that compression wood of Norway spruce has lower hydraulic safety than opposite wood. *Plant Cell and Environment* **26**: 1365-1371.

McDowell NG. **2010**. Mechanisms Linking Drought, Hydraulics, Carbon Metabolism, and Vegetation Mortality. *Plant Physiology* **155**: 1051-1059.

McDowell NG. **2011**. Mechanisms linking drought, hydraulics, carbon metabolism, and vegetation mortality. *Plant physiology* **155**: 1051-9.

McDowell NG, Pockman William T., Allen CD, Breshears DD, Cobb N, Kolb T, Plaut J, Sperry JS, West A, Williams DG, et al. 2008. Mechanisms of plant survival and mortality during drought: why do some plants survive while others succumb to drought? *New Phytologist* **178**: 719-739.

Meirmans PG, Philip WH. **2011**. Assessing population structure: FST and related measures. *Molecular Ecology* **11**: 1.

Mencuccini M, Comstock J. **1997**. Vulnerability to cavitation in populations of two desert species, Hymenoclea salsola and Ambrosia dumosa, from different climatic regions. *Journal of Experimental Botany* **48**: 1323-1334.

Michalakis Y, Excoffier L. **1996**. A generic estimation of population subdivision using distances between alleles with special reference for microsatellite loci. *Genetics* **142**: 1061-1064.

Miller JR, Wood BP, Hamilton MB. **2008**. FST and QST under Neutrality. *Genetics* **180**: 1023-1037.

Mueller JP, James JW. **1983**. Effect on linkage disequilibrium of selection for a quantitative character with epistasis. *Theoretical and Applied Genetics*: 25-30.

Navarro C, Cavers S, Pappinen A, Tigerstedt P, Lowe A, Merila Juha. **2005**. Contrasting quantitative traits and neutral genetic markers for genetic resource assessment of Mesoamerican Cedrela odorata. *Silvae Genetica* **54**: 281-292.

Neufeld HS, Grantz DA, Meinzer F. C., Goldstein G, Crisosto GM, Crisosto C. **1992**. Genotypic variability in vulnerability of leaf xylem to cavitation in water-stressed and well-irrigated sugarcane. *Plant physiology* **100**: 1020-8.

Ogle K, Barber JJ, Willson C, Thompson B. **2009**. Hierarchical statistical modeling of xylem vulnerability to cavitation. *New Phytologist* **182**: 541-554.

O'Hara RB, Merilä J. **2005**. Bias and precision in QST estimates: problems and some solutions. *Genetics* **171**: 1331-9.

Pammenter NW, Vander Willigen C. **1998**. A mathematical and statistical analysis of the curves illustrating vulnerability of xylem to cavitation. *Tree Physiology* **18**: 589-593.

Parey S. **2008**. Extremely high temperatures in France at the end of the century. *Climate Dynamics* **30**: 99-112.

Picon C, Guehl J-M, Ferhi A. **1996**. Leaf gas exchange and carbon isotope composition responses to drought in a drought-avoiding (Pinus pinaster) and a drought-tolerant (Quercus petraea) species under present and elevated atmospheric CO2 concentrations. *Plant Cell and Environment* **19**: 182-190.

Piepho HP. **2001**. A quick method to compute approximate LOD thresholds for QTL detection. Quantitative Genetics and Breeding Methods: the Way Ahead.286-287.

Pittermann J, Sperry JS. **2003**. Tracheid diameter is the key trait determining the extent of freezing-induced embolism in conifers. *Tree Physiology* **23**: 907-914.

Pittermann J, Choat B, Jansen S, Stuart SA, Lynn L, Dawson TE. **2010**. The Relationships between Xylem Safety and Hydraulic Efficiency in the Cupressaceae: The Evolution of Pit Membrane Form and Function. *Plant Physiology* **153**: 1919-1931.

Pittermann J, Sperry JS, Hacke UG, Wheeler JK, Sikkema EH. **2006**. Inter-tracheid pitting and the hydraulic efficiency of conifer wood: The role of tracheid allometry and cavitation protection. *American Journal of Botany* **93**: 1265-1273.

Potter CS. **2008**. Terrestrial Biomass and the Effects of Deforestation on the Global Carbon Cycle, results from a model of production using satellite observations. *Bioscience* **49**: 769-778.

Queitsch Christine, Sangster T a, Lindquist Susan. **2002**. Hsp90 as a capacitor of phenotypic variation. *Nature* **417**: 618-24.

Ramirez-Valiente JA, Sanchez-Gomez D, Aranda I, Valladares F. **2010**. Phenotypic plasticity and local adaptation in leaf ecophysiological traits of 13 contrasting cork oak populations under different water availabilities. *Tree Physiology* **30**: 618-627.

Rehfeldt GE, Tchebakova NM, Parfenova YI, Wykoff WR, Kuzmina NA, Milyutin LI. **2002**. Intraspecific responses to climate in Pinus sylvestris. *Global Change Biology* **8**: 912-929.

Rosner S, Klein A, Müller U, Karlsson B. **2007**. Hydraulic and mechanical properties of young Norway spruce clones related to growth and wood structure. *Tree physiology* **27**: 1165-78.

Le Rouzic A, Carlborg O. **2008**. Evolutionary potential of hidden genetic variation. *Trends in Ecology & Evolution* **23**: 33-37.

Le Rouzic A, Alvarez-Castro José M, Carlborg O. **2008**. Dissection of the genetic architecture of body weight in chicken reveals the impact of epistasis on domestication traits. *Genetics* **179**: 1591-9.

Sangster TA, Bahrami A, Wilczek A, Watanabe E, Schellenberg K, McLellan C, Kelley A, Kong SW, Queitsch C, Lindquist S. **2007**. Phenotypic Diversity and Altered Environmental Plasticity in Arabidopsis thaliana with Reduced Hsp90 Levels. *Plos One* **2**.

Sangster TA, Salathia N, Undurraga S, Milo R, Schelienberg K, Lindquist S, Queitsch C. **2008**. HSP90 affects the expression of genetic variation and developmental stability in quantitative traits. *Proceedings of the National Academy of Sciences of the United States of America* **105**: 2963-2968.

Santure AW, Wang J. **2009**. The joint effects of selection and dominance on the QST - FST contrast. *Genetics* **181**: 259-76.

Satterthwaite FE. **1946**. An Approximate Distribution of Estimates of Variance Components. *Biometrics Bulletin* **2**: 110-114.

Scheepens JF, Stocklin J, Pluess AR. **2010**. Unifying selection acts on competitive ability and relative growth rate in Scabiosa columbaria. *Basic and Applied Ecology* **11**: 612-618.

Scheiner SM. **1993**. Plasticity as a Selectable Trait - Reply. *American Naturalist* **142**: 371-373.

Scheiner SM, Lyman RF. **1989**. The Genetics of Phenotypic Plasticity .1. Heritability. *Journal of Evolutionary Biology* **2**: 95-107.

Scotti I. **2010**. Adaptive potential in forest tree populations: what is it, and how can we measure it? *Annals of Forest Science* **67**: 801.

Segrè D, Deluna A, Church GM, Kishony R. **2005**. Modular epistasis in yeast metabolism. *Nature genetics* **37**: 77-83.

Sparks JP, Black AR. **1999**. Regulation of water loss in populations of Populus trichocarpa: the role of stomatal control in preventing xylem cavitation. *Tree Physiology* **19**: 453-459.

Sperry JS, Donnelly JR. **1988**. A method for measuring hydraulic conductivity and embolism in xylem. *Solutions*: 35-40.

Sperry JS, Hacke UG. **2004**. Analysis of circular bordered pit function - I. Angiosperm vessels with homogenous pit membranes. *American Journal of Botany* **91**: 369-385.

Sperry JS, Tyree MT. **1990**. Water-stress-induced xylem embolism in three species of conifers. *Plant and cell & Environment* **13**: 427-436.

Sperry JS, Adler FR, Campbell GS, Comstock JP. **1998**. Limitation of plant water use by rhizosphere and xylem conductance□: results from a model. *Shoot*: 347-359.

Sperry JS, Saliendra NZ, Pockman W. T., Cochard H, Cruiziat P, Davis S. D., Ewers FW, Tyree MT. **1996**. New evidence for large negative xylem pressures and their measurement by the pressure chamber method. *Plant Cell and Environment* **19**: 427-436.

Spitze K. **1993**. Population structure in Daphnia obtusa: Quantitative genetic and allozymic variation. *Genetics* **135**: 367-374.

Steane DA, Conod N, Jones RC, Vaillancourt RE, Potts BM. **2006**. A comparative analysis of population structure of a forest tree, Eucalyptus globutus (Myrtaceae), using microsatellite markers and quantitative traits. *Tree Genetics & Genomes* **2**: 30-38.

Tripiana V, Bourgeois M, Verhaegen D, Vigneron P, Bouvet JM. **2007**. Combining microsatellites, growth, and adaptive traits for managing in situ genetic resources of Eucalyptus urophylla. *Canadian Journal of Botany-Revue Canadienne De Botanique* **2007**: 773-785.

Turelli M, Barton NH. **2006**. Will population bottlenecks and multilocus epistasis increase additive genetic variance? *Evolution; international journal of organic evolution* **60**: 1763-76.

Tyree MT, Zimmermann MH. **2002**. *Xylem Structure and the Ascent of Sap* (SS in W Science, Ed.). Berlin: Springer.

Valladares F, Sanchez-Gomez D, Zavala MA. **2006**. Quantitative estimation of phenotypic plasticity: bridging the gap between the evolutionary concept and its ecological applications. *Journal of Ecology* **94**: 1103-1116.

Wang TL, Aitken SN, Kavanagh KL. **2003**. Selection for improved growth and wood quality in lodgepole pine: effects on phenology, hydraulic architecture and growth of seedlings. *Trees-Structure and Function* **17**: 269-277.

Wei CF, Tyree MT, Steudle E. **1999**. Direct measurement of xylem pressure in leaves of intact maize plants. A test of the cohesion-tension theory taking hydraulic architecture into consideration. *Plant Physiology* **121**: 1191-1205.

Weir BS, Hill WG. **2002**. Estimating F-statistics. *Annual Review of Genetics* **36**: 721-750.

Wheeler TD, Stroock AD. **2009**. Stability limit of liquid water in metastable equilibrium with subsaturated vapors. *Langmuir□: the ACS journal of surfaces and colloids* **25**: 7609-22.

Whitlock MC. **1999**. Neutral additive genetic variance in a metapopulation. *Genetical Research* **74**: 215-221.

Whitlock MC. **2008**. Evolutionary inference from QST. *Molecular Ecology* **17**: 1885-1896.

Whitlock MC. **2011**. G'ST and D do not replace FST. *Molecular ecology* **20**: 1083-91.

Willson CJ, Manos PS, Jackson RB. **2008**. Hydraulic traits are influenced by phylogenetic history in the drought-resistant, invasive genus Juniperus (Cupressaceae). *American Journal of Botany* **95**: 299-314.

Wortemann R. **2011**. Etude de la variabilité génétique et la plasticité phénotypique de la vulnérabilité à la cavitation chez Fagus sylvatica. : 1-129.

Wortemann R, Herbette S, Barigah Têtè Sévérien, Fumanal B, Alia R, Ducousso A, Gomory D, Roeckel-Drevet P, Cochard H. **2011**. Genotypic variability and phenotypic plasticity of cavitation resistance in Fagus sylvatica L. across Europe. *Tree physiology*: 1-8.

Xu S. **2003**. Theoretical basis of the Beavis effect. *Genetics* **165**: 2259-68.

Yang RC, Yeh FC, Yanchuk AD. **1996**. A comparison of isozyme and quantitative genetic variation in Pinus contorta ssp. latifolia by FST. *Genetics* **142**: 1045-1052.

Yoshida Y, Honjo M, Kitamoto N, Ohsawa R. **2008**. Genetic variation and differentiation of floral morphology in wild Primula sieboldii evaluated by image analysis data and SSR markers. *Breeding Science* **58**: 301-307.

6 - Annexes

Plasmodesmatal pores in the torus of bordered pit membranes affect cavitation resistance of conifer xylem
Steven Jansen* and Jean-Baptiste Lamy*, Régis Burlett, Hervé Cochard, Peter Gasson, Sylvain Delzon (* co first author).
Pusblished in *Plant, Cell and Environement*

Uniform Selection as a Primary Force Reducing Population Genetic Differentiation of Cavitation Resistance across a Species Range
Jean-Baptiste Lamy, Laurent Bouffier, Régis Burlett, Christophe Plomion, Hervé Cochard, Sylvain Delzon
Pusblished in *PLoS ONE*

Genetic variation for resistance to cavitation among *Pinus hartwegii* populations
Cuauhtemoc Saenz-Romero, Sylvain Delzon, Jean-Baptiste Lamy, Esperanza Loya-Rebollar, Andrés Plaza-Aguilar, Régis Burlett, Philippe Lobit.
Submitted to *Acta Physiologiae Plantarum*

Evolutionary stasis of wood density in a pine species
Jean-Baptiste Lamy, Frédéric Lagane, Christophe Plomion, Hervé Cochard, Sylvain Delzon
Submitted to *Plant Ecology*

$\underline{Q}_{ST}<F_{ST}$ as a signature of canalization
Jean-Baptiste Lamy, Christophe Plomion, Antoine Kremer, Sylvain Delzon
In revision for *Molecular Ecology*

Genotypic and environmental variation in cavitation resistance in a pine species transplanted in wet and dry provenance tests
Jean-Baptiste Lamy, Sylvain Delzon, Pauline Bouche, Ricardo Alia, Giovanni Giuseppe Vendramin, Christophe Plomion, Hervé Cochard.
Submitted to *New-Phytologist*

Quand les arbres pleurent ou quand la sève surfe sur les lois de la thermodynamique.
Jean-Baptiste Lamy
Publié dans *Plume magazine* (vulgarisation scientifique)

Plant, Cell and Environment (2012) doi: 10.1111/j.1365-3040.2011.02476.x

Plasmodesmatal pores in the torus of bordered pit membranes affect cavitation resistance of conifer xylem

S. JANSEN[1]*, J.-B. LAMY[2], R. BURLETT[2], H. COCHARD[3], P. GASSON[1] & S. DELZON[2]

[1]Jodrell Laboratory, Royal Botanic Gardens, Kew, Richmond, Surrey TW9 3DS, UK, [2]INRA, University of Bordeaux, UMR BIOGECO, Talence, France and [3]INRA, UMR 547 PIAF, F-63100 Clermont-Ferrand, France

ABSTRACT

The pit membrane in bordered pits of conifer tracheids is characterized by a porous margo and central thickening (torus), which is traditionally considered to function as an impermeable safety valve against air-seeding. However, electron microscopy based on 33 conifer species, including five families and 19 genera, reveals that pores occur in the torus of 13 of the species studied. The pores have a plasmodesmatal origin with an average diameter of 51 nm and grouped arrangement. Evidence for embolism spreading via pores in tori is supported by the pore sizes, which correspond relatively well with the pressure inducing cavitation. Predictions based on earlier correlations between pit structure and cavitation resistance were only weakly supported for species with punctured tori. Moreover, species with punctured tori are significantly less resistant to cavitation than species with non-punctured tori. Nevertheless, absolute pore diameters must be treated with caution and correlations between theoretical and measured air-seeding pressures are weak. Because most pores appear not to traverse the torus but are limited to one torus pad, only complete pores would trigger air-seeding. Embolism spreading through a leaky torus is not universal across gymnosperms and unlikely to represent the only air-seeding mechanism.

Key-words: air-seeding; conifer wood; torus-margo; tracheid.

INTRODUCTION

The study of bordered pits and their biological significance in xylem has fascinated plant anatomists for centuries (Choat, Cobb & Jansen 2008). Soon after understanding that a pit membrane represents the primary wall that runs between the bordered pit cavities of a pit pair (Schacht 1859), much attention has been paid to conifer pit membranes with a 'torus', which represents the central thickening of the pit membrane and is surrounded by a porous 'margo' (Von Nägeli 1864; Sanio 1873; Russow 1883; Strasburger 1891; Liese 1965; Bauch, Schultze & Liese 1972). Pit membranes are of special interest for understanding structure – function relationships of water transport because they determine hydraulic efficiency for water flow between neighbouring tracheary elements, and limit the passage of air bubbles and pathogens into the sap stream (Tyree & Zimmermann 2002; Choat *et al*. 2008; Jansen, Choat & Pletsers 2009). Interest in the function of pit membranes is also due to their role in the movement of liquids and gas within wood and their influence on the permeability, drying and pulping of timber (Flynn 1995; Singh *et al*. 1999; Bao, Lu & Zhao 2001; Usta & Hale 2006).

As the porosity of tracheid walls is highest where there are pits, drought-induced cavitation is thought to occur at the pit level by a process called 'air-seeding' (Sperry & Tyree 1988, 1990; Tyree & Zimmermann 2002). The functional explanation for the nature of torus-margo pit membranes in conifers is that tori behave as safety valves, which are able to block off the pit aperture where there is a pressure difference between adjacent tracheids (Bailey 1913, 1916; Hart & Thomas 1967; Cochard *et al*. 2009). When a torus is in its relaxed, unaspirated position, the thin and porous margo is shown to offer a pit-area resistance that is on average 59 times lower than an angiosperm pit membrane (Hacke, Sperry & Pittermann 2004; Pittermann *et al*. 2005, 2010; Pittermann 2010). Aspirated tori, however, prevent the spreading of air into neighbouring tracheids. This sealing mechanism seems to be valid up to a certain threshold and air-seeding will occur when the pressure drop difference between adjacent tracheids exceeds a certain limit (Cochard *et al*. 2009; Delzon *et al*. 2010). The exact location of the air-seeding mechanism, however, remains unclear and two likely hypotheses have been proposed: (1) seal capillary-seeding (i.e. the torus does not perfectly seal the outer pit aperture, allowing air bubbles to pass through micropores at the edge of the torus); and (2) torus capillary-seeding (i.e. air-seeding through pores in the torus) (Delzon *et al*. 2010). Recent studies also demonstrate that anatomical features correlated with air-seeding in conifer tracheids mainly include torus thickness and the ratio of the torus to pit aperture diameter, but do not vary systematically with

Correspondence: S. Jansen. Fax: +49 731 502 3320; e-mail: steven.jansen@uni-ulm.de

*Present address: Institute of Systematic Botany and Ecology, Albert-Einstein-Allee 11, Ulm University, D-89081 Ulm, Germany.
Contributors: S.J. and J.-B.L. contributed equally to this study and are both considered as first authors.

margo porosity (Cochard *et al*. 2009; Hacke & Jansen 2009; Delzon *et al*. 2010; Pittermann *et al*. 2010).

The traditional understanding of air-seeding in bordered pits of conifers is based on the assumption that tori are impermeable to water and air, and that the valve mechanism depends on the elastic properties of the margo (Liese & Johann 1954; Liese 1965; Liese & Bauch 1967; Comstock & Côté 1968; Bao *et al*. 2001; Hacke *et al*. 2004). Therefore, the thick and non-porous nature of the torus plays a crucial role in the safety valve hypothesis. However, earlier observations suggested the presence of minute pores in the torus of *Abies firma*, *Abies sachalinensis*, *Pinus koraiensis*, *Pinus palustris*, *Pinus serotina*, *Pinus taeda*, *Pinus wallichiana* and *Tsuga sieboldii* (Thomas 1969; Thomas & Nicholas 1969; Fujikawa & Ishida 1972; Panshin & De Zeeuw 1980; Sano, Kawakami & Ohtani 1999; Dute, Hagler & Black 2008; Roth-Nebelsick, Voigt & Gorb 2010). Thomas (1969) suggested that the openings in tori of *Pinus* represent plasmodesmata because of their circular depression and raised central position. More recent observations in *A. firma* showed that the pores in tori of mature pit membranes correspond to channels of secondary (i.e. post-cytokinetically formed) plasmodesmata (Dute *et al*. 2008). Furthermore, Sano *et al*. (1999) demonstrated that the frequency of tori with pores varied from 45 to 81% across the innermost and middle area of the last three growth rings in *A. sachalinensis*. While some earlier observations of micropores in the torus of conifer pit membranes were interpreted as preparation artefact (Jansen, Pletsers & Sano 2008), cryo-scanning electron microscopy (SEM) demonstrated that pores detected in *P. wallichiana* represent real features associated with the native state of pit membranes (Roth-Nebelsick *et al*. 2010).

Taxonomic implications and functional consequences for conifers with punctured tori remain unclear. Minute openings in tori have recently been suggested as a functional explanation for the air-seeding mechanism in gymnosperms (Cochard *et al*. 2009; Delzon *et al*. 2010). Therefore, we hypothesize that the occurrence and the size of pores associated with tori are correlated with vulnerability to xylem cavitation, which is known to vary extensively within conifers (Maherali, Pockman & Jackson 2004; Delzon *et al*. 2010; Pittermann *et al*. 2010). The two major aims of this study are: (1) to explore the distribution of tori with pores across gymnosperms; and (2) to test whether these pores could represent sites of air-seeding associated with drought-induced cavitation. Both goals will be addressed by sampling across a broad taxonomic range of gymnosperms and by exploring in detail what aspects of pit structure are related to the variation in cavitation resistance. In particular, earlier hypotheses regarding cavitation resistance and pit morphology will be evaluated for the species with punctured tori. Overall, this paper aims to better understand the structural basis of cavitation resistance, which is a major issue in identifying the genetic background of drought resistance in plants.

MATERIALS AND METHODS

Plant material

A total of 33 conifer species was investigated, covering 5 families and 19 genera (Table 1). As we aimed to examine three to five specimens per species, criteria for species selection were: (1) the availability of three to five mature and healthy trees for each species; and (2) the taxonomic position, aiming to include species with a taxonomic range as broad as possible. For *Pinus nigra* and *P. wallichiana*, only one specimen was collected. Most trees sampled were growing at the Royal Botanic Gardens, Kew (UK) with an average daily temperature of 10.8 °C and 605 mm of annual rainfall.

Straight branches fully exposed to the sun were collected from each tree where they were most conveniently reached. The samples were longer than 40 cm and the xylem was 3–10 mm in diameter. Compression wood was avoided, and needles were removed as soon as possible in order to stop transpiration. The fresh stem segments were then immediately wrapped in wet paper towels and plastic bags, and brought to the laboratory.

Scanning electron microscopy

SEM observations were conducted on air-dried samples that were used for measuring cavitation resistance. Although intraspecific variation of pit morphology can be significant (Domec *et al*. 2008; Jansen *et al*. 2009; Schoonmaker *et al*. 2010; Gortan *et al*. 2011), qualitative features such as the presence or absence of punctured tori were assumed to be consistently present or absent for a given species. Although this assumption was only tested on observations for two species (*Pinus hartwegii* and *Pinus pinaster*), our approach mainly aimed at studying the taxonomic variation of pores in tori across various conifer genera and families. Therefore, SEM observations were limited to one sample for most species. We selected the sample that was closest to the average P_{50} value for each species.

SEM preparation followed standard protocols, except that the samples were briefly treated in an alcohol series (50, 70, 90, 100% ethanol) for a total of 5 min in order to remove pit membrane encrustations that could make detection of pores difficult (Thomas 1969; Jansen *et al*. 2008, 2009). Based on a total of 30 different preparation techniques applied by Jansen *et al*. (2008), the effect of chemical solutions and timing of treatment on pore size was examined for *P. wallichiana* and *Pinus radiata*. All SEM specimens were mounted on aluminium stubs using conductive carbon cement (Neubauer chemikaliën, Münster, Germany). Once dry, the mounted specimens were coated with platinum using an Emitech K550 sputter coater (Emitech Ltd, Ashford, UK) for 2 min, resulting in a ca. 10-nm-thick coating layer. Observations were carried out with a Hitachi cold-field emission SEM S-4700 (Hitachi High Technologies Corp., Tokyo, Japan) under 2 kV.

Table 1. List of the species studied with reference to their taxonomic family and origin; specimens in bold show pores in the torus of bordered pit pairs observed by electron microscopy

Family	Species	Authority	Origin and accession number	P_{50} (MPa) ± SE
Cephalotaxaceae	*Cephalotaxus fortunei*	Hook.	RBG Kew, 1969-16466	–7.21 ± 0.48
Cephalotaxaceae	***Cephalotaxus harringtonii***	**Knight ex J.Forbes**	**RBG Kew, 1969-16244**	**–7.21 ± 0.48**
Cupressaceae	*Callitris columellaris*[a]	F.Muell.	University of Tasmania, Hobart	–15.79 ± 0.18
Cupressaceae	*Callitris gracilis*[a]	R.T.Baker	University of Tasmania, Hobart	–12.26 ± 0.59
Cupressaceae	*Callitris preissii*[a]	Miq.	University of Tasmania, Hobart	–14.96 ± 0.50
Cupressaceae	*Callitris rhomboidea*[a]	R.Br.	University of Tasmania, Hobart	–9.60 ± 1.45
Cupressaceae	*Chamaecyparis obtusa*	Siebold & Zucc.	RBG Kew, 1969-10594	–3.70 ± 0.12
Cupressaceae	*Chamaecyparis pisifera*	(Siebold & Zucc.) Endl.	RBG Kew, 607-12-60702	–3.46 ± 0.21
Cupressaceae	*Cupressus dupreziana*	A.Camus	RBG Kew, 1970-6193	–10.29 ± 0.60
Cupressaceae	*Cupressus torulosa*	D.Don	RBG Kew, 1996-1799	–8.35 ± 0.60
Cupressaceae	*Metasequoia glyptostroboides**	Hu & W.C.Cheng	RBG Kew, 1980-6256	–2.91 ± 0.13
Cupressaceae	*Platycladus orientalis*	(L.) Franco	RBG Kew, 1976-3574	–9.04 ± 0.45
Cupressaceae	***Sequoia sempervirens***	**Endl.**	**University of Bordeaux, Château du Haut-carré**	**–4.38 ± 0.17**
Cupressaceae	***Sequoiadendron giganteum***	**(Lindl.) J.Buchholz**	**University of Bordeaux, Château du Haut-carré**	**–3.79 ± 0.07**
Cupressaceae	*Taiwania cryptomerioides*	Hayata	RBG Kew, 1994-900	–3.38 ± 0.29
Cupressaceae	*Thuja plicata**	Donn ex D.Don	RBG Kew, 1973-18600	–4.20 ± 0.13
Cupressaceae	*Thujopsis dolabrata*	Siebold & Zucc.	RBG Kew, 1969-16072	–5.63 ± 0.41
Cupressaceae	***Xanthocyparis nootkatensis***	**(D.Don) Farjon & D.K.Harder**	**RBG Kew, 1969-13806**	**–5.14 ± 0.25**
Pinaceae	***Abies balsamea***[*b]	**(L.) Mill.**	**University of Alberta, Edmonton, Canada**	**–3.64 ± 0.34**
Pinaceae	*Cedrus atlantica**	(Endl.) G.Manetti ex Carrière	RBG Kew, 2000-4686	–5.13 ± 0.08
Pinaceae	*Cedrus deodara*	Loudon	Clermont-Ferrand, France	–7.25 ± 0.41
Pinaceae	***Larix decidua****	**Mill.**	**RBG Kew, 1979-6300**	**–4.30 ± 0.37**
Pinaceae	***Picea glauca***[*b]	**(Moench) Voss**	**University of Alberta, Edmonton, Canada**	**–4.35 ± 0.26**
Pinaceae	***Picea mariana***[*b]	**(Mill.) BSP.**	**Edson, Canada**	**–5.21 ± 0.19**
Pinaceae	***Pinus hartwegii****	**Lindl.**	**RBG Kew, 1996-1016**	**–3.43 ± 0.18**
Pinaceae	***Pinus nigra****	**J.F.Arnold**	**RBG Kew, 1973-15503**	**–3.52**
Pinaceae	***Pinus pinaster****	**Aiton**	**Bordeaux, 503, 361, 441, 463B**	**–3.73 ± 0.07**
Pinaceae	***Pinus radiate***	**D.Don**	**University of Tasmania, Hobart**	**–4.38 ± 0.14**
Pinaceae	***Pinus wallichiana***[*c]	**A.B.Jacks**	**RBG Kew, 1979-2373**	**–2.39**
Sciadopityaceae	*Sciadopitys verticillata*	Siebold & Zucc.	RBG Kew, 1979-48	–3.94 ± 0.13
Taxaceae	*Torreya californica*	Torr.	RBG Kew, 1969-14196	–6.39 ± 0.30
Taxaceae	*Torreya grandis*	Fortune ex. Lindl.	RBG Kew, 1973-20815	–4.69 ± 0.25
Taxaceae	*Torreya nucifera*	Siebold & Zucc.	RBG Kew, 1969-15523	–5.94 ± 0.30

Air-dried material was used for scanning electron microscopy (SEM); transmission electron microscopy (TEM) was based on air-dried material for most species, but on fresh material for species followed by an asterisk (*). Average P_{50} values are based on three to five specimens and correspond to the pressure inducing 50% loss of hydraulic conductance; $n = 1$ specimen for *P. nigra* and *P. wallichiana*. [a]Material studied by Brodribb *et al*. (2010); [b]material studied by Hacke & Jansen (2009); [c]material studied by Jansen *et al*. (2008).

Transmission electron microscopy (TEM)

TEM was based on one wood sample per species, selecting the same branch that was also used for SEM. Air-dried wood from the two most recent growth rings was cut into 1 mm^3 blocks and dehydrated through a graded ethanol series. The ethanol was gradually replaced with LR White resin (London Resin Co, Reading, UK) over several days. The resin was polymerized in a Gallenkamp vacuum oven at 60 °C and 1000 mbar for 24 h. Embedded samples were trimmed with a Leica EM specimen trimmer (Leica Microsystems, Vienna, Austria) and sectioned on an ultramicrotome (Ultracut, Reichert-Jung, Austria). Transverse, ultra-thin sections were cut between 60 and 90 nm using a diamond knife, attached to Formvar (Agar Scientific, Stansted, UK) and 100 mesh copper grids, and stained with uranyl acetate and lead citrate using a Leica EM Stain Ultrostainer (Leica Microsystems). Observations were carried out with a JEOL JEM-1210 TEM (Jeol, Tokyo, Japan) at 80 kV accelerating voltage, and digital images were taken using a MegaView III camera (Soft Imaging System, Münster, Germany).

For 11 species (Table 1), TEM was applied to fresh material, which was cut into 1 mm^3 blocks and fixed overnight in Karnovsky's fixative at room temperature. After washing in a 0.05 M phosphate buffer, the specimens were postfixed in 1% buffered osmium tetroxide for 4 h at room temperature, and washed again. Further preparation followed the method given above.

Anatomical measurements

For each species a minimum of ca. 100 tori was observed using SEM, while the size of ultra-thin sections limited TEM observations to ca. 50 tori per species. SEM observations were mainly conducted on aspirated pit membranes at magnifications above 10 000. Both non-aspirated and aspirated pit membranes were seen with TEM, with higher frequencies of relaxed pit membranes in fresh material than air-dried wood.

Pit morphological features from earlywood tracheids were quantified for all 13 species with punctured tori. Pit membrane diameter (D_m), torus diameter (D_t) and pit aperture diameter (D_a) were measured at the widest point and in horizontal direction using SEM images. Pits with torus extensions (i.e. margo straps) were excluded from torus diameter measurements. Because of significant scaling between D_m, D_t and D_a (Hacke & Jansen 2009; Supporting Information Figure S2), a minimum of 15 aspirated pit membranes per species were measured, which allowed quantifying D_m, D_t and D_a on the same pit. Torus overlap (O) was defined following Delzon *et al*. (2010) as $(D_t - D_a)/D_t$, and as $(D_t - D_a)/(D_m - D_a)$ according to Hacke *et al*. (2004). The margo flexibility index ($F = (D_m - D_t)/D_t$) and valve effect ($V_{ef} = F \times O$) were estimated according to Delzon *et al*. (2010). The size of the pores associated with tori was consistently measured for a minimum of 25 pores per species. For most species, however, we measured more than 40 pores from ca. 20 pit membranes. For the *P. wallichiana* samples prepared according to Jansen *et al*. (2008), only conditions similar to 5 min of alcohol treatment were used to measure pore size.

Based on TEM images, the maximum margo thickness (M_t), the torus thickness (T_t) in the centre of the torus and the pit chamber depth (i.e. the maximum distance between overarching pit borders of a pit pair, D_p) were measured for all species with punctured tori except for *P. wallichiana* and *Sequoiadendron giganteum*. Average values for these TEM characteristics were determined based on a minimum of 10 measurements.

All anatomical measurements were conducted using ImageJ software (Rasband 1997–2011).

Xylem vulnerability to cavitation

To investigate intraspecific variation, vulnerability to cavitation was measured for three to five specimens per species. Except for the three species studied by Hacke & Jansen (2009; Table 1), vulnerability curves were based on the cavitron technique as described previously (Cochard 2002; Cochard *et al*. 2005; Delzon *et al*. 2010). Measurements were performed at the high-throughput phenotyping platform for hydraulic traits (CaviPlace, University of Bordeaux, Talence, France) using a custom-built honeycomb rotor (Precis 2000, Bordeaux, France) mounted on a Sorvall RC5 ultracentrifuge (Fisher Scientific, Schwerte, Germany). Samples were kept refrigerated and vulnerability to cavitation was determined within 2 weeks of collection. All samples were debarked to avoid resin exudation, re-cut under water to a standard length of 27 cm, and both ends were trimmed with a fresh razor blade to obtain perfectly smooth surfaces with open tracheids. A solution of ultrapure and degassed water including 10 mM KCl and 1 mM $CaCl_2$ was used as reference solution for hydraulic measurements. After measuring the maximum hydraulic conductance under low (i.e. close to zero) xylem pressure (P), the rotation speed of the centrifuge was gradually increased by 0.5 or 1 MPa to determine the percentage loss of hydraulic conductance (PLC). The rotor velocity was monitored using an electronic tachymeter (A2108-LSR232; Compact Inst, Bolton, UK) with a 10 r.p.m. resolution, and the xylem pressure was adjusted to ± 0.02 MPa. We used Cavi_soft software (version 1.5, University of Bordeaux) for conductance measurements and the computation of all vulnerability curves, which were adjusted according to Pammenter and Vander Willigen (1998). The P_{50} value was defined as the pressure corresponding to 50% PLC and averaged for each species. Similarly, P_{12} was defined as the pressure equivalent to 12% PLC, which corresponds to air entry in the xylem. S_{50} was defined as the slope of the vulnerability curve at the inflexion point (Pammenter & Vander Willigen 1998), which corresponds to the speed of embolism in the xylem system per unit of pressure (% MPa^{-1}).

The theoretical pressure gradient (ΔP, in MPa) required to pull an air bubble through the pore of a pit membrane was calculated based on the Young–Laplace equation as $\Delta P = 4\,(\tau \cos\theta / D)$, where D (nm) represents the diameter of the pit membrane pore and τ (N m^{-1}) is the surface tension of water. The contact angle (θ) between the air-water-pit membrane interface was assumed to be 0°.

Statistical analysis

Statistical differences between species with punctured tori ($n = 13$) and non-punctured tori ($n = 20$) were inferred using the following mixed model:

$$\boldsymbol{y} = \boldsymbol{X\beta} + \boldsymbol{Z\gamma} + \boldsymbol{\varepsilon}$$

$\boldsymbol{y}$ is the observation vector (here P_{50} and S_{50}). $\boldsymbol{X}$ represents a design matrix linking the observation to fixed effects and $\boldsymbol{\beta}$ is a vector of the fixed effect (here, *torus anatomy* with two levels 'punctured' and 'non-punctured tori'). $\boldsymbol{Z}$ is a random effect matrix linking observations to random effects and $\boldsymbol{\gamma}$ is a random effects vector (here, *family* with five levels and *genus* nested within *family* with one to five levels). At first, we ran the fixed part of this model to assess if there was an effect of torus anatomy on P_{50} and S_{50}. Afterwards, the full model was run to consider the putative phylogenetic autocorrelation between species (Chave *et al*. 2009). Differences were considered statistically significant at $P \leq 0.05$.

Classical linear regression analyses were used to determine the relationship between (1) torus capillary-seeding and resistance to cavitation; (2) pit dimensions (D_a, D_t, D_m); (3) pore diameter in tori and torus thickness; and (4) pit functional traits (O, F, V_{ef}).

Statistical analyses were performed using SAS software (SAS 9.2; SAS Institute, Cary, NC, USA).

RESULTS

The anatomy of punctured tori

Torus-margo pit membranes were found in all species studied. The torus could be distinguished from the margo due to its non-porosity and high electron density as seen with the SEM and TEM, respectively (Figs 1 & 2). Punctured tori were observed in 13 species using SEM (Table 1; Fig. 1b–j), while all other species studied showed tori without distinct pores (Fig. 1a). Punctured tori were consistently present in the two specimens of *P. hartwegii* and the four trees of *P. pinaster* studied.

The size of the pores varied from 12 to 144 nm, with a mean diameter of 49 (±9) nm (±SD) based on SEM

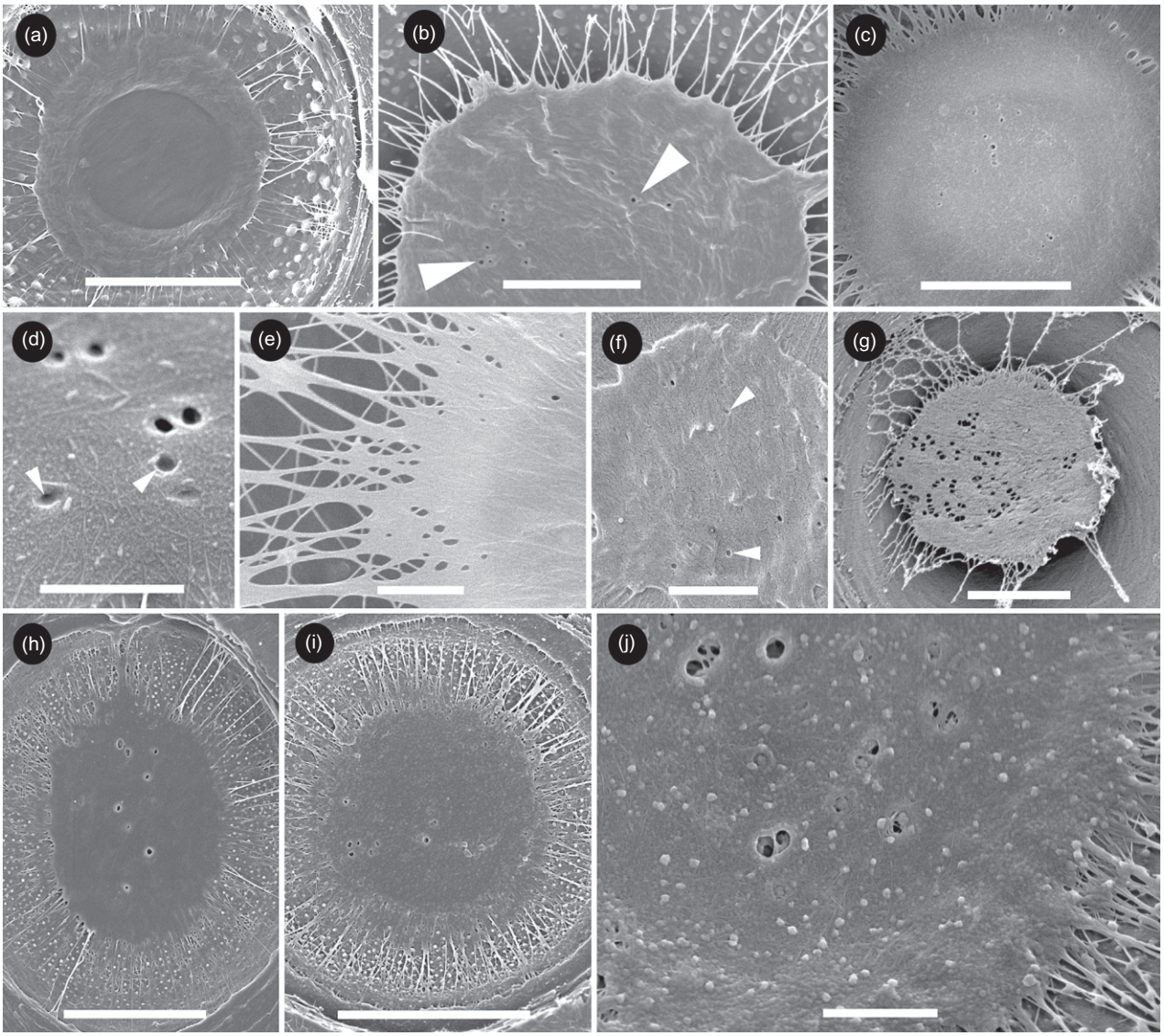

Figure 1. Scanning electron microscope images of bordered pit membranes in conifer tracheids showing the ultrastructure of the torus. (a) *Pinus radiata*, aspirated pit membrane, the outline of the inner pit aperture, which has a smaller diameter than the torus, can be seen through the torus, distinct warts occur on the surface of the pit border, scale bar = 5 μm; (b) *Pinus pinaster*, arrowheads indicate several pores in the torus, scale bar = 2 μm; (c) *Cephalotaxus harringtonii*, detail of torus with minute pores, scale bar = 2 μm; (d) *Picea mariana*, detail of torus with shallow (arrowheads) and deep pores, scale bar = 500 nm; (e) *Torreya californica*, detail of torus and margo, the pores occurring on the torus-margo border are interpreted as margo pores and not as plasmodesmatal pores, scale bar = 500 nm; (f) *Pinus wallichiana*, torus detail of oven dried (100 °C) sample, some of the pores appear superficial and partly filled with material (arrowheads), scale bar = 2 μm; (g) *P. wallichiana*, sample after critical point drying and treatment with 100% ethanol, which resulted in an increased pore size and reduced microfibril network of the margo, scale bar = 2.5 μm; (h) *Sequoia sempervirens*, aspirated pit membrane with punctured torus, scale bar = 5 μm; (i) *Sequoiadendron giganteum*, overview of a punctured torus, scale bar = 5 μm; (j) *S. giganteum*, detail of pores showing different levels of penetration into the torus, scale bar = 1 μm.

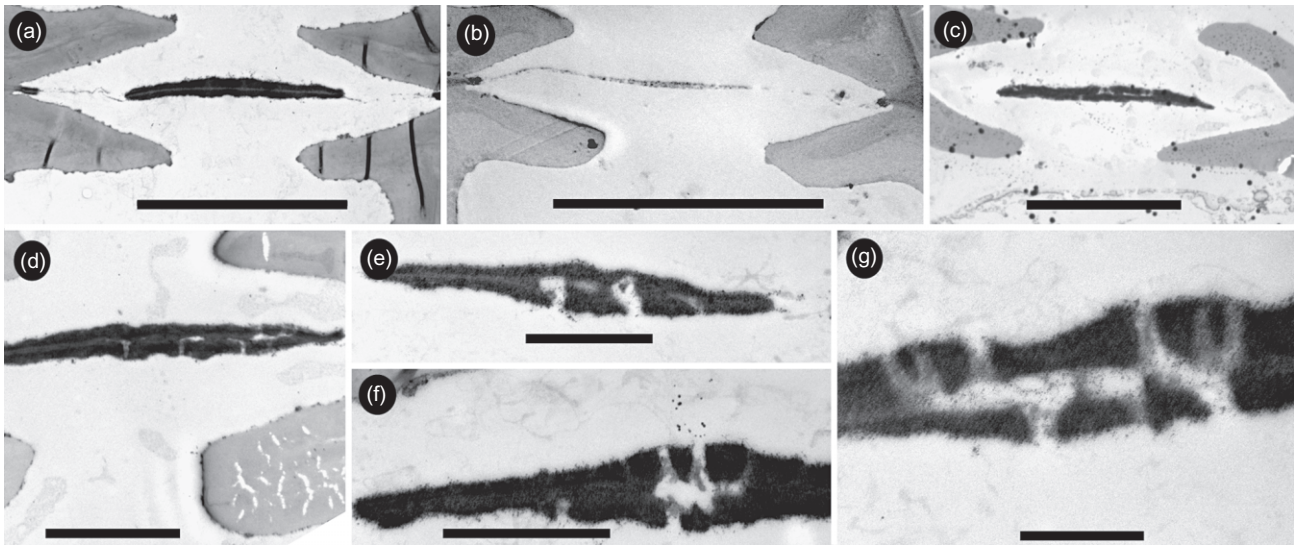

Figure 2. Transmission electron microscope images of bordered pit membranes in conifer tracheids showing details of the central torus and plasmodesmatal channels. (a) *Pinus hartwegii*, pit membrane showing a non-punctured, electron dense torus, thin margo and electron dense pit membrane annulus near the pit border, scale bar = 5 μm; (b) *Metasequoia glyptostroboides*, thin pit membrane consisting of a margo and indistinct, thin torus, scale bar = 5 μm; (c) *Larix decidua*, torus with minute pores, scale bar = 5 μm; (d) *Pinus pinaster*, detail of torus with several plasmodesmatal channels, scale bar = 2 μm; (e) *P. hartwegii*, two distinct plasmodesmatal channels seemingly terminating at the middle lamella, a third, indistinct pore can be seen on the right, scale bar = 1 μm; (f) *P. hartwegii*, pores piercing the entire torus and sharing a single median cavity, scale bar = 1 μm; (g) *P. hartwegii*, various plasmodesmatal pores with a typically branched pattern share a single median cavity and give the torus a sieve-like, permeable appearance, scale bar = 500 nm.

(Supporting Information Table S1). Treatment with alcohol and other dissolving solutions had a clear effect on the size of the pores in *P. wallichiana* (Fig. 1f,g). The average pore size in this species (61 nm ± 27) increased substantially after the following treatments: 85 (±42) nm (formalin-acetic-alcohol treatment), 135 (±57) nm (100% ethanol in combination with critical point drying; Fig. 1g), 116 (±42) nm (glacial acetic acid) and 100 (±17) nm (oven drying at 100 °C; Fig. 1f). However, no significant difference was found with respect to the pore size in *P. radiata* when comparing no alcohol treatment with 5 min of ethanol treatment. The only morphological difference was that pores in SEM material not treated with alcohol showed a circular depression with a slightly raised area in the centre, which was not seen after alcohol treatment (images not shown).

No difference was found in the occurrence of punctured tori between ray tracheid to longitudinal tracheid pit pairs and longitudinal tracheid bordered pit pairs. Overall, the frequency of the pores was low and rarely exceeded more than 10% of the pits. The highest frequencies were counted in *P. hartwegii*, in which tori with pores were found in 31% of the pits observed. The shape of the pores was usually round. Some pores appeared superficial and partly filled with material, while others penetrated more deeply into the torus (Fig. 1d,f,j). They were distributed across the entire torus, with similar frequency in the centre and peripheral areas of the torus. However, in most cases the pores were characteristically grouped in small pairs of two or more (Fig. 1b–j).

In some species, solitary pores near the edge of the torus as seen with SEM were not interpreted as plasmodesmatal pores because of their similarity in size and morphology to margo pores (Fig. 1e). The largest margo pores varied from 330 to 1060 nm. Margo pores near the periphery of the torus were especially common in species with torus extensions (*Cupressus dupreziana*, *Cupressus torulosa*, *Sequoia sempervirens*), and in species with a relatively thin torus (*Metasequoia glyptostroboides*, *Thujopsis dolabrata* and *Torreya grandis*; Fig. 2b). Minute pores (generally < 50 nm) could also be seen using SEM and TEM in the central part of the torus in the latter three species, which showed an average torus thickness around 100 nm as compared with a mean torus thickness of 503 nm for species with punctured tori (Fig. 5). Not only the size of the torus pores in *M. glyptostroboides*, *T. dolabrata* and *T. grandis*, but also their non-grouped distribution suggested that these pores did not represent plasmodesmatal pores, but were due to the thin torus nature.

TEM observations demonstrated the occurrence of punctured tori in six species, in which this feature was also seen with SEM (Fig. 2c–g). However, no pores could be detected with TEM in *Cephalotaxus harringtonia*, *Chamaecyparis nootkatensis*, *Picea glauca*, *P. wallichiana*, *P. radiata* and *S. sempervirens*, which showed pores based on SEM (Fig. 1c,f,g). TEM measurements of the pore size were larger than those based on SEM, but within the same order of magnitude. The average TEM pore size was 64 (±10) nm (±SD), and the largest pore measured based on TEM was 150 nm in *Larix decidua*. Most pores could not be seen to extend through the complete torus, but were limited to one torus pad and gave the impression of terminating in a cavity near the middle lamella (Fig. 2c–e). However, pores were

occasionally seen to traverse the entire torus (Fig. 2f,g), and TEM confirmed that the channels were usually arranged in a branched pattern, with several pores connected laterally to each other via an extensive median cavity at the level of the middle lamella (Fig. 2f,g). The branched channels occasionally resulted in a sieve-like appearance of the torus (Fig. 2g).

Xylem vulnerability to cavitation

P_{50} values varied from –15.79 to –2.39 MPa among the species studied (Table 1). There was a significant difference ($P = 0.01$) in vulnerability to cavitation (P_{50}) between species with and without punctured tori: species with punctured tori were less cavitation resistant than species with no plasmodesmatal pores associated with their tori, with average P_{50} values of –4.3 and –7.2 MPa, respectively (Fig. 3). Similarly, we found that species with punctured tori have a greater S_{50} compared with species without punctured tori (Supporting Information Figure S1; $P < 0.0001$), and that this trend remained significant with control for taxonomy ($P = 0.024$). However, there was no statistical significance when considering the taxonomic influence on the difference in P_{50} between species with and without punctured tori ($P = 0.21$).

The air-seeding pressures estimated using the largest margo pores varied from 0.27 to 0.88 MPa and were 10 times lower in absolute value than the measured air-seeding pressure (P_{50}). By contrast, the air-seeding pressures based on the SEM size of plasmodesmatal pores in tori were of the same order of magnitude than the measured air-seeding pressures, varying from 2.02 to 4.16 MPa. However, there were weak correlations between P_{50} values derived from vulnerability curves and the theoretical air-seeding pressures based on the maximum and average SEM pore sizes, which corresponded to the torus capillary-seeding pressures (Fig. 4a). Torus capillary-seeding pressures as based on the average SEM pore sizes were lower in absolute value than the P_{50} values in all species. There was a significant correlation between the P_{12} values and the torus capillary-seeding pressure based on the maximum SEM pore size (Fig. 4b). Weak correlations were found when plotting P_{50} versus air-seeding based on average SEM pore size ($P = 0.064$; Fig. 4a), and P_{12} values versus air-seeding pressures derived from average SEM pore sizes ($P = 0.074$; Fig. 4b).

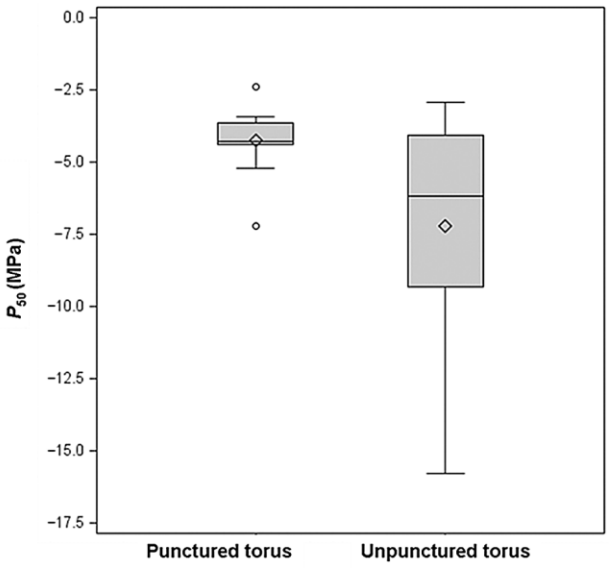

Figure 3. Box plot illustrating a significant difference ($P = 0.01$) in vulnerability to xylem cavitation (P_{50}, i.e. the pressure required to induce 50% loss of hydraulic conductance) between species with punctured tori ($n = 13$) and non-punctured tori ($n = 20$). This trend is not significant ($P = 0.21$) when including taxonomy based on a mixed model (see Materials and methods for details).

A strong allometry was found between D_m, D_t and D_a for species with punctured tori (Supporting Information Figure S2) with high coefficients of determination (Pearson correlation coefficients $R = 0.93$ for D_m versus D_t; $R = 0.88$ for D_m versus D_a; $R = 0.87$ for D_t versus D_a) and high significance ($P < 0.0001$). The slope of the regression lines was more or less similar for D_m versus D_t and D_t versus D_a (0.55 and 0.5, respectively), but lower for D_m versus D_a (0.30). Across the species with punctured tori, D_m, D_t and D_a decreased with increasing resistance to cavitation. However, only D_t showed a significant correlation with P_{50} (Pearson correlation = 0.63, $P = 0.02$).

Pit chamber depth (D_p), margo thickness (M_t) and torus thickness (T_t) showed no correlation with P_{50}. Interestingly, torus thickness (T_t) was positively correlated with the maximum diameter of plasmodesmatal pores, but not with the average pore diameter based on SEM (Fig. 5). P_{50} values were not correlated with valve effect (V_{ef}) and torus overlap (O), but weakly correlated with margo flexibility (F) (Fig. 6).

DISCUSSION

Our results suggest that torus capillary-seeding is a likely hypothesis in some conifers. Indeed, the size of the torus pores corresponds to the pressure inducing cavitation event and particularly to the xylem air-entry point (P_{12}, Fig. 4b): the larger the pore diameter, the less cavitation resistant the species (Jarbeau, Ewers & Davis 1995; Choat *et al*. 2008). Because air-seeding will always occur at the largest pore first, maximum pore sizes should in theory correlate more strongly with air-seeding thresholds than average values (Choat *et al*. 2003; Jansen *et al*. 2009). It is surprising that in our dataset no significant correlations are found between cavitation resistance with torus overlap, torus thickness, and the torus to aperture ratio, although measurements obtained for pit membrane diameter (D_m), aperture diameter (D_a) and especially torus diameter (D_t) are consistent with previous hypotheses explaining cavitation resistance in conifers (Hacke & Jansen 2009; Delzon *et al*. 2010; Pittermann *et al*. 2010). This finding suggests that the pores associated with tori are likely to explain variation in cavitation

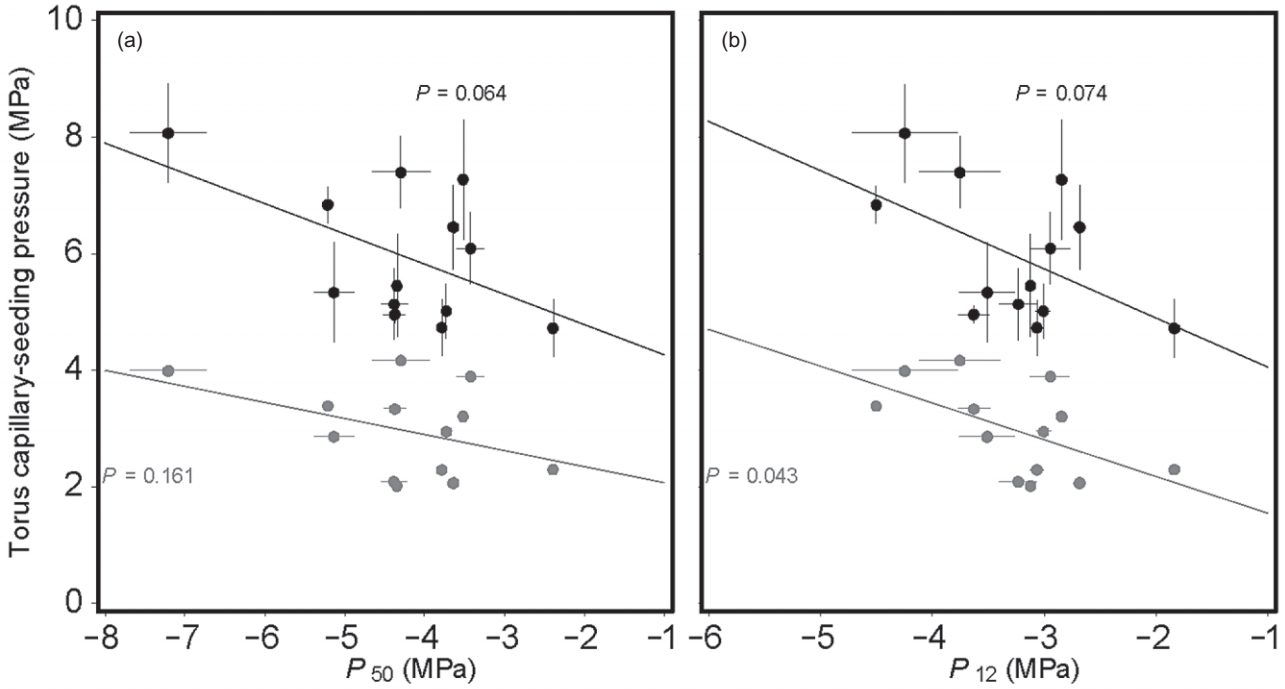

Figure 4. Xylem vulnerability to cavitation quantified as (a) P_{50} and (b) P_{12} (i.e. the pressure corresponding to 50 and 12% loss of hydraulic conductance, respectively) versus the torus capillary-seeding pressure (MPa). The latter was calculated based on the average (black circles) and maximum (grey circles) scanning electron microscopy (SEM) pore size ($n \geq 25$) for 13 conifer species with punctured tori. Data represent average values per species ± SE. A significant relationship was found between P_{12} values and the torus capillary-seeding pressures based on the maximum pore size, while non-significant correlations were found when analysing P_{50} values and torus capillary-seeding pressures based on the average and maximum pore size.

resistance equally as well as other pit morphological features.

Correlations between theoretical and measured air-seeding pressures among the 13 species with punctured tori are weak (Fig. 4) and absolute pore diameter measurements based on SEM should be interpreted with caution for various reasons. At first, only pores that traverse the torus are potential places for air-seeding. Although superficial pores can be distinguished from deeper ones in most cases (Fig. 1d,j), SEM does not allow the distinction between pores that completely pierce the torus from those that are limited to one torus pad. Our TEM observations illustrate that at least a few pores in each species with punctured tori completely traverse the torus (Fig. 2f,g). Careful TEM observation of serial sections would be most useful to quantify the number of pores running from one end of the torus to the other. Secondly, the diameter of the pore measured on the outermost surface of the torus may not correspond to the minimum diameter of the total channel, which determines at what pressure difference the air-water interface is pulled through the pore (Sperry & Tyree 1988; Sperry *et al.* 1996). Estimating the diameter of a pore at nanometer scale is not always free from bias, because the exact outline of the pore may not be clearly visible, even when using high magnifications and optimal contrast conditions with a cold-field emission SEM. Furthermore, the thickness of the coating layer (ca. 10 nm) could have an effect on the actual pore size in pit membranes (Jansen *et al.* 2008). Finally, pore size measurements based on SEM have been shown to offer relative estimates of air-seeding thresholds (Jansen *et al.* 2009) and should be complemented with other techniques such as air injection or particle perfusion experiments (Choat *et al.* 2004, 2005).

The plasmodesmatal nature of the pores can be confirmed based on two arguments: (1) the average pore size corresponds with the ca. 50 nm diameter of plasmodesmata (Murmanis & Sachs 1969; Roberts 2005; Bell & Oparka 2011); and (2) their grouped distribution and branched pattern reflect the characteristically uneven and branched arrangement of secondary plasmodesmata (Rabaey *et al.* 2008). Variation in average pore size between SEM and TEM (51 and 64 nm, respectively) is likely due to differences in sample preparation and observation. While detailed surface views of pores are possible with a field-emission SEM, ultra-thin sections prepared for TEM may show pores in an oblique way with more indistinct contours than SEM. Therefore, we believe that pore size measurements based on SEM are more accurate than TEM. The increase in pore size in *P. wallichiana* after treatment with various chemicals corresponds with earlier observations by Fujikawa & Ishida (1972). As illustrated in Fig. 5, the maximum pore diameter correlates positively with the torus thickness, which is contradictory to earlier findings in angiosperms (Jansen *et al.* 2009): larger pores are more

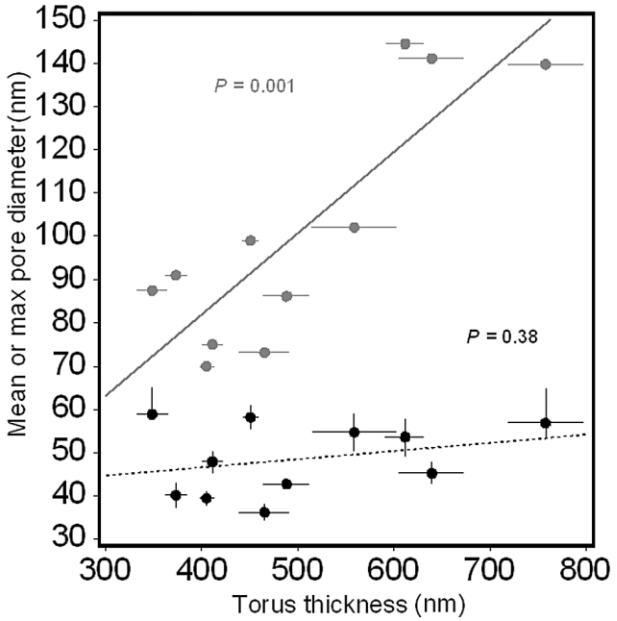

Figure 5. The ratio torus thickness to plasmodesmatal pore diameter showed a significant correlation for the maximum pore diameter, but not for the average pore diameter values for 11 species with punctured tori. Torus thickness was based on transmission electron microscopy (TEM) observations, while dimensions of pores in tori were measured using scanning electron microscopy (SEM). Data represent average values per species ± SE.

likely to occur in thin, flimsy pit membranes than in thick and solid pit membranes.

Given the plasmodesmatal origin of the pores associated with tori, it is not surprising that there is a relatively constant average pore size. Therefore, we believe that it is unlikely that plasmodesmatal pores with actual pore sizes below 30 nm (corresponding to air-seeding below 10 MPa) occur. Thus, rather limited variation in P_{50} values would be found among species with punctured tori, but more variation in cavitation resistance and more negative P_{50} values among species without punctured tori. This is supported by the finding that P_{50} values are more variable and higher in absolute value in species without punctured tori compared with species with punctured tori (Fig. 3). Likewise, the distribution of punctured tori may explain why a large and ecologically diverse genus such as *Pinus* shows relatively little variation with respect to P_{50} values, which generally ranges from –2.5 to –4.5 MPa, although more negative P_{50} values have been recorded in few species (Sperry & Tyree 1990; Piñol & Sala 2000; Hacke *et al*. 2004; Martínez-Vilalta, Sala & Piñol 2004; Martínez-Vilalta *et al*. 2009; Lamy *et al*. 2011). As there seems to be no true selective advantage of having punctured tori, one may also speculate that this phenomenon is tolerated in some conifer species with a particular life history. Incomplete plasmodesmatal sealing of the torus could be acceptable for instance in fast-growing conifers such as *Sequoia*, *Sequoiadendron* and various Pinaceae. Further research is clearly needed to consider possible trade-offs between species with punctured tori and habitat, growth rate and cavitation resistance to drought.

The most likely explanation why pores could not be detected with TEM in five species in which punctured tori were seen with SEM, is that punctured tori are only occasionally present and SEM allows the observation of a higher number of tori than TEM. In addition, TEM sections represent only small fragments of the entire torus, and even if pores would be present, it is possible that they cannot be seen in the ultra-thin sections either because of their arrangement in small groups, or because the pores are narrower than the 60–90 nm thickness of TEM sections. The latter may also explain why most pores seen in TEM sections are not completely open and free from matrix material (Fig. 2e–g). Again, careful examination of serial sections might be required to detect plasmodesmatal pores with TEM.

Based on the limited number of 33 species studied, punctured tori appear to be relatively common across conifer taxa and are not limited to particular taxonomic families or genera. It is possible that the occasional retention of plasmodesmatal pores in some conifer taxa reflects differences in the chemical composition of conifer tori. As far as we know, however, gymnosperm tori show an overall similarity in chemical composition and mainly consist of pectins (Bauch & Berndt 1973; Imamura, Harada & Saiki 1974; Hafrén, Daniel & Westmark 2000; Putoczki *et al*. 2008; Kim *et al*. 2011). Alternatively, the

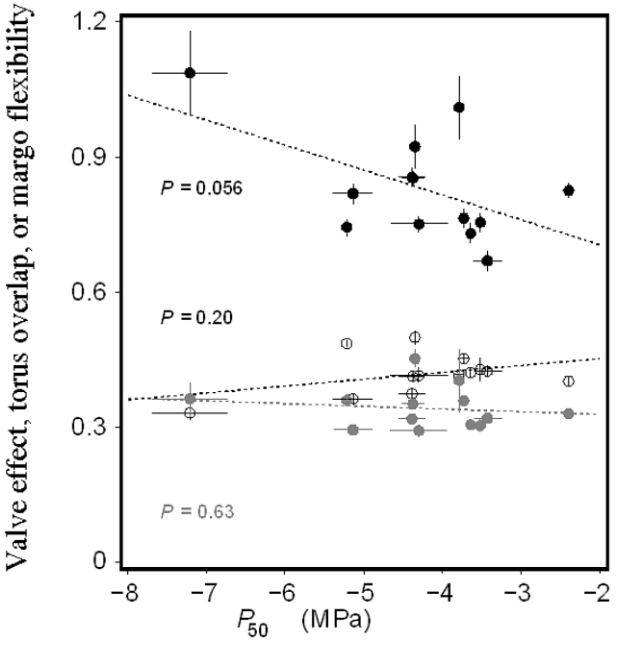

Figure 6. No significant relationship was found between P_{50} versus valve effect (V_{ef}, grey symbols) sensu Delzon *et al*. (2010), torus overlap (O, blank circles), and margo flexibility (F, black dots) for 13 species with punctured tori. Data represent average values per species ± SE. Furthermore, no significant relationship was found between P_{50} and torus overlap sensu Hacke *et al*. (2004) ($P = 0.12$; data not shown).

presence or absence of plasmodesmatal pores could be explained by differences in torus development among conifers. Plasmodesmata seem very common in developing pit membranes of conifer tracheids (Murmanis & Sachs 1969; Thomas 1969; Fengel 1972; Fujikawa & Ishida 1972; Dute 1994; Dute *et al*. 2008), although it is unclear whether their frequency in developing tori corresponds with similar frequencies of punctured tori in mature pit membranes. While secondary plasmodesmata associated with tori appear during the final stages of cell differentiation in *A. firma* (Pinaceae) and *M. glyptostroboides* (Cupressaceae), they are only retained in mature pit membranes of *A. firma*. In contrast, autolytic enzymes remove matrix from the torus in *M. glyptostroboides*, which results in a loss of the plasmodesmatal channels and rearrangement of microfibrils (Dute 1994; Dute *et al*. 2008). Whether or not plasmodesmatal openings remain present in the fully developed torus after autolysis may thus depend on the degree and conditions of the autolysis. Clearly, more developmental research will be needed to test this idea.

In conclusion, this study suggests that the torus in conifer pit membranes is not always as airtight as previously thought. While air-seeding through pores in the torus does not represent the only and universal mechanism for drought-induced cavitation in conifers, there is preliminary evidence indicating that plasmodesmatal pores could contribute to air-seeding, supporting the torus capillary-seeding hypothesis. In species without punctured tori, cavitation might occur between the torus and the outer pit chamber wall when the torus is not tightly sealed against the pit border (seal capillary-seeding). This finding will hopefully encourage further work on the structural basis behind cavitation resistance in woody plants, which will also be useful for untying the genetic mechanisms of drought resistance in plants.

ACKNOWLEDGMENTS

We thank Tony Kirkham (RBG Kew) for permission to collect samples from the living collections in Kew. Tim Brodribb (University of Tasmania) and Uwe Hacke (University of Alberta) are acknowledged for providing wood samples. Financial support to Kew and Bordeaux was provided by an International Joint grant from the Royal Society (UK). S.J. acknowledges a 'Juniorprofessorenprogramm' grant from the Ministry of Science, Research, and the Arts of Baden-Wurttemberg (Germany). Funding to S.D. and J.-B.L. was provided by grants from INRA-Project Innovant and a PhD grant from INRA-Région Auvergne, respectively. A mobility grant to J.-B.L. was provided by INRA (France).

REFERENCES

Bailey I.W. (1913) The preservative treatment of wood. II. The structure of the pit membranes in the tracheids of conifers and their relation to the penetration of gases, liquids, and finely divided solids into green and seasoned wood. *Forestry Quarterly* **11,** 12–20.

Bailey I.W. (1916) The structure of bordered pits of conifers and its bearing upon the tension hypothesis of the ascent of sap in plants. *Botanical Gazette* **62,** 133–142.

Bao F.C., Lu J.X. & Zhao Y. (2001) Effect of bordered pit torus position on permeability in Chinese yezo spruce. *Wood and Fiber Science* **33,** 193–199.

Bauch J. & Berndt H. (1973) Variability of the chemical composition of pit membranes in bordered pits of gymnosperms. *Wood Science and Technology* **7,** 6–19.

Bauch J., Schultze R. & Liese W. (1972) Morphological variability of bordered pit membranes in gymnosperms. *Wood Science and Technology* **6,** 165–184.

Bell K. & Oparka K. (2011) Imaging plasmodesmata. *Protoplasma* **248,** 9–25.

Brodribb T.J., Bowman D.J.M., Nichols S., Delzon S. & Burlett R. (2010) Xylem function and growth rate interact to determine recovery rates after exposure to extreme water deficit. *New Phytologist* **188,** 533–542.

Chave J., Coomes D., Jansen S., Lewis S., Swenson N. & Zanne A. (2009) Towards a worldwide wood economics spectrum. *Ecology Letters* **12,** 351–366.

Choat B., Ball M., Luly J. & Holtum J. (2003) Pit membrane porosity and water stress-induced cavitation in four co-existing dry rainforest tree species. *Plant Physiology* **131,** 41–48.

Choat B., Jansen S., Zwieniecki M.A., Smets E. & Holbrook N.M. (2004) Changes in pit membrane porosity due to deflection and stretching: the role of vestured pits. *Journal of Experimental Botany* **55,** 1569–1575.

Choat B., Lahr E.C., Melcher P.J., Zwieniecki M.A. & Holbrook N.M. (2005) The spatial pattern of air seeding thresholds in mature sugar maple trees. *Plant, Cell & Environment* **28,** 1082–1089.

Choat B., Cobb A. & Jansen S. (2008) Structure and function of bordered pits: new discoveries and impacts on whole plant hydraulic function. *New Phytologist* **177,** 608–626.

Cochard H. (2002) A technique for measuring xylem hydraulic conductance under high negative pressures. *Plant, Cell & Environment* **25,** 815–819.

Cochard H., Damour G., Bodet C., Tharwat I., Poirier M. & Ameglio T. (2005) Evaluation of a new centrifuge technique for rapid generation of xylem vulnerability curves. *Physiologia Plantarum* **124,** 410–418.

Cochard H., Hölttä T., Herbette S., Delzon S. & Mencuccini M. (2009) New insights into the mechanisms of water-stress-induced cavitation in conifers. *Plant Physiology* **151,** 949–954.

Comstock G.L. & Côté W.A. (1968) Factors affecting permeability and pit aspiration in coniferous wood. *Wood Science and Technology* **2,** 279–291.

Delzon S., Douthe C., Sala A. & Cochard H. (2010) Mechanism of water-stress induced cavitation in conifers: bordered pit structure and function support the hypothesis of seal capillary-seeding. *Plant, Cell & Environment* **33,** 2101–2111.

Domec J.-C., Lachenbruch B., Meinzer F.C., Woodruff D.R., Warren J.M. & McCulloh K.A. (2008) Maximum height in a conifer is associated with conflicting requirements for xylem design. *Proceedings of the National Academy of Sciences of the United States of America* **105,** 12069–12074.

Dute R.R. (1994) Pit membrane structure and development in *Ginkgo biloba*. *International Association of Wood Anatomists Journal* **15,** 75–90.

Dute R., Hagler L. & Black A. (2008) Comparative development of intertracheary pit membranes in *Abies firma* and *Metasequoia glyptostroboides*. *International Association of Wood Anatomists Journal* **29,** 277–289.

Fengel D. (1972) Structure and function of the membrane in softwood bordered pits. *Holzforschung* **26,** 1–9.

Flynn K.A. (1995) A review of the permeability, fluid-flow, and anatomy of Spruce (*Picea* spp.). *Wood and Fiber Science* **27,** 278–284.

Fujikawa S. & Ishida S. (1972) Study on the pit of wood cells using scanning electron microscopy. 3. Structural variation of bordered pit membrane on the radial wall between tracheids in Pinaceae species. *Mokuzai Gakkaishi* **18,** 477–483.

Gortan E., Nardini A., Salleo S. & Jansen S. (2011) Pit membrane chemistry influences the magnitude of ion-mediated enhancement of xylem hydraulic conductivity in four Lauraceae. *Tree Physiology* **31,** 48–58.

Hacke U.G. & Jansen S. (2009) Embolism resistance of three boreal conifer species varies with pit structure. *New Phytologist* **182,** 675–686.

Hacke U.G., Sperry J.S. & Pittermann J. (2004) Analysis of circular bordered pit function – II. Gymnosperm tracheids with torus-margo pit membranes. *American Journal of Botany* **91,** 386–400.

Hafrén J., Daniel G. & Westmark U. (2000) The distribution of acidic and esterified pectin in cambium, developing xylem and mature xylem of *Pinus sylvestris*. *International Association of Wood Anatomists Journal* **21,** 157–168.

Hart C.A. & Thomas R.J. (1967) Mechanism of bordered pit aspiration as caused by capillarity. *Forest Products Journal* **17,** 61–68.

Imamura Y., Harada H. & Saiki H. (1974) Embedding substances of pit membranes in softwood tracheids and their degradation by enzymes. *Wood Science and Technology* **7,** 189–205.

Jansen S., Pletsers A. & Sano Y. (2008) The effect of preparation techniques on SEM-imaging of pit membranes. *International Association of Wood Anatomists Journal* **29,** 161–178.

Jansen S., Choat B. & Pletsers A. (2009) Morphological variation of intervessel pit membranes and implications to xylem function in angiosperms. *American Journal of Botany* **96,** 409–419.

Jarbeau J.A., Ewers F.W. & Davis S.D. (1995) The mechanism of water-stress-induced embolism in two species of chaparral shrubs. *Plant, Cell & Environment* **18,** 189–196.

Kim J.S., Awano T., Yoshinaga A. & Takabe K. (2011) Temporal and spatial diversities of the immunolabelling of mannan and xylan polysaccharides in differentiating earlywood ray cells and pits of *Cryptomeria japonica*. *Planta* **233,** 109–122.

Lamy J.-B., Bouffier L., Burlett R., Plomion C., Cochard H. & Delzon S. (2011) Uniform selection as a primary force reducing population genetic differentiation of cavitation resistance across a species range. *PLoS One* **6,** e23476.

Liese W. (1965) The fine structure of bordered pits in softwoods. In *Cellular Ultrastructure of Woody Plants* (ed. W.A. Coté), pp. 271–290. Syracuse University Press, New York, USA.

Liese W. & Bauch J. (1967) On the closure of bordered pits in conifers. *Wood Science and Technology* **1,** 1–13.

Liese W. & Johann I. (1954) Elektronenmikroscopische Beobachtungen über eine besondere Feinstruktur der verholzten Zellwand bei einigen Coniferen. *Planta* **44,** 269–285.

Maherali H., Pockman W.T. & Jackson R.B. (2004) Adaptive variation in the vulnerability of woody plants to xylem cavitation. *Ecology* **85,** 2184–2199.

Martínez-Vilalta J., Sala A. & Piñol J. (2004) The hydraulic architecture of Pinaceae – a review. *Plant Ecology* **171,** 3–13.

Martínez-Vilalta J., Cochard H., Mencuccini M., *et al*. (2009) Hydraulic adjustment of Scots pine across Europe. *New Phytologist* **184,** 353–364.

Murmanis L. & Sachs I.B. (1969) Seasonal development of secondary xylem in *Pinus strobus* L. *Wood Science and Technology* **3,** 177–193.

Pammenter N.W. & Vander Willigen C. (1998) A mathematical and statistical analysis of the curves illustrating vulnerability of xylem to cavitation. *Tree Physiology* **18,** 589–593.

Panshin A.J. & De Zeeuw C. (1980) *Textbook of Wood Technology*. McGraw-Hill, New York, USA.

Piñol J. & Sala A. (2000) Ecological implications of xylem embolism for several Pinaceae in the Pacific Northern USA. *Functional Ecology* **14,** 538–545.

Pittermann J. (2010) The evolution of water transport in plants: an integrated approach. *Geobiology* **8,** 112–139.

Pittermann J., Sperry J.S., Hacke U.G., Wheeler J.K. & Sikkema E.H. (2005) The torus-margo pit valve makes conifers hydraulically competitive with angiosperms. *Science* **310,** 1924.

Pittermann J., Choat B., Jansen S., Stuart S., Lynn L. & Dawson T. (2010) The relationships between cavitation safety and hydraulic efficiency in the pit membranes of conifers belonging to the Cupressaceae: the evolution of form and function. *Plant Physiology* **153,** 1919–1931.

Putoczki T.L., Gerrard J.A., Butterfield B.G. & Jackson S.L. (2008) The distribution of un-esterified and methyl-esterified pectic polysaccharides in *Pinus radiata*. *International Association of Wood Anatomists Journal* **29,** 115–127.

Rabaey D., Lens F., Huysmans S., Smets E. & Jansen S. (2008) The ultrastructure and development of pit membranes with plasmodesmata associated thickenings in secondary xylem. *Protoplasma* **233,** 255–262.

Rasband W.S. (1997–2011) *ImageJ*. National Institutes of Health, Bethesda, MD, USA. URL http://rsbweb.nih.gov/ij/.

Roberts A.G. (2005) Plasmodesmal structure and development. In *Plasmodesmata* (ed. K.J. Oparka), pp. 1–23. Blackwell, Oxford, UK.

Roth-Nebelsick A., Voigt D. & Gorb S. (2010) Cryo-scanning electron microscopy studies of *Pinus wallichiana* and *Mallotus japonicus*. *International Association of Wood Anatomists Journal* **31,** 257–267.

Russow E. (1883) Zur Kenntniss des Holzes, insonderheit des Coniferenholzes. *Botanisches Zentralblatt* **13,** 134–144.

Sanio K. (1873) Anatomie der gemeinen Kiefer (*Pinus silvestris* L.). *Jahrbücher für wissenschaftliche Botanik* **9,** 50–126.

Sano Y., Kawakami Y. & Ohtani J. (1999) Variation in the structure of intertracheary pit membranes in *Abies sachalinensis*, as observed by field-emission scanning electron microscopy. *International Association of Wood Anatomists Journal* **20,** 375–388.

Schacht H. (1859) Über die Tüpfel der Gefäss-und Holzzellen. *Botanische Zeitung* **17,** 238–239.

Schoonmaker A.L., Hacke U.G., Landhausser S.M., Lieffers V.J. & Tyree M.T. (2010) Hydraulic acclimation to shading in boreal conifers of varying shade tolerance. *Plant, Cell & Environment* **33,** 382–393.

Singh A., Dawson B., Franich R., Cowan F. & Warnes J. (1999) The relationship between pit membrane ultrastructure and chemical impregnability of wood. *Holzforschung* **53,** 341–346.

Sperry J.S. & Tyree M.T. (1988) Mechanism of water stress-induced xylem embolism. *Plant Physiology* **88,** 581–587.

Sperry J.S. & Tyree M.T. (1990) Water-stress-induced xylem embolism in three species of conifers. *Plant, Cell & Environment* **13,** 427–436.

Sperry J.S., Saliendra N.Z., Pockman W.T., Cochard H., Cruiziat P., Davis S.D., Ewers F.W. & Tyree M.T. (1996) New evidence for large negative xylem pressure and their measurements by the pressure chamber method. *Plant, Cell & Environment* **19,** 427–436.

Strasburger E. (1891) *Über den bau und die Verrichtungen der Leitungsbahnen in den Pflanzen*. Gustav Fischer, Jena, Germany.

Thomas R.J. (1969) The ultrastructure of southern pine bordered pit membranes as revealed by specialized drying techniques. *Wood and Fiber* **1,** 110–123.

Thomas R.J. & Nicholas D.D. (1969) The ultrastructure of the ray tracheid bordered pit membranes in southern pine. *Technical*

Association of the Pulp and Paper Industry Journal **52,** 2160–2163.

Tyree M.T. & Zimmermann M.H. (2002) *Xylem Structure and the Ascent of Sap*. Springer-Verlag, Berlin, Germany.

Usta I. & Hale M.D. (2006) Comparison of the bordered pits of two species of spruce (Pinaceae) in a green and kiln-dried condition and their effects on fluid flow in the stem wood in relation to wood preservation. *Forestry* **79,** 467–475.

Von Nägeli C. (1864) Aufquellende Epidermiszellen von Samen und Früchten. Sitzungsberichte der königliche bayerische Akademie der Wissenschaften Jahrgang 1864 Band II, 114–170.

Received 20 June 2011; accepted for publication 9 December 2011

SUPPORTING INFORMATION

Additional Supporting Information may be found in the online version of this article:

Figure S1. Box plot illustrating a significant difference ($P < 0.0001$) in S_{50} between species with punctured tori ($n = 13$) and non-punctured tori ($n = 20$). This difference remained significant ($P = 0.024$) when controlling for taxonomy based on a mixed model (see Material and methods for details).

Figure S2. Scaling of pit aperture diameter (D_a) versus pit membrane diameter (D_m, grey dots), and D_a versus torus diameter (D_t, black dots) as based on average values (±SD) for 13 species with punctured tori. All linear regressions were highly significant. These relationships remain significant ($P < 0.0001$) when controlling for taxonomy.

Table S1. List of pit morphological dimensions for 13 conifer species with punctured tori. Average and maximum pore sizes per species were based on SEM ($n \geq 25$) and TEM ($n \geq 5$) measurements. D_m, D_t and D_a were measured on a minimum of 15 aspirated pit membranes in order to obtain these parameters from the same pit. The TEM characters T_t and D_p were averaged for a minimum of 10 measurements. Av = average; Max = maximum; D_m = pit membrane diameter; D_t = torus diameter; D_a = aperture diameter; T_t = torus thickness; D_p = depth of the pit chamber; / = no pores were detected with TEM; X = species not studied with TEM.

Please note: Wiley-Blackwell are not responsible for the content or functionality of any supporting materials supplied by the authors. Any queries (other than missing material) should be directed to the corresponding author for the article.

OPEN ACCESS Freely available online

PLoS one

Uniform Selection as a Primary Force Reducing Population Genetic Differentiation of Cavitation Resistance across a Species Range

Jean-Baptiste Lamy[1,2,3], Laurent Bouffier[1,4], Régis Burlett[1,2], Christophe Plomion[1,2], Hervé Cochard[3], Sylvain Delzon[1,2]*

1 INRA, UMR 1202 BIOGECO, F-33610 Cestas, France, **2** Université de Bordeaux, UMR 1202 BIOGECO, F-33610 Cestas, France, **3** INRA, UMR 547 PIAF, University of Blaise Pascal, F-63100 Clermont-Ferrand, France, **4** FCBA, Station Sud-Ouest, Domaine de Sivaillan, F-33480 Moulis en Médoc, France

Abstract

Background: Cavitation resistance to water stress-induced embolism determines plant survival during drought. This adaptive trait has been described as highly variable in a wide range of tree species, but little is known about the extent of genetic and phenotypic variability within species. This information is essential to our understanding of the evolutionary forces that have shaped this trait, and for evaluation of its inclusion in breeding programs.

Methodology: We assessed cavitation resistance (P_{50}), growth and carbon isotope composition in six *Pinus pinaster* populations in a provenance and progeny trial. We estimated the heritability of cavitation resistance and compared the distribution of neutral markers (F_{ST}) and quantitative genetic differentiation (Q_{ST}), for retrospective identification of the evolutionary forces acting on these traits.

Results/Discussion: In contrast to growth and carbon isotope composition, no population differentiation was found for cavitation resistance. Heritability was higher than for the other traits, with a low additive genetic variance ($h^2_{ns} = 0.43 \pm 0.18$, $CV_A = 4.4\%$). Q_{ST} was significantly lower than F_{ST}, indicating uniform selection for P_{50}, rather than genetic drift. Putative mechanisms underlying $Q_{ST} < F_{ST}$ are discussed.

Citation: Lamy J-B, Bouffier L, Burlett R, Plomion C, Cochard H, et al. (2011) Uniform Selection as a Primary Force Reducing Population Genetic Differentiation of Cavitation Resistance across a Species Range. PLoS ONE 6(8): e23476. doi:10.1371/journal.pone.0023476

Editor: Pär K. Ingvarsson, University of Umeå, Sweden

Received February 25, 2011; **Accepted** July 19, 2011; **Published** August 12, 2011

Funding: This research was supported by grants from INRA (innovative project 2010) and the European Union: i) the provenance trial was set up in 2003 by the experimental unit at INRA Pierroton, as part of the TREESNIP-QLK3-CT2002-01973 project. ii) measurements of carbon isotope discrimination and cavitation resistance were funded by the NOVELTREE project (FP7-211868). J-BL was supported by a doctoral fellowship from INRA and the Auvergne Region. The funders had no role in study design, data collection and analysis, decision to publish, or preparation of the manuscript.

Competing Interests: The authors have declared that no competing interests exist.

* E-mail: sylvain.delzon@u-bordeaux1.fr

Introduction

The climatic niches of forest tree species are moving faster than the maximum rate of migration, measured by palynology or gene flow analysis, as a direct consequence of the current increase in temperatures due to global warming [1,2]. Forest tree populations are thus facing new selection pressures and are unable to track their bioclimatic envelope [3] over the time scale at which these changes are occurring. The local adaptation and survival of tree populations in a rapidly changing environment with warmer temperatures and more frequent water shortage is a major concern in efforts to ensure the sustainability of forest ecosystem services. In addition to this trend, climate experts are predicting more extreme climatic events, such as periods of severe drought [4], which will increase mortality rates [5,6,7]. These effects on tree mortality highlight the way in which the impact of climate change may depend on the changes associated with extreme events rather than trends [8]. In this context, there is a need to investigate relevant drought tolerance-related traits, to quantify both genetic variation and phenotypic plasticity, which together define the capacity of tree populations to adapt.

From a physiological point of view cavitation resistance is an important trait to estimate drought tolerance. Indeed, dysfunctions of the vascular system of the tree, such as xylem embolism due to cavitation events, is likely to be a key factor governing the mortality of these long-lived organisms [9].When a cavity is formed in the xylem sap under tension (negative pressure), it may spread in the vascular system through intervessel or intertracheid pits, thus compromising the capacity of the plant to transport water [10].

A direct causal link between survival (fitness) and cavitation resistance during extreme drought has been highlighted, based on two lines of evidence suggesting that cavitation resistance is an important adaptive trait. Firstly, assessments of the correlation between cavitation resistance and lethal water potential [11,12] demonstrated a highly significant linear relationship ($r^2 = 0.9$) between these two traits. Secondly, global surveys of cavitation resistance in woody species showed that xeric species are more resistant to embolism than hydric species [13,14,15]. These interspecific studies, with adaptive inferences concerning cavitation resistance being rendered robust by the incorporation of phylogenetic information [15,16,17], concluded that cavitation

resistance-related traits are under natural selection [15,18]. To validate this evolutionary pattern, a population-level perspective is appropriate, because variation observed across species cannot be assumed to reflect patterns within species.

At the intraspecific level, cavitation resistance can be analyzed by provenance or progeny trials. The few studies carried out to date (reviewed in Table S1) have included only small numbers of individuals (<9) and populations (<5), and it has therefore not been possible to estimate environmental and genetic effects on phenotypic variation accurately. We therefore still know little about the genetic determinism and micro-evolutionary pattern of this hydraulic trait, but such information is absolutely necessary if this trait is to be incorporated into breeding programs and for a more fundamental understanding of the evolutionary basis of tolerance to severe drought.

The aim of this study was to provide the first estimates of heritability, additive variance and population differentiation for cavitation resistance-related traits. We carried out a case study of maritime pine (*Pinus pinaster* Ait.), a species with a fragmented distribution in the western part of the Mediterranean region. The scattered distribution of this species may have prevented or limited gene flow between different groups of populations, promoting high levels of genetic divergence between ecotypes due to genetic drift [19] and/or natural selection (Quezel and Barbero 1998 in [20]). Here, we took advantage of a new technology (high-throughput phenotyping platform for cavitation resistance) to screen for the first time a large number of genotypes from six ecotypes to test the hypothesis that *Pinus pinaster* populations have been subjected to diversifying selection for cavitation resistance. More specifically, this experiment aimed to address the following questions: what is the level intraspecific variation and heritability for cavitation resistance? Can we separate the relative roles of drift and selection in population differentiation for this trait?

Methods

Provenance trial and climatic data

We carried out a provenance-progeny trial, in which young trees (six-year-old plants) were planted in December 2003 at the INRA forestry station in the Aquitaine Region (44°44'N, 00°46'W). The mean annual temperature at this site is 13.2°C and mean annual rainfall is 836 mm (1984–2006). The soil is a sandy podzol with a water table rising to about 0.5 m below the surface in winter and descending to a depth of 2 m in late summer. Seedlings were grown in the nursery from open-pollinated seeds collected from 24 natural populations (or ecotypes) in France, Spain, Morocco and Tunisia, to cover the fragmented distribution of *Pinus pinaster*. Each population was represented by 20 to 30 half-sib families. The trial was arranged in a randomized block design (15 blocks) with single-tree plots. Each block contained at least one tree from each half-sib family. There were 600 seedlings per block, giving 9,000 seedlings for the entire experiment.

Choice of populations

The assessment of cavitation resistance is a intensively time-consuming process [21]. We therefore designed a procedure for the selection of a subset of populations representing all the variability of climatic envelope of maritime pine. For a total of 754 grid points covering the entire natural range of the species [22], we first extracted climatic data from the CRU CL 2.0 10′ global dataset for the period 1961–1990 [23,24,25]. These data included monthly average precipitation, mean, minimum and maximum temperature, diurnal temperature range, water vapor pressure, cloud cover, wet day frequency, ground frost frequency, radiation, wind, Martonne index, Turc's potential evapotranspiration and soil water deficit. We also derived the vapor pressure deficit from these parameters. Principal component analysis (PCA) was then used to reduce the number of dimensions for the whole set of climate variables (Figure 1). The data were centered and scaled before PCA. The 14 populations were finally placed on the main plane of the PCA (accounting for 76% of the variation, Table S2) and six of these populations (Table 1) were selected as a representative subset of the climatic envelope covered by *Pinus pinaster* species. In each population, eight families (5 half-sibs/family/block) were randomly selected for further analysis.

Sample preparation for the assessment of cavitation resistance

We collected branches, according to the sampling procedure described below, during winter 2009, before 10 am, to avoid native embolism. Needle water potential was lower than -1 MPa, far from the minimum needle water potential in summer (−2 MPa) of *Pinus pinaster* [26]. The branch sample corresponded to the 2007 and 2008 growth units on the 2007 whorl when possible, in order to measure on the same number of rings in each sample. Sampled branches were fully exposed to the sun, longer than 40 cm and with a diameter of 0.3 to 1 cm (<4 years of age). The current needles were removed and the branches were wrapped in wet paper towels and bagged upon collection to prevent dehydration. In the lab, samples were cut under water just before measurement to obtain 0.28 m segments (*i.e.*, much longer than the longest tracheid). Bark was removed from all segments before measurements.

Assessment of cavitation resistance

Cavitation resistance was measured on 240 genotypes (6 populations * 8 families * 5 offsprings), with the Cavitron technique [21,27,28]. Centrifugal force was used to establish negative pressure in the xylem and to provoke water stress-induced cavitation, using a custom-built honeycomb rotor (Precis 2000, Bordeaux, France) mounted on a high-speed centrifuge (HS18, MSE Scientific, London, UK). This technique enables measurement of the hydraulic conductance of a branch under negative pressure. Xylem pressure (P_x) was first set to a reference pressure (−0.5 MPa) and maximal conductance (k_{max}) was determined by measuring the flux of a reference ionic solution (10 mmol dm^{-3} KCl and dm^{-3} mmol dm^{-3} $CaCl_2$ in deionized water) through the sample. The centrifugation speed was then set to a higher value for 3 min to expose the sample at a more negative pressure. Conductance (k_i) were measured 4 times for each step, and the average was used to compute percent of loss of xylem of conductance (PLC in %) following $PLC = 100\ (1-k_i/k_{max})$. The procedure was repeated for at least eight pressure step with a −0.5 MPa step increment until PLC reached at least 90%. The percent loss of xylem conductance as a function of xylem pressure (MPa) represents the sample's vulnerability curve (Figure 2). Rotor velocity was monitored with a 10 rpm resolution electronic tachymeter (A2108-LSR232, Compact Inst, Bolton, UK) and xylem pressure was adjusted to about ±0.02 MPa. We used Cavi_soft software (version1.5, University of Bordeaux) for conductance measurements and computation of all vulnerability curves (VCs). The 10,800 measurements of conductance were performed at the new high-throughput phenotyping platform for hydraulic traits (CavitPlace, University of Bordeaux, Talence, France).

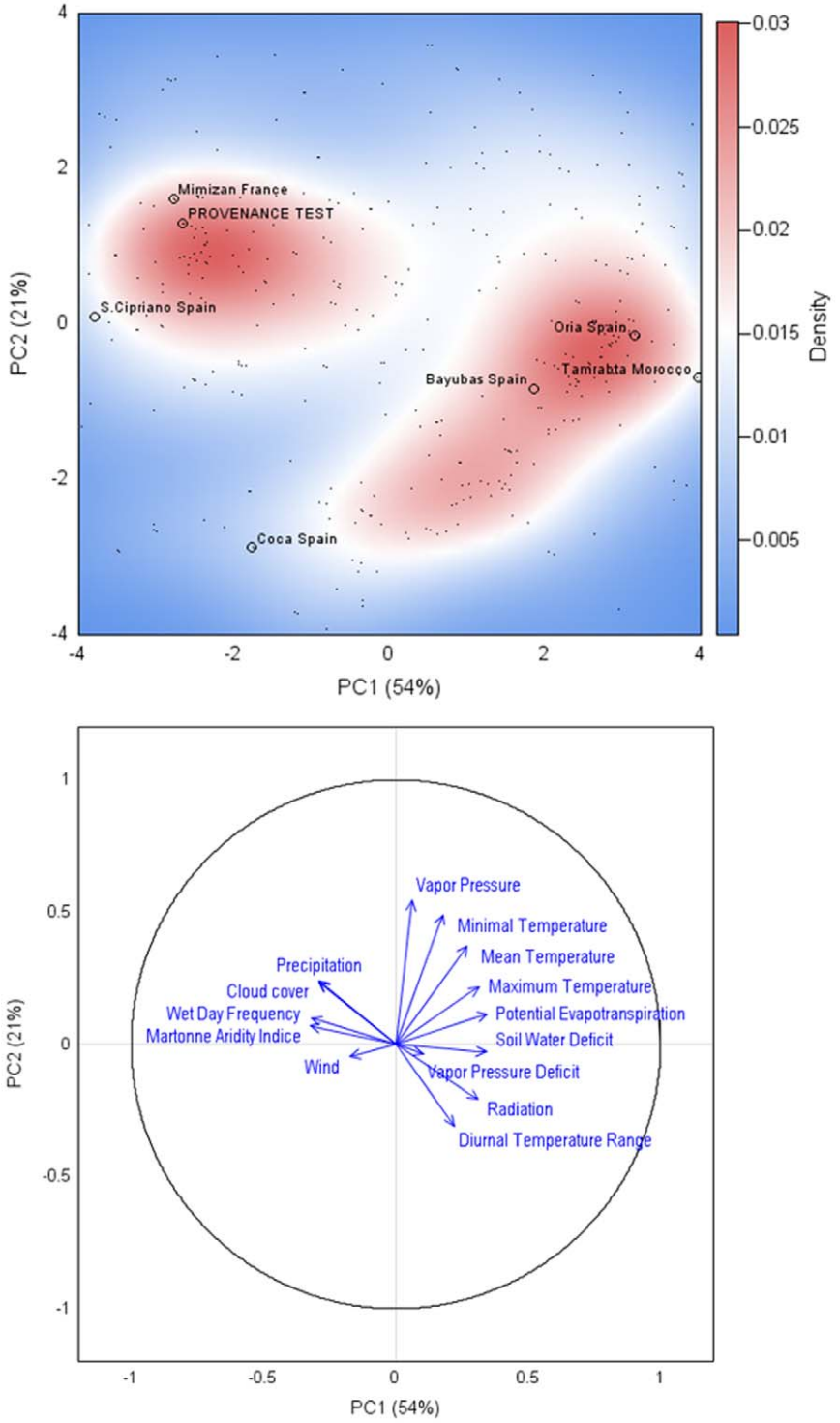

Figure 1. Principal component analysis (PCA) on the [763 population locations x 14 climatic variables] data matrix. Upper panel: The contour plot represents the presence's probability (kernel density estimate) of *Pinus pinaster* population (small black dot) within the bioclimatic envelope representing by PC1 and PC2 axes, accounted for 54% and 21% of the variance, respectively. The studied populations and provenance test are indicated by black circles. PCA was performed with the variables indicated in the methods section. See Table S2, for additional information about the relative contribution of climatic variables to the axes. Lower panel: projection of 14 climatic variables on the subspace spanned by the first two eigenvectors (correlation circle).
doi:10.1371/journal.pone.0023476.g001

Based on a sensitivity analysis (data not shown) and graphical checking (Figure 2), we retained the reparameterized sigmoid function fitted to the conductance data (k_i) (see [29] and [30] for an exhaustive review) rather than the Weibull model, for determination of the pressure at which the sample lost 50% of its conductance (P_{50}) and the slope of the curve at P_{50} (S_{50}).

Table 1. Climatic data, location and elevation of the studied maritime pine populations.

Sampling location	Longitude (°)	Latitude (°)	*n*	Elevation (m)	P_i (mm)	T_m (°C)	VPD_{max} (hPa)	*ETP* (mm)
Bayubas de Abajo (Central Spain)	−2.87	41.52	39	955	561	10.5	11.42	882.9
Coca (Central Spain)	−4.08	41.37	40	788	452	11.9	14.23	718.7
Mimizan (South-western France)	−1.30	44.13	40	37	1176	13.2	7.26	751.59
Oria (South-eastern Spain)	−2.62	37.87	40	1232	451	13.4	14.29	922.59
San Cipriano (Northern Spain)	−8.70	42.13	40	310	1625	13.8	8.54	721.91
Tamrabta (Southern Morocco)	−5.02	33.66	40	1760	550	15.1	18.56	976.54

n, number of sampled individuals for hydraulic measurements; P_i , mean annual precipitation; T_m, mean annual air temperature; VPD_{max}, maximal of water vapor pressure deficit (in July for all the provenance); *ETP*, annual sum of potential evapotranspiration.
doi:10.1371/journal.pone.0023476.t001

$$k_i = k_{\max} \times \left\{ 1 - \left(1 + \left(\frac{100}{X} - 1 \right) \times \exp\left(\frac{100 \times S_X \times (\mathrm{Pr}\,essure - P_X)}{X \times (X - 100)} \right) \right)^{-1} \right\} \quad (1)$$

where $k_{\max}$ is the highest conductance measured for each sample (equivalent to k_{sat} in the original Ogle's model), k_i is the mean conductance at a given pressure concerned, X is the percentage loss of conductance of interest (in %), P_X (in MPa) is the pressure inducing X% loss of conductance and S_X (in MPa.% $^{-1}$) is the slope of the tangent at the P_X abscissa point on the curve. Analysis has been performed for pressures and slopes corresponding to $X = 12$, 50 and 88 % loss of conductivity (P_{12}, P_{50}, P_{88}, S_{12}, S_{50} and S_{88} respectively).

Carbon isotope ratio and growth measurement

Carbon isotope ratio (δ^{13}C in ‰) was obtained as previously described [32,33]. Needles of the growth unit used for cavitation analysis were harvested and 20 needles were sampled at random. The needles were dried and ground to a powder and 3 mg sample was analyzed with an isotope ratio mass spectrometer (FISONS Isochrom, Manchester, UK) at INRA facility in Reims (France). Total height was measured at the ages of two (2004) and three (2005) years, on the same six populations and eight families, for all 15 blocks. The annual increase in height (Δ_h) was calculated as the difference between these two measurements (in 2004 and 2005).

Quantitative genetic analysis

Genetic analysis was conducted with the following mixed model:

$$y = Xb + Z_1 pop + Z_2 f + \varepsilon \quad (2)$$

where $\boldsymbol{y}$ is the vector of observation for a trait, $\boldsymbol{b}$ is the vector (number of block) of fixed block effects, $\boldsymbol{pop}$ is the vector (number of populations) of random population effects, $\boldsymbol{f}$ is the vector (number of mother trees) of the random genetic effects of mother tree within the population, $\boldsymbol{\varepsilon}$ is the vector (number of individuals) of residuals, $\mathbf{X}$ is called the design matrix, $\mathbf{Z_1}$ and $\mathbf{Z_2}$ are the incidence matrices linking the observations to the effects. A variance was fitted for each random effect: σ^2_{pop} is the genetic variance between populations, $\sigma^2_{f(pop)}$ is the genetic variance between mother trees nested within a population and $\sigma^2_e$is the residual variance.

Variance or covariance components were estimated by the restricted maximum likelihood (REML) method, assuming a normal distribution of the random effects. The significance of variance components were tested using log-likelihood ratio tests. We included population as a random effect to draw inference at species levels [34] and to obtain an unbiased estimate of heritability and genetic population differentiation [35]. The normality, identity and independency of residuals of each trait were graphically checked by plotting studentized marginal and conditional residuals (available on request), which confirmed that the data match with the assumption of mixed model. We estimated narrow-sense heritability as follows:

$$h^2_{ns} = \frac{\left(4\sigma^2_{f(pop)}\right)}{\left(\sigma^2_{\varepsilon} + \sigma^2_{f(pop)}\right)} = \frac{\sigma^2_A}{\left(\sigma^2_{\varepsilon} + \sigma^2_{f(pop)}\right)} \quad (3)$$

where σ^2_A is the within-population additive variance. In our study, σ^2_A was estimated by $\sigma^2_A = 4\sigma^2_{f(pop)}$ as trees from the same family were presumed to be half-sibs (open-pollinated seeds). We did not include the population effect in the heritability calculation, because natural selection appeared to occur within each population [36]. The standard deviation of heritability was calculated with the equations of delta method (see Appendix in [37]).

Variance components were standardized by the trait mean [38] as follows, $CV_X = 100\sqrt{(\text{Variance})}/\text{Mean}_X$ where X is the trait considered, and CV is the coefficient of variation. Each variance component is expressed with a CV (CV_A: additive coefficient of variation; CV_{BP} ($V_{BP} = \sigma^2_{pop}$): coefficient of variation between populations; CV_P: phenotypic coefficient of variation; CV_R: residual coefficient of variation). The variance of each component was extracted from the asymptotic covariance matrix. The significance of mean population difference was estimated using the same model (Eq. 2) with a proc GLM with a Student-Neuman-Keuls post hoc test.

Correlation between traits

To facilitate interpretation of correlation, negative value of P_{50} and δ^{13}C were converted from negatives to positives. Genetic correlations between traits were evaluated by calculating Pearson's coefficient on the family Best Linear Unbiased Predictor estimation (BLUP, for additional information see [37] p745). BLUP estimation ensures that data are corrected for block effect. We will refer to these correlations as genetic correlations. For phenotypic correlation, all Pearson correlations were computed over the BLUP family plus BLUP population and the grand-mean.

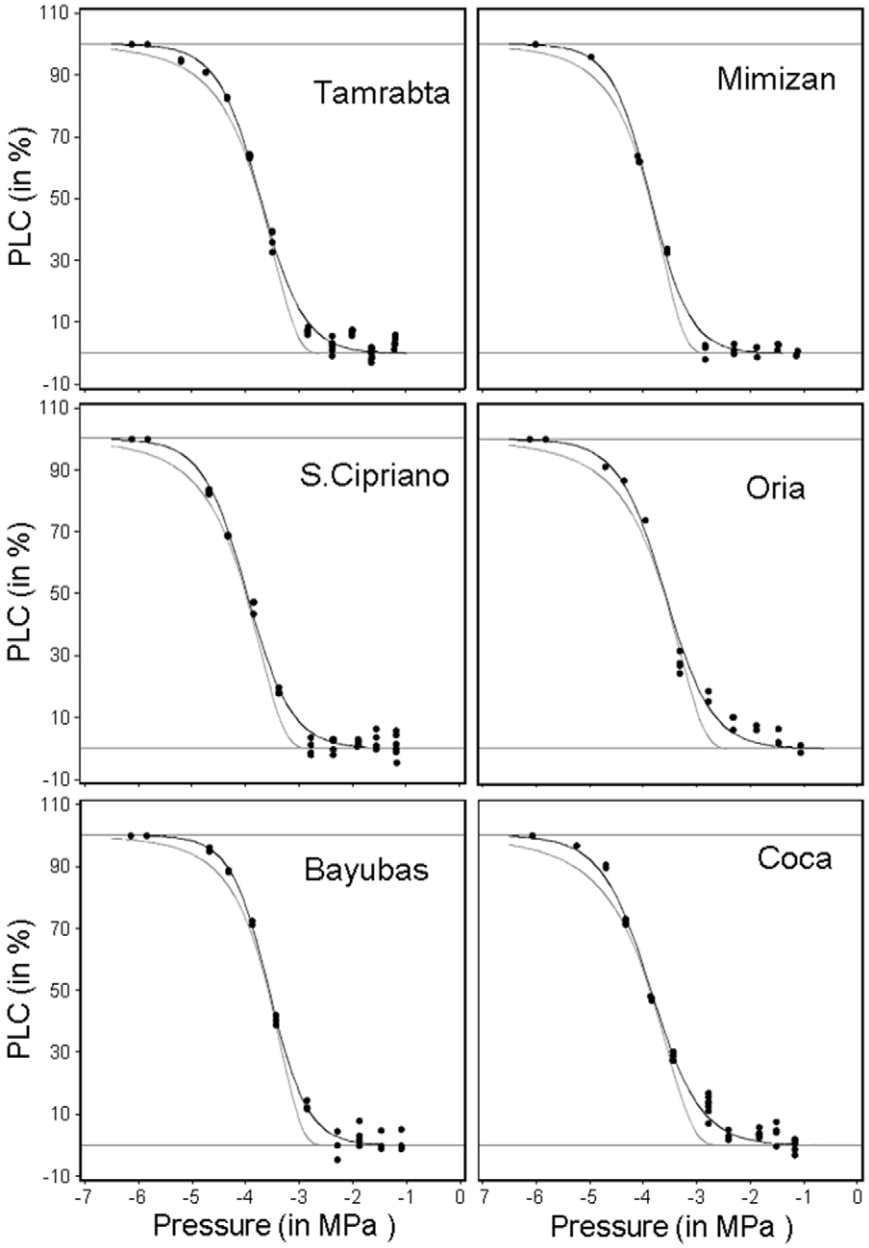

Figure 2. Vulnerability curves of one genotype for each studied population. Black dot are the raw measure of percent of loss of conductance (PLC in %) along the negative pressure gradient (in MPa). The grey line is the Weibull reparameterized model and the black line is the sigmoid reparameterized Model.
doi:10.1371/journal.pone.0023476.g002

Estimation of population differentiation

The estimate of phenotypic differentiation between populations, Q_{ST} [39], was calculated as

$$Q_{st} = \frac{\sigma^2_{pop}}{\left(\sigma^2_{pop} + 2\sigma^2_A\right)} \quad (4)$$

Putatively neutral nuclear microsatellites (nuSSRs) were used to account for genetic differentiation (F_{ST}) caused by demographic and other processes not related to selection (e.g., genetic drift resulting from geographic isolation or population expansion). Eight polymorphic nuSSRs were selected from those previously developed by [40] (NZPR413, NZPR1078, ctg64), [41,42] (ctg275, FRPP91, FRPP94, ITPH4516) and [43] (A6F03). The markers were selected to be evenly distributed over the various linkage groups of the maritime pine genetic linkage map, with, at least, 4 alleles and multiplexing capacity. Genotyping was performed on genomic DNA isolated from the needles of 20 to 30 individuals from each of the six selected populations, as previously described [44,45]. We used F_{ST} (which is estimated from the allelic frequency) rather than R_{ST} (which also takes into account allele size) because genetic drift affects allele frequency but not mutation rate. F_{ST} values for each locus were estimated with Genepop [46] using the framework developed by [47] adapted for SSR data [48].

F_{ST} and Q_{ST} comparison

For the comparison of Q_{ST} and F_{ST}, to disentangle the effects of genetic drift from those of selection, we develop a new test to avoid previously reported limitations [49,50,51,52] and allow to test $Q_{ST} > F_{ST}$ and $Q_{ST} < F_{ST}$. We explicitly derive the F_{ST} and Q_{ST} distribution using in both case a parametric bootstrap as follows.

$$F_{ST}^{*} = F_{ST}^{boot} \times \frac{\chi^2_{loci-1}}{loci-1} \quad (5)$$

F_{ST}^{*} is a parametric bootstrap replicate of F_{ST}. First, nuSSR loci were randomly resampled with replacement, to estimate the sampling variance of F_{ST}. Each of this F_{ST} replicate (F_{ST}^{boot}) value was then multiplied by a random number drawn from the Lewontin-Krakauer distribution, a chi-squared distribution with a number of degree of freedom equal to the number of loci minus 1, divided by degree of freedom equal to the number of loci minus 1. This distribution has been shown to take into account most of the deviation from the neutral model due to demographic history [51,53]. We will refer to this distribution of F_{ST}^{*} as the "drift distribution".

We estimated the sampling variance of Q_{ST} (Eq 4), by simulating the distribution of each variance component (σ^2_{pop},σ^2_A) with a parametric bootstrap [50], using the Satterthwaite approximation [54]. This distribution is highly conservative and takes into account the deviation from homogeneity of variance [54].

$$\sigma_i^{*} = \sigma_i \times \frac{\chi^2_{dfe_i}}{dfe_i} \quad (6)$$

σ_i^{*} is a parametric bootstrap replicate of variance component of i factor. It is obtained by multiplying σ_i (observed variance component) by a chi-square distribution scaled with an "effective" degree of freedom (dfe_i).

$$dfe_i = df_i - 1 \times \left[1 + \frac{2\sigma_i^2}{n\sigma_{i-1}^2} + \left(\frac{\sigma_i^i}{\sigma_{i-1}^2}\right)^2 \times \left(\frac{1}{n^2 + \frac{j-1}{n^3 j - n}}\right)\right]^{-1} \quad (7)$$

dfe_i is the effective degree of freedom for the variance component of i factor. df_i is the observed degree of freedom. σ_i is observed variance component due to i factor. σ_{i-1} is observed variance component due to *i-1* factor (nested or residuals factor). n is the total size of the sample. j is the number of level of factor i. We calculate a Q_{ST}^{*} for each replicate from σ^{2*}_{pop} and σ^{2*}_A (Eq. 6). We will refer to this distribution of Q_{ST}^{*} as the "phenotypic distribution", although Q_{ST} is a standardized measurement of additive genetic variance between populations.

Finally, we compared the F_{ST}^{*} and Q_{ST}^{*} distributions, using nonparametric and free distribution two-sample test for equality of the 2.5 and the 97.5 quantile (see [55] for theoretical proof) with a Bonferroni correction for multiple comparisons. We also applied a studentized bootstrap, which gave similar results but required more computation time [56,57,58]. All the analyses were performed with SAS version 9.2. Codes are available on request.

Results

1. Between-population variation

For each population, vulnerability curves showed similar sigmoid shape with the air-entry (P_{12}) around -3.25 ± 0.006 MPa (see Figure 2). Linear curves were discarded from the analysis [59]. The between-population effect (V_{BP}) was significant for $\delta^{13}C$ and Δ_h but not for P_{50} (Table 2). Similarly, no difference was found for the other cavitation resistance-related traits (S_{12}, S_{88}, S_{50}, P_{12}, P_{88}, data not shown). Cavitation resistance-related traits had much lower coefficients of variation than Δ_h (Table 2). This was particularly true for the between-population coefficient of variation ($CV_{BP} = 1\%$ and 18% for P_{50} and Δ_h, respectively). It should be noted that CVs for $\delta^{13}C$ are not comparable with those of other traits, because they are estimated relative to a standard [60] and are therefore independent of scale change but not of origin. The fixed block effect was significant for all the traits studied, indicating that some of the environmental variation was taken into account by the experimental design.

The populations from the wettest areas (Mimizan and San Cipriano) had the highest Δ_h values (Figure 3a), whereas Tamrabta population (from Morocco) presented the lowest value. Iberian populations from very different climatic areas (Coca, Bayubas, Oria) had intermediate values, with no detectable trend as a function of environmental aridity.

No significant difference between populations was detected for P_{50} (Figure 3b), although Tamrabta surpassed the other populations and was the most cavitation-resistant population. Tamrabta also presented the lowest $\delta^{13}C$ value (Figure 3c), demonstrating a significantly lower water-use efficiency than the other populations, all other populations presented similar $\delta^{13}C$ values.

2. Within-population variation

Heritabilities and normalized measurements of trait dispersion (i.e. CVs) were estimated to evaluate the within-population additive variance, evolvability (through the analysis of CV_A) and micro-environmental sensitivity (through the analysis of CV_R) (Table 2). Narrow-sense heritability (h^2_{ns}) for P_{50} was higher (0.44 ± 0.18) than those estimated for $\delta^{13}C$ (0.21 ± 0.10) and Δ_h (0.35 ± 0.06), showing that cavitation resistance was genetically controlled, although the standard error was high, probably due to the small number of progenies per mother tree analyzed. The CVs of P_{50} and Δ_h presented contrasting patterns, with a lower coefficient of additive variation for P_{50} ($CV_A = 4.4\%$) than for Δ_h ($CV_A = 16.2\%$), suggesting limited evolvability of P_{50}.

3. Evolutionary forces driving population differentiation

Q_{ST} and F_{ST} comparisons have three possible outcomes [39]: (i) if $Q_{ST} > F_{ST}$, the degree of differentiation for quantitative traits exceeds that attainable by genetic drift alone (ii) if Q_{ST} and F_{ST} are not significantly different, the observed degree of differentiation for quantitative traits could have been reached by genetic drift alone, and (iii) if $Q_{ST} < F_{ST}$ the observed degree of differentiation is lower than expected from genetic drift alone. Consistent with previous reports [50,61] , we found that F_{ST}^{*} and Q_{ST}^{*} presented skewed distributions (Figure 4). Only Δ_h and P_{50} had a Q_{ST}^{*} distribution different from the F_{ST}^{*} distribution ($P = 0.003$ and $P < 0.0001$ respectively). For, $\delta^{13}C$, the difference between Q_{ST}^{*} and F_{ST}^{*} values was centered on 0 (see Figure 4c right panel), and it was therefore not possible to distinguish between drift and selection ($P = 0.88$). Conversely, differences between the Q_{ST}^{*} and F_{ST}^{*} distributions for P_{50} were centered on -0.18, suggesting that the studied populations were less differentiated than would be expected in the presence of drift alone (Figure 4b), which means that natural selection favored the same mean phenotype in different populations (consequence of uniform selection) . For Δ_h, the difference between Q_{ST}^{*} and F_{ST}^{*} distributions was centered around 0.27, suggesting that the studied populations displayed more differentiation than would be expected with drift alone

Table 2. Variance components (V_P, V_{BP}, V_A, V_R), narrow-sense heritability (h^2_{ns}), coefficient of variation (CV_P, CV_A, CV_{BP}, CV_R) and population differentiation (Q_{ST}) for all studied maritime pine populations.

Traits	V_P	V_{BP}	V_A	V_R	$h^2_{ns}\pm SE$	CV_P	CV_A	CV_{BP}	CV_R	Q_{ST}
P_{50}	0.067	0.002 ^{ns}	0.028*	0.058	0.438±0.18	6.6	4.4	1	6.2	0.027
$\delta^{13}C$	0.284	0.030 **	0.059*	0.269	0.213±0.10	1.7[a]	0.8[a]	0.6[a]	1.7[a]	0.197
Δ_h	112.7	55.0 ***	40.96***	102.5	0.363±0.06	26.9	16.2	18.8	25.7	0.188

h^2_{ns} is the narrow-sense heritability and **SE** is the standard error of heritability, **V_P** is the phenotypic genetic variance, **V_A** is the additive genetic variance, **V_{BP}** is the between-population variance, **V_R** is the residual variance. **CV_A** is the variation coefficient of additive variance after adjustment for the block effect. **CV_P** is the variation coefficient of phenotypic variance after adjustment for the block effect. **CV_R** is the residual coefficient of variation. **CV_{BP}** is between-population coefficients of variation. **Q_{ST}** is the genetic quantitative variation between populations (Spitze, 1993). The significance of random effects is indicated after each variance estimator: ^{ns} $P > 0.05$, * $P<0.05$, ** $P<0.01$, *** $P<0.001$. [a] CVs for $\delta^{13}C$ are not comparable with other traits as they are estimated relative to a standard.

doi:10.1371/journal.pone.0023476.t002

(Figure 4c) which is interpreted as a consequence of diversifying selection.

4. Correlation between traits

We found a significant positive phenotypic correlation between absolute value of P_{50} and $\delta^{13}C$ at the phenotypic level ($r = 0.30$, $P = 0.035$ see Figure S1), indicating that the more cavitation-resistant genotypes tended to be less water-use efficient. However, this relationship was not significant at the genetic level ($r = 0.14$, $P = 0.320$). No relationship between P_{50} and Δ_h was found at either phenotypic or genetic level. A significant negative phenotypic correlation between Δ_h and $\delta^{13}C$ was detected ($r = -0.68$, $P<0.0001$). This correlation was barely significant at the genetic level ($r = -0.29$, $P = 0.053$).

Discussion

We reliably estimated for the first time the genetic variability of cavitation resistance, a functional trait that allows plants to survive under severe drought. We also provided evidence of natural selection acting on this trait. These results were based on the greatest number of genotypes ever measured to date in an experimental design (Table S1 and supplementary references). Despite the high level of variation of cavitation resistance between species [15], we detected no significant differences between maritime pine populations from a wide range of environments. Moreover, the between-population variability of cavitation resistance was significantly lower than would be expected under a hypothesis of genetic drift alone (Q_{ST}- F_{ST} comparison). We can therefore reject the hypothesis of diversifying selection. We suggest instead that uniform selection has shaped the phenotypic variability of this trait. Uniform selection could be seen as a stabilizing selection acting within each population with the same selection optimum in each population despite the steep climatic gradient [62,63]. Conversely, growth and water-use efficiency displayed different patterns and were found to be subject to strong diversifying selection and genetic drift, respectively. Quantitative genetics analysis also showed that cavitation resistance presented a significant heritability, higher than that estimated for growth and water-use efficiency. This is the first evidence of uniform selection in woody plants and the underlying mechanisms are discussed below from a micro-evolutionary point of view.

Intra- vs. interspecific variability of cavitation resistance

Despite the steepest climatic gradient (precipitation ranging from 400 to 1,600 mm in the sampled populations) and strong phylogeographic structure between the six studied populations [22,64]. Very low between-population variance for cavitation resistance were found ($CV_{BP} = 1\%$). The few studies published to date (reviewed in Table S1) tended to skim over the issue of intraspecific variation of cavitation resistance in provenance or progeny trials and reported little or no difference between populations [65,66]. As these studies were not designed to assess the genetic component of phenotypic variation, further investigations are required, to generalize our finding to other species. In addition, phenotypic variation for cavitation resistance was low ($CV_P = 6.6\%$), but consistent with the range reported for wood properties of maritime pine, such as mean ring density, lignin content and fiber morphology ([67,68] Lamy, unpunblished data). However, we are lacking information about the intraspecific variation of pit pair anatomical traits that are known to be implicated in cavitation resistance [69,16]. The low within-species variability for cavitation resistance is remarkable ($P_{50} = -3.93\pm0.04$ MPa, estimated over the whole dataset), given that substantial variability has been described between species. For instance, Delzon et al (2010) showed that cavitation resistance ranged from −3 to −12 MPa in a sample of 40 coniferous species. This variability was interpreted as the effect of natural selection rather than phylogenetic legacy [15].

In contrast, the population differentiation observed for growth and water-use efficiency (WUE) was significant and consistent with previous results for this species [70]. The Moroccan population had the lowest WUE, consistent with previous findings based on both gas exchange measurements and carbon isotope discrimination [71,72,73,74]. In a provenance trial carried out in south-western France, this Moroccan population displayed lower stomatal sensitivity to water stress (delayed stomatal closure), leading to greater water loss throughout the summer period and a lower WUE (as reflected by carbon isotope composition). Genotype × environment interaction could potentially alter differences between populations [75,76]. Our results therefore require confirmation in provenance trials carried out in drier climates.

Relationships between traits

The weak but significant positive correlation found between absolute value of cavitation resistance and water-use efficiency (carbon isotope composition) suggested that drought-tolerant genotypes had lower water-use efficiency. In dry environments, genotypes that allocate more carbon to the construction of cavitation-resistant wood in order to avoid runaway embolism might be able to maintain higher stomatal conductance and hydraulic conductance at low leaf water potential, resulting in a decrease in water-use efficiency. Our results are consistent with previous findings [77] of a strong and positive relationship between these two traits in two cedar species. However, little or no correlation has generally been reported [78,79,80]. The

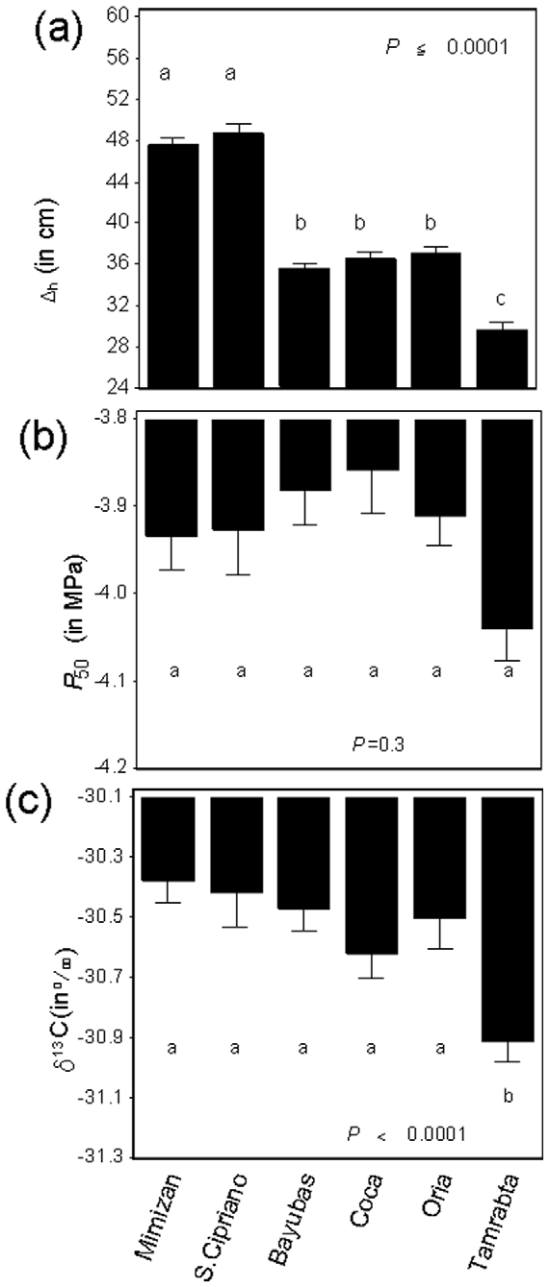

Figure 3. Mean values of height increment (Δ_h, (a)) (n = 297 per population). Mean values of cavitation resistance (P_{50}, (b)) and carbon isotope composition ($\delta^{13}C$, (c)) for each studied population (n = 40 per population). The error bars represents the standard errors. Different letters indicate significant differences between populations at $\alpha = 0.05$.
doi:10.1371/journal.pone.0023476.g003

negative correlation between carbon isotope composition and growth has been reported in previous studies [77,81,82], assuming that growth is a function of carbon assimilation and carbon isotope composition is an index of retrospective gas exchanges.

Evidence of uniform selection for cavitation resistance

The phenotypic distribution of cavitation resistance was significantly lower than the expected distribution under the drift hypothesis. This may be interpreted as a consequence of uniform selection (also called homogenous, spatially homogenizing, convergent selection, uniform stabilizing selection or stabilizing selection across population). This inference ($Q_{ST}<F_{ST}$) may result from an underestimation of Q_{ST} variance [52], leading to a false positive result. However, the F_{ST} estimate was more than five times greater that the Q_{ST} estimate. We thus believe that this difference is biologically meaningful and not due to a statistical artifact [52]. The robustness of this result is, also, supported by fourth lines of evidence: (i) the different patterns obtained for growth and WUE in the same experimental design. (ii) Selection procedure of population (see methods) increase the probability to find diversifying selection because we selected extreme populations in term of climatic origin and evolutionary history (different mitotypes and chlorotypes, see [64]), consequently uniform selection could not be interpreted as a sampling bias. (iii) Wood density (measured by X ray on the same data set) showed exactly the same pattern (Lamy, unpunblished). (iv) Willson et al (2008) showed from interspecific data with narrow taxon sampling (limited to the *Juniperus* genus), that cavitation resistance gave strong phylogenetic conservatism, suggestive of uniform selection for the maintenance of ancestral traits.

For growth, diversifying selection was highlighted by Q_{ST} being greater than F_{ST} [83]. For WUE, we detected no signature of selection, as the phenotypic and drift distributions did not differ significantly, as previous reported by [84] for *Quercus suber* (P_{ST}/F_{ST} comparison). However, the distribution (Q_{ST}-F_{ST}) of this trait was shifted to the right (integral probability above 0 > integral probability below 0, Figure 4c right panel), suggesting that diversifying selection was slightly more pronounced than drift.

What are the mechanisms behind "uniform selection" for cavitation resistance?

The causal mechanisms underlying uniform selection or leading to evolutionary stasis are not well understood [63,85,86,87,88]. We discuss here only the processes most likely to account for the observed pattern ($Q_{ST}<F_{ST}$).

Weak molecular variation. Lethal or sublethal mutations may limit the variability of the genes they affect, thereby controlling trait variation. In conifers, cavitation resistance is known to be determined by xylem anatomy, including, in particular, the characteristics of intertracheid pits [16,69]. As knowledge about the nucleotide diversity of different functional categories of genes accumulates, it may become possible to test the hypothesis that genes involved in intertracheid pit formation (once these genes have been identified) display lower levels of diversity.

Genetic constraints. If selection acts on a trait that is negatively correlated with another trait (or traits) also under selection, than the decrease of rate of evolution for the first trait is proportional to the strength of the correlation [94]. A multi-trait approach could be used to explore this hypothesis indirectly [95], but could fail if the trait is canalized.

Canalized trait. This hypothesis suggest that cavitation resistance is canalized to buffer the variation of this key hydraulic trait against all kinds of disturbance, being of genetic (mutation, hybridization, recombination) and/or environmental nature [89,90,91]. Emergent properties of molecular networks could buffer molecular variability [92], to maintain phenotypic function, in accordance with the robustness theory [93]. In zoology, dipterian wings shape or centroid size (or mammalian body temperature) are the best known cases of canalized traits [90]. Indeed they reported a similar wing shape between species despite a great variability of climatic niche and a low additive genetic variance between populations for this trait. Except for leaf shape in *Arabidopsis thaliana*, there is no evidence of canalized trait in plants nowadays. For cavitation resistance, two arguments lead

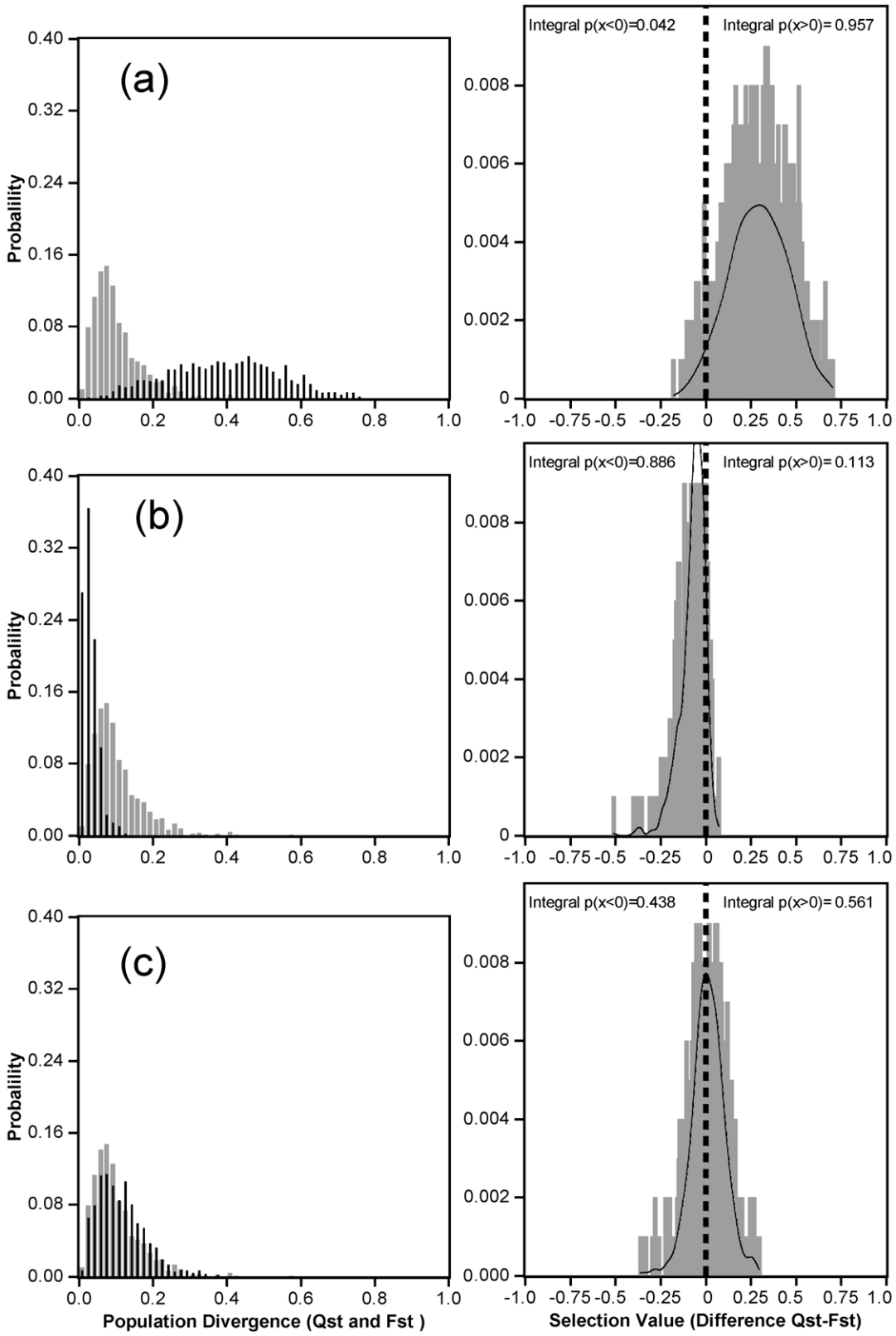

Figure 4. Comparison between F_{ST} (histogram in gray) and Q_{ST} (histogram in black) distributions for growth rate (Δ_h, (a)), cavitation resistance (P_{50}, (b)) and carbon isotope composition ($\delta^{13}C$, (c)) in the left panel. The observed distribution (gray histogram) and the kernel density (black curves) of the Q_{ST}-F_{ST} difference are represented in the right panel for each trait. On the right panel, we also show the integral probability of the distribution (using the kernel density estimator) above (see "Integral p(x>0)" on the right panel) and below (see "Integral p(x<0)" on the right panel) zero (marked with the tick and dotted line).
doi:10.1371/journal.pone.0023476.g004

us to consider canalization as the most likely mechanism: (i) low additive genetic variance between populations (V_{BP}) and (ii) the similarity of cavitation resistance values among all the *Pinus* species [69].

Variance component analysis

Variance component analysis for cavitation resistance resulted in the first estimates of the heritability of this trait ($h^2_{ns} = 0.4$) and its additive coefficient of variation ($CV_A = 4.4\%$). These values suggest that this trait may respond to truncation selection frequently practiced in breeding. However, for a given selection intensity, genetic gain for cavitation resistance would be limited by the low additive variance, although long-term artificial selection experiments have shown that quantitative traits have a non negligible mutational variance [91,96,97], which could supply further additive variance at each generation. However, due to the small number of half-sib families and progenies within each family, which could inflate the value for heritability [37], this estimate should be interpreted with caution. Additional studies with a larger sample size are required for further exploration of the genetic determinism of this hydraulically important trait.

The much higher CV_A value (16.2%) for height increment is consistent with previous reports and accounts for the genetic gain achieved for this trait over successive generations in breeding programs [98,99,100]. For $\delta^{13}C$, a previous study [31] reported a slightly lower heritability ($h^2_{ns} = 0.17$ vs. 0.21 here), but with estimation based on a diallel cross of limited size, with a narrow genetic background restricted to 12 elite trees from south-western France.

Future directions

Phenotypic variation is a fundamental prerequisite for evolution because natural selection acts on phenotype. Adaptation and evolution via natural selection requires the presence of genetic variation among individuals in a population upon which natural selection can act. Intra-population genetic variability can thus be seen as the fuel for future adaptation. However, an environmentally induced shift in phenotype is also a major component of the variation we see in nature. Recent studies [80,101] showed a weak but significant phenotypic variability for cavitation resistance. Our results suggest that this between populations variability might be under environmental control rather than genetic determinism. These considerations call for more research (ongoing) aiming at quantifying the *in situ* phenotypic variability of cavitation resistance and the extent of phenotypic plasticity using provenance trials installed under different edapho-climatic environments. Further studies are also being pursued to dissect the genetic architecture of cavitation resistance to determine the number, map location and effects of Quantitative Trait Loci controlling part of the variation of this trait.

Supporting Information

Figure S1 Genetic (right panel) and phenotypic (left panel) correlation between traits. For ease of interpretation, we have converted all the negative values to positive values (P_{50}, δC^{13}). For the genetic correlation, all Pearson correlations (r) were computed over the best linear unbiased prediction (BLUP) (n = 48 for P_{50}, δ^{13} and n = 151 for Δh). For phenotypic correlation, all Pearson correlations were computed over the BLUP family plus BLUP population and the grand-mean, to ensure that the order of degree of freedom remained the same and the block effects are removed. P_{50}, pressure at 50 % loss of conductivity in MPa, Δh the annual increment between 2004 and 2005, in mm, $\delta^{13}C$ is the isotope discrimination for carbon 13 in ‰.
(TIF)

Table S1 Review of intraspecific studies for cavitation resistance estimated using P_{50} or related parameters (as indicated in the table). Npop: number of populations used, Nind: number of individuals per population used to assess cavitation resistance. The table is divided in two parts, the first part corresponds to provenance or progeny trials, and the second to "*in situ*" studies.
(DOC)

Table S2 Result of the principal component (PC) analysis (PCA) for climatic data of *Pinus pinaster* populations (listed in the methods section, n = 763). Contributions to the first, second, third and fourth axes are indicated for each variable (PC1, PC2, PC3, PC4). The eigenvalues of PC1 = 7.65, PC2 = 3.059, PC3 = 0.97, PC4 = 0.86. *W* is mean wet ground days (days). *I* is mean Martonne's index ($P_i/(T_a+10)$). P_i is the mean precipitation ($mm.days^{-1}$). *C* is percent of cloud cover (%). *S* is the mean of wind speed ($m.s^{-1}$). *V* is the water vapor pressure in air (hPa). *VPD* is the water vapor pressure deficit of air (hPa). T_{min} is the minimum temperature (°C). Δ_{DT} is the mean diurnal temperature range (°C). T_m is mean temperature (°C). R_G is mean global radiation ($W.m^2$). T_{max} is the maximum temperature (°C). *H* is mean soil water deficit (P_i-ETP, in mm). *ETP* is mean Truc's potential evapotranspiration (mm).
(DOC)

Acknowledgments

We thank Ricardo Alia for providing seeds from the Spanish populations, Steven Jansen for discussions about phylogeny, Stephanie Mariette for sharing her knowledge on neutral diversity in *Pinus pinaster* and Chantal Hélou for laboratory assistance, Hadrien Lalagüe for photography credit (www.hadrien-Lalague.com). We thank Pauline Granier-Géré, Emmanuelle Eveno and the experimental unit of INRA pierroton for providing height growth data.

Author Contributions

Conceived and designed the experiments: J-BL CP. Performed the experiments: J-BL RB SD. Analyzed the data: J-BL LB SD. Contributed reagents/materials/analysis tools: J-BL LB SD RB. Wrote the paper: J-BL CP HC SD. Organized the funding of the study: CP HC SD.

References

1. Pearson RG (2006) Climate change and the migration capacity of species. Trends in Ecology & Evolution 21: 111–113.
2. Thuiller W (2004) Patterns and uncertainties of species' range shifts under climate change. Global Change Biology 10: 2020–2027.
3. Lindner M, Maroschek M, Netherer S, Kremer A, Barbati A, et al. (2010) Climate change impacts, adaptive capacity, and vulnerability of European forest ecosystems. Forest Ecology and Management 259: 698–709.
4. Beniston M, Stephenson DB, Christensen OB, Ferro CAT, Frei C, et al. (2007) Future extreme events in European climate: an exploration of regional climate model projections. Climatic Change 81: 71–95.
5. Breshears DD, Myers OB, Meyer CW, Barnes FJ, Zou CB, et al. (2009) Tree die-off in response to global change-type drought: mortality insights from a decade of plant water potential measurements. Frontiers in Ecology and the Environment 7: 185–189.

6. Martinez-Meier A, Sanchez L, Pastorino M, Gallo L, Rozenberg P (2008) What is hot in tree rings? The wood density of surviving Douglas-firs to the 2003 drought and heat wave. Forest Ecology and Management 256: 837–843.
7. Martinez-Vilalta J, Pinol J (2002) Drought-induced mortality and hydraulic architecture in pine populations of the NE Iberian Peninsula. Forest Ecology and Management 161: 247–256.
8. Jentsch A, Kreyling J, Beierkuhnlein C (2007) A new generation of climate-change experiments: events, not trends. Frontiers in Ecology and the Environment 5: 365–374.
9. McDowell N, Pockman WT, Allen CD, Breshears DD, Cobb N, et al. (2008) Mechanisms of plant survival and mortality during drought: why do some plants survive while others succumb to drought? New Phytologist 178: 719–739.
10. Tyree MT (2003) The ascent of water. Nature 423: 923–923.
11. Brodribb TJ, Bowman D, Nichols S, Delzon S, Burlett R (2010) Xylem function and growth rate interact to determine recovery rates after exposure to extreme water deficit. New Phytologist 188: 533–542.
12. Brodribb TJ, Cochard H (2009) Hydraulic Failure Defines the Recovery and Point of Death in Water-Stressed Conifers. Plant Physiology 149: 575–584.
13. Cochard H, Barigah ST, Kleinhentz M, Eshel A (2008) Is xylem cavitation resistance a relevant criterion for screening drought resistance among Prunus species? Journal of Plant Physiology 165: 976–982.
14. Hacke UG, Sperry JS (2001) Functional and ecological xylem anatomy. Perspectives in Plant Ecology Evolution and Systematics 4: 97–115.
15. Maherali H, Pockman WT, Jackson RB (2004) Adaptive variation in the vulnerability of woody plants to xylem cavitation. Ecology 85: 2184–2199.
16. Pittermann J, Choat B, Jansen S, Stuart SA, Lynn L, et al. (2010) The Relationships between Xylem Safety and Hydraulic Efficiency in the Cupressaceae: The Evolution of Pit Membrane Form and Function. Plant Physiology 153: 1919–1931.
17. Willson CJ, Manos PS, Jackson RB (2008) Hydraulic traits are influenced by phylogenetic history in the drought-resistant, invasive genus Juniperus (Cupressaceae). American Journal of Botany 95: 299–314.
18. Jacobsen AL, Ewers FW, Pratt RB, Paddock WA, Davis SD (2005) Do xylem fibers affect vessel cavitation resistance? Plant Physiology 139: 546–556.
19. Ribeiro MM, LeProvost G, Gerber S, Vendramin GG, Anzidei M, et al. (2002) Origin identification of maritime pine stands in France using chloroplast simple-sequence repeats. Annals of Forest Science 59: 53–62.
20. Richardson DM, ed (1998) Ecology and biogeography of Pinus. Cambridge: Press Syndicate of the University of Cambridge. xvii +527.
21. Cochard H, Damour G, Bodet C, Tharwat I, Poirier M, et al. (2005) Evaluation of a new centrifuge technique for rapid generation of xylem vulnerability curves. Physiologia Plantarum 124: 410–418.
22. Bucci G, Gonzalez-Martinez SC, Le Provost G, Plomion C, Ribeiro MM, et al. (2007) Range-wide phylogeography and gene zones in Pinus pinaster Ait. revealed by chloroplast microsatellite markers. Molecular Ecology 16: 2137–2153.
23. New M, Hulme M, Jones P (1999) Representing twentieth-century space-time climate variability. Part I: Development of a 1961-90 mean monthly terrestrial climatology. Journal of Climate 12: 829–856.
24. New M, Hulme M, Jones P (2000) Representing twentieth-century space-time climate variability. Part II: Development of 1901-96 monthly grids of terrestrial surface climate. Journal of Climate 13: 2217–2238.
25. New M, Lister D, Hulme M, Makin I (2002) A high-resolution data set of surface climate over global land areas. Climate Research 21: 1–25.
26. Delzon S, Sartore M, Burlett R, Dewar R, Loustau D (2004) Hydraulic responses to height growth in maritime pine trees. Plant Cell and Environment 27: 1077–1087.
27. Cai J, Hacke U, Zhang SX, Tyree MT (2010) What happens when stems are embolized in a centrifuge? Testing the cavitron theory. Physiologia Plantarum 140: 311–320.
28. Cochard H (2002) A technique for measuring xylem hydraulic conductance under high negative pressures. Plant Cell and Environment 25: 815–819.
29. Pammenter NW, Vander Willigen C (1998) A mathematical and statistical analysis of the curves illustrating vulnerability of xylem to cavitation. Tree Physiology 18: 589–593.
30. Ogle K, Barber JJ, Willson C, Thompson B (2009) Hierarchical statistical modeling of xylem vulnerability to cavitation. New Phytologist 182: 541–554.
31. Brendel O, Pot D, Plomion C, Rozenberg P, Guehl JM (2002) Genetic parameters and QTL analysis of delta C-13 and ring width in maritime pine. Plant Cell and Environment 25: 945–953.
32. Farquhar GD, Oleary MH, Berry JA (1982) On the relationship between carbon isotope discrimination and the inter-cellular carbon-dioxide concentration in leaves. Australian Journal of Plant Physiology 9: 121–137.
33. Farquhar GD, Richards RA (1984) Isotopic composition of plant carbon correlates with water-use efficiency of wheat genotypes. Australian Journal of Plant Physiology 11: 539–552.
34. SAS II (2008) SAS/STAT® 9.2 User's Guide. Cary, NC: SAS Institute Inc.
35. Wilson AJ (2008) Why h^2 does not always equal V_A/V_P? Journal of Evolutionary Biology 21: 647–650.
36. Visscher PM, Hill WG, Wray NR (2008) Heritability in the genomics era - concepts and misconceptions. Nature Reviews Genetics 9: 255–266.
37. Lynch M, Walsh B, eds (1998) Genetics and analysis of quantitative traits: Sinauer Associates, Inc.. xvi + 980.
38. Houle D (1992) Comparing evolvabiliy and variability of quantitative traits. Genetics 130: 195–204.
39. Spitze K (1993) Population-Structure in Daphnia-Obtusa - Quantitative Genetic and Allozymic Variation. Genetics 135: 367–374.
40. Chagne D, Chaumeil P, Ramboer A, Collada C, Guevara A, et al. (2004) Cross-species transferability and mapping of genomic and cDNA SSRs in pines. Theoretical and Applied Genetics 109: 1204–1214.
41. Mariette S, Chagne D, Decroocq S, Vendramin GG, Lalanne C, et al. (2001) Microsatellite markers for Pinus pinaster Ait. Annals of Forest Science 58: 203–206.
42. Mariette S, Chagne D, Lezier C, Pastuszka P, Baffin A, et al. (2001) Genetic diversity within and among Pinus pinaster populations: comparison between AFLP and microsatellite markers. Heredity 86: 469–479.
43. Guevara MA, Chagne D, Almeida MH, Byrne M, Collada C, et al. (2005) Isolation and characterization of nuclear microsatellite loci in Pinus pinaster Ait. Molecular Ecology Notes 5: 57–59.
44. Eveno E (2008) Drought adaptation in *Pinus pinaster*: diversity pattern and nucleotidic differentiation of candidats genes and phenotypic variability [PhD thesis,]. Bordeaux, aquitaine, FRANCE: :University of Bordeaux 1: 399.
45. Eveno E, Collada C, Guevara MA, Leger V, Soto A, et al. (2008) Contrasting patterns of selection at Pinus pinaster Ait. drought stress candidate genes as revealed by genetic differentiation analyses. Molecular Biology and Evolution 25: 417–437.
46. Rousset F (2008) GENEPOP ' 007: a complete re-implementation of the GENEPOP software for Windows and Linux. Molecular Ecology Resources 8: 103–106.
47. Weir BS, Hill WG (2002) Estimating F-statistics. Annual Review of Genetics 36: 721–750.
48. Michalakis Y, Excoffier L (1996) A generic estimation of population subdivision using distances between alleles with special reference for microsatellite loci. Genetics 142: 1061–1064.
49. Le Corre V, Kremer A (2003) Genetic variability at neutral markers, quantitative trait loci and trait in a subdivided population under selection. Genetics 164: 1205–1219.
50. O'Hara RB, Merila J (2005) Bias and precision in Q_{ST} estimates: Problems and some solutions. Genetics 171: 1331–1339.
51. Whitlock MC (2008) Evolutionary inference from Q_{ST}. Molecular Ecology 17: 1885–1896.
52. Whitlock MC, Guillaume F (2009) Testing for Spatially Divergent Selection: Comparing Q_{ST} to F_{ST}. Genetics 183: 1055–1063.
53. Lewontin RC, Krakauer J (1973) Distribution of gene frequency as a test of theory of selective neutrality of polymorphisms. Genetics 74: 175–195.
54. Satterthwaite FE (1946) An Approximate Distribution of Estimates of Variance Components. Biometrics Bulletin 2: 110–114.
55. Kosorok MR (1999) Two-sample quantile tests under general conditions. Biometrika 86: 909–921.
56. Boos DD (2003) Introduction to the bootstrap world. Statistical Science 18: 168–174.
57. Field CA, Pang Z, Welsh AH (2008) Bootstrapping data with multiple levels of variation. Canadian Journal of Statistics-Revue Canadienne De Statistique 36: 521–539.
58. Field CA, Welsh AH (2007) Bootstrapping clustered data. Journal of the Royal Statistical Society Series B-Statistical Methodology 69: 369–390.
59. Cochard H, Herbette S, Barigah T, Badel E, Ennajeh M, et al. (2010) Does sample length influence the shape of xylem embolism vulnerability curves? A test with the Cavitron spinning technique. Plant Cell and Environment 33: 1543–1552.
60. Brendel O, Le Thiec D, Scotti-Saintagne C, Bodenes C, Kremer A, et al. (2008) Quantitative trait loci controlling water use efficiency and related traits in Quercus robur L. Tree Genetics & Genomes 4: 263–278.
61. Waldmann P, Garcia-Gil MR, Sillanpaa MJ (2005) Comparing Bayesian estimates of genetic differentiation of molecular markers and quantitative traits: an application to Pinus sylvestris. Heredity 94: 623–629.
62. Leinonen T, O'Hara RB, Cano JM, Merila J (2008) Comparative studies of quantitative trait and neutral marker divergence: a meta-analysis. Journal of Evolutionary Biology 21: 1–17.
63. Merila J, Crnokrak P (2001) Comparison of genetic differentiation at marker loci and quantitative traits. Journal of Evolutionary Biology 14: 892–903.
64. Burban C, Petit RJ (2003) Phylogeography of maritime pine inferred with organelle markers having contrasted inheritance. Molecular Ecology 12: 1487–1495.
65. Matzner SL, Rice KJ, Richards JH (2001) Intra-specific variation in xylem cavitation in interior live oak (Quercus wislizenii A. DC.). Journal of Experimental Botany 52: 783–789.
66. Wang TL, Aitken SN, Kavanagh KL (2003) Selection for improved growth and wood quality in lodgepole pine: effects on phenology, hydraulic architecture and growth of seedlings. Trees-Structure and Function 17: 269–277.
67. Bouffier L, Charlot C, Raffin A, Rozenberg P, Kremer A (2008) Can wood density be efficiently selected at early stage in maritime pine (Pinus pinaster Ait.)? Annals of Forest Science 65, doi:10.1051/forest 2007078.
68. Pot D, Chantre G, Rozenberg P, Rodrigues JC, Jones GL, et al. (2002) Genetic control of pulp and timber properties in maritime pine (Pinus pinaster Ait.). Annals of Forest Science 59: 563–575.

69. Delzon S, Douthe C, Sala A, Cochard H (2010) Mechanism of water-stress induced cavitation in conifers: bordered pit structure and function support the hypothesis of seal capillary-seeding. Plant, Cell & Environment in Press.
70. Gonzalez-Martinez SC, Alia R, Gil L (2002) Population genetic structure in a Mediterranean pine (Pinus pinaster Ait.): a comparison of allozyme markers and quantitative traits. Heredity 89: 199–206.
71. Correia I, Almeida MH, Aguiar A, Alia R, David TS, et al. (2008) Variations in growth, survival and carbon isotope composition (delta C-13) among Pinus pinaster populations of different geographic origins. Tree Physiology 28: 1545–1552.
72. Guehl JM, Ferhi A, Loustau D, Nguyen A (1993) Spatial and between-tree variability of cellulose delta13C in the wood of maritime pine trees. Agricoltura Ricerca 15: 31.
73. Guehl JM, Fort C, Ferhi A (1995) Differential response of leaf conductance, carbon-isotope discrimination and water-use efficiency to nitrogen deficiency in Maritime Pine and Pedunculate Oak plants. New Phytologist 131: 149–157.
74. Guyon JP, Kremer A (1982) Phenotypic stability of the height growth and daily kinetics of sap pressure and transpiration in the maritime pine (*Pinus pianster*). Canadian Journal of Forest Research-Revue Canadienne De Recherche Forestiere 12: 936–946.
75. Alia R, Moro J, Denis JB (1997) Performance of Pinus pinaster provenances in Spain: interpretation of the genotype by environment interaction. Canadian Journal of Forest Research-Revue Canadienne De Recherche Forestiere 27: 1548–1559.
76. Rehfeldt GE, Tchebakova NM, Parfenova YI, Wykoff WR, Kuzmina NA, et al. (2002) Intraspecific responses to climate in Pinus sylvestris. Global Change Biology 8: 912–929.
77. Ducrey M, Huc R, Ladjal M, Guehl JM (2008) Variability in growth, carbon isotope composition, leaf gas exchange and hydraulic traits in the eastern Mediterranean cedars Cedrus libani and C. brevifolia. Tree Physiology 28: 689–701.
78. Fichot R, Barigah TS, Chamaillard S, Le Thiec D, Laurans F, et al. (2010) Common trade-offs between xylem resistance to cavitation and other physiological traits do not hold among unrelated Populus deltoidesx Populus nigra hybrids. Plant Cell and Environment 33: 1553–1568.
79. Maherali H, Walden AE, Husband BC (2009) Genome duplication and the evolution of physiological responses to water stress. New Phytologist 184: 721–731.
80. Martinez-Vilalta J, Cochard H, Mencuccini M, Sterck F, Herrero A, et al. (2009) Hydraulic adjustment of Scots pine across Europe. New Phytologist 184: 353–364.
81. Baltunis BS, Martin TA, Huber DA, Davis JM (2008) Inheritance of foliar stable carbon isotope discrimination and third-year height in Pinus taeda clones on contrasting sites in Florida and Georgia. Tree Genetics & Genomes 4: 797–807.
82. Johnsen KH, Flanagan LB, Huber DA, Major JE (1999) Genetic variation in growth, carbon isotope discrimination, and foliar N concentration in Picea mariana: analyses from a half-diallel mating design using field-grown trees. Canadian Journal of Forest Research-Revue Canadienne De Recherche Forestiere 29: 1727–1735.
83. Goudet J, Buchi L (2006) The effects of dominance, regular inbreeding and sampling design on Q_{ST}, an estimator of population differentiation for quantitative traits. Genetics 172: 1337–1347.
84. Ramirez-Valiente JA, Lorenzo Z, Soto A, Valladares F, Gil L, et al. (2009) Elucidating the role of genetic drift and natural selection in cork oak differentiation regarding drought tolerance. Molecular Ecology 18: 3803–3815.
85. Brent Burt D (2001) Evolutionary stasis, constraint and other terminology describing evolutionary patterns. Biological Journal of the Linnean Society 72: 509–517.
86. Caruso CM (2004) The quantitative genetics of floral trait variation in Lobelia: Potential constraints on adaptive evolution. Evolution 58: 732–740.
87. Caruso CM, Maherali H, Mikulyuk A, Carlson K, Jackson RB (2005) Genetic variance and covariance for physiological traits in Lobelia: Are there constraints on adaptive evolution? Evolution 59: 826–837.
88. Caruso CM, Maherali H, Sherrard M (2006) Plasticity of physiology in Lobelia: Testing for adaptation and constraint. Evolution 60: 980–990.
89. Hansen TF, Alvarez-Castro JM, Carter AJR, Hermisson J, Wagner GP (2006) Evolution of genetic architecture under directional selection. Evolution 60: 1523–1536.
90. Hansen TF, Houle D (2004) Evolvability, stabilizing selection, and the problem of stasis. In:Pigliucci M, Preston K, eds. Evolutionary Biology of Complex Phenotypes. Oxford UK: Oxford University Press. pp 130–150.
91. Le Rouzic A, Carlborg O (2008) Evolutionary potential of hidden genetic variation. Trends in Ecology & Evolution 23: 33–37.
92. Fu J, Keurentjes JJB, Bouwmeester H, America T, Verstappen FWA, et al. (2009) System-wide molecular evidence for phenotypic buffering in Arabidopsis. Nature Genetics 41: 166–167.
93. Kitano H (2004) Biological robustness. Nature Reviews Genetics 5: 826–837.
94. Kruuk LEB, Merila J, Sheldon BC (2001) Phenotypic selection on a heritable size trait revisited. American Naturalist 158: 557–571.
95. Martin G, Chapuis E, Goudet J (2008) Multivariate Q(st)-F-st Comparisons: A Neutrality Test for the Evolution of the G Matrix in Structured Populations. Genetics 180: 2135–2149.
96. Houle D, Morikawa B, Lynch M (1996) Comparing mutational variabilities. Genetics 143: 1467–1483.
97. Moose SP, Dudley JW, Rocheford TR (2004) Maize selection passes the century mark: a unique resource for 21st century genomics. Trends in Plant Science 9: 358–364.
98. Bouffier L, Raffin A, Kremer A (2008) Evolution of genetic variation for selected traits in successive breeding populations of maritime pine. Heredity 101: 156–165.
99. Kremer A (1979) Genetic control of height increment in Pinus pinaster, annual rhythm and interannual behaviour. Comptes-rendus du 104eme Congres National des Societes Savantes. pp 340–352.
100. Rweyongeza DM, Yeh FC, Dhir NK (2005) Heritability and correlations for Biomass production and allocation in white spruce seedlings. Silvae Genetica 54: 228–235.
101. Herbette S, Wortemann R, Awad H, Huc R, Cochard H, et al. (2010) Insights into xylem vulnerability to cavitation in *Fagus sylvatica* L.: phenotypic and environmental sources of variability. Tree Physiology.

Acta Physiologiae Plantarum

Genetic variation for resistance to cavitation among Pinus hartwegii populations

--Manuscript Draft--

Manuscript Number:	
Full Title:	Genetic variation for resistance to cavitation among Pinus hartwegii populations
Article Type:	Original Research
Corresponding Author:	Cuauhtemoc Saenz-Romero, Ph.D. Universidad Michoacana de San Nicolás de Hidalgo Tarímbaro, Michoacán MEXICO
Corresponding Author Secondary Information:	
Corresponding Author's Institution:	Universidad Michoacana de San Nicolás de Hidalgo
Corresponding Author's Secondary Institution:	
First Author:	Cuauhtemoc Saenz-Romero, Ph.D.
First Author Secondary Information:	
Order of Authors:	Cuauhtemoc Saenz-Romero, Ph.D.
	Sylvain Delzon, Ph.D.
	Jean-Baptiste Lamy, Ph.D.
	Esperanza Loya-Rebollar, M.Sc.
	Andrés Plaza-Aguilar, M.Sc.
	Régis Burlett, M.Sc.
	Philippe Lobit, Ph.D.
Order of Authors Secondary Information:	
Abstract:	Hydraulic failure can cause massive die-back of forest trees during drought. With extreme climatic events set to become more frequent and severe due to climatic change, it is essential to study resistance to water-stress induced cavitation. We investigated the genetic differentiation for cavitation resistance among Pinus hartwegii populations, the pine species growing at the treeline in México. Open-pollinated seeds were collected from 10 natural populations along an altitudinal gradient (3150 to 3700 m of altitude, one population in general every 50 m of altitudinal difference), from Pico de Tancítaro, Michoacán, western México. Seedlings were raised in a nursery and then established in a randomized complete block design in a common garden experiment. Resistance to cavitation (P50, xylem pressure inducing 50% loss of hydraulic conductance and S, slope of the vulnerability curve), was evaluated on branches of 5-years-old seedlings, using the Cavitron technique. No significant genetic differentiation was detected between populations for P50, whereas a significant altitudinal cline was found for S. Mean value (± standard error) of cavitation resistance (P50) was -3.42 ± 0.047 MPa, indicating that Pinus hartwegii is highly vulnerable to cavitation as previously observed for most of Pinus genus species. Within the Pinus genus, we also found that pines growing at the treeline are more vulnerable to cavitation than those from lowland. The low cavitation resistance and the lack of genetic differentiation among P. hartwegii populations, represent a limitation for adapting to warmer and drier climates that will occur in México due to climatic change

Genetic variation for resistance to cavitation among *Pinus hartwegii* populations

Cuauhtémoc Sáenz-Romero[1*], Sylvain Delzon[2], Jean-Baptiste Lamy[2], Esperanza Loya-Rebollar[1], Andrés Plaza-Aguilar[2], Régis Burlett[2] and Philippe Lobit[1]

[1]*Universidad Michoacana de San Nicolás de Hidalgo, Instituto de Investigaciones Agropecuarias y Forestales (UMSNH-IIAF). Km 9.5 Carretera Morelia-Zinapécuaro, Tarímbaro Michoacán 58880, México.*

[2]*INRA – Université de Bordeaux, UMR 1202 BIOGECO, F-33610 Cestas, France.*

Phone: +52 (443) 334-0475 ext. 118. Fax: ext. 200.

*Corresponding author. Email: csaenzromero@gmail.com

Abstract

Hydraulic failure can cause massive die-back of forest trees during drought. With extreme climatic events set to become more frequent and severe due to climatic change, it is essential to study resistance to water-stress induced cavitation. We investigated the genetic differentiation for cavitation resistance among *Pinus hartwegii* populations, the pine species growing at the treeline in México. Open-pollinated seeds were collected from 10 natural populations along an altitudinal gradient (3150 to 3700 m of altitude, one population in general every 50 m of altitudinal difference), from Pico de Tancítaro, Michoacán, western México. Seedlings were raised in a nursery and then established in a randomized complete block design in a common garden experiment. Resistance to cavitation (P_{50}, xylem pressure inducing 50% loss of hydraulic conductance and *S*, slope of the vulnerability curve), was evaluated on branches of 5-years-old seedlings, using the Cavitron technique. No significant genetic differentiation was detected between populations for P_{50}, whereas a significant altitudinal cline was found for *S*. Mean value (± standard error) of cavitation resistance (P_{50}) was -3.42 ± 0.047 MPa, indicating that *Pinus hartwegii* is highly vulnerable to cavitation as previously observed for most of *Pinus* genus species. Within the *Pinus* genus, we also found that pines growing at the treeline are more vulnerable to cavitation than those from lowland. The low cavitation resistance and the lack of genetic differentiation among *P. hartwegii* populations, represent a limitation for adapting to warmer and drier climates that will occur in México due to climatic change.

Keywords: *Pinus hartwegii, altitudinal genetic variation, climatic change, drought stress, timberline, resistance to cavitation.*

Introduction

There are predictions for México that climatic change will cause (in comparison with the average 1961-1990) an increase of mean annual temperature of 1.5 ºC by year 2030, 2.3 ºC by year 2060 and 3.7 ºC by year 2090, while precipitation would decrease 6.7 % by year 2030, 9.0 % by year 2060 and 18.2 % by year 2090 (Saénz-Romero et al 2010). In this situation, Mexican mountain ranges were conifer forests occur are expected to have a dryer climate (Rehfeldt et al. 2011) with more frequent droughts. There is cumulative evidence of sudden decline of tree populations linked to climatic change, for example, for *Pinus edulis* at low altitudinal limits in south-western USA (Breshears et al 2005), for *Populus tremuloides* in the Rocky Mountains, USA (Rehfeldt et al 2009), for *Cedrus atlantica* in the Moyen Atlas mountain range, Morocco (Mátyás 2010), and for *Fagus sylvatica* in South-west Hungary (Mátyás et al 2010). In Catalonia, northeast Spain, declining species already are being replaced by more drought-tolerant species, that is, *Fagus sylvatica* being replaced by *Quercus ilex* (Peñuelas et al 2007). Another recent study revealed global forest die-backs due to drought and heat stress (Allen et al. 2010), that are likely to be caused by tree hydraulic failure (McDowell et al. 2008).

Pinus hartwegii Lindl is a pine species from the temperate-cold zones of Mexico and Central América. It grows at one of the world's highest treelines. Since it is confines at altitudesbetween 3000 and 4000 m, where it constitutes the upper altitudinal limit of tree vegetation (Lauer 1978; Perry, 1991). Its extreme altitudinal distribution makes of *P. hartwegii* a highly vulnerable species due to global warming, since its exclusive habitat could be reduced (Gómez-Mendoza and Arriaga 2007; Viveros-Viveros et al 2009). There are predictions that by the end of the current century, suitable climates for the conifer forests in the Trans-Mexican Volcanic Belt in México could be reduced 92 % (Rehfeldt et al 2011).

Resistance to cavitation is a good estimator of a species tolerance to drought in vascular plants (Brodribb and Cochard 2009; Brodribb et al. 2010). Recent studies have reported a high variability of P_{50} (proxy of cavitation resistance, corresponding to the pressure inducing 50% loss

of hydraulic conductance) among conifer species, ranging from -3 to -11 MPa (Delzon et al 2010, Pittermmann et al. 2010). However, only few studies have investigated the intra-specific variability of cavitation resistance so far. Indeed, former measurement techniques of cavitation resistance did not allow to screen a great number of genotypes in order to quantify genetic variations for this trait.

In this work, we have studied cavitation resistance on *Pinus hartwegii* Lindl., for which as far as we know there is a single previous report, obtained from only one tree growing in a botanical garden (Janzen et al. 2012). We investigated the genetic differentiation for cavitation resistance among *Pinus hartwegii* populations on seedlings growing in a provenance test, collected along an altitudinal gradient. We also compared several pine species growing at low and high altitudes in the north hemisphere in order to determine whether there is a general relation between altitude and cavitation resistance, and how *Pinus hartwegii* compares with other pine species.

Materials and Methods

Sample collection

Open-pollinated seeds were collected from 13 natural populations along an altitudinal gradient, from 3150 m of altitude (19° 25.967' N, 102° 16.972' W), to 3750 m (19° 25.120' N, 102° 18.750' W), one population every 50 m of altitudinal difference (lapse rate of 0.5 °C for every 100 m of altitudinal difference), from Pico de Tancítaro, Michoacán, western México (same provenances than Viveros-Viveros 2009; we made a correction of provenance altitude of 150 m upward). The trees represented by these samples are termed populations while the location of a population is called the provenance. Seedlings were raised in a nursery (380 cm^3 rigid containers with commercial Creciroot® substrate), and then established in a randomized complete block design in a common garden provenance test when seedlings were 19 months old.

Common garden conditions consisted of two rectangular wooden-structure raised beds, 12.3 m long x 1.5 m wide x 0.6 m high each; the wooden-structures were filled with a 20-cm layer of extrusive volcanic coarse stones for improving drainage (particle size: 28.4-37.3 mm), and then a 40 cm of a 4:1 mixture of local Andosol pine-oak forest top-soil, and commercial Creciroot® substrate. Seedlings were placed in plots of five-seedlings in a row, spaced 0.3 m within plots and 0.3 m among plots. The first and the last plot of each wooden-structure were flanked by a row of randomly selected seedlings, to control the edge effect. The test was covered by a 35 % shade net.

Test was located at a Universidad Michoacana de San Nicolás de Hidalgo facility, at Morelia, Michoacán (101° 14’ 59’’ Long W, 19° 41’ 20’’ Lat N, 1955 masl, mean annual temperature 17.0 °C, average annual precipitation 881 mm).

Resistance to cavitation was evaluated on branches collected when seedlings were 5-years-old. Only were collected branches fully exposed to the sun, as straight as possible, 30 cm long, and near to 1 cm diameter (including bark), due to equipment requirements. Because the small size of branches on the provenance test, a trend more pronounced on seedlings originated from the high elevation provenances, we did not have analyzed samples representing populations from 3550, 3650 and 3750 m of altitude. Also, we had single samples for populations from 3350, 3450, 3600 and 3700 m of altitude. In order to have a more balanced analysis, we merged the single samples of 3350 and 3450 with the samples of 3400 m, and the ones from 3600 and 3700 were merged to represent a population at 3650 m. Thus, the average sample size for each of the seven populations examined was 4.6 individuals, and a total of six individuals were represented by more than one branch. All needles were immediately removed, and then the branches were labeled, wrapped in wet paper towels, placed in black bags, and immediately posted to France, where vulnerability was determined at the new high-throughput phenotyping platform for hydraulic traits (CavitPlace, University of Bordeaux, Talence, France; http://sylvain-delzon.com/caviplace). These were then kept wet and cool (3°C) until cavitation resistance was measured within three weeks after collection. Prior to measurement, all branches were cut under water to a standard length of 27 cm, and bark was removed with a razor blade.

Measurement of resistance to cavitation

Xylem cavitation was assessed with the CAVITRON, a centrifuge technique following the procedure described by Cochard (Cochard 2002; Cochard et al. 2005). Centrifugal force was used to establish negative pressure in the xylem and to provoke water stress-induced cavitation, using a custom-built honeycomb rotor (Precis 2000, Bordeaux, France) mounted on a high-speed centrifuge (Sorvall RC5, USA). This technique enables measurement of the hydraulic conductance of a branch under negative pressure. Xylem pressure (P_i) was first set to a reference pressure (-0.5 MPa) and hydraulic conductance (k_i) was determined by measuring the flux of a reference ionic solution (10 mmol dm^{-3} KCl and dm^{-3} mmol dm^{-3} $CaCl_2$ in deionized water) through the sample. The centrifugation speed was then set to a higher value for 3 min to expose the sample at a more

negative pressure. Conductance were measured four times for each step, and the average was used to compute the percent loss of xylem conductance (PLC in %). PLC was determined at each pressure step following the equation:

$$PLC = 100 \times \left(1 - \frac{k_i}{k_{\max}}\right) \quad \text{Eqn 1}$$

where k_{max} corresponds to the maximum hydraulic conductance measured at low speed. The procedure was repeated for at least eight pressure steps with a -0.5 MPa step increment until PLC reached at least 90%. Rotor velocity was monitored with a 10 rpm resolution electronic tachymeter and xylem pressure was adjusted to about -0.02 MPa. We used Cavisoft software (version 2.0, BIOGECO, University of Bordeaux) for conductance measurements and computation of all vulnerability curves (VC).

The percent loss of xylem conductance as a function of xylem pressure (MPa) represents the sample's vulnerability curve (VC). A sigmoid function (Pammenter & Van der Willigen, 1998) was fitted to the VC from each sample using the following equation:

$$PLC = \frac{100}{\left[1 + \exp\left(\frac{S}{25} * \left(P - P_{50}\right)\right)\right]} \quad \text{Eqn 2}$$

where P_{50} (MPa) is the xylem pressure inducing 50% loss of conductance and S (% MPa^{-1}) is the slope of the vulnerability curve at the inflexion point. The xylem specific hydraulic conductance (k_s, m^2 MPa^{-1} s^{-1}) was calculated by divided k_{max} by the sapwood area of the sample.

Statistical analysis

Genetic differentiation among populations were tested by an analysis of variance (ANOVA), using the Procedure GLM of SAS (SAS Institute, 2004). Measurements of more than one branch of the same individual were previously averaged. The statistical model used was:

$$Y_{ij} = \mu + \tau_i + \varepsilon_{ij} \quad \text{Eqn 3}$$

Where: Y_{ij} = value of the *ij*-th observation, μ = general mean, τ_j = effect of the *i*-th population, and ε_{ij} = experimental error. Population was considered as random effect. Variance components were estimated using the Procedure VARCOMP with the method of restricted maximum likelihood (REML), of SAS (SAS Institute, 2004).

In order to determine the altitudinal pattern of genetic variation, if any, the relationship existing among the mean values per population of the assessed characteristics with altitude above sea level of the sites was modeled, using the procedure REG of SAS, (SAS Institute, 2004) with the following statistic model:

$$Y_{ij} = \beta_0 + \beta_1 X_i + \varepsilon_{ij} \qquad \text{Eqn 4}$$

Where: Y_{ij} = population mean of P_{50}, k_s, or S; β_0 = intercept, β_1 = regression parameter, X_i = altitude (m) of *i*-th provenance, and ε_{ij} = error.

Results and Discussion

Cavitation resistance at treeline

For each provenance, vulnerability curves showed similar sigmoid shape (see as example Figure 1) that allows us to robustly estimate P_{50} and S using the Pammenter model (Pammenter and Van der Willigen, 1998). More negative P_{50} (xylem pressure inducing 50% loss of conductance), values indicate higher resistance to cavitation, while the slope of the vulnerability curve, S, indicates how fast cavitation progresses around P_{50}. The overall average value for P_{50}, was -3.42 ± 0.047 MPa (± standard error, SE) and the average value for S was 121 ± 9 % MPa^{-1}. The estimated P_{50} average value is very close to the single available reported value (P_{50} = -3.43 ± 0.18; Jansen et al. 2012).

Both P_{50} and S values found in *Pinus hartwegii* fall within the range found on other treeline pine species. Similar P_{50} value were found for *Pinus cembra* (-3.02 ± 0.17 MPa), *Pinus albicaulis* (-3.19 ± 0.1 MPa) and *Pinus mugo* (-3.75 ± 0.17 MPa) (Delzon et al 2010), three species that also conform the timberline, at high altitude, cold and humid sites. *Pinus albicaulis* in western USA and Canada mountain ranges, mostly at Rocky Mountains (Bower and Aitken 2008) and *Pinus cembra* and *Pinus mugo* at the Alps and Carpathian mountains, Europe (Critchfield and Little 1966; Christensen 1987).

When comparing P_{50} values between pine species previously studied, and grouped according to their altitudinal position (treeline or low altitude), treeline pine species are more vulnerable to cavitation (Table 1). The average P_{50} is significantly less negative (Snedekor test, α=0.05) for treeline species (P_{50} = -3.39 MPa) than for middle-lowland pine species (P_{50} = -3.96 MPa, Table 1).

Like all pine studies previously characterized, *Pinus hartwegii* is highly vulnerable to cavitation. In other conifers, reported values for P_{50} range from - 2.91 MPa for *Metasequoia glyptostroboides*, down to between -9 to -10 MPa *Juniperus osteoperma* and *J. scopulorum*, which distribute in semiarid regions (Delzon et al 2010) and even -11.32 MPa for *Cupressus glabra* (Delzon et al 2010). Generally, species from dry environment are more resistant to cavitation (Maherali et al. 2004). Concerning the slope of the cavitation curve, Delzon et al. (2010) consider that slope values larger than 50 % MPa^{-1} indicate a very fast rate of embolism. On the other hand, when comparing *P. hartwegii* to other pine species, its P_{50} is within the range of other treeline species but its S value is the lowest among all treeline species.

Genetic differentiation among populations

Between-population genetic differentiation in ecophysiological traits has been poorly documented for tree species so far (but see Arntz and Delph 2001; Dang et al. 1994; Rowland 2001), especially for hydraulic traits.

In the present study, cavitation resistance (P_{50}) did not show significant differences among populations (P = 0.3038, Table 2), and there was no detectable altitudinal trend among P_{50} population means in relation to the altitude of the provenance (r^2 = 0.001, P = 0.9541; Figure 2a). In contrast with the absence of altitudinal trend for P50, we found significant relationships between provenance altitude and ks and S. There were significant differences in k_s between populations (P = 0.0039, Table 2), and a significant correlation was found between the population average and the provenance altitude (r^2 = 0.577, P = 0.0475, Fig. 1c). Similarly, a significant negative correlation was found between S and altitude (r^2 = 0.816, P = 0.0053, Fig. 1b), with higher S values in populations from low altitudes . No significant differences between populations were found, however (P = 0.2445, Table 2).

Genetic differentiation among populations for traits such as P_{50} has being studied very scarcely and recently. The data available for conifers has documented mostly differences among species (Delzon et al 2010). One studied explored in deep genetic differentiation among *Pinus pinaster* populations for cavitation resistance, including populations growing in disparate environments, from warm and dry sites in Tamrabta, Southern Morocco, to less warm and much more humid sites in Mimizan, South-western France; results indicate no significant differentiation among populations for cavitation resistance (P_{50}), and suggests that canalization (or uniform

selection) has shaped the phenotypic variability of this trait (Lamy et al 2011). In other word, the genetic architecture narrows trait variability to preserve functional phenotype. How canalization appears during evolution is still a debate.

Given the low coefficient of variation (2.3 %, Table 2) (for the between population variance component) of cavitation resistance, our results supports the hypothesis that P_{50} is a canalized trait. In this study, the number of *P. hartwegii* populations (7) is twice as large as the average of previous intrapopulation studies for cavitation resistance (3.04 populations in average) and the sampling fully represent the thermal amplitude of this species, at least in the studied region. However, for investigating genetic differences among populations, the average number of individuals measured for each provenance (4.6), is the largest limitation of the present work. For example, in the Lamy et al (2011) study, 40 individuals per population were measured. Our inference needs to be confirmed by larger sample sizes.

Recent studies on altitudinal gradient showed significant clines in the wild for several leaf functional traits, but weak effect of genetic variation measured in common garden, suggesting a strong effect of the environment on functional traits (Bresson et al. 2009; Bresson et al. 2011 TP; Premoli and Brewer 2007).

Implications for management

The combination of the low average value of cavitation resistance, fast rate of embolism and lack of genetic differentiation among populations, represent a potential risk of a limited ability of *Pinus hartwegii* populations to adapt to future climates warmer and dryer, as predicted for climate change scenarios for México (Sáenz-Romero et al 2010). Populations of other high altitude pines that conform a timberline, with similar cavitation resistance values, have started to show a severe decline, like *Pinus albicaulis* (Bower and Aitken 2008; Bower and Aitken 2011). Also *Pinus hartwegii* populations have decreased their growth rate due to the climatic change that has occurred already (Ricker et al 2007). The fact that *P. hartwegii* conforms the timberline in high altitude mountains in México, limit its options for conducting an assisted migration to higher altitudes, because sometimes it is at the summit of the mountains already, as it is the case at Pico de Tancítaro, state of Michoacán (Viveros-Viveros et al 2009), and in cases when the mountain has higher elevation (like Popocatépetl and Iztaccíhuatl volcanoes), the soils typically are poor

above the timberline, due to lack of organic material and abundance of sand and stones of volcanic origin (Lauer 1978).

Conclusions

Our results showed that *Pinus hartwegii* is a rather high vulnerable species to cavitation in regards to the conifer cavitation resistance spectrum. This finding confirms that pine species growing at the treeline have a less resistance xylem to cavitation compared to those growing in lowland as demonstrated by our literature survey.

There were not significant differences among populations for resistance to cavitation and for slope of vulnerability curve (S), supporting the hypothesis that uniform selection has shaped the variability among populations of this trait. However, there were significant differences among populations for the xylem specific hydraulic conductance (k_s), and a clear altitudinal trend, were low altitude populations have larger k_s values, than higher elevation populations, with smaller k_s values.

Acknowledgements

Funding was provided to CSR by the joint research funds between the Mexican Council of Science and Technology (CONACYT), and the State of Michoacán (CONACyT-Michoacán, grant 2009-127128), and the Mexican National Forestry Commission (CONACYT-CONAFOR, grant 2005- C02-14783); and funds from the Coordination for Scientific Research of the Universidad Michoacana de San Nicolás de Hidalgo (CIC-UMSNH). This study was also supported by the Institut Scientifique de Recherche Agronomique (INRA) innovative project (2010) to SD and JBL.

References

Allen CD, Macalady AK, Chenchouni H, Bachelet D, McDowell N, Vennetier M, Kizberger T, Rigling A, Breshears DD, Hogg EH, Gonzalez P, Fensham R, Zhang Z, Castro J, Demidova N, Lim JH, Allard G, Running SW, Semerci A, Cobb N (2010) A global overview of drought and heat-induced tree mortality reveals emerging climate change risks for forests. Forest Ecology and Management 259:660–684

Arntz AM, Delph LF (2001) Pattern and process: evidence for the evolution of photosynthetic traits in natural populations. Oecologia 127:455-467

Bower AD, Aitken SN (2008) Ecological genetics and seed transfer guidelines for *Pinus albicaulis* (Pinaceae). American Journal of Botany 95(1):66-76

Bower AD, Aitken SN (2011) Changes in genetic diversity of whitebark pine (*Pinus albicaulis* Engelm.) associated with inbreeding and white pine blister rust infection. Silvae Genetica 60(3–4):113-123

Breshears DD, Cobb NS, Rich PM, Price KP, Allen CD, Balice RG, Romme WH, Kastens JH, Floyd ML, Belnap J, Anderson JJ, Myers OB, Meyer CW (2005) Regional vegetation die-off in response to global-change-type drought. Proceedings of National Academy of Sciences 102:15144-15148

Bresson CC, Kowalski AS, Kremer A, Delzon S (2009) Evidence of altitudinal increase in photosynthetic capacity: gas exchange measurements at ambient and constant CO_2 partial pressures. Ann For Sci 66:505

Bresson CC, Vitasse Y, Kremer A, Delzon S (2011) To what extent is altitudinal variation of functional traits driven by genetic adaptation in European oak and beech? Tree Physiology doi:10.1093/treephys/tpr084

Brodribb TJ, Cochard H (2009) Hydraulic failure defines the recovery and point of death in water-stressed conifers. Plant Physiology 149:575–584

Brodribb TJ, Bowman DJMS, Nichols S, Delzon S, Burlett R (2010) Xylem function and growth rate interact to determine recovery rates after exposure to extreme water deficit. New Phytologist 188: 533–542

Christensen, KI (1987) Taxonomic revision of the *Pinus mugo* complex and *P.* x *rhaetica* (*P. mugo* x *sylvestris*) (Pinaceae). Nord J Bot 7:383-408

Cochard H (2002) A technique for measuring xylem hydraulic conductance under high negative pressures. Plant Cell and Environment 25:815-819

Cochard H, Damour G, Bodet C, Tharwat I, Poirier M, Ameglio T (2005) Evaluation of a new centrifuge technique for rapid generation of xylem vulnerability curves. Physiologia Plantarum 124:410–418

Critchfield WB, Little ELJr (1966) Geographic distribution of the pines of the world. Miscellaneous Publication 991. USDA-Forest Service, Washington DC

Dang QL, Xie CY, Ying C, Guy RD (1994) Genetic variation of ecophysiological traits in red alder (*Alnus rubra* Bong.). Can J For Res 24:2150–2156

Delzon S, Douthe C, Sala A, Cochard H (2010) Mechanism of water-stress induced cavitation in conifers: bordered pit structure and function support the hypothesis of seal capillary-seeding. Plant, Cell and Environment 33(12): 2101–2111

Gomez-Mendoza L, Arriaga L (2007) Modeling the effect of climate change on the distribution of oak and pine species of México. Conservation Biology 21(6):1545-1555

Jansen S, Lamy JB, Burlett R, Cochard H, Gasson P, Delzon S (2012) Plasmodesmatal pores in the torus of bordered pit membranes affect cavitation resistance of conifer xylem. Plant Cell and Environment. In press. Doi: 10.1111/j.1365-3040.2011.02476.x.

Lamy J-B, Bouffier L, Burlett R, Plomion C, Cochard H, Delzon S (2011) Uniform selection as a primary force reducing population genetic differentiation of cavitation resistance across a species range. PLoS ONE 6(8):e23476

Lauer, W (1978) Timberline studies in central Mexico. Arctic and Alpine Research 10:383-396

Maherali H, Pockman WT, Jackson RB (2004) Adaptive variation in the vulnerability of woody plants to xylem cavitation. Ecology 85:2184–2199

Mátyás C (2010) Forecasts needed for retreating forests. Nature 464:1271

McDowell N, Pockman WT, Allen CD, Breshears DD, Cobb N, Kolb T, Plaut J, Sperry J, West A, Williams DG, Yepez EA (2008) Mechanisms of plant survival and mortality during drought: why do some plants survive while others succumb to drought? New Phytologist (2008) 178: 719–739

Pammenter NW, Van der Willigen C (1998) A mathematical and statistical analysis of the curves illustrating vulnerability of xylem to cavitation. Tree Physiology 18: 589–593

Peñuelas J, Oyaga R, Boada M, Jump AS (2007) Migration, invasion and decline: changes in recruitment and forest structure in a warming-linked shift of European beech forest in Catalonia (NE Spain). Ecography 30:830-838

Perry JP, (1991) The pine of Mexico and Central America. Timber Press, Portland, Oregon

Pittermann J, Choat B, Jansen S, Stuart SA, Lynn L, Dawson TE (2010) The relationships between xylem safety and hydraulic efficiency in the Cupressaceae: the evolution of pit membrane form and function. Plant Physiology 153:1919–1931

Premoli AC, Brewer C (2007) Environmental v. genetically driven variation in ecophysiological traits of *Nothofagus pumilio* from contrasting elevations. Austr. J. Bot. 55: 585–591

Rehfeldt GE, Ferguson DE, Crookston NL (2009) Aspen, climate, and sudden decline in western USA. Forest Ecology and Management 258:2353-2364

Rehfeldt GE, Crookston NL, Sáenz-Romero C, Campbell E (2011) North American vegetation analysis for land use planning in a changing climate: A statistical solution to large classification problems. Ecological Applications. In press

Ricker M, Gutiérrez-García G, Daly DC (2007) Modeling long-term tree growth curves in response to warming climate: test cases from a subtropical mountain forest and a tropical rainforest in México. Can J For Res 37:977-989

Rowland DL (2001) Diversity in physiological and morphological characteristics of four cottonwood (*Populus deltoides* var. *wislizenii*) populations in New Mexico: evidence for a genetic component of variation. Can J For Res 31:845–853

Saenz-Romero C, Rehfeldt GE, Crookston NL, Pierre D, St-Amant R, Bealieau J, Richardson B (2010). Contemporary and projected spline climate surfaces for Mexico and their use in understanding climate-plant relationships. Climatic Change 102:595-623

SAS Institute Inc. (2004) SAS/ STAT 9.1 User's Guide. SAS Institute Inc., Cary, North Carolina

Viveros-Viveros H, Sáenz-Romero C, Vargas-Hernández JJ, López-Upton J, Ramírez-Valverde G, Santacruz-Varela A (2009) Altitudinal genetic variation in *Pinus hartwegii* Lindl. I. : height growth, shoot phenology, and frost damage in seedlings. Forest Ecology and Management 257:836-842

Figure Captions

Figure 1. Examples of vulnerability curves as loss of xyleme conductance (PLC, in %, see Equation 1) against pressure, of six seedlings from a single *Pinus hartwegii* provenance (3250 m of altitude).

Figure 2. Evolution of hydraulic safety (cavitation resistance) and efficiency (hydraulic conductance) according to altitude of provenance origin: (a) P_{50} in MPa, xylem pressure inducing 50% loss of hydraulic conductance; (b) S in % MPa^{-1}, slope of the vulnerability curve at the inflexion point, and (c) k_s in m^2 MPa^{-1} s^{-1}, xylem specific hydraulic conductance. Vertical bars represent standard errors.

Tables

Table 1. Comparative values (means and standard errors) for cavitation resistance (P_{50}) and slope of the vulnerability curve for several pine species, grouped for range of altitudinal distribution and sorted by average P_{50} values.

Altitudinal Range	Species	Mean		Standard error		n	Citation
		P_{50}	Slope	P_{50}	Slope		
High or Treeline	*Pinus wallichiana*	-2.83	147	0.112	23.8	5	3
High or Treeline	*Pinus cembra*	-3.02	159	0.170	18.6	3	1
High or Treeline	*Pinus albicaulis*	-3.19	189	0.101	11.6	4	1
High or Treeline	*Pinus hartwegii*	-3.42	121	0.047	9.0	32	This study
High or Treeline	*Pinus mugo*	-3.75	169	0.066	17.9	3	1
High or Treeline	*Pinus uncinata*	-4.18	127	0.169	8.7	4	1
	Mean	-3.39	135				
Mid or Low elev.	*Pinus sylvestris*	-3.20	129	0.021	8.7	5	1
Mid or Low elev.	*Pinus flexilis*	-3.71	100	0.180	10.7	4	1
Mid or Low elev.	*Pinus pinaster*	-3.73	69	0.070	0.5	2	2
Mid or Low elev.	*Pinus ponderosa*	-3.86	152	0.051	18.4	3	1
Mid or Low elev.	*Pinus contorta*	-3.90	168	0.180	22.4	5	1
Mid or Low elev.	*Pinus edulis*	-4.03	102	0.061	15.1	5	1
Mid or Low elev.	*Pinus pinea*	-4.34	89	0.161	6.4	3	1
Mid or Low elev.	*Pinus radiata*	-4.38	67	0.143	5.4	5	3
Mid or Low elev.	*Pinus halepensis*	-4.67	78	0.050	8.4	3	1
	Mean	-3.96	109				

1 = Delzon *et al* (2010). 2 = Lamy et al. (2011). 3 = Jansen et al. (2012).

Table 2. Analysis of variance of xylem cavitation resistance traits (P_{50}, xylem pressure inducing 50% loss of conductance and *S*, slope of the vulnerability curve at the inflexion point) and xylem transport efficiency (k_s, xylem specific hydraulic conductance), for 5-year-old seedlings originated from 7 *Pinus hartwegii* populations collected along an altitudinal gradient.

Trait	Population			Error
	CV	RV	*P*	RV
P_{50}	2.3	9.1	0.3038	90.9
S	12.4	8.6	0.2445	91.4
k_s	48.5	47.4	0.0039	52.6

CV = Coefficient of variation (in %) for the between population variance component. RV = Ratio (in %) of variance component of each random effect to total variance estimated. *P* = Significance value.

Figure 1

Click here to download Figure: SaenzRomero_CavPhartw_Fig1.xlsx

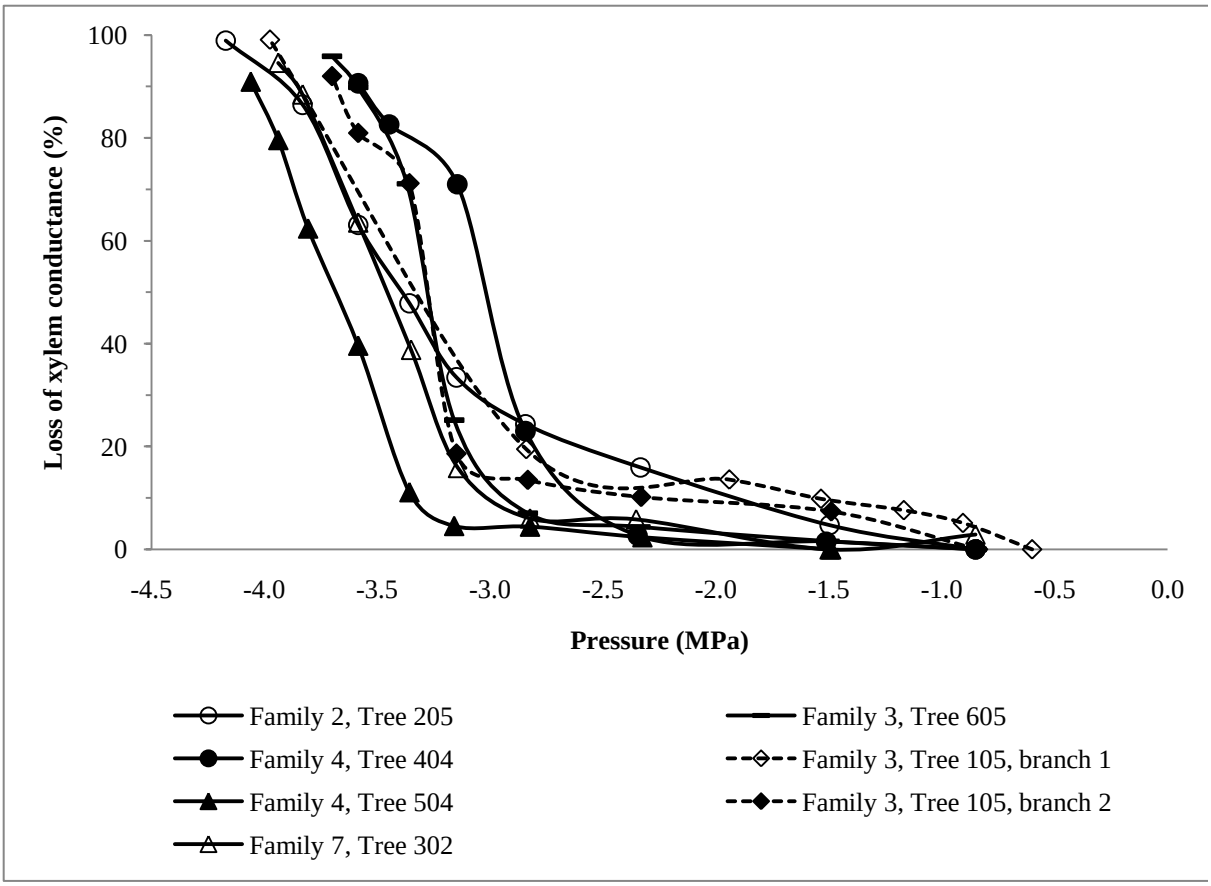

Altitude	Provenance	progeny	Tree	Block	Branch	Codesample	speed_class	mean_Lp_cor
3250	11	2	5	2	1	11-2-5-2	a	7.51
3250	11	2	5	2	1	11-2-5-2	b	7.16
3250	11	2	5	2	1	11-2-5-2	c	6.32
3250	11	2	5	2	1	11-2-5-2	d	5.69
3250	11	2	5	2	1	11-2-5-2	e	5.00
3250	11	2	5	2	1	11-2-5-2	f	3.92
3250	11	2	5	2	1	11-2-5-2	g	2.77
3250	11	2	5	2	1	11-2-5-2	h	1.02
3250	11	2	5	2	1	11-2-5-2	i	0.08
3250	11	3	5	1	1	11-3-5-1	a	0.74
3250	11	3	5	1	1	11-3-5-1	b	0.70
3250	11	3	5	1	1	11-3-5-1	c	0.68
3250	11	3	5	1	1	11-3-5-1	d	0.66
3250	11	3	5	1	1	11-3-5-1	e	0.64
3250	11	3	5	1	1	11-3-5-1	f	0.59
3250	11	3	5	1	1	11-3-5-1	g	0.01
3250	11	3	5	1	2	11-3-5-1b	a	8.17
3250	11	3	5	1	2	11-3-5-1b	b	7.57
3250	11	3	5	1	2	11-3-5-1b	c	7.34
3250	11	3	5	1	2	11-3-5-1b	d	7.07
3250	11	3	5	1	2	11-3-5-1b	e	6.65
3250	11	3	5	1	2	11-3-5-1b	f	2.36
3250	11	3	5	1	2	11-3-5-1b	g	1.56
3250	11	3	5	1	2	11-3-5-1b	h	0.66
3250	11	3	5	6	1	11-3-5-6	a	1.86
3250	11	3	5	6	1	11-3-5-6	b	1.84
3250	11	3	5	6	1	11-3-5-6	c	1.78
3250	11	3	5	6	1	11-3-5-6	d	1.73
3250	11	3	5	6	1	11-3-5-6	e	1.40
3250	11	3	5	6	1	11-3-5-6	f	0.54
3250	11	3	5	6	1	11-3-5-6	g	0.19
3250	11	3	5	6	1	11-3-5-6	h	0.08
3250	11	4	4	4	1	11-4-4-4	a	0.82
3250	11	4	4	4	1	11-4-4-4	b	0.81
3250	11	4	4	4	1	11-4-4-4	c	0.80
3250	11	4	4	4	1	11-4-4-4	d	0.63
3250	11	4	4	4	1	11-4-4-4	e	0.24
3250	11	4	4	4	1	11-4-4-4	f	0.14
3250	11	4	4	4	1	11-4-4-4	g	0.08
3250	11	4	4	5	1	11-4-4-5	b	0.44
3250	11	4	4	5	1	11-4-4-5	c	0.43
3250	11	4	4	5	1	11-4-4-5	d	0.42
3250	11	4	4	5	1	11-4-4-5	e	0.42
3250	11	4	4	5	1	11-4-4-5	f	0.39
3250	11	4	4	5	1	11-4-4-5	g	0.27

3250	11	4	4	5	1	11-4-4-5	h	0.17
3250	11	4	4	5	1	11-4-4-5	i	0.09
3250	11	4	4	5	1	11-4-4-5	j	0.04
3250	11	7	2	3	1	11-7-2-3	a	1.00
3250	11	7	2	3	1	11-7-2-3	b	1.03
3250	11	7	2	3	1	11-7-2-3	c	0.97
3250	11	7	2	3	1	11-7-2-3	d	0.97
3250	11	7	2	3	1	11-7-2-3	e	0.87
3250	11	7	2	3	1	11-7-2-3	f	0.63
3250	11	7	2	3	1	11-7-2-3	g	0.38
3250	11	7	2	3	1	11-7-2-3	h	0.12
3250	11	7	2	3	1	11-7-2-3	i	0.06

Label	pressure	PLC2
Family 2, Tree 205	-0.851	0.0
Family 2, Tree 205	-1.497	4.7
Family 2, Tree 205	-2.335	15.9
Family 2, Tree 205	-2.844	24.3
Family 2, Tree 205	-3.150	33.4
Family 2, Tree 205	-3.358	47.9
Family 2, Tree 205	-3.585	63.1
Family 2, Tree 205	-3.831	86.4
Family 2, Tree 205	-4.172	98.9
Family 3, Tree 105, branch 1	-0.600	0.0
Family 3, Tree 105, branch 1	-0.906	5.1
Family 3, Tree 105, branch 1	-1.168	7.6
Family 3, Tree 105, branch 1	-1.535	9.8
Family 3, Tree 105, branch 1	-1.941	13.6
Family 3, Tree 105, branch 1	-2.841	19.5
Family 3, Tree 105, branch 1	-3.976	99.1
Family 3, Tree 105, branch 2	-0.840	0.0
Family 3, Tree 105, branch 2	-1.490	7.4
Family 3, Tree 105, branch 2	-2.332	10.2
Family 3, Tree 105, branch 2	-2.834	13.5
Family 3, Tree 105, branch 2	-3.150	18.6
Family 3, Tree 105, branch 2	-3.358	71.2
Family 3, Tree 105, branch 2	-3.585	80.9
Family 3, Tree 105, branch 2	-3.701	92.0
Family 3, Tree 605	-0.845	0.0
Family 3, Tree 605	-1.497	1.6
Family 3, Tree 605	-2.335	4.4
Family 3, Tree 605	-2.834	7.0
Family 3, Tree 605	-3.160	25.1
Family 3, Tree 605	-3.369	71.1
Family 3, Tree 605	-3.585	89.8
Family 3, Tree 605	-3.701	95.9
Family 4, Tree 404	-0.851	0.0
Family 4, Tree 404	-1.512	1.5
Family 4, Tree 404	-2.347	2.7
Family 4, Tree 404	-2.844	23.0
Family 4, Tree 404	-3.146	71.0
Family 4, Tree 404	-3.448	82.6
Family 4, Tree 404	-3.585	90.6
Family 4, Tree 504	-1.490	0.0
Family 4, Tree 504	-2.326	2.4
Family 4, Tree 504	-2.824	4.4
Family 4, Tree 504	-3.160	4.6
Family 4, Tree 504	-3.358	11.1
Family 4, Tree 504	-3.585	39.6

Family 4, Tree 504	-3.807	62.4
Family 4, Tree 504	-3.939	79.6
Family 4, Tree 504	-4.061	91.0
Family 7, Tree 302	-0.851	2.9
Family 7, Tree 302	-1.497	0.0
Family 7, Tree 302	-2.354	5.8
Family 7, Tree 302	-2.824	6.0
Family 7, Tree 302	-3.143	15.8
Family 7, Tree 302	-3.351	38.8
Family 7, Tree 302	-3.585	63.5
Family 7, Tree 302	-3.831	88.4
Family 7, Tree 302	-3.939	94.6

Figure 2a
Click here to download Figure: SaenzRomero_CavPhartw_Fig2a.xlsx

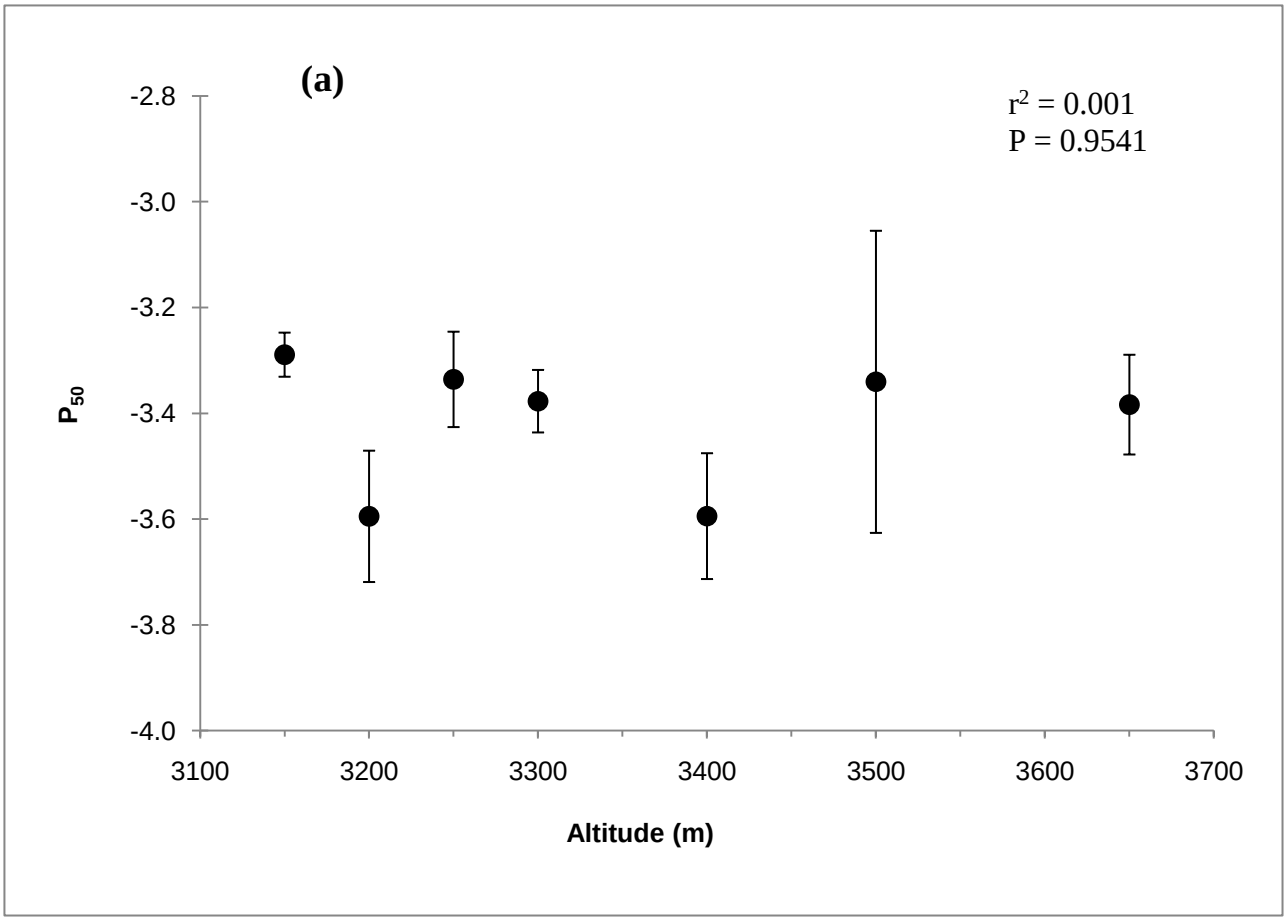

Population	Altitude (m)	P_{50}	Standard Error
2	3700		
3	3650	-3.38365	0.09431
4			
6	3500	-3.34055	0.28565
7	3450		
8	3400	-3.59448	0.11894
9	3350		
10	3300	-3.37714	0.05909
11	3250	-3.33594	0.09019
12	3200	-3.59491	0.12417
13	3150	-3.28922	0.0417

Figure 2b
Click here to download Figure: SaenzRomero_CavPhartw_Fig2b.xlsx

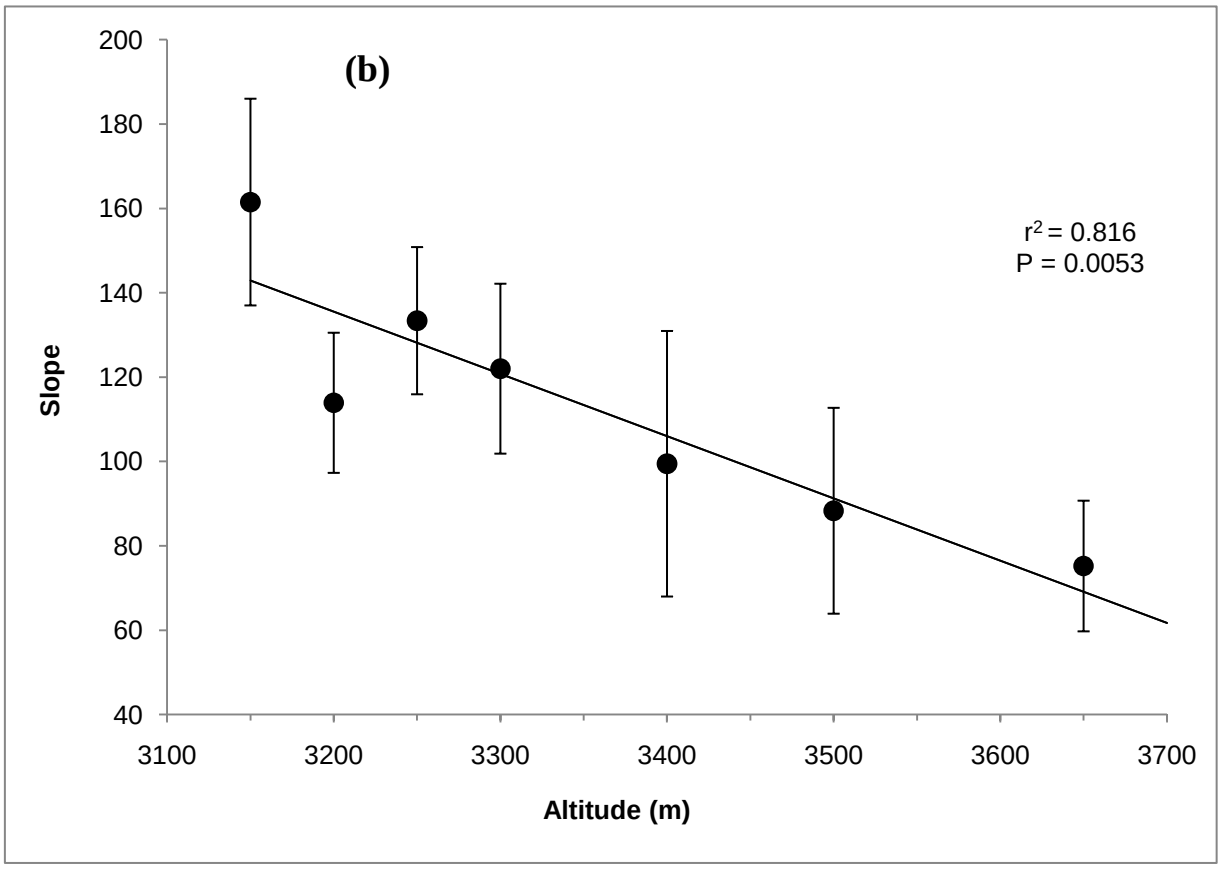

Population	Altituden (m)	Slope (%)	Standard error
2	3700		
3	3650	75.219	15.4877
4	3600		
6	3500	88.321	24.4041
7	3450		
8	3400	99.464	31.4774
9	3350		
10	3300	122.004	20.1439
11	3250	133.383	17.4498
12	3200	113.917	16.6113
13	3150	161.503	24.5052

Figure 2c
Click here to download Figure: SaenzRomero_CavPhartw_Fig2c.xlsx

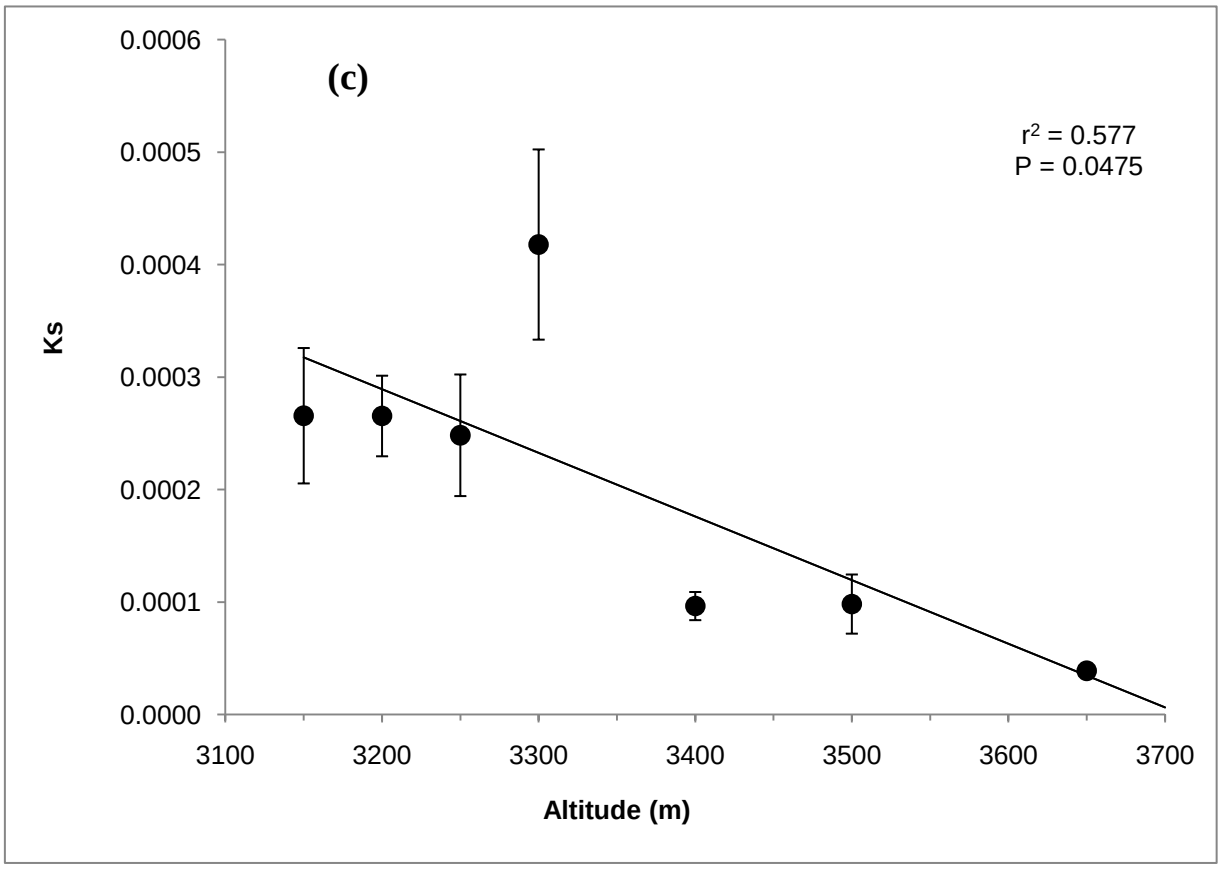

Population	Altitude (m)	K max	Standard error
2	3700		
3	3650	3.8899E-05	0.000005823
4	3600		
6	3500	9.8246E-05	0.000026294
7	3450		
8	3400	9.6465E-05	0.000012527
9	3350		
10	3300	0.00041788	0.000084556
11	3250	0.00024831	0.000054047
12	3200	0.00026546	0.000035825
13	3150	0.0002657	0.000060191

Micro-evolutionary patterns of juvenile wood density in a pine species

Jean-Baptiste Lamy, Frédéric Lagane, Christophe Plomion, Hervé Cochard & Sylvain Delzon

Plant Ecology
An International Journal

ISSN 1385-0237
Volume 213
Number 11

Plant Ecol (2012) 213:1781-1792
DOI 10.1007/s11258-012-0133-2

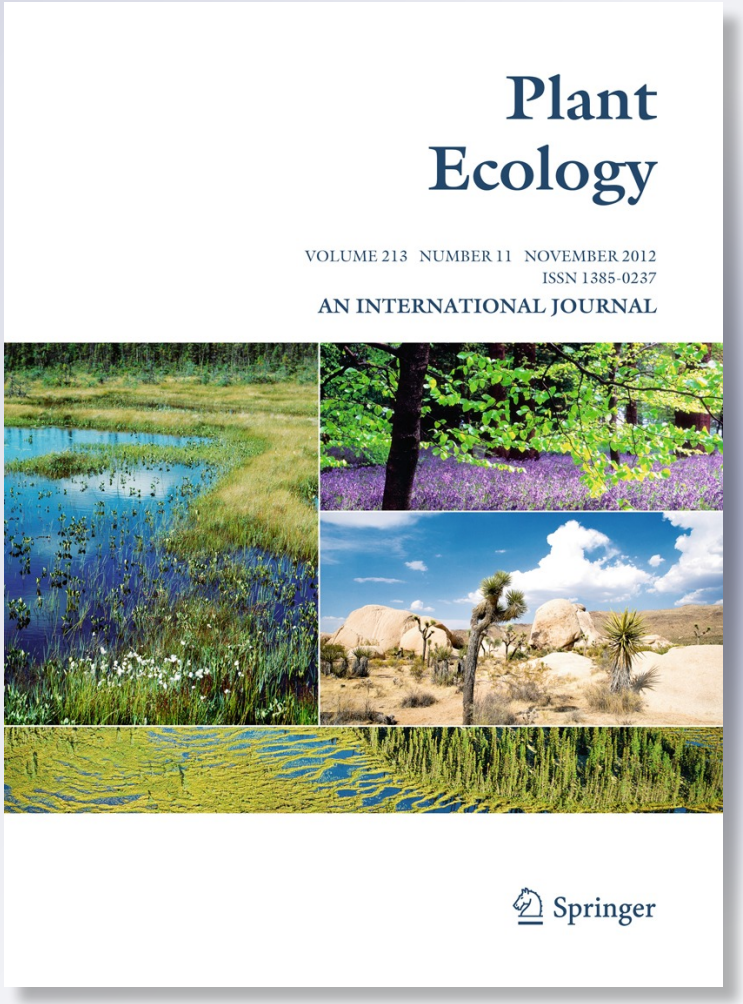

Springer

Plant Ecol (2012) 213:1781–1792
DOI 10.1007/s11258-012-0133-2

Micro-evolutionary patterns of juvenile wood density in a pine species

Jean-Baptiste Lamy · Frédéric Lagane · Christophe Plomion · Hervé Cochard · Sylvain Delzon

Received: 13 February 2012 / Accepted: 26 September 2012 / Published online: 5 October 2012

Abstract Wood density can be considered an adaptive trait, because it ensures the safe and efficient transport of water from the roots to the leaves, mechanical support for the body of the plant and the storage of biological chemicals. Its variability has been extensively described in narrow genetic backgrounds and in wide ranges of forest tree species, but little is known about the extent of natural genetic and phenotypic variability within species. This information is essential to our understanding of the evolutionary forces that have shaped this trait, and for the evaluation of its inclusion in breeding programs. We assessed juvenile wood density, leaf area, total aboveground biomass, and growth in six *Pinus pinaster* populations of different geographic origins (France, Spain, and Morocco) growing in a provenance-progeny trial. No genetic differentiation was found for wood density, whereas all other traits significantly differed between populations. Heritability of this trait was moderate, with a low additive genetic variance. For retrospective identification of the evolutionary forces acting on juvenile wood density, we compared the distribution of neutral markers (F_{ST}) and quantitative genetic differentiation (Q_{ST}). We found that Q_{ST} was significantly lower than F_{ST}, suggesting evolutionary stasis. Furthermore, we did not detect any relationship between juvenile wood density and drought tolerance (resistance to cavitation), suggesting that this trait could not be used as a proxy for drought tolerance at the intraspecific level.

Keywords Canalization · Heritability · Q_{ST}/F_{ST} comparison · Pine · Evolutionary stasis · Juvenile wood density

J.-B. Lamy · F. Lagane · C. Plomion · S. Delzon
INRA, UMR 1202 BIOGECO, 33610 Cestas, France

J.-B. Lamy · F. Lagane · C. Plomion · S. Delzon (✉)
Université de Bordeaux, UMR 1202 BIOGECO, Avenue des Facultés, 33405 Talence, France
e-mail: sylvain.delzon@u-bordeaux1.fr

J.-B. Lamy · H. Cochard
INRA, UMR 547 PIAF, University of Blaise Pascal, 63100 Clermont-Ferrand, France

Present Address:
S. Delzon
Department of Agriculture, Food & Natural Resources, University of Sydney, 1 Central Avenue, Australian Technology Park, Eveleigh, NSW 2015, Australia

Introduction

Recent ecological theories have included wood density (mass of wood per unit volume) as key dimension of the variation between woody plant strategies (Westoby et al. 2002; Westoby and Wright 2006; Chave et al. 2009; Zanne et al. 2010). Wood density describes the proportion of cell walls in a given woody tissue. This proportion reflects three functions: the safe

and efficient transport of water from the roots to the leaves, mechanical support for the body of the plant, and the storage of biological chemicals. Wood density is strongly constrained by a trade-off between these functions (Chave et al. 2009) that has influenced the evolution of woody plants over millions of years. It is possible to extrapolate some of the features of the tree, such as growth rate and hydraulic strategy, from the wood density of the species concerned (McCulloh et al. 2011). Species with high wood density are expected to grow more slowly and to have a lower hydraulic efficiency and a higher resistance to embolism than species with a lower wood density (Poorter et al. 2010; Markesteijn et al. 2011). Wood density is also thought to be a good proxy for drought tolerance (i.e., survival of extreme drought events) (Hacke and Sperry 2001; Brodribb and Cochard 2009). For example, after the 2003 heatwave in Europe, *Pseudotsuga menziesii* trees with denser wood and a higher proportion of late wood had higher survival rates than trees with a lower wood density (Martinez-Meier et al. 2008). In *Pseudotsuga menziesii* and *Picea abies* clones, Rosner et al. (2008) and Dalla-Salda et al. (2011) found that wood density was negatively correlated with resistance to cavitation.

Chave et al. (2006) countered the widespread belief that wood density is determined principally by environmental conditions, by suggesting that there is a strong phylogenetic signal controlling interspecific wood density variation. However, in temperate region, wood density may vary considerably in the environment of an individual plant (increasing from the early to the late wood), but the variation between individuals of a given species remains limited and, more importantly, the mean wood density for a given species is generally highly conserved. Many studies have investigated the intraspecific variability of wood density, dissecting the phenotypic variation of wood density into genetic and environmental components (and their interaction) for most commercial forest tree species (Aguiar et al. 2003; Bouffier et al. 2008; Martinez-Meier et al. 2011; Apiolaza 2011). The phenotypic coefficient of variation for wood density is generally low, as is the genetic additive coefficient of variation (these conclusions do not apply to interspecific crosses, such as *Eucalyptus* sp.) (Apiolaza 2011). However, these quantitative estimators have often been measured in narrow genetic backgrounds (or hybrids), without reference to the natural variation of wood density within the species concerned. Even in studies in which wood density was measured in several populations, efforts were rarely made to determine whether the observed variation between populations was caused by genetic drift or past selective events, even though knowledge about the mechanisms shaping the variability of this trait would be useful if this trait was to be incorporated into a breeding program. Some traits are known to be robust to genetic alterations (e.g., wing shape in *Drosophila* sp., mammalian body temperature), such as mutation, drift, or recombination events, and these traits generally have a low variability (phenotypic and/or genetic) (Gilchrist and Partridge 2001; Hansen and Houle 2004). In a breeding context, it is difficult to manipulate these traits: genetic gains at each generation are limited by the low additive genetic variance. However, such "canalized" traits provide a guarantee of a certain level of trait constancy in diverse environmental conditions (Knap 2005; Mormede et al. 2011).

Most of the previous studies dealt with wood density measured on mature trees and very little work has been devoted to juvenile wood density from an evolutionary ecology point of view. The seedling stage is the woody plant life stage with the greatest mortality (the strongest selection pressure) (Petit and Hampe 2006). Young seedling performance may be more important than mature individual performance in determining species distributions and evolution (Figueroa and Lusk 2001). This study had three main objectives: (i) to assess between- and within-population variation of juvenile wood density, using genetic material originating from contrasting climatic environments, (ii) to determine the main evolutionary forces responsible for shaping the genetic variability of juvenile wood density between populations (i.e., contributing to population differentiation), and (iii) to assess the strength of the correlation between juvenile wood density and drought tolerance (resistance to cavitation). We carried out a case study in maritime pine (*Pinus pinaster* Ait.), a species with a fragmented distribution in the western part of the Mediterranean region. The scattered distribution of this species may have prevented or limited gene flow between different groups of populations, promoting high levels of genetic divergence between ecotypes, due to genetic drift (Ribeiro et al. 2002) and/or natural selection (Quezel and Barbero 1998 in Richardson 1998).

Materials and methods

Plant material

We used the same material described in a recent paper by Lamy et al. (2011). Briefly, a provenance-progeny trial was established in December 2003 at the INRA forestry station (Cestas, France, 44°44′N, 00°46′W), with 1-year-old seedlings from open-pollinated seeds collected from 24 natural populations (or ecotypes) in France, Spain, Morocco, and Tunisia, to cover the fragmented distribution of *Pinus pinaster* (see Lamy et al. 2011). Each population was represented by 20–30 half-sib families. The trial was arranged in a randomized block design (15 blocks in total) with single-tree plots. Each block contained at least one tree from each half-sib family. A selective sampling of 6-year-old saplings was carried out as described by Lamy et al. (2011), leading to the selection of six populations representative of the maritime pine climatic envelope. Climate and location of the studied population are presented in Table 1. We sampled eight families with one half-sib in each block (6 populations/8 families/5 blocks = 240 genotypes) at random for further analysis.

Assessment of wood density

Wood density (D, g cm^{-3}) was measured on a section of dry branch. The samples corresponded to the 2007 and 2008 growth units on the 2007 whorl when possible. Sampled branches were fully exposed to the sun, more than 40 cm long and had a diameter of 0.3–1 cm. The number of trees for which wood density data were available per cambial year was as follows: 10 for 2 years old, 151 for 3 years old, 76 for 4 years old, and nine for 5 years old. No difference of branch age was found between populations ($F_{1/221} = 0.07$ and $P = 0.79$), reducing the risk of sampling procedure bias. Mean wood density was measured for 240 genotypes. For each sample, we used a double-bladed saw to cut a transverse section with a constant thickness of 2 mm. Wood density was measured with an indirect-reading X-ray densitometer (Polge 1966). Two orthogonal (longest and shortest axes) radial density profiles were obtained by analyzing the scanned images with WinDENDRO software (Guay et al. 1992). Ring limits were determined automatically, checked manually, and then corrected with this software. For each genotype, we derived three parameters from the distribution of wood density values (after removing the values corresponding to the pith), the mean value (D_{mean}), the 10th percentile (D_{min}) and the 90th percentile (D_{max}). D_{min} was strongly correlated with the mean density of earlywood, whereas D_{max} was correlated with the mean density of latewood (data not shown, $r > 0.8$). We carried out the analysis on both radial density profiles separately to check the impact of compression and normal wood on the variance estimation. Similar patterns were observed for both profiles (not in absolute values, but in terms of significance) because the sampled branches were orthotropic, so we pooled the data.

Biomass, collar diameter, leaf area, and cavitation resistance measurement

At the age of 3 years, all the saplings in six blocks (blocks 1–6) were cut at the collar position. Total

Table 1 Climatic data, location, and elevation of the studied maritime pine populations

Sampling location	Longitude (°)	Latitude (°)	n	Elevation (m)	P_i (mm)	T_m (°C)	VPD_{max} (hPa)	ETP (mm)
Bayubas de Abajo (Central Spain)	−2.87	41.52	39	955	561	10.5	11.42	882.9
Coca (Central Spain)	−4.08	41.37	40	788	452	11.9	14.23	718.7
Mimizan (South-western France)	−1.30	44.13	40	37	1176	13.2	7.26	751.59
Oria (South-eastern Spain)	−2.62	37.87	40	1232	451	13.4	14.29	922.59
San Cipriano de Ribarteme (Northern Spain)	−8.70	42.13	40	310	1625	13.8	8.54	721.91
Tamrabta (Southern Morocco)	−5.02	33.66	40	1760	550	15.1	18.56	976.54

n number of sampled individuals for wood density measurements, P_i mean annual precipitation, T_m, mean annual air temperature, VPD_{max} maximum water vapor pressure deficit (in July for all provenances), ETP annual sum of potential evapotranspiration

above-ground biomass (W_a, g), including the main stem, branches, and needles, was determined by weighing after the material had been dried in an oven at 55 °C for 72 h (Eveno 2008). Needle biomass (W_{needle}, g) was also determined separately. For this study, we used a subset of data corresponding to the selected populations.

On the other blocks (blocks 7–12), collar diameter (ø, mm) was measured on the selected populations and families only at the age of 6 years, in 2007. Specific leaf area (SLA, in $m^2\,kg^{-1}$) was also determined for 20 needles per genotype. Total leaf area (A_{Leaf} in m^2) was estimated retrospectively, by multiplying total W_{needle} (blocks 1–6) by family mean of SLA (blocks 7–12). Resistance to cavitation was determined in a previous study (Lamy et al. 2011).

Quantitative genetic analysis

Genetic analysis was conducted with the following mixed model:

$$\boldsymbol{y} = \boldsymbol{Xb} + \boldsymbol{Z}_1\mathrm{pop} + \boldsymbol{Z}_2\boldsymbol{f} + \boldsymbol{\varepsilon}, \quad (1)$$

where $\boldsymbol{y}$ is the vector of observation for a trait, $\boldsymbol{b}$ is the vector (number of blocks) of fixed block effects, **pop** is the vector (number of populations) of random population effects, $\boldsymbol{f}$ is the vector (number of mother trees) of the random genetic effects of mother tree within the population, $\boldsymbol{\varepsilon}$ is the vector (number of individuals × 1) of residuals, $\boldsymbol{X}$ is called the design matrix, $\boldsymbol{Z}_1$ and $\boldsymbol{Z}_2$ are the incidence matrices linking the observations to the effects. A variance was fitted for each random effect: σ^2_{pop} is the genetic variance between populations, $\sigma^2_{f(pop)}$ is the genetic variance between mother trees nested within a population and σ^2_e is the residual variance for repeated analyses. As the density record for each year constitutes a new measurement for the same tree (Littell et al. 2000; Apiolaza and Garrick 2001), there is an autocorrelation between measurements, which was taken intaccount using a special variance–covariance $\boldsymbol{R}$ matrix structure for repeated analysis. Several covariance structures were considered for specification of the $\boldsymbol{R}$ matrix in the mixed model (autoregressive, heterogeneous autoregressive, first-order autoregressive moving-average, toeplitz, banded correlation). On the basis of Akaike's information criterion and Bayes' information criterion, a banded correlation structure for additive genetic effects was found to be the most appropriate (data not shown). We also ran the analysis with the seed mass as covariate to control potential maternal effect, but it did not change the observed patterns.

Variance and covariance components were estimated by the restricted maximum likelihood (REML) method, assuming a normal distribution of the random effects. The significance of variance components was assessed in log-likelihood ratio tests. We included population as a random effect, for inference at the species level and to obtain an unbiased estimate of heritability and genetic population differentiation (Wilson 2008). The normality, identity, and independence of the residuals of each trait were checked graphically by plotting studentized marginal and conditional residuals. These plots confirmed that the data conformed to the assumptions of the mixed model. We estimated narrow-sense heritability as follows: $h^2_{ns} = 4\sigma^2_{f(pop)} \Big/ \left(\sigma^2_\varepsilon + \sigma^2_{f(pop)}\right)$. In our study, σ^2_A was estimated as $\sigma^2_A = 4\sigma^2_{f(pop)}$ because trees from the same family were presumed to be half-sibs (open-pollinated seeds). We did not include the population effect in the heritability calculation, because natural selection appeared to occur within each population (Visscher et al. 2008). The standard deviation of heritability was calculated with the delta method (Lynch and Walsh 1998). Phenotypic differentiation between populations, Q_{ST} (Spitze 1993), was estimated as $Q_{ST} = \sigma^2_{pop} \Big/ \left(\sigma^2_{pop} + 2\sigma^2_A\right)$. Variance components were standardized with the trait mean (Houle 1992) as follows: $CV = \frac{\sqrt{\sigma^2_{trait}}}{\bar{X}_{trait}} 100$,, where CV is the coefficient of variation. Each variance component was expressed with a CV (CV_A: additive coefficient of variation; CV_{BP} ($V_{BP} = \sigma^2_{pop}$): between-population coefficient of variation; CV_P: phenotypic coefficient of variation; CV_R: residual coefficient of variation). The variance of each component was extracted from the asymptotic covariance matrix. The significance of mean population differences was estimated with model (#1), with the GLM procedure and Student–Newman–Keuls post hoc tests.

Correlation between traits and climatic variable

Genetic correlations between traits were evaluated by calculating Pearson's coefficients for the family best

linear unbiased predictor (BLUP) estimate. These correlations are referred to hereafter as genetic correlations. Phenotypic correlations were evaluated by calculating Pearson's coefficients for the family BLUP plus the population BLUP and the grand-mean. Data from a previous study (Lamy et al. 2011) were also included, to assess the correlation between density parameters and cavitation resistance (estimated from P_{50}, the xylem pressure at which a sample lost 50 % of its conductance).

We also explore relationships between climatic variables from population origin and the population performance in the provenance-progeny trial. The first PCA axis was used as an aridity index because soil water deficit and evapotranspiration are the main contributors.

Q_{ST} and F_{ST} comparison

We investigated the contribution of selection to the differentiation of phenotypic traits, as previously described (Lamy et al. 2011) by comparing the distribution of phenotypic differentiation (Q_{ST}) with the distribution of genetic differentiation (F_{ST}) assessed with molecular markers assumed to be neutral. Briefly, the F_{ST} distribution (F^*_{ST}) was constructed from a dataset for eight neutral nuclear microsatellites previously genotyped in the populations studied (Eveno et al. 2008). Neutral expectations were simulated by randomly resampling 10^3 times with replacement between loci, to estimate the sampling variance of F_{ST}. Each F_{ST} replicate value was multiplied by a random number drawn from the (Lewontin and Krakauer 1973) distribution, which accounts for demographic deviations from the neutral model (Whitlock 2008; Whitlock and Guillaume 2009). Q_{ST} distributions (Q^*_{ST}) were constructed by performing a parametric bootstrap resampling procedure 10^3 times (O'Hara and Merilä 2005), making it possible to estimate the distribution of each variance component (σ^2_A, σ^2_{pop}) by Satterthwaite's approximation (Satterthwaite 1946). Finally, the two resulting distributions were compared in a non-parametric test on the 2.5 and 97.5 quantiles (Kosorok 1999). A more classical Whitlock test was also performed. All analyses were performed with SAS software (2008, version 9.2 SAS Institute, Cary, NC, USA). Codes are available on request.

Results

Between-population variation

No significant difference between populations (V_{BP}) was detected for wood density (D_{mean}, D_{min}, and D_{max}), whereas significant differences were found for W_a, A_{Leaf}, and ø (Fig. 1; Table 2). Wood density-related traits had much lower coefficients of variation than W_a (Table 2), particularly at the between-population level ($CV_{BP} = 1$ % and 19 % for D_{mean} and W_a, respectively). The fixed block effect was significant for all the traits studied; indicating that environmental variations were significant and taken into account by the model.

The populations from the wettest areas (Mimizan and San Cipriano) had the highest A_{Leaf} and ø values (Fig. 1), whereas the Tamrabta population (from Morocco) had the lowest values. Iberian populations from the central and southern part of Spain (Coca, Bayubas, Oria) had intermediate values, with no detectable trend in terms of environmental aridity.

Within-population variation

Heritabilities and normalized measurements of trait dispersion (i.e., CVs) were estimated to evaluate within-population additive variance (through the analysis of CV_A) and micro-environmental sensitivity (through the analysis of CV_R) (Table 2). The values of narrow-sense heritability (h^2_{ns}) for D_{mean} (0.38 ± 0.20) and D_{max} (0.51 ± 0.20) indicated that wood density was moderately genetically determined, although the standard error was high, due to the small number of progenies per mother tree analyzed for this trait. The CVs of wood density and growth traits presented contrasting patterns, with a lower coefficient of additive variation ($CV_A \leq 7$ %) for wood density than for other traits ($CV_A > 20$ %), suggesting that evolvability is limited for wood density.

Evolutionary forces driving population differentiation

Comparisons of Q_{ST} and F_{ST} may have three possible outcomes (Spitze 1993): (i) if $Q_{ST} > F_{ST}$, the degree of differentiation for quantitative traits exceeds that attainable by genetic drift alone, (ii) if Q_{ST} and F_{ST} are not significantly different, the observed degree of

Table 2 Variance components (V_P, V_{BP}, V_A, V_R), narrow-sense heritability ($h^2_{ns} \pm$ SE), coefficient of variation (CV_P, CV_A, CV_{BP}, CV_R) and population differentiation (Q_{ST})

Traits	V_P	V_{BP}	V_A	V_R	h^2_{ns}	CV_P	CV_A	CV_{BP}	CV_R	Q^a_{ST}
D_{mean}	0.001	1.9 10^{-5} ns	0.5 10^{-3}*	0.001	0.38 ± 0.20	11	7	1	10	0.02*/**
D_{max}	0.001	1.7 10^{-5}ns	0.7 10^{-3}*	0.001	0.49 ± 0.20	10	7	1	9	0.01 */**
D_{min}	0.001	1.6 10^{-5}ns	0.2 10^{-3}ns	0.001	0.22 ± 0.21	12	5	1	11	0.03 */**
$ø_{2007}$	50.63	31.92***	17.55*	46.24	0.34 ± 0.12	37	22	29	36	0.47 ***/***
B_{tot}	16124	3246***	9207***	13822	0.57 ± 0.08	43	32	19	40	0.14 ns/ns
A_{Leaf}	0.427	0.104***	0.1817**	0.382	0.425 ± 0.14	37	24	35	35	0.22 */ns

h^2_{ns} narrow-sense heritability and SE is the standard error of heritability, V_P phenotypic variance, V_A additive genetic variance, V_{BP} between-population variance, V_R residual variance, CV_A additive variation coefficient after adjustment for the block effect, CV_P phenotypic variation coefficient after adjustment for the block effect, CV_R residual coefficient of variation, CV_{BP} between-population coefficient of variation, Q_{ST} quantitative genetic variation between populations (Spitze 1993)

[a] We provide P value for Q_{ST} and F_{ST} comparison based on Whitlock's method and our method based on Kosorok test

The significance of random effects is indicated after each variance estimator: [ns] $P > 0.05$, * $P < 0.05$, ** $P < 0.01$, *** $P < 0.001$

differentiation for quantitative traits could have been reached by genetic drift alone, and (iii) if $Q_{ST} < F_{ST}$, the observed degree of differentiation is lower than expected from genetic drift alone. Consistent with previous reports (Waldmann et al. 2005; O'Hara and Merilä 2005), we found that F^*_{ST} and Q^*_{ST} had skewed distributions (Fig. 2). Only ø and D_{mean} (together with D_{min}, D_{max}, data not shown) had a Q^*_{ST} distribution that differed from the F^*_{ST} distribution ($P < 0.0001$ and $P = 0.0008$, respectively). For, A_{Leaf} (and W_a, data not shown), the difference between Q^*_{ST} and F^*_{ST} values was centered on 0 (see Fig. 2c, right panel), and it was, therefore, not possible to distinguish between drift and selection ($P = 0.23$). Conversely, differences between the Q^*_{ST} and F^*_{ST} distributions for D_{mean} were centered on −0.13, suggesting that the studied populations were less differentiated than would be expected in the presence of drift alone (Fig. 2a). Thus, natural selection favors the same phenotypic mean in different populations. For ø, the difference between Q^*_{ST} and F^*_{ST} distributions was centered on 0.34, suggesting that the studied populations displayed more differentiation than would be expected with drift alone (Fig. 2b). The population sampling protocol lead us to select population bearing different mitotypes and chlorotypes reflecting different evolutionary histories (Vendramin et al. 1998; Burban and Petit 2003). It is worth noticing that this procedure did not bias the population genetic differentiation upward because our F_{ST} estimation (0.10) was close to the lower bound of F_{ST} estimated for this species (0.10–0.14, Bucci et al. 2007).

Correlation between traits and climate

We found a significant negative phenotypic correlation between D_{mean} and ø ($r = -0.33$, $P = 0.02$), indicating that individuals with denser wood tended to have a smaller stem diameter. However, the genetic correlation was not significant ($r = -0.20$, $P = 0.16$). We observed no significant phenotypic correlation between D_{mean} (or D_{max} and D_{min}) and cavitation resistance (P_{50}) (Fig. 3). No significant correlations were found between D_{mean} and W_a, A_{Leaf}. Soil water deficit and evapotranspiration are the main contributors to the first axis of the PCA of climatic variable at population origin (see "Plant material" section). Therefore, this axis represents an index of aridity for each provenance site. No significant relationships were found between population's traits and aridity, except for ø ($P = 0.02$, data not shown).

Discussion

We here evidenced that juvenile wood density (D_{min}, D_{mean}, and D_{max}) had a low additive variance and moderate heritability. Although the studied populations originated from contrasting climates and presented different evolutionary histories, no significant difference between populations was detected and the variability between populations was smaller than expected under genetic drift alone ($Q_{ST} < F_{ST}$). In other words, these populations from different climates

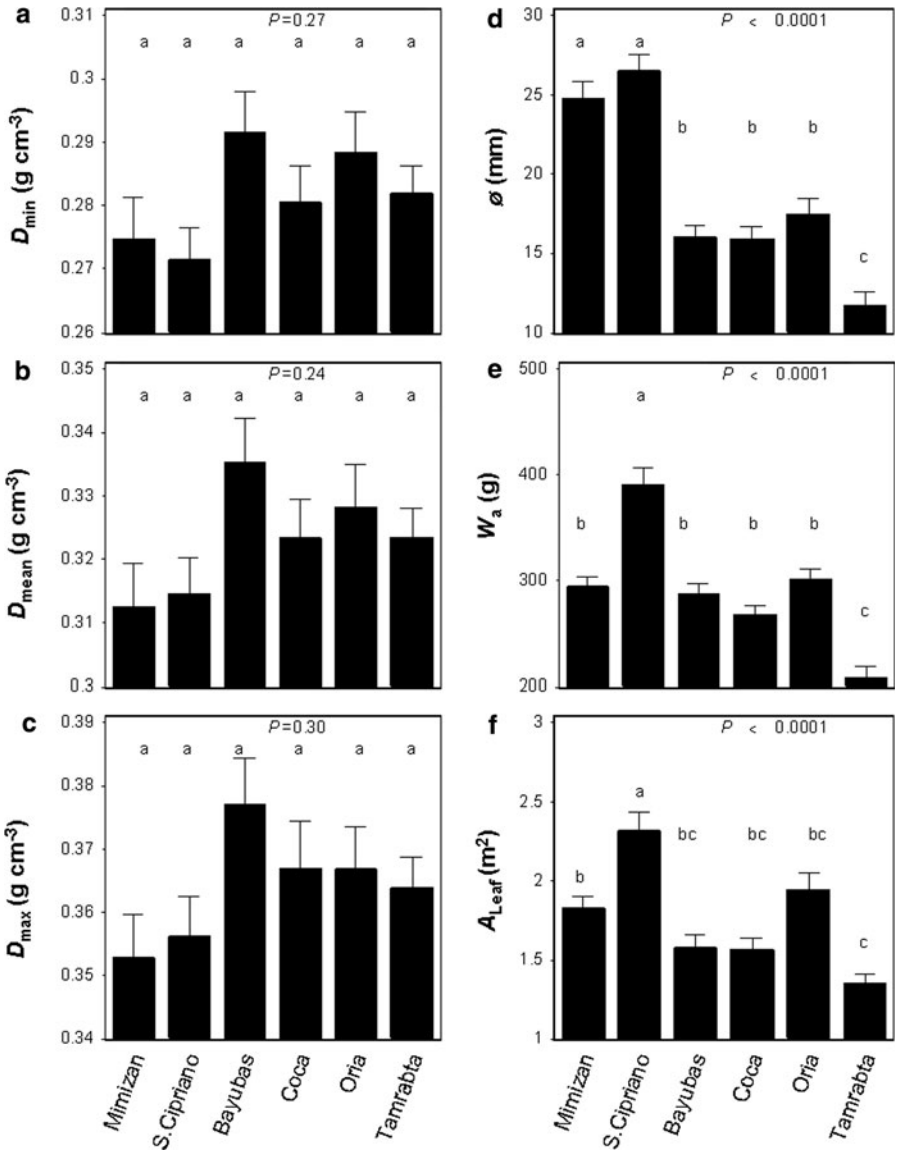

Fig. 1 Histogram showing, for each population, the 10th percentile of wood density distribution (D_{min} **a**), mean values of mean wood density (D_{mean} **b**), 90th percentile of wood density distribution (D_{max} **c**), stem diameter in 2007 (ø **d**), total above-ground tree dry biomass in 2005 (W_a **e**), total tree leaf (needle) area (A_{Leaf} **f**), for each studied population ($n = 40$ per population). *Error bars* standard errors. The *P* value is that for the mixed model and indicates whether the population effect is significant. *Different letters* indicate significant differences between populations at the $\alpha = 0.05$ level (from a fixed effect model)

and with different evolutionary histories shared the same trait value, suggesting an evolutionary process had driven the trait variability. Conversely, growth (collar diameter) presented a higher additive genetic variance and differentiation between populations, consistent with the action of diversifying selection on the studied populations. Concerning other biomass estimates (W_a, A_{Leaf}), we were unable to disentangle the effects of genetic drift and natural selection. We discuss below the possible evolutionary mechanisms underlying the low degree of variability of juvenile wood density between populations.

Juvenile wood density variability

Our results showed that mean juvenile wood density did not change between *Pinus pinaster* ecotypes. Wood density variability has been thoroughly dissected in previous studies (Gapare et al. 2009), but generally in mature tree with a narrow genetic backgrounds (elite trees, crossing between local populations) or mature interspecific hybrids. Conversely, few studies have considered the between-population variability of wood density because this information is usually not required for classical

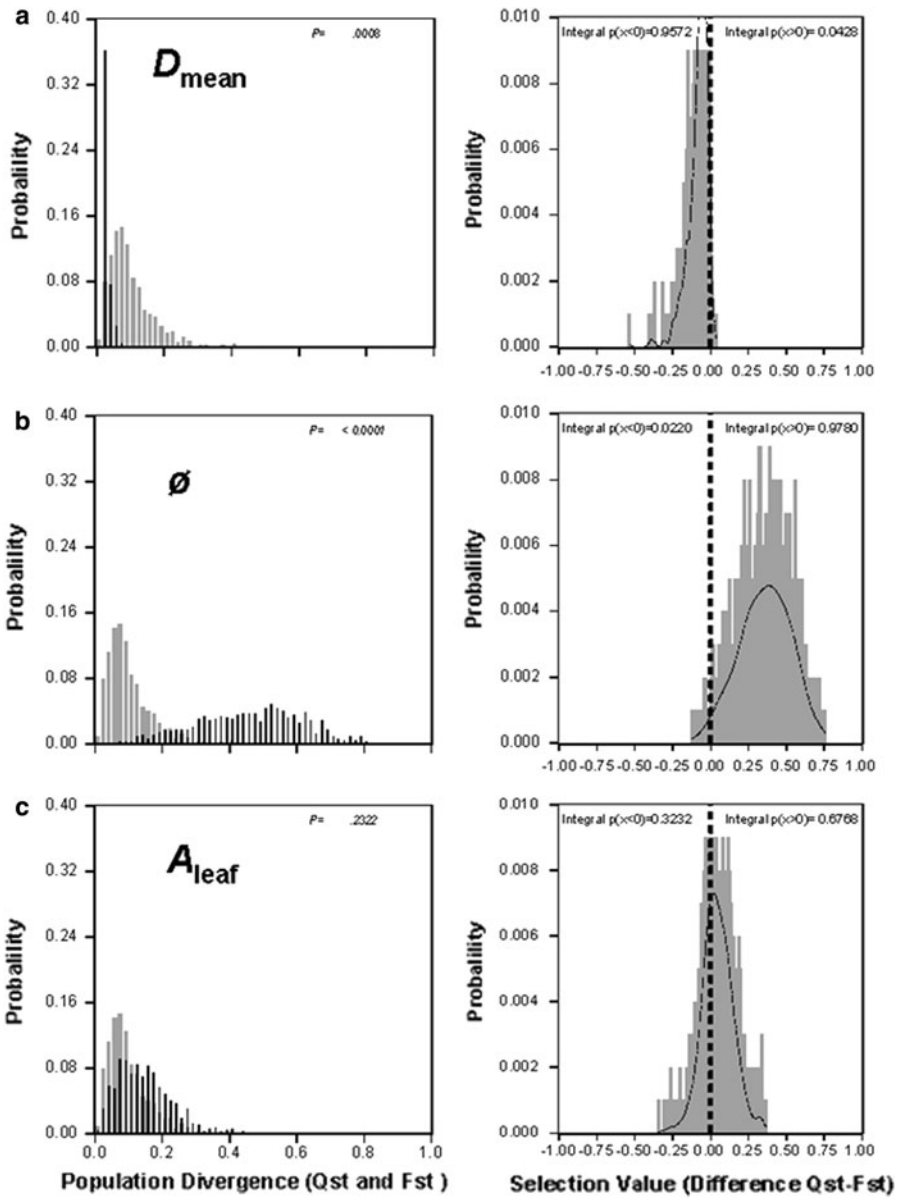

Fig. 2 Comparison between F_{ST} (histogram in *gray*) and Q_{ST} (histogram in *black*) distributions for mean wood density (D_{mean} **a**), stem diameter (ø **b**), total tree leaf (needle) area in 2006 (A_{Leaf} **c**), in the *left panel*. The observed distribution (*gray* histogram) and kernel density (*black* curves) of the $Q_{ST} - F_{ST}$ difference are represented on the *right panel* for each trait. On the *right panel*, we also show the integral probability of the distribution (using the kernel density estimator) above (see "Integral $p(x > 0)$" on the *right panel*) and below (see "Integral $p(x < 0)$" on the *right panel*) zero (marked with the *dashed* and *dotted lines*)

breeding programs. In some instance, evolutionary biologists have compared between-population variability and expectations under genetic drift for wood density as for *Picea glauca*, *Eucalyptus globulus*, and *Pinus contorta* (Yang et al. 1996; Jaramillo-Correa et al. 2001; Steane et al. 2006). In some studies, between-population variation was detected, but comparisons with ours remain difficult because: (i) these previous studies were not designed to assess the level and structure of variation across a wide range of ecotypes. Population sampling was usually restricted to a subset of the distribution area. The results were, therefore, biased toward low F_{ST} values (<0.1). For instance, Jaramillo-Correa et al. (2001) obtained an F_{ST} of 0.02, much lower than that found by Tremblay and Simon (1989) ($F_{ST} = 0.11$) for broader sampling in *Picea Glauca*, (ii) the protocols for assessing wood density differ between studies: with the use of pilodyn (Steane et al. 2006) or the water displacement method to estimate wood-specific gravity (Yang et al. 1996), (iii) the age at which wood density was measured also differed considerably between studies. Apiolaza

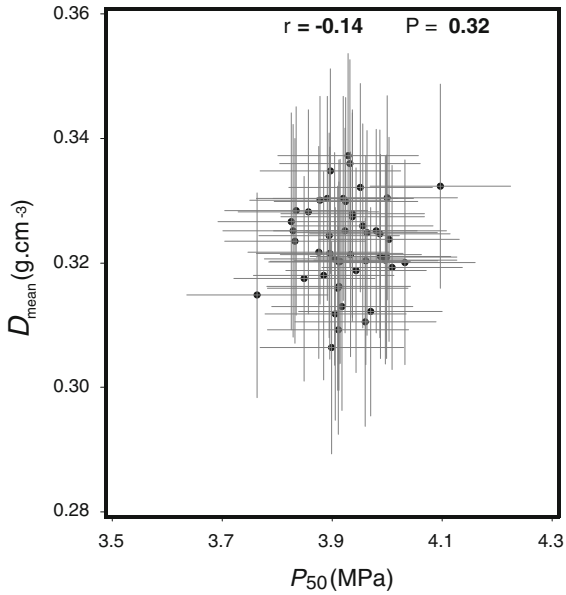

Fig. 3 Adjusted mean values of wood density (D_{mean}) versus cavitation resistance (P_{50}, xylem pressure inducing 50 % loss of hydraulic conductance). *Dots* correspond to the composite BLUP estimate and the *error bar* to the associated standard error ($n = 48$). The BLUP estimate for each family is calculated as the sum of population BLUP, family BLUP and the grand mean

(2011) and Zamudio et al. (2002) showed that genetic variability in *Pinus radiata* increases with age for wood density, and mature wood and juvenile wood are known to be the subject of different genetic controls (Plomion et al. 2001). The ring's age in our studies is much more younger compare to Jaramillo-Correa et al. (2001) and Yang et al. (1996), who worked on 22-year-old and 10-year-old trees, respectively. Our conclusions could, therefore, not be extrapolated to mature wood (and mature tree) even for *Pinus pinaster*. Low variability within population for juvenile wood density and the lack of genetic differentiation between populations may have different consequences; (i) breeding different ecotypes will not bring much more genetic variation for this trait; (ii) it may be more valuable to select for a better diameter growth and/or for a greater proportion of the latewood in the juvenile wood. It is important to keep in mind that all the above-mentioned studies, including our own, have sample size (<1,000 individuals) still far from the standard required by quantitative genetics theory (≫1000 individuals), more studies are needed to draw robust conclusions.

Impact of environment variation on wood density

Comparing CV_R between traits, it seems that wood density is less sensitive to environmental variance compare to growth-related traits. Wood density should exhibit some phenotypic plasticity but in a less extent compare to growth trait, and it may be possible that such phenotypic plasticity is sterotyped. To specifically study the reaction norm of mean wood density, multi-site approach would be valuable to draw robust conclusion about the environmental sensitivity of such trait (Vitasse et al. 2010). Another alternative to explore phenotypic plasticity is to study reaction norm of wood density along the whole profile (Martinez-Meier et al. 2011). It was not possible to investigate more deeply the reaction norm of wood density in this study because of the low number of wood rings (3-year-old branches). In addition, the extraction of phenotypic plasticity out of the total wood density signal is still a conceptual (no mechanistic model of wood density genesis) and statistical challenge (none-linearity with time). However, there are some pertinent approaches at the intra-annual level (Martinez-Meier et al. 2011).

Evolutionary significance of trait conservatism and underlying mechanisms

In our study, variance between populations (Q_{ST}) was lower than expected under a hypothesis of genetic drift (F_{ST}, from neutral markers), suggesting an evolutionary stasis for wood density. Such a pattern of variability was recently described for cavitation resistance-related traits in a study based on the same experiment (Lamy et al. 2011). Here, we demonstrated, using another complex trait (wood density), that functional traits are not always labile and prone to diversifying selection or homoplasy. Explaining trait conservatism (the extreme form of conservatism lead to stasis) is one of the most challenging questions in evolutionary biology (Bradshaw 1991). Uniform selection is often proposed as a classical explanation of narrow between-population trait variation resulting in evolutionary stasis. According to this model, independent stabilizing selection events act within each population, with the same selection optimum. However, this model provides no clues as to why the selection optimum should be the same. Genetic constraints (such as canalization) could also represent alternative explanations, particularly for

traits still displaying some degree of variability within populations (Gould and Lewontin 1979; Bradshaw 1991; Lamy et al. 2011). Simulations have also shown that the $Q_{ST} < F_{ST}$ pattern can be obtained for traits that are non additively genetically controlled (Goudet and Buchi 2006; Lopez-Fanjul et al. 2007). Deciphering uniform selection from canalization hypotheses is a difficult task. Across 21 *Pinus* species, Creese et al. (2011) have shown that wood density presented the lowest coefficient of variation among plant mass, hydraulic conductivity, and transpiring surface on the conductive surface ratio, and they found no relation with climatic variables despite a large range of mean annual precipitation (500–2,000 mm). If closely related species living in different climate have the same value of trait (i.e., evolutionary stasis), it is difficult to conceive that all the populations of each species share the same value of selective optima as it is assumed in the uniform selection hypothesis. Therefore, the alternative hypothesis that evolutionary stasis is due to a robust genetic architecture that narrows trait variability (i.e., canalization) should be considered with more attention.

Wood density and other adaptive traits

Juvenile wood density is negatively correlated with growth trait as diameter and/or height in mature tree (Bouffier et al. 2008). Between water use efficiency and wood density, the relationships are difficult to predict as a ring could be build up with the carbon from the previous years. Indeed, theoretically, the correlation is very loose between these two processes. For hydraulic safety traits (drought tolerance), at the interspecific level, Hacke and Sperry (2001) showed that cavitation resistance is correlated with wood density, species with higher wood density being more resistant to cavitation. In *Pseudotsuga menziesii* and *Picea abies* clones, a negative correlation was found between wood density and cavitation resistance (Rosner et al. 2008; Dalla-Salda et al. 2011). Even with considerable statistical power compared to these previous studies, we found no relationship between wood density and cavitation resistance within species (Fig. 3). In provenance tests, Corcuera et al. (2011) and Wortemann (2011) also found no relationship between wood density and cavitation resistance. In *Pinus sylvestris,* Martinez-Vilalta et al. (2009) did not detect any correlation between these traits in situ in natural populations. We propose two hypotheses to account for these discrepancies: (i) despite the greater statistical power of our design, the relationship between cavitation resistance and wood density does not seem to be robust to environmental variation and genetic variation and (ii) from a physiological point of view, this lack of correlation is unsurprising, because there is no direct causal link between wood density and cavitation resistance (Delzon et al. 2010; Jansen et al. 2012) in *Pinus* genera. For instance, Delzon et al. (2010) showed that bordered pit dimensions are much more important for cavitation resistance than total tracheid lumen area. However, even if these two traits are not correlated, they have other features in common: they both have a low CV_A (<7 %) and display extremely low levels of variation between populations ($CV_{BP} \leq 1$ %), suggesting that this trend follows a general rule for wood anatomy-related traits. These findings indicate that additional, more detailed investigations of the naturally occurring variability of wood anatomy-related traits (e.g., cell wall thickness, aperture pit dimensions, torus diameter, margo pore diameter, etc.) are required to gain greater insight into canalization. However, it should be pointed out that our study focused on juvenile wood, and trait values at the start of ontogeny are known to be canalized (Milton et al. 2003; Sangster et al. 2008). Further studies are required to confirm that conservatism for mean wood density is also conserved in mature trees.

Acknowledgments SD and JBL received funding from INRA-EFPA (innovative project Grant) and a PhD Grant from INRA Région Auvergne, respectively. This trial was set up by the experimental unit of INRA Pierroton within the Treesnips EC-funded project (QLK3-CT-2002-01973). Cavitation resistance, wood density and leaf area were measured with fundings from the European Union (Noveltree project, FP7-21868). We thank Emmanuelle Eveno and Pauline Garnier-Géré for sharing biomass data.

References

Aguiar A, Almeida MH, Borralho N (2003) Genetic control of growth, wood density and stem characteristics of *Pinus pinaster* in Portugal. Genetica 11:131–139

Apiolaza LA (2011) Basic density of radiata pine in New Zealand: genetic and environmental factors. Tree Genet. Genomes. doi:10.1007/s11295-011-0423-1

Apiolaza LA, Garrick DJ (2001) Analysis of longitudinal data from progeny tests: some multivariate approaches. For Sci 47:129–140

Bouffier L, Rozenberg P, Raffin A, Kremer A (2008) Wood density variability in successive breeding populations of maritime pine. Can J For Res 38:2148–2158

Bradshaw AD (1991) The Croonian Lecture, 1991. Genostasis and the limits to evolution. Philos Trans R Soc Lond B 333:289–305

Brodribb TJ, Cochard H (2009) Hydraulic failure defines the recovery and point of death in water-stressed conifers. Plant Physiol 149:575–584

Burban C, Petit RJ (2003) Phylogeography of maritime pine inferred with organelle markers having contrasted inheritance. Mol Ecol 12:1487–1495

Chave J, Muller-Landau HC, Baker TR, Easdale TA, Ter Steege H, Webb CO (2006) Regional and phylogenetic variation of wood density across 2456 neotropical tree species. Ecol Appl 16:2356–2367

Chave J, Coomes D, Jansen S, Lewis SL, Swenson NG, Zanne AE (2009) Towards a worldwide wood economics spectrum. Ecol Lett 12:351–366

Corcuera L, Cochard H, Gil-Pelegrin E, Notivol E (2011) Phenotypic plasticity in mesic populations of Pinus pinaster improves resistance to xylem embolism (P_{50}) under severe drought. Trees. doi:10.1007/s00468-011-0578-2

Creese C, Benscoter A, Maherali H (2011) Xylem function and climate adaptation in Pinus. Am J Bot 98(9):1437–1445

Dalla-Salda G, Martinez-Meier A, Cochard H, Rozenberg P (2011) Genetic variation of xylem hydraulic properties shows that wood density is involved in adaptation to drought in Douglas-fir (*Pseudotsuga menziesii* (Mirb.)). Ann For Sci 68:747–757

Delzon S, Douthe C, Sala A, Cochard H (2010) Mechanism of water-stress induced cavitation in conifers: bordered pit structure and function support the hypothesis of seal capillary-seeding. Plant Cell Environ 33:2101–2111

Eveno E (2008) L'adaptation à la sécheresse chez le pin maritime (*Pinus pinaster*): patrons de diversité et différenciation nucléotidiques de gènes candidats et variabilité de caractères phénotypiques. Thesis, University of Bordeaux 1, pp 1–390

Eveno E, Collada C, Guevara MA, Léger V, Soto A, Díaz L, Léger P, González-Martínez SC, Cervera MT, Plomion C et al (2008) Contrasting patterns of selection at *Pinus pinaster* drought stress candidate genes as revealed by genetic differentiation analyses. Mol Biol Evol 25:417–437

Figueroa JA, Lusk CH (2001) Germination requirements and seedling shade tolerance are not correlated in a Chilean temperate rain forest. New Phytol 152:483–489

Gapare WJ, Ivković M, Baltunis BS, Matheson CA, Wu HX (2009) Genetic stability of wood density and diameter in *Pinus radiata* D. Don plantation estate across Australia. Tree Genet Genomes 6:113–125

Gilchrist AS, Partridge L (2001) The contrasting genetic architecture of wing size and shape in *Drosophila melanogaster*. Heredity 86:144–152

Goudet J, Buchi L (2006) The effects of dominance, regular inbreeding and sampling design on Q_{ST}, an estimator of population differentiation for quantitative traits. Genet. 172:1337–1347

Gould SJ, Lewontin RC (1979) Spandrels of San-Marco and the panglossian paradigm—a critique of the adaptationist program. Proc R Soc Lond B 205:581–598

Guay R, Gagnon R, Morin H (1992) A new automatic and interactive tree ring measurement system based on a line scan camera. For. Chron. 68:138–141

Hacke UG, Sperry JS (2001) Functional and ecological xylem anatomy. Perspect Plant Ecol Evol Syst 4:97–115

Hansen TF, Houle D (2004) Evolvability, stabilizing selection and the problem of stasis. In: Pigliucci M, Preston K (eds) The evolutionary biology of complex phenotypes. Oxford University Press, Oxford, pp 1–27

Houle D (1992) Comparing evolvabiliy and variability of quantitative traits. Genet. 130:195–204

Jansen S, Lamy J-B, Burlett R, Cochard H, Gasson P, Delzon S (2012) Plasmodesmatal pores in the torus of bordered pit membranes affect cavitation resistance of conifer xylem. Plant and cell Environ. doi: 10.1111/j.1365-3040.2011.02476.x

Jaramillo-Correa JP, Beaulieu J, Bousquet J (2001) Contrasting evolutionary forces driving population structure at expressed sequence tag polymorphisms, allozymes and quantitative traits in white spruce. Mol Ecol 10:2729–2740

Knap PW (2005) Breeding robust pigs. Aust J Exp Agric 45:763–773

Kosorok MR (1999) Two-sample quantile tests under general conditions. Biometrika 86:909–921

Lamy J-B, Bouffier L, Burlett R, Plomion C, Cochard H, Delzon S (2011) Uniform selection as a primary force reducing population genetic differentiation of cavitation resistance across a species range. PLoS ONE 6:e23476

Lewontin RC, Krakauer J (1973) Distribution of gene frequency as a test of theory of selective neutrality of polymorphisms. Genetics 74:175–195

Littell RC, Pendergast J, Natarajan R (2000) Modelling covariance structure in the analysis of repeated measures data. Stat Med 19:1793–1819

Lopez-Fanjul C, Fernandez A, Toro MA (2007) The effect of dominance on the use of the QST-FST contrast to detect natural selection on quantitative traits. Genetics 176:725–727

Lynch M, Walsh B (1998) Genetics and analysis of quantitative traits. Sinauer Associates, Sunderland, pp 1–980

Markesteijn L, Poorter L, Bongers F, Paz H, Sack L (2011) Hydraulics and life history of tropical dry forest tree species: coordination of species' drought and shade tolerance. N Phytol 191:480–495

Martinez-Meier A, Sanchez L, Pastorino M, Gallo L, Rozenberg P (2008) What is hot in tree rings? The wood density of surviving Douglas-firs to the 2003 drought and heat wave. For Ecol Manag 256:837–843

Martinez-Meier A, Gallo L, Pastorino M, Mondino V, Rozenberg P (2011) Phenotypic variation of basic wood density in *Pinus ponderosa* plus trees. Bosque (Valdivia) 32:221–226

Martinez-Vilalta J, Cochard H, Mencuccini M, Sterck F, Herrero A, Korhonen JFJ, Llorens P, Nikinmaa E, Nole A, Poyatos R et al (2009) Hydraulic adjustment of Scots pine across Europe. N Phytol 184:353–364

McCulloh KA, Meinzer FC, Sperry JS, Lachenbruch B, Voelker SL, Woodruff DR, Domec J-C (2011) Comparative hydraulic architecture of tropical tree species representing a range of successional stages and wood density. Oecologia 167:27–37

Milton CC, Huynh B, Batterham P, Rutherford SL, Hoffmann AA (2003) Quantitative trait symmetry independent of Hsp90 buffering: distinct modes of genetic canalization and developmental stability. Proc Natl Acad Sci USA 100:13396–13401

Mormede P, Foury A, Terenina E, Knap PW (2011) Breeding for robustness: the role of cortisol. Animal 5:651–657

O'Hara RB, Merilä J (2005) Bias and precision in Q_{ST} estimates: problems and some solutions. Genetics 171:1331–1339

Petit RJ, Hampe A (2006) Some evolutionary consequences of being a tree. Annu Rev Ecol Evol Syst 37:187–214

Plomion C, Leprovost G, Stokes A (2001) Wood formation in trees. Plant Physiol 127:1513–1523

Polge H (1966) Etablissement des courbes de variation de la densité du bois par exploration densitométrique de radiographie d'échantillons prélevés à la tarière sur des arbres vivants. Ann Sci For 23:1–206

Poorter L, McDonald I, Alarcon A, Fichtler E, Licona JC, Pena-Claros M, Sterck F, Villegas Z, Sass-Klaassen U (2010) The importance of wood traits and hydraulic conductance for the performance and life history strategies of 42 rainforest tree species. N Phytol 185:481–492

Ribeiro MM, Mariette S, Vendramin GG, Szmidt AE, Plomion C, Kremer A (2002) Comparison of genetic diversity estimates within and among populations of maritime pine using chloroplast simple-sequence repeat and amplified fragment length polymorphism data. Mol Ecol 11:869–877

Richardson DM (1998) Ecology and biogeography of Pinus. Cambridge University Press, Cambridge, pp 1–527

Rosner S, Klein A, Müller U, Karlsson B (2008) Tradeoffs between hydraulic and mechanical stress responses of mature Norway spruce trunk wood. Tree Physiol 28:1179–1188

Sangster TA, Salathia N, Undurraga S, Milo R, Schelienberg K, Lindquist S, Queitsch C (2008) HSP90 affects the expression of genetic variation and developmental stability in quantitative traits. Proc Natl Acad Sci USA 105:2963–2968

SAS II (2008) SAS/STAT® 9.2 User's Guide. SAS Institute Inc, Cary

Satterthwaite FE (1946) An approximate distribution of estimates of variance components. Biom Bull 2:110–114

Spitze K (1993) Population structure in *Daphnia obtusa*: quantitative genetic and allozymic variation. Genetics 135:367–374

Steane DA, Conod N, Jones RC, Vaillancourt RE, Potts BM (2006) A comparative analysis of population structure of a forest tree, *Eucalyptus globutus* (Myrtaceae), using microsatellite markers and quantitative traits. Tree Genet Genomes 2:30–38

Tremblay M, Simon JP (1989) Genetic-structure of marginal populations of white spruce (*Picea glauca*) at its northern limit of distribution in nouveau-Québec. Can J For Res 19:1371–1379

Vendramin GG, Anzidei M, Madaghiele A, Bucci G (1998) Distribution of genetic diversity in *Pinus pinaster* Ait. as revealed by chloroplast microsatellites. Theor Appl Genet 97:456–463

Visscher PM, Hill WG, Wray NR (2008) Heritability in the genomics era—concepts and misconceptions. Nat Rev Genet 9:255–266

Vitasse Y, Bresson CC, Kremer A, Michalet R, Delzon S (2010) Quantifying phenological plasticity to temperature in two temperate tree species. Funct Ecol 24:1211–1218

Waldmann P, García-Gil MR, Sillanpää MJ (2005) Comparing Bayesian estimates of genetic differentiation of molecular markers and quantitative traits: an application to *Pinus sylvestris*. Heredity 94:623–629

Westoby M, Wright IJ (2006) Land-plant ecology on the basis of functional traits. Trends Ecol Evol 21:261–268

Westoby M, Falster DS, Moles AT, Vesk PA, Wright IJ (2002) Plant ecological strategies: some leading dimensions of variation between species. Ann Rev Ecol Syst 33:125–159

Whitlock MC (2008) Evolutionary inference from Q_{ST}. Mol Ecol 17:1885–1896

Whitlock MC, Guillaume F (2009) Testing for spatially divergent selection: comparing Q_{ST} to F_{ST}. Genetics 183:1055–1063

Wilson AJ (2008) Why h^2 does not always equal V_A/V_P? J Evol Biol 21:647–650

Wortemann R (2011) Etude de la variabilité génétique et la plasticité phénotypique de la vulnérabilité à la cavitation chez *Fagus sylvatica*. Thesis, University of Blaise Pascal, pp 1–154

Yang RC, Yeh FC, Yanchuk AD (1996) A comparison of isozyme and quantitative genetic variation in *Pinus contorta* ssp. latifolia by F_{ST}. Genetics 142:1045–1052

Zamudio F, Baettyg R, Vergara A, Guerra F (2002) Genetic trends in wood density and radial growth with cambial age in a radiata pine progeny test. Ann For Sci 59:541–549

Zanne AE, Westoby M, Falster DS, Ackerly DD, Loarie SR, Arnold SEJ, Coomes DA (2010) Angiosperm wood structure: globla patterns in vessel anatomy and their relation to wood density and potential conductivity. Am J Bot 97:207–215

MOLECULAR ECOLOGY

Molecular Ecology (2012)

NEWS AND VIEWS

OPINION

$Q_{ST} < F_{ST}$ As a signature of canalization

JEAN-BAPTISTE LAMY,*†‡ CHRISTOPHE PLOMION,*† ANTOINE KREMER*† and SYLVAIN DELZON*†

Univ. Bordeaux, UMR 1202 BIOGECO, F-33400, Talence, France; †INRA, UMR 1202 BIOGECO, F-33610, Cestas, France; ‡INRA, UMR 547 PIAF, F-63100, Clermont-Ferrand, France

Abstract

A key aim of evolutionary biology – inferring the action of natural selection on wild species – can be achieved by comparing neutral genetic differentiation between populations (F_{ST}) with quantitative genetic variation (Q_{ST}). Each of the three possible outcomes of comparisons of Q_{ST} and F_{ST} ($Q_{ST} > F_{ST}$, $Q_{ST} = F_{ST}$, $Q_{ST} < F_{ST}$) is associated with an inference (diversifying selection, genetic drift, uniform selection, respectively). However, published empirical and theoretical studies have focused on the $Q_{ST} > F_{ST}$ outcome. We believe that this reflects the absence of a straightforward biological interpretation of the $Q_{ST} < F_{ST}$ pattern. We here report recent evidence of this neglected evolutionary pattern, provide guidelines to its interpretation as either a canalization phenomenon or a consequence of uniform selection and discuss the significant importance this issue will have for the area of evolutionary biology.

Keywords: Canalization, diversifying selection, evolutionary stasis, phylogeny signal, Q_{ST}/F_{ST} comparison, stabilizing selection, uniform selection

Received 10 January 2012; revised 27 July 2012; accepted 31 July 2012

Introduction: comparison of Q_{ST} and F_{ST} and inferences

The relative contributions of genetic drift and natural selection to evolutionary change have long been debated in evolutionary biology (Galpern 2000; McKay & Latta 2002; Hansen & Houle 2004; Leinonen *et al.* 2008; Meirmans & Philip 2011). Comparisons of the differentiation of phenotypic traits (as measured by Q_{ST}) with that of neutral molecular markers (as measured by F_{ST}) provide one of the most accessible frameworks and universal tools for inferring the role of natural selection in population differentiation for quantitative traits (DeWoody *et al.* 2010).

Correspondence: Sylvain Delzon, Fax: 33 (0)5 40 00 36 57; E-mail: sylvain.delzon@u-bordeaux1.fr

Underlying assumptions for comparison of Q_{ST} and F_{ST}

Comparisons of Q_{ST} and F_{ST} are based on the rationale that F_{ST} values at neutral markers are estimators of the degree of population differentiation only due to the interplay between genetic drift and migration, assuming that mutation rates are negligible in comparison with migration rates (Spitze 1993; Merilä & Crnokrak 2001). If the quantitative traits are exposed only to the same neutral evolutionary forces as neutral genetic markers and they are genetically controlled by purely additive genes (without pleiotropy), then their level of differentiation between populations would be expected to be equal to that for neutral loci (*i.e.* $Q_{ST} = F_{ST}$). The comparison of these two quantities (Q_{ST} and F_{ST}) can therefore be used to detect the effects of selection, including the effect of cumulative past selection events in the absence of current selection (Whitlock 2008).

Inferring the action of natural selection on wild species

In comparisons of Q_{ST} and F_{ST}, three outcomes are possible, for which a different inference can be drawn. If the trait is neutral and additively determined, then Q_{ST} should be equal to F_{ST}. By contrast, $Q_{ST} > F_{ST}$ is predicted under conditions of diversifying (or divergent) selection for different local optima and $Q_{ST} < F_{ST}$ is predicted under conditions of uniform selection (also called homogeneous, spatially homogenizing, convergent or stabilizing selection across populations). Hereafter, we refer to 'uniform selection', to distinguish this situation from that of stabilizing selection (see Glossary) within a population.

Uniform selection is conceptualized and modelled as n stabilizing selection events acting within n different populations with the same selection optimum for each population (Fig. 1), despite the partial genetic isolation (assessed by determining F_{ST}) (Le Corre & Kremer 2003; Whitlock & Guillaume 2009). This process reproduces trait conservatism and eventually leads to stasis (see Glossary), but unfortunately, this model does not provide suggestions for the biological hypothesis constraining the local selective optima across populations or subspecies living in different environments. In evolutionary ecology, most of the literature is oriented towards the explanation of the variation between populations (or related species), but discard experimental results leading to the absence of trait differentiation despite the great variability of environment. Therefore, it does not seem that the explanation for trait conservatism (and stasis) can lie only in selection regimes;

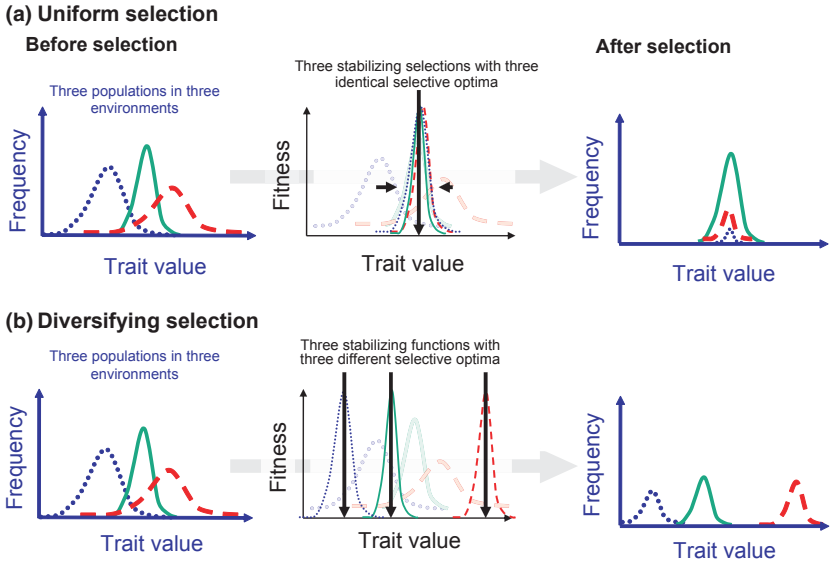

Fig. 1 Conceptual relationship between uniform or diversifying selection and stabilizing selection. On the left part, there are three populations inhabiting different environments across the species distribution range, symbolized by blue, green and red colours; they represent three different trait distributions. The central part shows the relationship between the fitness and the trait value (selection function). In the background of the selection function, we also reported the initial trait distribution. The horizontal black arrow illustrated the location of selective optima, while the vertical one symbolized the selective intensity of the selection function. (a) The upper panel shows the conceptual relationship between stabilizing selection and uniform selection. Uniform selection is the joint effect of *n* stabilizing selection events within *n* populations centred on the same selective optimum. Following this uniform selection event, populations exhibit the same mean trait value and a reduced variance. This selection process decreases the between-population variance. (b) The lower panel shows the conceptual relationship between stabilizing selection and diversifying selection. Diversifying selection could be modelled through stabilizing selections or other selection functions (disruptive, directional and divergent) with different selective optima between populations. Within-population consequences of diversifying selection depend on the selection function, but this selection process generally leads to increased between-population variance.

constraints due to genetic architecture are too readily dismissed (Bradshaw 1991; Brent Burt 2001; Merilä & Crnokrak 2001; Hansen & Houle 2004).

Methodological limits of comparison of Q_{ST} and F_{ST}

The empirical estimation of Q_{ST} is labour intensive [(O'Hara & Merila 2005; Navarro *et al.* 2005; Goudet & Buchi 2006; Whitlock & Guillaume 2009) recommend >20 populations × five families × five progenies], and rigorous statistical comparisons between Q_{ST} and F_{ST} are not simple to perform. On the one hand, estimates of Q_{ST} and F_{ST} are subject to statistical and evolutionary stochasticity. The first leads to estimation error, while the second which is due to the randomness of evolutionary processes has not always been dealt with appropriately, particularly in comparisons between Q_{ST} and F_{ST}. Approaches for comparing these two parameters taking both types of error into account have only recently been developed, for univariate (Whitlock & Guillaume 2009; Lamy *et al.* 2011) and multivariate tests (Martin *et al.* 2008; Ovaskainen *et al.* 2011). On the other hand, the use of F_{ST} values estimated for neutral markers with rates of mutation higher than those for quantitative traits has been criticized, as it could potentially lead to spurious inferences of diversifying selection (Kronholm *et al.* 2010; Edeelar & Björklund 2011; Meirmans & Philip 2011; Whitlock 2011). Another extreme situation is presented by small populations with very low levels of gene flow, which is not the most appropriate situation for comparisons of Q_{ST} and F_{ST} (high neutral variance compared to putative selective variance, see Kremer & Le Corre 2012). Q_{ST} estimations are also subject to various sources of bias [reviewed by Whitlock (2008)]. For instance, Cano *et al.* (2004) demonstrated experimentally that Q_{ST} could be influenced by genotype x environment interactions, suggesting that such an impact of phenotypic plasticity on Q_{ST} and F_{ST} estimator should be tested more often. Bearing these methodological problems in mind, we aim here to provide guidelines for the interpretation of the $Q_{ST} < F_{ST}$ pattern.

$Q_{ST} < F_{ST}$: publication bias and cryptic published evidence

A recent review (Leinonen *et al.* 2008) showed that 70% of Q_{ST} values exceed the associated F_{ST} values (see Fig. 2 for an updated comparison). The authors pointed out two potential biases in such a pattern: (i) a sampling bias, due to the deliberate selection, by researchers, of populations from contrasting environments or based on prior knowledge of phenotypic divergence and (ii) a publication bias

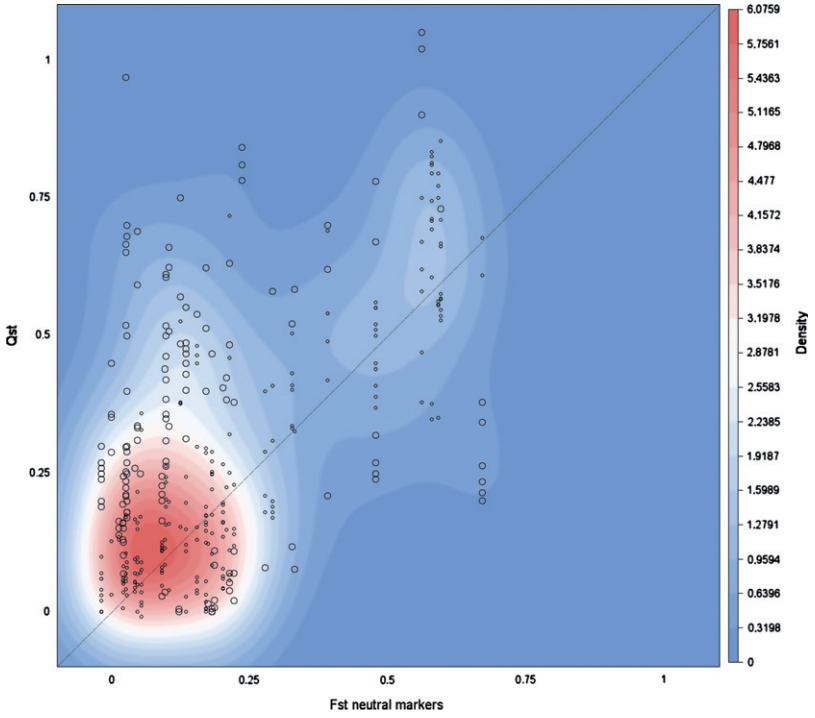

Fig. 2 Relationship between Q_{ST} and F_{ST} estimates from empirical published studies (based on and updated* from Leinonen *et al.* 2008 see Table S1 and Table S2). The thin dashed black line shows the 1:1 ratio. Circles represent Q_{ST} estimates of individual traits plotted against F_{ST} estimates for presumably neutral markers, small circles for no significant results, and large circles for significant results. It is worth noticing that statistical significance of Q_{ST} versus F_{ST} is diversified with different statistical power and robustness (*P*-value from the literature). For the sake of clarity, P_{ST} estimates were discarded because they do not control for the effect of the environment (Pujol *et al.* 2008; Brommer 2011); most were therefore located above the 1:1 line and close to zero on the F_{ST} axis. The contour plot highlights the nonuniform nature of the distribution of Q_{ST} and F_{ST} comparison results. *Updated references are Andersen *et al.* (2008); Badri *et al.* (2008a,b); Chenoweth & Blows (2008); Demont *et al.* (2008); Kinnison *et al.* (2008); Kohn *et al.* (2008); Olivieri *et al.* (2008); Vonlanthen *et al.* (2009); Yoshida *et al.* (2008); Chun *et al.* (2009a,b); Eroukhmanoff *et al.* (2009); Liang *et al.* (2009); Meyer *et al.* (2009); Ramírez-Valiente *et al.* (2009); Yoshida *et al.* (2009); Antoniazza *et al.* (2010); Lind *et al.* (2010); Santure *et al.* (2010); Scheepens *et al.* (2010); Alberto *et al.* (2011); J. B. Lamy & S. Delzon, unpublished data.

favouring studies reporting an outcome $Q_{ST} > F_{ST}$ (Fig. 2), possibly due to the difficulties involved in interpreting a $Q_{ST} < F_{ST}$ pattern. These difficulties have epistemological and scientific foundations as selection is classically invoked to account for differences, rather than similarities, between populations and there is no widely accepted consensus concerning the most probable evolutionary interpretation of the '$Q_{ST} < F_{ST}$' pattern.

Studies dealing with several traits tend to focus on traits with a $Q_{ST} > F_{ST}$ pattern, and interpretation of traits for which $Q_{ST} < F_{ST}$ tends to be discreet or entirely absent. Nevertheless, some studies have provided cryptic, but well-supported examples of the $Q_{ST} < F_{ST}$ pattern. Chapuis *et al.* (2008) showed (with a randomization procedure and a highly replicated design) that early traits of freshwater snails, such as morphological characters measured before maturity, have the same population means between 17 populations from permanent or temporary ponds (i.e. $Q_{ST} < F_{ST}$). Two studies also found that copepod subspecies (*Eurytemora affinis* and *Tigriopus californicus*) displayed morphological stasis (see Glossary) for secondary sexual and life history traits (Lee & Frost 2002; Edmands & Harrison 2003). In plant sciences, Lamy *et al.* (2011) showed that cavitation resistance, a physiological trait related to survival in conditions of extreme drought, displayed no differentiation between populations originating from contrasting climates. Other studies (Navarro *et al.* 2005; Yoshida *et al.* 2008; Chun *et al.* 2009a,b; Santure *et al.* 2010) reported that Q_{ST} values were significantly lower than F_{ST} values, for various types of trait (floral morphology, vegetative morphology, growth, competitive ability). There is therefore enough evidence of trait conservatism in changing environments to now pay more attention on the evolutionary underpinnings of stasis.

Theoretical expectation of $Q_{ST} < F_{ST}$

From a theoretical standpoint, occurrences of $Q_{ST} < F_{ST}$ have been explored by simulations under different evolutionary scenarios, with various levels of uniform selection, divergent selection and gene flow (Le Corre & Kremer 2003; Miller *et al.* 2008). Under uniform selection,

regardless of the level of gene flow and the strength of within-population selection, Q_{ST} is always lower than F_{ST}. Indeed, under uniform selection, negative covariance between genes effects (which may be seen as linkage disequilibrium, a nonrandom association of genes) builds up, decreasing the between-population variance to levels lower than those predicted on the basis of gene flow alone (Kremer & Le Corre 2012). It is also worth noting that a $Q_{ST} < F_{ST}$ pattern may occur under diversifying selection (Le Corre & Kremer 2012). Under strong genetic drift (small effective population under limited gene flow), the between-population variance due to drift can become larger than the between-population variance generated by the differences in local optima [for more explanation about the underlying process, see Kremer & Le Corre (2012) and Le Corre & Kremer (2012)].

Other simulations and theoretical studies have tested departure from two implicit hypotheses (i.e. single traits and additive genetic determinism) underlying comparisons of Q_{ST} and F_{ST}: multitrait approach and nonadditive genetic determinism of the underlying genes. Phenotypic traits are often correlated, due to pleiotropy (see Glossary), and the response of a single trait to selection could be slowed down by these correlation constraints (Kruuk *et al.* 2008). Several statistical methods have been proposed to take the whole additive genetic variance–covariance matrix (**G**) for Q_{ST} and F_{ST} comparison into account (Kremer *et al.* 1997; Martin *et al.* 2008; Ovaskainen *et al.* 2011). However, detecting $Q_{ST} < F_{ST}$ comparison in a multivariate framework is more complex than previously thought. Using a modelling approach, Guillaume (2011) showed that the interplay between migration and genetic correlations among phenotypic traits can generate substantial phenotypic divergence in traits under uniform selection, and this could lead to false case of diversifying selection.

The effect of genetic architecture (nonadditive effects: dominance and epistasis, see Glossary) on Q_{ST} has also been investigated. It has been shown that dominance generally leads to the $Q_{ST} < F_{ST}$ outcome, in at least two evolutionary scenarios [the island model, see Goudet & Buchi (2006) and the pure drift model, see Goudet & Martin (2007)]. Moreover, epistasis generally decreases Q_{ST} relative to F_{ST} in the island model (Whitlock 1999) and in a pure drift model (Lopez-Fanjul *et al.* 2003). These analytical studies thus demonstrate that a nonadditive genetic architecture can lead to $Q_{ST} < F_{ST}$ without the need for uniform selection.

$Q_{ST} < F_{ST}$: underlying mechanisms

The biological mechanisms resulting in the $Q_{ST} < F_{ST}$ pattern are generally skimmed over in scientific publications. We review here two evolutionary processes that might potentially account for this pattern.

True uniform selection and other selection-based hypotheses

An inference of uniform selection requires a demonstration that stabilizing selection drives independently each population to the same selective optimum (Fig. 1). Stabilizing selection is documented in empirical literature (Kingsolver *et al.* 2001), but the variance of the associated phenotypic optima is less documented due to the difficulty in assessing these optima for life history and morphological traits. The demonstration of independent stabilizing selection (with the same selective optimum among populations) would require specific experimental designs, such as local measurements of selection on each population from contrasting environments, as described by Lande & Arnold (1983). These experiments would be very time-consuming and expensive, and the study of this type has therefore seldom been carried out. It must also be borne in mind that the explanation of stasis by uniform selection requires not only common stabilizing selection, but also the variation in selective optima within only a narrow range (Hansen & Houle 2004). Other selection-based hypotheses could be invoked to explain $Q_{ST} < F_{ST}$: for instance, DeWoody *et al.* (2010) showed by simulation that frequency-dependent selection applied in a multitrait framework maintains a high variance within populations. Extrapolating this mechanism to subdivided populations, this selection process will inflate variance within population relative to variance among populations, which might result in a $Q_{ST} < F_{ST}$ pattern. Sexually selected traits or traits involved in biotic relationship are prone to be targeted by frequency-dependent selection.

Simulation studies show that selection-based hypotheses are likely, but maybe not for all traits. For instance, cavitation resistance, which is a core fitness-related trait allowing plants to survive under extreme drought conditions (Maherali *et al.* 2004; Brodribb & Cochard 2009; Brodribb *et al.* 2010), is expected to diverge between populations from the most contrasted part of the species distribution range. Yet, despite high contrasted water-stress conditions (different selective optima), no difference between populations was reported for two angiosperm and conifer species with a broad distribution in Europe (Lamy *et al.* 2011; Wortemann *et al.* 2011) and Q_{ST} was significantly lower than F_{ST} (Lamy *et al.* 2011). For this drought-resistance trait, it is therefore less than likely that selection-based hypotheses would explain this pattern.

Canalization. Canalization (also called robustness, see Glossary) refers to any inheritable structure or process, adaptive or otherwise, reducing the sensitivity of a phenotype to changes or disturbances to the underlying genetic (mutation and recombination) and/or nongenetic (environmental variation) factors determining its expression [see Flatt (2005) for a complete review]. In the original meaning, a trait becomes canalized because the insensitivity to perturbations was considered to increase fitness (Waddington 1942, 1953; Wagner *et al.* 1997; Debat & David 2001). Nowadays, canalization concept is widely used in developmental sciences (Felix & Wagner 2008) and in the expanding evo-devo field (Carroll 2008). Such a concept should be taken into consideration in evolutionary ecology because, from a functional point of view, phenotype should be seen as a core of functions [*Bauplan*, see Gould & Lewontin

(1979) and Williams (1992)] inherited from the deep evolutionary history, and functions with more genetic variation allows for short-term adaptation.

Is it possible to infer canalization in the wild?

Canalization is a relative term that can be defined only in a comparative framework. It was first demonstrated in *Drosophila*, through comparisons of wild-type and modified inbred lines [based on artificial mutagenesis or abiotic stress, Waddington (1942) and Stearns (1994)]. However, Felix & Wagner (2008) proposed a comparative approach for the inference of canalization, by making use of the genetic variation naturally accumulating during evolution, and comparing the genetic variation between individuals or populations of the same species. These authors argued that the application of this approach 'in the wild' might be more powerful, as it would allow the comparison of genotypes that had accumulated genetic change over long periods of evolution, whereas laboratory experiments are much more short-term. Here, we propose the use of Q_{ST} and F_{ST} for such comparisons. As Q_{ST} is a standardized measure of genetic variation between populations (even between closely related species), then a $Q_{ST} < F_{ST}$ signature could be interpreted as the presence of a genetically canalized trait.

Some traits are known from the literature to be invariant, that is, canalized traits, for example, the body temperature of mammalian, segmentation of blastoderm and wing shape (intersection veins position and the derived multivariate estimators) in Drosophila (Hansen & Houle 2004; Gilchrist & Partridge 2001; Manu *et al.* 2009; Williams 1992). Wing shape trait in *Drosophila* has been studied in developmental science and evolutionary quantitative genetics. For instance, Andersen *et al.* (2008) showed that populations from highland or lowland environments (contrasted atmospheric conditions) generally presented a low Q_{ST} (low genetic variance between populations), which is always lower than the F_{ST}. At this stage, it is difficult to define a threshold between uniform selection and canalization. But comparing the wing shape between species from the same genus (same *Bauplan* = same genetic architecture) but living in different ecological niches and having different geographical distributions (different selective optima) could give more clues about the underlying processes. Among 21 species of *Drosophila* with diverse ecological specialization (Table 1), Hansen & Houle (2004) noticed that wing shape trait in *Drosophila* species is a conserved trait ($CV_P = 8.1\%$, $n = 21$, see also Galpern 2000). Trait conservatism is classically explained by uniform selection, meaning that, for a given species, stabilizing selections must occur in all populations with nearly the same selective optima. However if a single global optimum does exist over contrasted conditions for *Drosophila*, why then would thousands of similarly-sized hymenopterans have such different wings? Surprisingly, little work has been devoted to this problem. The same reasoning could be applied to cavitation resistance in pine species. In *Pinus pinaster*, a significant $Q_{ST} < F_{ST}$ pattern was reported for this trait among

Table 1 Comparison of a well-known (wing traits in *Drosophila*) and a putative (cavitation resistance in *Pinus*) canalized trait

Species	*Drosophila buzzatii*	*Pinus pinaster*
Trait	Wing traits	Cavitation resistance
Interspecific level	In the *Drosophila* genus*	In the *Pinus* genus[†]
CV_P	8.1	13.0
Intraspecific level	Natural populations and hybrids (3 generations)[‡]	Natural populations[§]
Q_{ST}	0.06	0.02
F_{ST}	0.25	0.11

CV_P (%) is the coefficient of phenotypic variation for a given genus (*Drosophila* genus $n = 21$ and *Pinus* genus $n = 17$). Q_{ST} is the additive quantitative genetic variation between populations (phenotyped individuals: *Drosophila buzzatii* $n = 593$ and *Pinus pinaster* $n = 240$). F_{ST} is the neutral genetic difference between populations (number of loci: for *Drosophila buzzatii* $n = 10$ and for *Pinus pinaster* $n = 8$).
*Galpern (2000).
[†]Delzon *et al.* (2010).
[‡]Andersen *et al.* (2008).
[§]Lamy *et al.* (2011).

populations from extreme climatic origin (Lamy *et al.* 2011), while a high degree of conservation within the *pinus* lineage (36 species) showed that cavitation resistance strongly reflects phylogenetic history (strong evolutionary conservatism; S. Delzon, unpublished data). These examples might provide some clues that $Q_{ST} < F_{ST}$ could be also interpreted as canalization (genetic constraints) rather than only selection-based hypothesis.

However, selection-based and canalization hypotheses are not exclusives as demonstrated by some modelling studies in phylogenetic and evolutionary quantitative genetic fields. Over the very long term, assuming additive genetic model, canalization results from a phenomenon of stabilizing selection centred on the same selective optimum on average (Waddington 1942; Stearns & Kawecki 1995; Falconer & Mackay 1996; Bergman & Siegal, 2003; de Visser *et al.* 2003; Lande 2009). This scenario of apparition of canalization has been addressed and questioned by recent studies (Wagner *et al.* 1997; Zhang 2006): for instance, under fluctuating selection, Kawecki (2000) showed that modifier genes reducing phenotypic variance will be favoured leading to canalization. Adopting a new quantitative genetic formalism to described genetic architecture (Hansen & Wagner 2001b), Hansen and co-workers found the counterintuitive conclusion that the selection regime might be less important than the sign of functional epistasis (see Glossary) in determining the evolvability [for novel perspectives, see Hermisson *et al.* (2003); Carter *et al.* (2005); Hansen (2006)]. For instance, they showed that directional rather than stabilizing selection could lead to canalization if the underlying genes of a trait exhibit

negative directional epistasis (Carter *et al.* 2005). A task of future research is to further disentangle the complex relationship between these two phenomena.

Some guidelines to interpret $Q_{ST} < F_{ST}$

For nonmodel species, the use of classical methods (*i.e.* artificial mutagenesis or abiotic stress) for inferring canalization remains impracticable. This obstacle could be partially overcome by utilizing a bottom-up approach that combines information from Q_{ST}/F_{ST} comparisons and phylogenetic information (see Fig. 3). For a given trait, if Q_{ST} is lower than F_{ST} and closely related species living in different environmental conditions showed a trait conservatism, then canalization could be an alternative to the classical uniform selection hypothesis. Canalization could explain the constancy of a trait within species (low or lack of genetic variance between populations) and across species (evolutionary stasis). In other words, it means that species genetic backgrounds share the same genetic constraints (same *Bauplan*) rather than the same selective optima. This inference may be crucial for the identification of dimensions in which phenotype variation is constrained, impeding the use of classical models for the prediction of past or future phenotypic evolution.

Future directions

Several future directions could be suggested: (i) Traits of known function and for which selective optima could be inferred a priori should be explored more extensively for their interpopulation differentiation. The comparison between the a priori selective optima and the inferred ones could give some clues about the underlying process (uniform selection or canalization). (ii) Recent genomic studies revealed that epistasis and pleiotropy seem to be the rule rather than exception (Hill *et al.* 2008; Weedon & Frayling 2008; Visscher 2008; Cheverud *et al.* 2004; Wagner *et al.* 2008; Wagner & Zhang 2011). However, Q_{ST} and F_{ST} comparisons are usually made in the traditional quantitative genetic context ignoring epistasis and pleiotropy. Therefore, more theoretical work is needed to quantify the impact of complex genetic architecture (for instance using Hansen's formalism) on the inference made from Q_{ST} and F_{ST} comparison. (iii) Multitrait approaches should be implemented more often to explore the effects of multivariate genetic

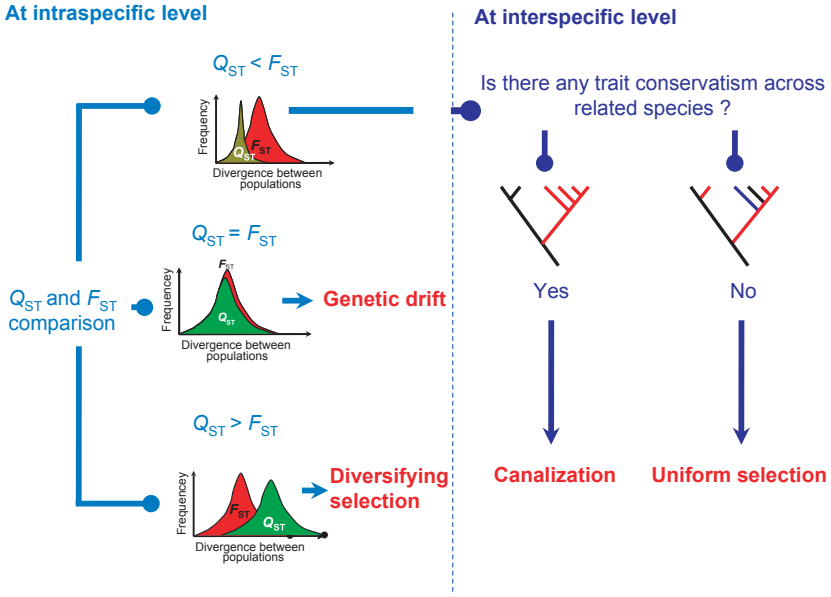

Fig. 3 Decision tree for the comparison of Q_{ST} and F_{ST}. This decision tree combines two levels of information for a given trait: (i) information relating to populations, based on comparisons of Q_{ST} and F_{ST} (light blue, left panel); (ii) the degree of evolutionary conservatism between closely related species living in different ecological conditions based on phylogenetic analyses. As indicated by the arrows and the red text, $Q_{ST} = F_{ST}$ and $Q_{ST} > F_{ST}$ are straightforwardly interpreted as genetic drift and diversifying selection, respectively. In the case of $Q_{ST} < F_{ST}$, more information is required for a robust inference indicated by the final circle and the blue text. Closely related species inhabiting different ecological niches (or any proxy which allows to assess a priori selective optima) and sharing the same value of trait (trait conservatism) provides clues about a potential canalization phenomenon (i.e. the genetic architecture narrows trait variability). It is worth noticing that trait conservatism concept excludes cases where trait evolution followed a Brownian model (an approximation of interspecific genetic drift motion). $Q_{ST} < F_{ST}$ associated with substantial variability between species for the studied trait could be interpreted as true uniform selection. Q_{ST} (in green) and F_{ST} (in red) are represented as distributions because these estimators are subjected to two types of errors (evolutionary and sampling errors).

constraints on phenotype evolution *in natura* (Martin *et al.* 2008; Ovaskainen *et al.* 2011).

Acknowledgements

We thank Stefan Andersson, Pascal Vonlanthen, Louis Bernatchez and Emmanuelle Porcher for kindly sharing published data. We thank Rémy J. Petit, Vincent Debat, Ivan Scotti and Maximilien Larter for helpful comments on the manuscript about quantitative genetics, canalization concepts and English syntax. This study has been carried out with financial support from the European commission under FP7 (FP7-211868 Noveltree).

Glossary

Canalization

A trait is canalized if the underlying genetic architecture buffers its variation against all kinds of disturbance, being of genetic (mutation, hybridization, recombination) and/or environmental nature (Hansen & Houle 2004).

Directional epistasis

Functional epistasis (see definition of Epistasis) is said to be directional if genes systematically modify each other (genes effects) in particular patterns or directions in the phenotypic space. (i) Positive epistasis, where genes tend to reinforce each other's effects along the direction of selection, will accelerate the response, (ii) while negative epistasis, where genes tend to diminish each other's effects in the direction of selection, will reduce the response (Hansen & Wagner 2001a,b). Obviously, functional epistasis sign can lead to dramatic qualitative changes in evolutionary dynamics.

Epistasis

A phenomenon by which the effects of one gene are modified by one or several other genes. Despite this simple definition, there are several ways to conceptualize and quantify epistasis. A distinction should be made between statistical (Falconer & Mackay 1996; Lynch & Walsh 1998) and functional (or physiological) epistasis (Cheverud & Routman 1995; Hansen & Wagner 2001b). (i) Statistical epistasis refers to the standard quantitative genetic definition of epistasis as the third interaction terms in a regression of trait value on the presence of alleles. It is a population property and is a function of both allele frequencies and the biological interactions among genes. (ii) Functional epistasis refers to nonadditive interactions among loci in the mapping from specific genotypes to phenotype and is not a population property [see Hansen (2006) p126]. In other words, functional epistasis means that gene or genotype effects depend on the genetic background, suggesting that these effects might change due to selection, drift, mutation or any other mechanisms. Both statistical and functional epistasis definitions are partially overlapping, but not univocal. Functional epistasis can contribute to additive and dominance genetic variance component, whereas statistical epistasis is associated only with the third interaction genetic component. In the present article, the use of epistasis alone means functional epistasis (epistatic effect of allele, gene or genotype).

Genetic architecture

The number of genes underlying the trait, their redundancy (gene duplication and alternate pathways) and/or the resulting network due to interallelic interaction (additive effect and dominance) and interloci interaction (epistasis).

Pleiotropy

Pleiotropy is due to two mechanisms: pleiotropic gene (gene affects more than one character) and linkage disequilibrium (the statistical associations between alleles at different loci). Pleiotropy is the underlying cause of genetic covariation between characters at the population level (Flatt 2005; Hansen 2006).

Stasis

Taxa, such as genera, species or populations, displayed the same value of trait despite significant genetic isolation and environmental distance between taxa. In evolutionary ecology field, stasis is, most of the time, assessed by a synchronic study through a comparative analysis.

Stabilizing selection

Selection-based process on the fitness value of an individual as it has been defined by Turelli (1984). In this model, the fitness is the function of selection intensity (ω^2), selection optimum (Z_{opt}) and trait value (Z). An individual has the higher fitness when its value of phenotypic trait equals to Z_{opt}, which does not imply it is the most abundant phenotype (Z).

References

Alberto F, Bouffier L, Louvet J-M, Delzon S, Lamy J-B, Kremer A (2011) Adaptive responses for seed and leaf phenology in natural populations of sessile oak along an altitudinal gradient. *Journal of Evolutionary Biology*, **24**, 1442–1454.

Andersen HD, Pertoldi C, Loeschcke V, Cavicchi S, Scali V (2008) Divergence at neutral and non-neutral loci in *Drosophila buzzatii* populations and their hybrids. *Evolutionary Ecology*, **22**, 593–605.

Antoniazza S, Burri R, Fumagalli L, Goudet J, Roulin A (2010) Local adpatation maintains clinal variation in melanin-based coloration of european barn owls (*Tyto alba*). *Evolution*, **64**, 1944–1954.

Badri M, Zitoun A, Houcine I, Huguet T, Aouani ME (2008a) Morphological and microsatellite diversity associated with ecological factors in natural populations of *Medicago laciniata* Mill. (Fabaceae). *Indian Academy of Sciences*, **87**, 241–255.

Badri M, Zitoun A, Soula S, Houcine I, Huguet T, Aouani ME (2008b) Low levels of quantitative and molecular genetic differentiation among natural populations of *Medicago ciliaris* Kroch. (Fabaceae) of different Tunisian eco-geographical origin. *Conservation Genetics*, **9**, 1509–1520.

Bergman A, Siegal ML (2003) Evolutionary capacitance as a general feature of complex gene networks. *Nature*, **424**, 549–552.

Bradshaw AD (1991) The Croonian lecture, 1991: genostasis and the limits to evolution. *Philosophical Transactions of the Royal Society of London Series B-Biological Sciences*, **333**, 289–305.

Brent Burt D (2001) Evolutionary stasis, constraint and other terminology describing evolutionary patterns. *Biological Journal of the Linnean Society*, **72**, 509–517.

Brodribb TJ, Cochard H (2009) Hydraulic failure defines the recovery and point of death in water-stressed conifers. *Plant Physiology*, **149**, 575–584.

Brodribb TJ, Bowman DJMS, Nichols S, Delzon S, Burlett R (2010) Xylem function and growth rate interact to determine recovery rates after exposure to extreme water deficit. *New Phytologist*, **188**, 533–542.

Brommer JE (2011) Whither PST? The approximation of QST by PST in evolutionary and conservation biology. *Journal of Evolutionary Biology*, **24**, 1160–1168.

Cano JM, Laurila A, Palo J, Merilä J (2004) Population differentiation in G matrix structure due to natural selection in *Rana temporaria*. *Evolution*, **58**, 2013–2020.

Carroll SB (2008) Evo-devo and an expanding evolutionary synthesis: a genetic theory of morphological evolution. *Cell*, **134**, 25–36.

Carter AJR, Hermisson J, Hansen TF (2005) The role of epistatic gene interactions in the response to selection and the evolution of evolvability. *Theoretical Population Biology*, **68**, 179–196.

Chapuis E, Martin G, Goudet J (2008) Effects of selection and drift on G matrix evolution in a heterogeneous environment: a multivariate Q_{ST}-F_{ST} test with the freshwater snail *Galba truncatula*. *Genetics*, **180**, 2151–2161.

Chenoweth SF, Blows MW (2008) Q_{ST} meets the **G** matrix: the dimensionality of adaptive divergence in multiple correlated quantitative traits. *Evolution*, **62**, 1437–1449.

Cheverud JM, Routman EJ (1995) Epistasis and its contribution to genetic variance-components. *Genetics*, **139**, 1455–1461.

Cheverud JM, Ehrich TH, Vaughn TYT, Koreishi SF, Linsey RB, Pletscher LS (2004) Pleiotropic effects on mandibular morphology II: differential epistasis and genetic variation in morphological integration. *Journal of Experimental Zoology Part B-Molecular and Developmental Evolution*, **302B**, 424–435.

Chun YJ, Le Corre V, Bretagnolle F (2009a) Adaptive divergence for a fitness-related trait among invasive *Ambrosia artemisiifolia* populations in France. *Molecular Ecology*, **20**, 1378–1388.

Chun YJ, Nason JD, Moloney KA (2009b) Comparison of quantitative and molecular genetic variation of native vs. invasive populations of purple loosestrife (*Lythrum salicaria* L., Lythraceae). *Molecular Ecology*, **18**, 3020–3035.

Debat V, David P (2001) Mapping phenotypes: canalization, plasticity and developmental stability. *Trends in Ecology & Evolution*, **16**, 555–561.

Delzon S, Douthe C, Sala A, Cochard H (2010) Mechanism of water-stress induced cavitation in conifers: bordered pit structure and function support the hypothesis of seal capillary-seeding. *Plant, Cell & Environment*, **33**, 2101–2111.

Demont M, Blanckenhorn WU, Hosken DJ, Garner TWJ (2008) Molecular and quantitative genetic differentiation across Europe in yellow dung flies. *Journal of Evolutionary Biology*, **21**, 1492–1503.

DeWoody AJ, Bickham WJ, Nichols MK, Rhodes OEJ, Woeste EW (2010) *Molecular Approaches in Natural Resource Conservation and Management* (ed. Press CU), p. 374. Cambridge University Press, Cambridge.

Edeelar P, Björklund M (2011) If F_{ST} does not measure neutral genetic differentiation, then comparing it with Q_{ST} is misleading. Or is it ? *Molecular Ecology*, **20**, 1805–1812.

Edmands S, Harrison JS (2003) Molecular and quantitative trait variation within and among populations of the intertidal copepod *Tigriopus californicus*. *Evolution*, **57**, 2277–2285.

Eroukhmanoff F, Hargeby A, Svensson EI (2009) Rapid adaptive divergence between ecotypes of an aquatic isopod inferred from F_{ST}-Q_{ST} analysis. *Molecular Ecology*, **18**, 4912–4923.

Falconer DS, Mackay TFC (1996) Introduction to quantitative genetics. Introduction to quantitative genetics., xv + 464 pp.

Felix MA, Wagner A (2008) Robustness and evolution: concepts, insights and challenges from a developmental model system. *Heredity*, **100**, 132–140.

Flatt T (2005) The evolutionary genetics of canalization. *Quarterly Review of Biology*, **80**, 287–316.

Galpern P (2000) The use of common principal component analysis in studies of phenotypic evolution: An example from the Drosophilidae, PhD Thesis, University of Toronto, Canada.

Gilchrist AS, Partridge L (2001) The contrasting genetic architecture of wing size and shape in Drosophila melanogaster. *Heredity*, **86**, 144–152.

Goudet J, Buchi L (2006) The effects of dominance, regular inbreeding and sampling design on Q_{ST}, an estimator of population differentiation for quantitative traits. *Genetics*, **172**, 1337–1347.

Goudet J, Martin G (2007) Under neutrality, Q_{ST}<=F_{ST} when there is dominance in an island model. *Genetics*, **176**, 1371–1374.

Gould SJ, Lewontin R (1979) Spandrels of San-Marco and the Panglossian paradigm – A critique of the adaptationist program. *Proceedings of the Royal Society of London Series B-Biological Sciences*, **205**, 581–598.

Guillaume F (2011) Migration-induced phenotypic divergence: the migration-selection balance of correlated traits. *Evolution*, **65**, 1723–1738.

Hansen TF (2006) The evolution of genetic architecture. *Annual Review of Ecology Evolution and Systematics*, **37**, 123–157.

Hansen TF, Houle D (2004) Evolvability, stabilizing selection, and the problem of stasis. In: *Evolutionary Biology of Complex Phenotypes* (eds Pigliucci M, Preston K), pp. 130–150. Oxford University Press, Oxford.

Hansen TF, Wagner GP (2001a) Epistasis and the mutation load: a measurement-theoretical approach. *Genetics*, **158**, 477–485.

Hansen TF, Wagner GP (2001b) Modeling genetic architecture: a multilinear theory of gene interaction. *Theoretical Population Biology*, **59**, 61–86.

Hermisson J, Hansen TF, Wagner GP (2003) Epistasis in polygenic traits and the evolution of genetic architecture under stabilizing selection. *American Naturalist*, **161**, 708–734.

Hill WG, Goddard ME, Visscher PM (2008) Data and theory point to mainly additive genetic variance for complex traits. *PLoS Genetics*, **4**, e1000008.

Kawecki TJ (2000) The evolution of genetic canalization under fluctuating selection. *Evolution*, **54**, 1–12.

Kingsolver JG, Hoekstra HE, Hoekstra JM *et al*. (2001) The strength of phenotypic selection in natural populations. *The American Naturalist*, **157**, 245–261.

Kinnison MT, Unwin MJ, Quinn TP (2008) Eco-evolutionary vs. habitat contributions to invasion in salmon: experimental evaluation in the wild. *Molecular Ecology*, **17**, 405–414.

Kohn HJ, Shapiro J, Wu C-I (2008) Decoupled differentiation of gene expression and coding sequence among *Drosophila* populations. *Genes, Genetics and Systematics*, **83**, 265–273.

Kremer A, Le Corre V (2012) Decoupling of differentiation between traits and their underlying genes in response to divergent selection. *Heredity*, **108**, 375–385.

Kremer A, Zanetto A, Ducousso A (1997) Multilocus and multitrait measures of differentiation for gene markers and phenotypic traits. *Genetics*, **145**, 1229–1241.

Kronholm I, Loudet O, de Meaux J (2010) Influence of mutation rate on estimators of genetic differentiation - lessons from *Arabidopsis thaliana*. *BMC Genetics*, **11**, 18.

Kruuk LEB, Slate J, Wilson AJ (2008) New answers for old questions: the evolutionary quantitative genetics of wild animal populations. *Annual Review of Ecology Evolution and Systematics*, **39**, 525–548.

Lamy J-B, Bouffier L, Burlett R, Plomion C, Cochard H, Delzon S (2011) Uniform selection as a primary force reducing population genetic differentiation of cavitation resistance across a species range. *PLoS ONE*, **6**, e23476.

Lande R (2009) Adaptation to an extraordinary environment by evolution of phenotypic plasticity and genetic assimilation. *Journal of Evolutionary Biology*, **22**, 1435–1446.

Lande R, Arnold SJ (1983) The measurement of selection on correlated characters. *Evolution*, **37**, 1210–1226.

Le Corre V, Kremer A (2003) Genetic variability at neutral markers, quantitative trait loci and trait in a subdivided population under selection. *Genetics*, **164**, 1205–1219.

Le Corre V, Kremer A (2012) The genetic differentiation at quantitative trait loci under local adaptation. *Molecular Ecology*, **21**, 1548–1566.

Lee CE, Frost BW (2002) Morphological stasis in the *Eurytemora affinis* species complex (Copepoda: Temoridae). *Hydrobiologia*, **480**, 111–128.

Leinonen T, O'Hara RB, Cano JM, Merila J (2008) Comparative studies of quantitative trait and neutral marker divergence: a meta-analysis. *Journal of Evolutionary Biology*, **21**, 1–17.

Liang ZC, Huang P, Yang J, Rao GY (2009) Population divergence in the amphicarpic species *Amphicarpaea edgeworthii* Benth. (Fabaceae): microsatellite markers and leaf morphology. *Biological Journal of the Linnean Society*, **96**, 505–516.

Lind MI, Ingvarsson PK, Johansson H, Hall D, Johansson F (2010) Gene flow and selection on phenotypic plasticity in an island system of *Rana temporaria*. *Evolution*, **65**, 684–697.

Lopez-Fanjul C, Fernandez A, Toro MA (2003) The effect of neutral nonadditive gene action on the quantitative index of population divergence. *Genetics*, **164**, 1627–1633.

Lynch M, Walsh B (1998) Genetics and analysis of quantitative traits. In: *Genetics and analysis of quantitative traits*., p. xvi + 980 pp. Sinauer Associates, Inc.

Maherali H, Pockman WT, Jackson RB (2004) Adaptive variation in the vulnerability of woody plants to xylem cavitation. *Ecology*, **85**, 2184–2199.

Manu, Surkova S, Spirov AV *et al.* (2009) Canalization of gene expression in the Drosophila blastoderm by gap gene cross regulation. *PLoS Biology*, **7**, 0591–0603.

Martin G, Chapuis E, Goudet J (2008) Multivariate Q_{ST}-F_{ST} comparisons: a neutrality test for the evolution of the G matrix in structured populations. *Genetics*, **180**, 2135–2149.

McKay JK, Latta RG (2002) Adaptive population divergence: markers, QTL and traits. *Trends in Ecology & Evolution*, **17**, 285–291.

Meirmans PG, Philip WH (2011) Assessing population structure: F_{ST} and related measures. *Molecular Ecology*, **11**, 5–18.

Merilä J, Crnokrak P (2001) Comparison of genetic differentiation at marker loci and quantitative traits. *Journal of Evolutionary Biology*, **14**, 892–903.

Meyer C-L, Kostecka A, Saumitou-Laprade P *et al.* (2009) Variability of zinc tolerance among and within populations of the pseudometallophyte *Arabidopsis halleri* and possible role of directional selection. *New Phytologist*, **185**, 130–142.

Miller JR, Wood BP, Hamilton MB (2008) F_{ST} and Q_{ST} under Neutrality. *Genetics*, **180**, 1023–1037.

Navarro C, Cavers S, Pappinen A *et al.* (2005) Contrasting quantitative traits and neutral genetic markers for genetic resource assessment of Mesoamerican *Cedrela odorata*. *Silvae Genetica*, **54**, 281–292.

O'Hara RB, Merila J (2005) Bias and precision in Q_{ST} estimates: problems and some solutions. *Genetics*, **171**, 1331–1339.

Olivieri I, Singer CM, Magalhães S *et al.* (2008) Genetic, ecological, behavioral and geographic differentiation of populations in a thistle weevil: implications for speciation and biocontrol. *Evolutionary Applications*, **1**, 112–128.

Ovaskainen O, Karhunen M, Zheng C, Cano Arias JM, Merilä J (2011) A new method to uncover signatures of divergent and stabilizing selection in quantitative traits. *Genetics*, **189**, 621–U729.

Pujol B, Wilson AJ, Ross RIC, Pannell JR (2008) Are Q_{ST}-F_{ST} comparisons for natural populations meaningful? *Molecular Ecology*, **17**, 4782–4785.

Ramírez-Valiente JA, Lorenzo Z, Soto A, Valladares F, Gil L, Aranda I (2009) Elucidating the role of genetic drift and natural selection in cork oak differentiation regarding drought tolerance. *Molecular Ecology*, **18**, 3803–3815.

Santure AW, Ewen JG, Sicard D, Roff DA, Moller AP (2010) Population structure in the barn swallow, *Hirundo rustica*: a comparison between neutral DNA markers and quantitative traits. *Biological Journal of the Linnean Society*, **99**, 306–314.

Scheepens JF, Stocklin J, Pluess AR (2010) Unifying selection acts on competitive ability and relative growth rate in *Scabiosa columbaria*. *Basic and Applied Ecology*, **11**, 612–618.

Spitze K (1993) Population structure in *Daphnia obtusa*: quantitative genetic and allozymic variation. *Genetics*, **135**, 367–374.

Stearns S (1994) The evolutionary links between fixed and variable traits. *Acta Palaenotologica Polonica*, **38**, 215–232.

Stearns SC, Kawecki TJ (1995) Fitness sensitivity and the canalization of life-history traits. *Evolution*, **48**, 1438–1450.

Turelli M (1984) Heritable genetic variation via mutation-selection balance: Lerch's zeta meets the abdominal bristle. *Theoretical and Population Biology*, **25**, 138–193.

Visscher PM (2008) Sizing up human height variation. *Nature genetics*, **40**, 489–490.

de Visser JAGM, Hermisson J, Wagner GP *et al.* (2003) Perspective: evolution and detection of genetic robustness. *Evolution*, **57**, 1959–1972.

Vonlanthen P, Roy D, Hudson AG, Largiadèr CR, Bittner D, Seehausen O (2009) Divergence along a steep ecological gradient in lake whitefish (*Coregonus sp.*). *Journal of Evolutionary Biology*, **22**, 498–514.

Waddington CH (1942) Canalization of development and the inheritance of acquired characters. *Nature*, **150**, 563–565.

Waddington CH (1953) Epigenetics and evolution. *Journal of Experimental Zoology*, **7**, 187–199.

Wagner GP, Zhang JZ (2011) The pleiotropic structure of the genotype-phenotype map: the evolvability of complex organisms. *Nature Reviews Genetics*, **12**, 204–213.

Wagner GP, Booth G, Bagheri HC (1997) A population genetic theory of canalization. *Evolution*, **51**, 329–347.
Wagner GP, Kenney-Hunt JP, Pavlicev M, Peck JR, Waxman D, Cheverud JM (2008) Pleiotropic scaling of gene effects and the "cost of complexity". *Nature*, **452**, 470–U9.
Weedon MN, Frayling TM (2008) Reaching new heights: insights into the genetics of human stature. *Trends in genetics*, **24**, 595–603.
Whitlock MC (1999) Neutral additive genetic variance in a metapopulation. *Genetical Research*, **74**, 215–221.
Whitlock MC (2008) Evolutionary inference from Q_{ST}. *Molecular Ecology*, **17**, 1885–1896.
Whitlock MC (2011) G'_{ST} and D do not replace F_{ST}. *Molecular Ecology*, **20**, 1083–1091.
Whitlock MC, Guillaume F (2009) Testing for spatially divergent selection: comparing Q_{ST} to F_{ST}. *Genetics*, **183**, 1055–1063.
Williams GC (1992) *Natural Selection: Domains, Levels and Challenges*. Oxford University Press, USA.
Wortemann R, Herbette S, Barigah TS *et al.* (2011) Genotypic variability and phenotypic plasticity of cavitation resistance in *Fagus sylvatica* L. across Europe. *Tree physiology*, **31**, 1175–1182.
Yoshida Y, Honjo M, Kitamoto N, Ohsawa R (2008) Genetic variation and differentiation of floral morphology in wild *Primula sieboldii* evaluated by image analysis data and SSR markers. *Breeding Science*, **58**, 301–307.
Yoshida Y, Honjo M, Kitamoto N, Ohsawa R (2009) Reconsideration for conservation units of wild *Primula sieboldii* in Japan based on adaptive diversity and molecular genetic diversity. *Genetics Research*, **91**, 225–235.
Zhang X-S (2006) The phenotypic variance within plastic traits under migration-mutation-selection balance. *Evolution*, **60**, 1125–1136.

J.-B.L.'s interests are centered on the processes that drive or limit adaptation, population differentiation, in order to quantify adaptive capacities of tree species.

C.P.'s interests are centered on combining different approaches (genomics, quantitative and population genetics, ecology) for understanding the interplay between genetic adaptation, plasticity and their interaction in the response of forest trees to past, present and future edapho-climatic conditions.

A.K.'s interests are centered on the evolution of genetic diversity and differentiation between natural populations, at various hierarchical levels where diversity is expressed (from genes to phenotypic traits). The main emphasis of my research activities is the understanding of evolutionary forces that contribute to the distribution of diversity and differentiation.

S.D.'s interests are centered on the processes that drive the evolution of ecophysiological traits and the adaptation of populations, with a particular interest in drought resistance, tree hydraulic and leaf phenology.

doi: 10.1111/mec.12017

Data accessibility

All the data used in this study have been provided as supplementary material.

Supporting information

Additional Supporting Information may be found in the online version of this article.

Table S1 Synopsis of comparative studies of marker and quantitative genetic population structure (based on and updated from Leinonen *et al.* (2008).

Table S2 The full length dataset.

Genotypic and environmental variation in cavitation resistance in a pine species transplanted in wet and dry provenance tests

Jean-Baptiste Lamy[1,2,3,4], Sylvain Delzon[1,2], Pauline Bouche, Ricardo Alia[4], Giovanni Giuseppe Vendramin[5], Christophe Plomion[1,2], Hervé Cochard[3,4].

[1] INRA, UMR 1202 BIOGECO, F-33610 Cestas, France

[2] Univ. Bordeaux, UMR 1202 BIOGECO, F-33400 Talence, France.

3 INRA, UMR547 PIAF, F-63100 Clermont-Ferrand, France

4 Clermont Université, Université Blaise Pascal, UMR547 PIAF, BP 10448, F-63000 Clermont-Ferrand, France

[4] Departamento de Sistemas y Recursos Forestales, CIFOR — INIA, Carretera de La Coruña km 7.5, 28040 Madrid, Spain

[5] Instituto di Genetica Vegetale, Sezione di Firenze, Consiglio Nazionale delle Ricerche, via Madonna del Piano 10, 50019 Sesto Fiorentino (FI), Italy

Author for correspondence: Hervé Cochard,
Phone: + 033 (0)473624471
Email: cochard@clermont.inra.fr

For submission to: **New-phytologist**
Total word count: 5564
Number of figures: 4
Number of tables: 4
Number of supplementary tables: 2
Number of supplementary figures: 1

Running title: Intraspecific variation of cavitation resistance

Abstract

- Cavitation resistance is one of the best proxy of tree survival to severe drought. The interspecific variation of this trait is well known, but data at intraspecific level remains scare. Quantifying genetic variation and phenotypic plasticity is therefore critical to estimate the adaptive potential of these perennial organisms in the context of climate change .
- Combining for the first time the *in situ* characterization of natural populations with common garden experiments in xeric and mesic sites, we estimated variance components (genetic G, environmental E, and GxE) of resistance to cavitation based on 506 genotypes of *Pinus pinaster*.
- Surprisingly, resistance to cavitation displayed low phenotypic (CV_P<7%) and genetic (CV_A=4.9%) variances and limited phenotypic plasticity compared to height growth.
- This pattern of variation strongly suggests resistance to cavitation is buffered against environmental and genetic variations. The underlying evolutionary mechanisms are discussed.

Key words: Drought tolerance, cavitation resistance, provenance-progeny trial, *Pinus pinaster*, hydraulic physiology, phenotypic plasticity, genetic variation, Q_{ST}/F_{ST} comparison.

Introduction

Terrestrial plants need to absorb water to replace the evaporation that occurs while atmospheric CO_2 is diffusing into photosynthetic tissues. This constraint has shaped plant structure and functioning since they have colonised emerged lands and can explain the evolution of plant tissues to achieve efficient water transport (such as hydroids, tracheids, vessels) and to regulate water flow (stomata) (Sperry, 2003; Pittermann, 2010). The evolution of the hydraulic system from hydroids to vessels reflects a trade-off between hydraulic safety (resistance to cavitation) and hydraulic efficiency (maximum conductance). Plants have since been able to adapt to the natural climatic fluctuations and to colonize most of the arid places in the world. However, given the recent abnormal increase in world average temperature and the frequency of extreme climatic events (Beniston et al., 2007; Della-Marta & Beniston, 2008), the rate of natural adaptation may no longer follow the rate of climate change (Bréda, 2006; Riou-Nivert et al., 2008; Bréda & Badeau, 2008; Lindner et al., 2010). Indeed several authors noticed that recent forests die-back could be linked to a severe drought event (Allen & Breshears, 1998; Breshears et al., 2005; Bréda et al., 2006; Granier et al., 2007; Allen, 2009; Allen et al., 2010). In this context, an effort should be made to quantify and then improve drought tolerance of domesticated and natural plant species (Allen & Breshears, 1998) to ensure the maintenance of economic and ecological services.

Due to the complex nature of most quantitative traits and the cost of phenotyping, researchers should select crucial trait(s) for drought tolerance (Houle, 2009, 2010). This is particularly true for drought tolerance which encompasses multiple dimensions, with involves various morphological and physiological responses difficult to assess. Usually, to circumvent these obstacle agronomists use a series of morphological traits, such as the leaf rolling delay in *Zea*

mays (Dhanda et al., 2004; Blum, 2009a), or a more easy to measure and cost effective physiological trait such as carbon isotope composition to trace the ratio of carbon assimilation and transpiration (Brendel et al., 2002, 2008; Cumbie et al., 2011). However, these above-mentioned traits are related to growth maintenance during moderate drought rather than survival during and after extreme drought (Blum, 2009b). It is now time to pay attention on traits clearly related to drought survival.

The importance of cavitation resistance in plant physiology under drought is grounded by several lines of evidence: (i) Thank to experimental drought and recovery monitoring Brodribb & Cochard, (2009) and Brodribb et al., (2010) demonstrated a good correlation between the tree lethal water potential and its cavitation resistance (i.e. in conifers, 50% loss of conductance in the seedling stem lead to death by dehydration, r= 0.9), more cavitation resistant species survived to stronger drought, (ii) In average, species from drier climates are more cavitation resistant compared to species from wetter climates (Maherali et al., 2004). (iii) Tyree et al., (1994) and Rood et al., (2000) related massive branch die-back in *Populus deltoides* and *P. fremontii* to extensive events of cavitation in tree's limb. Cavitation resistance is therefore the best proxy for tree drought tolerance, still no extensive dataset exist nowadays, even less at the intra-specific level.

Along the course of evolution, adaptation to the changing environment is possible through at least, two non-exclusives mechanisms: genetic diversity and phenotypic plasticity:

(i) Genetic diversity can be seen as a pool of variants among which natural selection keeps the fittest. Indeed genetic diversity is the necessary fuel for genetic adaptation. Such diversity appears naturally with time by the interplay of evolutionary forces (migration, genetic drift, natural selection, recombination and mutation). To cope with the rapid rate of current climate change, human actions can also enhance genetic adaptation through the increase of genetic

diversity (artificial mutation, transgenesis, assisted migration) (Scotti, 2010). An other condition is needed to be targeted by natural selection, the strong correlation between the studied trait and fitness. Based on the previous arguments, we assumed that cavitation resistance is the best available and fitness related-trait to trace survival during extreme droughts. The variation of cavitation resistance has been extensively studied between species (Maherali et al., 2004; Delzon et al., 2010), although estimates of the amount of genetic variation are still scarce. Three recent studies have assessed the genetic variation of cavitation resistance for *Pinus Pinaster* and *Fagus sylvatica* (Lamy et al., 2011; Corcuera et al., 2011; Wortemann et al., 2011). Overall, cavitation resistance has a low phenotypic variation, (coefficient of variation is less than 10%) and most part of the genetic variation resides within each population, the variation between populations being very low or null. Lamy et al (2011) have proposed that cavitation resistance is a canalized trait in *Pinus pinaster*. In other words, the average value of this trait is the same for populations from contrasted climates; in other words this trait seems to be robust to genetic and environmental perturbations.

(ii) Phenotypic plasticity is a second component of adaptation. A genotype expresses a given phenotypic value in a given environment. Phenotypic plasticity could be dissected in two parts, first, the reaction norms is the function (linear, quadratic or sigmoid) that links the phenotypic changes to the environmental changes; second it is the genetic variability of the reaction norm, also called genotype by environment interaction (Debat & David, 2001). Indeed, like any other trait, reaction norms can evolve in response to environmental pressures. The genotype by environment interaction is of major concern in the attempt to develop adapted crop plants to wide geographical ranges. It is also of considerable concern for undomesticated species because it provides clues to understand mechanisms that have shaped local adaptation. The term “phenotypic plasticity” can be found in most of the discussion section of papers dealing with ecological implication of cavitation resistance variation; but

they consider qualitative estimations (K.J. Kolb & Sperry, 1999; Maherali & DeLucia, 2000; Maherali et al., 2002; Jacobsen et al., 2007; Martinez-Vilalta et al., 2009; Beikircher & Mayr, 2009). These speculations are based on the discrepancy between phenotypic variation (cavitation resistance assessed *in situ*) and genetic variation (cavitation resistances assessed in provenance trials). Some authors stated that there is a lot of phenotypic plasticity for cavitation resistance while others stated the opposite. Clearly, a definitive conclusion could only be drawn out of a larger amount of studies regarding phenotypic plasticity but as far as we know there are only two quantitative estimation of phenotypic plasticity for cavitation resistance (Corcuera et al., 2011; Wortemann et al., 2011). Therefore a major concern is to quantify the relative amount of genetic variation and phenotypic plasticity in the variation of tree drought resistance.

We carried out a case study on maritime pine (*Pinus pinaster* Ait.), a tree species with a fragmented distribution in the western part of the Mediterranean region. The scattered distribution of this species may have prevented or limited gene flow between different groups of populations, promoting high levels of genetic divergence between ecotypes due to genetic drift (M. M. Ribeiro, LeProvost, et al., 2002; M. M. Ribeiro, Mariette, et al., 2002) and/or natural selection (Quezel and Barbero 1998 in (Richardson, 1998)). We screened 506 six-year-old trees from six populations from the most contrasted climatic provenances using two twin provenance-progeny trials, with contrasting water availability conditions and sampling in *in situ* natural populations. The aims of this study were: (i) to quantify the magnitude of the phenotypic variation of cavitation resistance traits in natural populations, (ii) to study the determinism of these traits by quantifying both the genetic variation and the phenotypic plasticity (iii) the correlation between cavitation resistance and climatic variable.

Table 1. Climatic data, location, elevation, soil and genetic information of each selected populations and eachprovenance-progeny trials

Populations	Longitude (°)	Latitude (°)	*n*	Elevation (m)	P_i (mm)	T_m (°C)	VPD_{max} (hPa)	*ETP* (mm)	*Mito*	*Chloro*
Bayubas de Abajo (Spain)	-2.87	41.52	37- 182	955	561	10.5	11.42	882.9	*W*	a
Coca (Spain)	-4.08	41.37	37- 122	788	452	11.9	14.23	718.7	*W*	a
Mimizan (France)	-1.30	44.13	38- 154.5	37	1176	13.2	7.26	751.59	*W*	a
Oria (Spain)	-2.62	37.87	32- 155.5	1232	451	13.4	14.29	922.59	*W*	j
San Cipriano (Spain)	-8.70	42.13	35- 114	310	1625	13.8	8.54	721.91	*W*	g
Tamrabta (Morocco)	-5.02	33.66	38- 113	1760	550	15.1	18.56	976.54	*M*	k

Trials	Longitude (°)	Latitude (°)	*n*	Elevation (m)	P_i (mm)	T_m (°C)	VPD_{max} (hPa)	*ETP* (mm)	Soil
Dry, Calcena (Spain)	-1.72	41.62	196-1857	997	452	11.1	11.1	778.2	Shaly sandstone
Wet, Cestas (France)	-0.78	44.74	240-5569	61	800	12.7	6.70	743.8	Sandy podzol

n, number of individuals for cavitation resistance and tree height traits, respectively; P_i , mean annual precipitation; T_m, mean annual air temperature; VPD_{max}, maximal of water vapor pressure deficit (in July for all provenances); *ETP*, annual sum of potential evapotranspiration. *Mito* and *chloro* corresponds to the most frequent chloroplastic and mitochondrial haploptype bearing by the populations (Burban & Petit, 2003).

Material and Methods

Provenance trial

We established a replicated provenance-progeny trial (i.e. same families of the same populations, Figure 1): in Calcena (Spain, Aragon, 41° 3'N, 01°43'W) hereafter called the "dry" trial, and in Cestas (France, Aquitaine, 44°44'N, 00°46'W) called the "wet" trial (see Table 1 and Figure 2). Seedlings were grown in a nursery from open-pollinated seeds collected from 24 natural populations (or ecotypes) in France, Spain, Morocco, Italy and Tunisia, to cover the fragmented distribution of *Pinus pinaster*. Each population was represented by 20 to 30 half-sib families. Each trial was planted using an incomplete randomized block design (a multi-tree plot in the dry trial and a single tree plot in the wet trial). The wet trial was planted in winter 2003 and the dry trial in winter 2004 (Eveno, 2008), respectively. In both trials, trees were 6 old years at the time of cavitation resistance assessment (2009 and 2010 respectively).

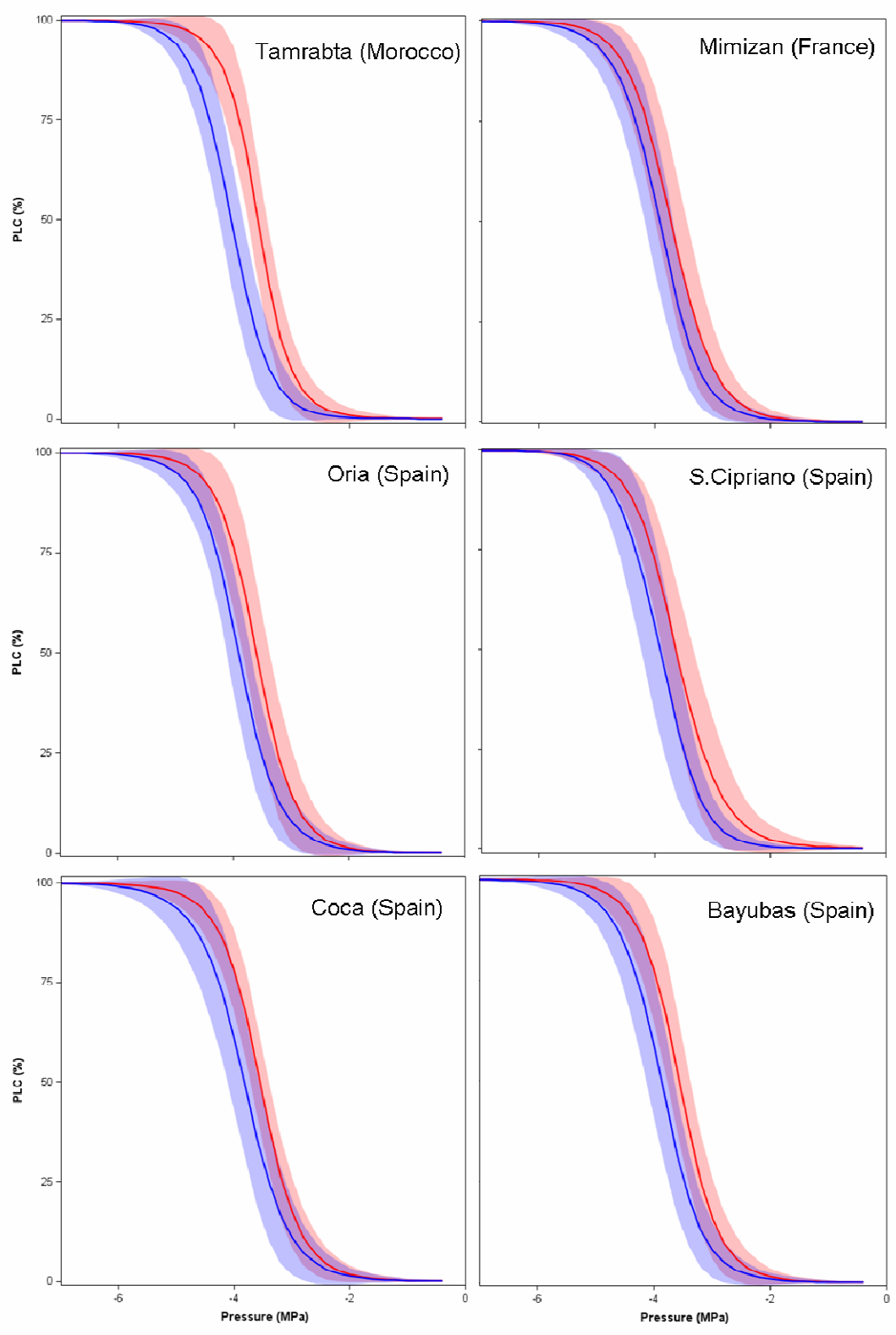

Fig. 1 Mean vulnerability curves for each of the 6 populations in each trial (wet and dry, n=36±1). The shaded band represents the standard deviation. In red, mean vulnerability curve for the dry trial. In blue, mean vulnerability curve for the wet trial.

Selection of populations

We designed a procedure for selecting 6 populations representing the extreme range of the climatic envelope of maritime pine. For a total of 754 grid points covering the entire natural range of the species (Gabriele Bucci et al., 2007) we first extracted climatic data from the CRU CL 2.0 10' global dataset for the period 1961-1990 (New et al., 1999, 2000, 2002). These data included monthly precipitation, mean, minimum and maximum temperature, diurnal temperature range, water vapor pressure, cloud cover, wet day frequency, ground frost frequency, mean global radiation, mean wind speed, Martonne index, Turc's potential evapotranspiration and soil water deficit. We also derived the air vapor pressure deficit from these parameters (H.G. Jones, 1992). A principal component analysis (PCA) was then used to reduce the number of dimensions (14 climatic variables * 12 months) for the whole set of climate variables (Figure 2). The data were centered and scaled prior to PCA. All the populations available in the provenance-progeny trials were finally placed on the main plane of the PCA (accounting for 70% of the variation) and six of these populations were selected to cover the climatic envelope covered by *Pinus pinaster* (Table 1). In addition, to their distribution over the whole climatic range, we selected populations bearing different mitochondrion and chloroplastic haplotypes, a good proxy of contrasted evolutionary history using genetic maps (Gabriele Bucci et al., 2007) and literature (Vendramin et al., 1998; Burban & Petit, 2003).

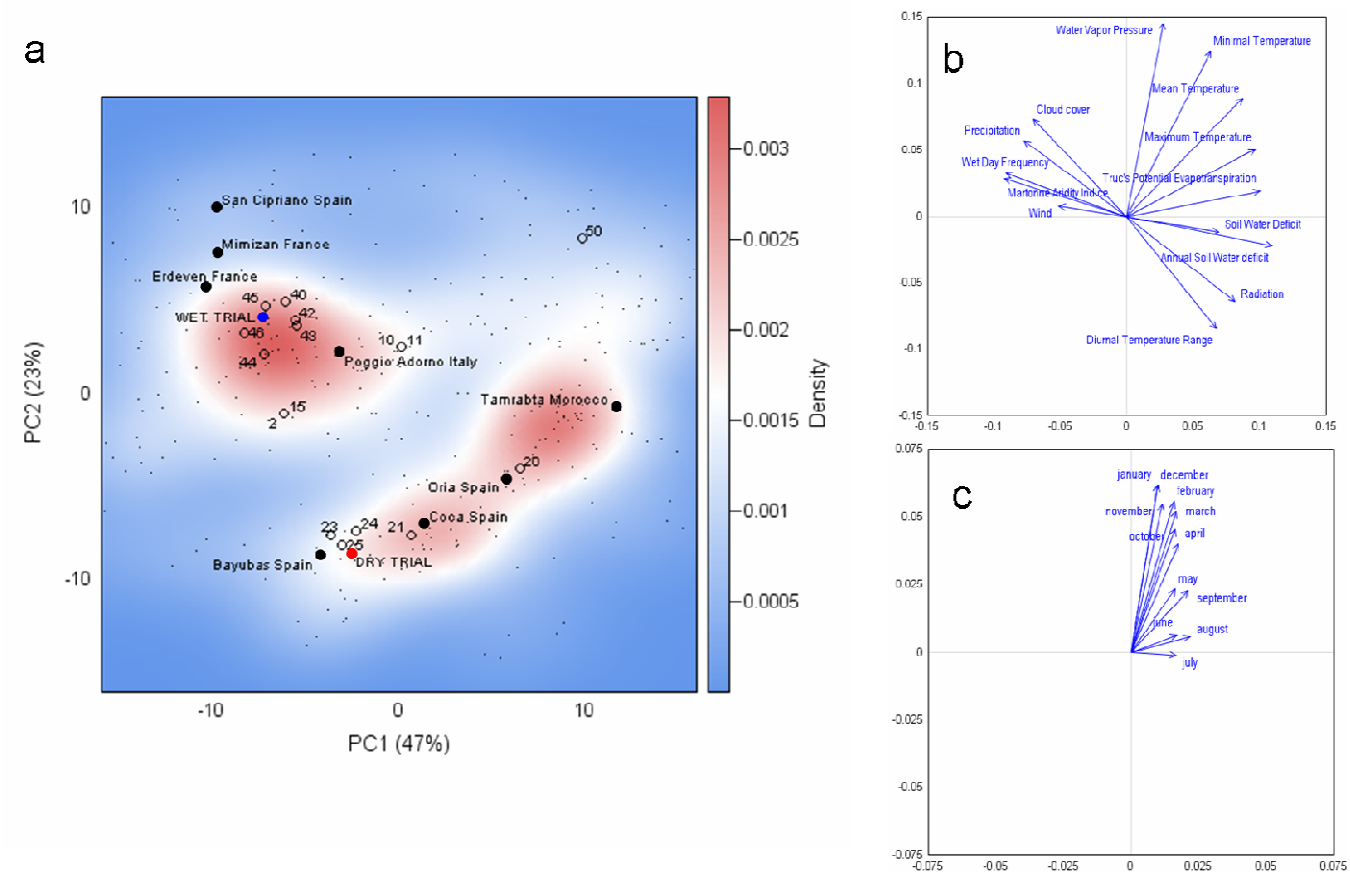

Fig. 2 Principal component analysis (PCA) based on 769 population locations x 168 monthly derived climatic variables. (a) Main plain (PC1 and PC2) with a contour plot representing the presence's probability (kernel density estimate) of *Pinus pinaster* populations (small black dots) within the bioclimatic envelope. Red and blue colour means respectively high and low probability of presence of *Pinus pinaster* populations within the bioclimatic envelope. PC1 and PC2 account for 47% and 23% of the variance, respectively. PC1 can be interpreted as an aridity index and PC2 as a continentality index (see results section).

- Open circles ID correspond to the populations studied for growth traits in the twin provenance-progeny trial as follows: #2: Restonica, Corsica; #10: Aullène, Corsica; #11: Pineta, Corsica; #15: Pinia, Corsica; #21: Arenas de San Pedro, Spain; #23: Cuellar, Spain; #24: Valdemaqueda, Spain; #25: San Leonardo de Yagüe, Spain; #40: Petrock, France; #42: Hourtin, France; #43: Le Verdon, France; #44: Olonne sur mer, France; #45: Saint Jean de Monts, France; #46: Pleucadec, France; #50, Tabarka, Tunisia (geographical coordinates as available in supplementary file).
- Closed black dots labelled with a lower case text correspond to i/ populations selected for cavitation resistance and growth traits analyses in the RPPT, as well as ii/ natural populations sampled *in situ*.
- Coloured dots are the RPPT, red for the "dry" provenance-progeny test (Calcena, Spain) and blue for "wet" provenance-progeny test (Cestas, France).

PCA was performed with the variables indicated in the material and methods section. Because of the high number of climatic variables (168), we provide two correlation circles (b) shows the averaged eigenvectors for each category of climatic variable, and (c) displays the eigenvectors averaged by month.

Sampling in provenance-progeny trials and in situ natural populations

In both provenance-progeny trials, we randomly sampled eight families per population with at least one half-sib on each block (6 populations/8 families/5-4 blocks) (see table 1). To assess phenotypic variation for *in situ* natural populations, we used a simplified sampling with 11 individuals per site (66 genotypes in total) spaced by at least 50m to avoid genetic autocorrelations due to relatedness between individuals (González-Martínez et al., 2003). On the same trees, we also measured collar diameter (electronic calipper, mm), total height (instrument, m), determine tree age (counting stem's whorl) and harvested two branches per individuals for cavitation resistance measurements on the two last growth units (see cavitation resistance and height growth trait section).

Cavitation resistance and height growth

To assess the variation of cavitation resistance, we established the whole vulnerability curve for each of the 506 genotypes (see figure 1). Vulnerability curves were based on the Cavitron technique as described previously in (Cochard, 2002; Cochard et al., 2005). Measurements were performed at the high-throughput phenotyping platform for hydraulic traits (CaviPlace, University of Bordeaux, Talence, France) using a custom-built honeycomb rotor (SamPrecis 2000, Bordeaux, France) mounted on a Sorvall RC5 ultra-centrifuge (Thermo Fisher Scientific, Munich, Germany). Samples were kept refrigerated and vulnerability to cavitation was determined within two weeks of collection. All samples were debarked to avoid resin exudation, re-cut under water to a standard length of 27 cm, and both ends were trimmed with a fresh razor blade to obtain perfectly smooth surfaces with open tracheids. A solution of

ultrapure and degassed water including 10 mM KCl and 1 mM $CaCl_2$ was used as reference solution for hydraulic measurements. After measuring the maximum hydraulic conductance under low (i.e., close to zero) xylem pressure (*P*), the rotation speed of the centrifuge was gradually increased by 0.5 MPa to determine the percentage loss of hydraulic conductance (*PLC*). The rotor velocity was monitored with a 10 rpm resolution electronic tachymeter (A2108-LSR232, 202 Compact Inst, Bolton, UK) and the xylem pressure was adjusted to about ± 0.02 MPa. We used Cavi_soft software (version 1.5, University of Bordeaux) for conductance measurements and the computation of all vulnerability curves, which were adjusted according to (Pammenter & Vander Willigen, 1998). The P_{50} (MPa) value was defined as the pressure corresponding to 50% PLC. S_{50} was defined as the slope (% MPa^{-1}) of a tangent at the inflexion point (P_{50}) and corresponds to the speed of cavitation spread.

To compare growth performance between trials and *in situ* natural stands, we used tree height at four years old (*h* m) corresponding to years 2008 for the dry trial and 2007 for the wet trial. For *in situ* natural populations, we estimated the height at four by dividing the height by the actual age (we obtained an average annual increment) and then multiply by four.

Single site analysis

We used the following mixed model which is robust enough to handle non normality and unbalanced data:

$$\mathbf{y = Xb + Z_0 block + Z_1 pop + Z_2 f + \varepsilon} \quad (1)$$

where ***y*** is the vector of observation for a trait, **b** is the vector of fixed mean effects, **block** is the vector of random block effects, **pop** is the vector of random population effects, **f** is the vector of the random genetic effects of mother trees within the population, **ε** is the vector of residuals, **X** is called the design matrix, $\mathbf{Z_0}$, $\mathbf{Z_1}$ and $\mathbf{Z_2}$ are the incidence matrices linking the observations to the effects. A variance was fitted for each random effect: σ^2_{pop} is the genetic

variance between populations, $\sigma^2_{f(pop)}$ is the genetic variance between mother trees nested within a population and ε is the vector of residuals. Residuals were assumed to be independent ($\boldsymbol{R} = \sigma^2_e \boldsymbol{I}$). However, there are some spatial autocorrelations in field trial due to soil and microclimatic effects between individuals. To avoid a biased estimation of variance components, we used a covariance structure that assumes separable first-order autoregressive processes in rows and columns with spatially dependant and independent error variances (Dutkowski et al., 2002, 2006). Spatially explicit model were performed only for *h* because P_{50} data were spatially too sparse (see table 2).

Variance or covariance components were estimated by the restricted maximum likelihood method, assuming a normal distribution of the random effects. The significance of variance components were tested using log-likelihood ratio tests. We included population as a random effect to draw inference at the species level and to obtain an unbiased estimate of heritability and genetic population differentiation (Wilson, 2008). The normality, identity and independency of residuals of each trait were graphically checked by plotting studentized marginal and conditional residuals, which confirmed that the data match with the assumption of mixed model.

Multisite analysis

We used the following mixed model to analyze the whole data set:

$$\boldsymbol{y} = \boldsymbol{X}site + \boldsymbol{Z}_0 block + \boldsymbol{Z}_1 pop + \boldsymbol{Z}_2 site.pop + \boldsymbol{Z}_3 f + \boldsymbol{Z}_4 site.f + \boldsymbol{\varepsilon} \quad (2)$$

where ***y*** is the vector of observation for a trait, ***site*** is the vector of fixed site effects, ***block*** is the vector of random block effects, ***pop*** is the vector of random population effects, ***site.pop*** the vector of random population by site effects, ***f*** is the vector of the random genetic effects of mother trees within the population, ***site.f*** is the vector of the random genetic effects of mother trees within the population by each site, **ε** is the vector of residuals, **X** is called the design

matrix, $\mathbf{Z_1}$, $\mathbf{Z_2}$, $\mathbf{Z_3}$ and $\mathbf{Z_4}$ are the incidence matrices linking the observations to the effects. A variance was fitted for each random effect: σ^2_{pop} is the genetic variance between populations, $\sigma^2_{site.pop}$ is the variance of the interaction term between population and site, $\sigma^2_{f(pop)}$ is the genetic variance between mother trees nested within population, and σ^2_e is the residual variance.

The full model (2) implies the homogeneity of error variance between sites. We also tested another formulation of the previous multisite model which allows different error variance terms for each site and estimated the correlation between sites at the population and family levels (i.e. custom ***G*** and ***R*** variance-covariance matrices: uniform correlation structure and heterogeneous diagonal structure, respectively) as follows:

$$y = Xsite + Z_0 block + Z_1 site.pop + Z_2 site.f + \varepsilon \quad (3)$$

where ***y*** is the vector of observation for a trait, ***site*** is the vector of fixed site effects, ***block*** is the vector of random block effects, ***site.pop*** is the vector of random site by population effects, ***site.f*** is the vector of random site by genetic effects of mother trees within the population, **ε** is the vector of residuals, **X** is called the design matrix, $\mathbf{Z_0}$, $\mathbf{Z_1}$, and $\mathbf{Z_2}$ are the incidence matrices linking the observations to the effects. Two variance estimates (one for each site) plus a correlation term (between sites) were fitted for ***site.pop*** and ***site.f*** random effects ($r_{\text{site.pop}}$ and $r_{\text{site.f}}$). This alternative formulation did not change the result of the analysis (see supplementary file), thus it was decided to present the results from model (2). Mixed models were run with SAS (SAS, 2008) and ASReml (Gilmour et al., 2009).

Given the difference in terms of sample size between P_{50} and h, we also run all the analysis on a reduced dataset for h, with the same sample size to that of P_{50}. While the absolute values of variances were different as expected, orders of magnitude between analysis on reduced dataset and full dataset were similar, therefore it was decided to present the most accurate estimates using the whole dataset for h.

Quantitative genetic parameters

For the single site analysis, we estimated narrow-sense heritability as follows: $h^2_{ns} = 4\sigma^2_{f(pop)} / (\sigma^2_{\varepsilon} + \sigma^2_{f(pop)})$. In our study, σ^2_A was estimated by $\sigma^2_A = 4\sigma^2_{f(pop)}$ as trees from the same family were presumed to be half-sibs (open-pollinated seeds). We did not include the population effect in the heritability calculation, because natural selection appeared to occur within each population (Visscher et al., 2008). The standard deviation of heritability was calculated with the equations of delta method (Lynch & Walsh, 1998). Variance components were standardized by the trait mean (Houle, 1992) as follows: $CV = \frac{\sqrt{\sigma^2_{trait}}}{\overline{X}_{trait}} 100$, where CV is the coefficient of variation. Each variance component is expressed with a CV (CV_A: additive coefficient of variation; CV_{BP} ($V_{BP} = \sigma^2_{pop}$): between population coefficient of variation; CV_P: phenotypic coefficient of variation; CV_R: residual coefficient of variation).

The estimate of phenotypic differentiation between populations, Q_{ST} (Spitze, 1993), was calculated as $Q_{ST} = \sigma^2_{pop} / (\sigma^2_{pop} + 2\sigma^2_A)$. For more detail about the methodology used for Q_{ST} and F_{ST} comparisons see Lamy et al (2011).

Assessment of phenotypic plasticity

There are various ways to estimate phenotypic plasticity. Assuming that the total phenotypic variance of a population can be written as (Falconer & Mackay, 1996)

$$\sigma^2_P = \sigma^2_G + \sigma^2_E + 2\,\mathrm{cov}_{GE} + I_{GE} + \sigma^2_{\varepsilon}$$

where σ^2_P is the population phenotypic variance, σ^2_G is the genetic variance of a population, σ^2_E is the general environmental effect (also called macro-environmental effect). The greatest conceptual difficulty is in the interpretation of $2\,\mathrm{cov}_{GE}$ and I_{GE}. $2\,\mathrm{cov}_{GE}$ corresponds to the

genotype-environment covariance which measures of the physical association of particular genotypes with particular environmental effects. I_{GE} is the genotype-environment interaction which is the variation in the phenotypic response of specific genotypes to specific environments. In other words, if individuals are randomly distributed with respect to macroenvironments (as it is the case in experimental designs) then $2\mathrm{cov}_{GE} = 0$ but $I_{GE} \neq 0$ if genotypic values and environmental effects are non-randomly distributed. Assuming that $2\mathrm{cov}_{GE} = 0$ in our provenance-progeny trials, then the phenotypic plasticity (σ^2_{PP}) can be written as: $\sigma^2_{PP} = \sigma^2_E + I_{GE}$

The most intuitive and common way (in ecology and genetics) to estimate phenotypic plasticity is to use the interaction term from a mixed model analysis (see model #2), and calculate a Scheiner's phenotypic plasticity index: $S = (\sigma^2_E + I_{GE}) / \left(I_{GE} + \sigma^2_G + \sigma^2_E + \sigma^2_\varepsilon\right)$ adapted from (Scheiner & Lyman, 1989). This index includes both terms of the phenotypic plasticity. Another way to estimate phenotypic plasticity is to consider that the same character measured in two environments can be treated as two different traits. Phenotypic plasticity can then be treated from the genetic correlation between the two traits. If genetic effects do not change across environments then the genetic correlation across environments is equal to one (see model #3). To facilitate the interpretation of such a genetic correlation (see explanation of model 3, r_x), we report $C = 1\text{-}r_x$, which means that a trait with a high *C* value is a trait with a high phenotypic plasticity. This *C* index mainly reflects the I_{GE} term. A thrid approach to estimate phenotypic plasticity is to use Relative Distances Plasticity Index (*RDPI*) from (Valladares et al., 2006), defined as the absolute phenotypic distances between individuals of the same genotype (here family) placed in different environments, divided by the highest of the two phenotypic values. This index relies less on the implicit assumption made on data distribution.

Results

Table 2. Variance component estimates for the (a) multi-site and (b) single site models.

(a)

	Overall			
	h		***P_{50}***	
Effects	**Variances**	***P*value**	**Variances**	***P*value**
Site	3424	<0.001	0.054	<0.001
Block(site)	37.00		0.001	
Population	438.7	<0.001	0.001	0.08
Site*population	76.84	<0.001	0.002	0.23
Family(Population)	10.85	<0.001	$7\ 10^{-9}$	0.003
Site*Family(Population)	28.27	<0.001	0.008	0.03
Residuals	374.7		0.052	

(b)

	Dry trial, Calcena (Spain)				Wet trial, Cestas (France)			
	h		***P_{50}***		***h***		***P_{50}***	
Effects	**Varianc es**	***P*value**	**Variances**	***P*value**	**Variances**	***P*value**	**Variances**	***P*value**
Block	1058	<0.001	12.87	<0.001	13830	<0.001	15.30	<0.001
Population	8.03	<0.001	0.0003	0.173	204.14	<0.001	0.0028	0.06
Family(Population)	6.79	<0.001	0.0083	0.009	47.51	<0.001	0.0088	0.003
Spatial residuals	102.14	<0.001	na	na	307.10	<0.001	na	na
Non spatial Residual	42.25		0.0456		216.23		0.059	
Spatial autocorrelation (row)	0.92	<0.001	na	na	0.87	<0.001	na	na
Spatial autocorrelation (colums)	0.92	<0.001	na	na	0.91	<0.001	na	na

Variance estimators are from full mixed model. The Site effect (in grey) was not declared as random effect for statistical reasons (see Material and Methods section) but we calculated a variance from the values estimated for each sites (fixed effects) and the *P-value* is from the fixed model. This model assumes the same error variance for both sites. Results from a full model assuming two different error variances for each site are provided in Table S6. Variance estimators are from mixed model for single site analysis. Spatial residuals, spatial autocorrelation coefficients are given for growth trait only because data were too spatialy to sparse for cavitation resistance. “na” not available. In both models *P*-values are from a log-likelihood ratio test, this is why block effects do not have *P-value*.

1. Phenotypic plasticity

From the full model analysis

For both cavitation resistance and height growth traits, a site effect was significant but the relative contribution of environmental variance (σ_E^2) to total variance was stronger for *h* compare to P_{50} (79% for *h* and 46% for P_{50}). The interaction term at population levels (I_{GE} for population) was only significant for *h*, not for P_{50}. The interaction term at family level (I_{GE} for family) was significant for both traits. To summarize, P_{50} and especially *h* displayed phenotypic plasticity mainly driven by σ_E^2.

Table 3. Phenotypic plasticity estimators for cavitation resistance (P_{50}) and tree height (*h*).

	Population		Family		Overall	
	P_{50}	*h*	P_{50}	*h*	P_{50}	*h*
C	0	0.15	0.88	0.78	na	na
S	0.51	0.90	0.90	0.98	na	na
RDPI	na	na	na	na	0.08	0.65

C is one minus the correlation coefficient calculated from mixed model with custom G and R matrices (see material and methods section). *S* is the Scheiner's index for phenotypic plasticity using variance components from mixed model 2. RDPI is the Relative Distances Plasticity Index which is the absolute phenotypic distances between individuals of same genotype (here family) and different environments, divided by one of the two phenotypic values.

From phenotypic index

The previous results were drawn from model #2, which could be biased by the implicit assumption made on the same error variance in both site (scale effect). From model #3, which allows two error variances, we calculated *C* index (for explanation see material and methods) and compared the results to the *S* index calculated from model #2 (Table 3). Both index showed the same trend as (i) at the population level, *h* displayed much more phenotypic plasticity compare to P_{50}. (ii) At family

level, both traits displayed phenotypic plasticity but that of P_{50} is lower than *h*. The most robust estimator (*RDPI*) of phenotypic plasticity clearly shows that P_{50} is less plastic compare to *h*. It should be noticed that trend was not driven by the unbalanced data between *h* and P_{50} because the same trend was found on the reduced dataset.

2. Genetic variation

Within population

The micro-environmental sensitivity (through the analysis of CV_R) and the evolvability (through the analysis of CV_A) were lower for P_{50} compare to *h*. In other words, P_{50} is less influenced by the micro-environemental variations and its amount of additive genetic variation is limited compare *h* (Table 4).

Between population variation and Q_{ST} and F_{ST} comparisons

In both trials, the same pattern was found: (i) No significant population effect was detected for P_{50}, whereas significant population effect was found for *h* (Table 2). In average, across trials, the between-population coefficient of variation (CV_{BP}) was 0.7% for P_{50}, much lower than the value measured for *h* (10.5%) (Table 4), (ii) For P_{50}, Q_{ST} distribution was lower compare to F_{ST} distribution, i.e. the observed variation between populations was less than the expectation under genetic drift alone. It means that a mechanism (uniform selection and/or genetic constraints, see discussion) must be favoring the same phenotypic mean in the studied populations from contrasted climates,. For *h*, the opposite trend was detected; Q_{ST} distribution was higher compared to F_{ST} distribution, suggesting that the studied populations displayed more differentiation than would be expected with drift alone (Figure S5).

Table 4. Variance components (V_P, V_{BP}, V_A, V_R), narrow-sense heritbility (h^2_{ns}), coefficient of variation (CV_P, CV_A, CV_{BP}, CV_R) and population differentiation (Q_{ST}).

Site	Traits	V_P	V_{BP}	V_A	V_R	h^2_{ns}	CV_P	CV_A	CV_{BP}	CV_R	Q_{ST}
Dry trial	*h*	151.2	8.043	27.13	144.4	0.17 ± 0.07	34.96	14.8	8.0	34.1	0.12
Dry trial	P_{50}	0.053	0.0004	0.034	0.045	0.61 ± 0.27	6.43	5.06	0.4	5.9	0.005
Wet trial	*h*	570.8	204.1	190.0	523.3	0.33 ± 0.03	21.7	12.5	13	20.8	0.34
Wet trial	P_{50}	0.067	0.0027	0.035	0.058	0.51 ± 0.23	6.60	4.75	1	6.1	0.04
In situ	*h*	2514	1789 [a]	na	724.9	na	47.2	na	39.8 [a]	25.3	na
In situ	P_{50}	0.064	0.010 [a]	na	0.053	na	6.97	na	2.83[a]	9.64	na

Variance component are from single site mixed model analysis. h^2_{ns} is the narrow-sense heritability and **SE** is the standard error of heritability, V_P is the phenotypic genetic variance, V_A is the additive genetic variance, V_{BP} is the between-population variance, V_R is the residual variance. CV_A is the variation coefficient of additive variance after adjustment for the block effect. CV_P is the variation coefficient of phenotypic variance after adjustment for the block effect. CV_R is the residual coefficient of variation. CV_{BP} is between-population coefficients of variation. Q_{ST} is the genetic quantitative variation between populations (Spitze, 1993). *In situ* variance components are from a mixed model with one random parameter (population). [a] this variance component (or the associated coefficient of variation) is not fully equally to the same variance estimated in the provenance-progeny trial because it include variation from the family level.

Experimental effects and spatial analysis

Block effects was significant for all the traits and models, which means that environmental variation was captured by the experimental design. Spatial analysis for *h* showed a high autocorrelation (> 0.85) between closely spatially related individuals (Table 2). However, changes in terms of variance estimation between a spatial analysis and a classical analysis were low (around 2-5%, data not shown).

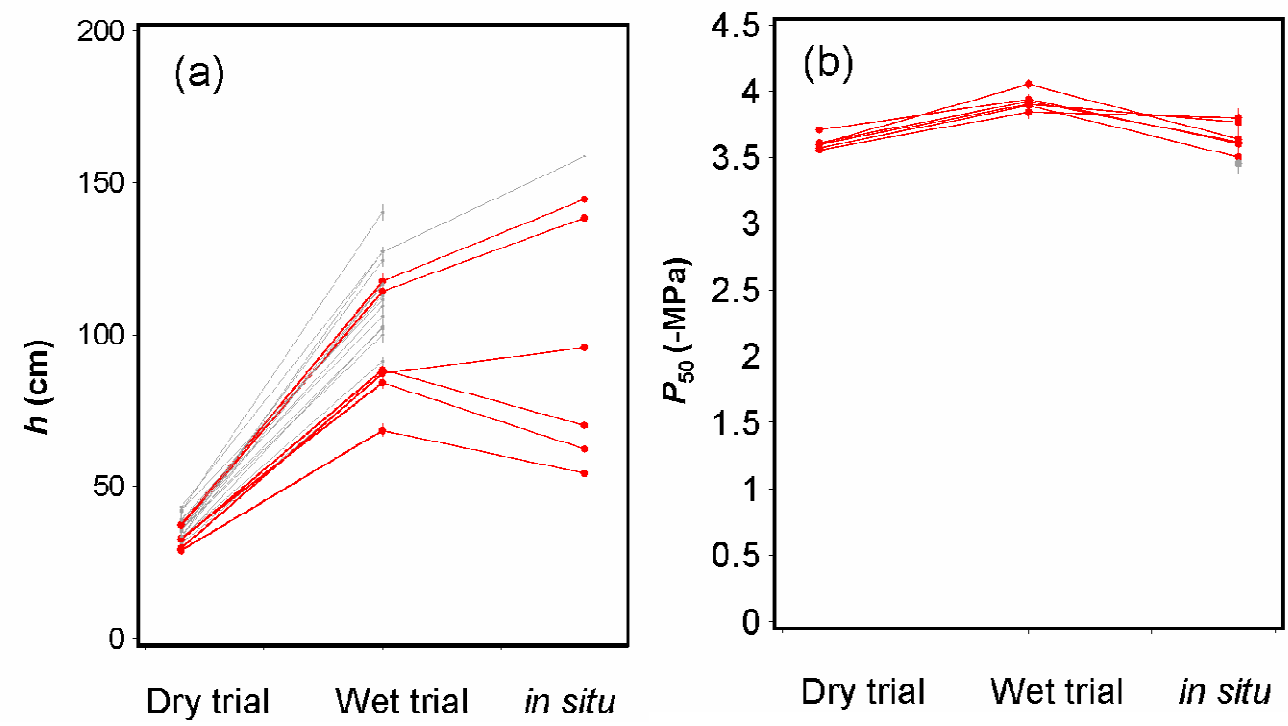

Fig. 3 Chart showing population means in each provenance-progeny trial (dry and wet) connected by plain lines, and means for natural population collected *in situ* : (a) For *h* assessed at four years old in both trials, n =163 ± 14.56 individuals per populations, and for *h* estimated at 4-year old from 11-year old trees, n=11 individuals per natural population. (b) for P_{50} n = 36 ± 1 individuals per populations of both trials, and n = 11 individuals per natural population. The error bars represent the standard errors. Red dots are used for the six selected populations, while grey dots are used for the other populations present in the dataset.

17

18 **3. Phenotypic variabilityl**

19 For cavitation resistance, CV_P *in situ* natural population ($CV_P^{in-situ}$) and CV_P from
20 provenance-progeny trial (CV_P^{ppt}) were equal to 6.9 and 6.4 respectively (given the error done
21 on the estimation of variance component for *in situ* population). It means that phenotypic
22 variation of *in situ* natural population was close to what we found in the provenance-progeny
23 trial.

24 The coefficient of variation between populations was higher *in situ* ($CV_{bp}^{in-situ}$) than in the
25 provenance-progeny trial (CV_{bp}^{ppt}). From a statistical point of view, it is however more
26 rigorous to compare $CV_{bp}^{in-situ}$ to the sum CV_{bp}^{ppt} and the coefficient of variation due to family
27 $CV_{f(pop)}^{ppt}$. After this correction, the estimation of $CV_P^{in-situ}$ was to the same order of magnitude
28 as that estimated in the provenance-progeny test ($CV_P^{in-situ}$ = 2.8, $\overline{CV_{bp}^{ppt}} + \overline{CV_{f(pop)}^{ppt}}$ = 1.92
29 (we average *CV* across trials)). The small difference between both estimators of variation
30 between populations is likely due to phenotypic plasticity and/or microenvironmental
31 heterogeneity.

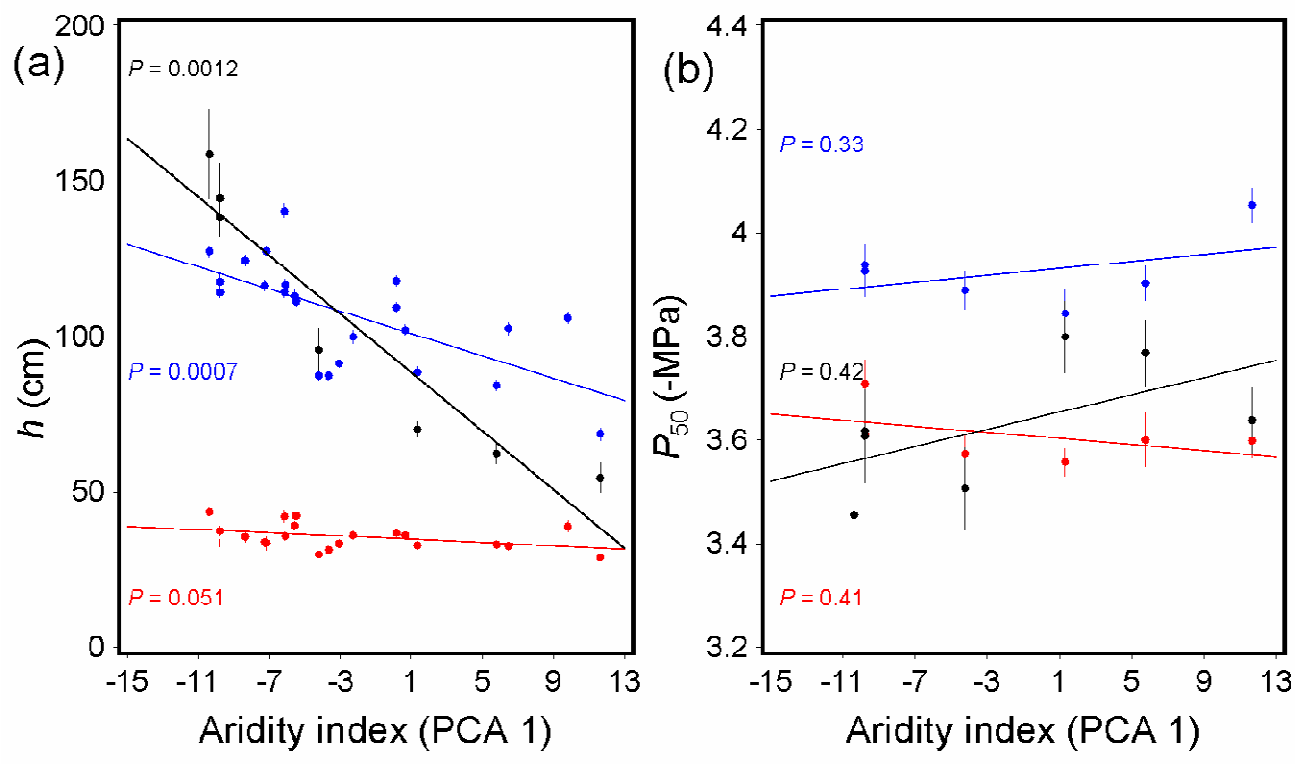

Fig. 4 The population mean for (a) tree height (*h)* and (b) cavitation resistance (P_{50}) according to aridity index. The aridity index corresponds the projection on the first principal component axis (PC1) of population position within the main plain space described by the PCA. Red, bleu and black colours correspond to regression in the dry, wet provenance-progeny trial and *in situ* natural stand respectively. The *P-value* was from a linear model and the error bars represent standard errors.

4. Link between climate and traits

The first principal component (PC 1) axis was interpreted as an aridity index, since it was positively correlated with atmospheric water demand, soil water deficit and negatively correlated with number of wet day frequency (Figure 2b).

Mean population *h* values showed a negative correlation with the composite aridity index (*P*-value = 0.056, 0.007 and 0.0012 in dry, wet trials and *in situ* Figure 5a). Populations from mesic provenances had a better growth compared to population from xeric provenances in both trials and *in situ* natural stand. We have observed the same trend with the reduced

dataset (*P*-value = 0.051, 0.009 and 0.0012 in dry, wet trial and *in situ*, data not shown). For P_{50}, we did not detect any relationship in both trials (*P*-value = 0.33, 0.41 and 0.42 in dry, wet trial and *in situ*, Figure 5b).

Discussion

We here carried out the first comprehensive study on the determinism of cavitation resistance variation, by simultaneously quantifying phenotypic variation, genetic variation and phenotypic plasticity in a pine species. Three major conclusions can be drawn: (i) the phenotypic variance for cavitation resistance (P_{50}) was relatively low ($CV_P^{in-situ}$ = 6.9 % and CV_P^{ppt} = 6.4%); (ii) the additive genetic variance and the genetic variance between populations were also low for P_{50} compared with growth trait (*h*); (iii) Cavitation resistance displayed phenotypic plasticity mainly driven by environmental variance as growth trait (no significant interaction between population and environment). However, plasticity of cavitation resistance was substantially lower than growth plasticity. All together, these results suggest that this drought tolerance key trait seems to be buffered against genetic perturbation and to a lesser extent against environmental variation.

Low phenotypic variation of cavitation resistance

Despite the recurrent demand of evolutionary ecology literature about natural variation of physiological traits (Leinonen et al., 2008), such studies were rarely performed (but see (Arntz & Delph, 2001)). Recently, Martinez-Vilalta et al., (2009), Corcuera et al., (2011) and Wortemann et al., (2011) provided a such work with enough statistical power to make robust inference about variability pattern at the species level for *Pinus sylvestris, Pinus pinaster* and *Fagus sylvatica,* respectively. In two provenance trials conducted on *Pinus pinaster*, Corcuera et al., (2011) measured a $\overline{CV_P^{ppt}} \approx 5\%$ which agree with our estimate ($\overline{CV_P^{ppt}}$) = 6.4%.

Martinez-Vilalta et al., (2009) estimated for cavitation resistance in *Pinus sylvestris* rounded $CV_P^{in-situ} \approx 8\%$ was similar to our $CV_P^{in-situ} = 6.9\%$ for *Pinus pinaster*. Therefore, our results matched well with previous experiments on *in situ* natural populations as well as populations grown in provenance trials for conifer species. On a broadleaved species, Wortemann et al., (2011) reported higher $\overline{CV_P^{ppt}} = 11.27$ value for *Fagus Sylvatica* (averaged on three provenance trials). The discrepancy between estimates gathered for conifers and those for *Fagus* could be due to the differences in wood anatomy (homoxyleous versus heteroxyleous woods).

Cavitation resistance is not linked with an aridity index

Like Martinez-Vilalta et al., (2009), Herbette et al., (2010) and Corcuera et al., (2011) together with this one, failed to detect a phenotypic or genetic clinal (or counter-clinal) variation of cavitation resistance with climatic variables. In this line, the following results were found in our study: (i) the mean values for cavitation resistance in the dry trial was lower compared to the one in the wet trial, which is opposite to what we could be expected. However, this result provides good evidence that P_{50} measurements in the dry trial were not be biased by native embolism (though K_{max} parameter), (ii) no correlation was found between genetic variation cavitation resistance (mean population in provenance-progeny test), either with phenotypic variation (mean population *in situ* natural stand) and the provenance climatic data (Figure 4). Several hypotheses could explain this unexpected result. First, we may not have targeted all the potential driving climatic variables for this trait since frost could also induce cavitation and the soil abiotic compartment was not directly considered. However, frost induced cavitation seems highly improbable low since, we did not detect significant trends between the second PCA axis (correlated with minimal annual temperature) and cavitation resistance (*P*-value= 0.09 and 0.47 in dry and wet trials), and since gymnosperms

are not prone to frost induced-cavitation (Pittermann & Sperry, 2003, 2006). Although we targeted only the atmospheric abiotic compartment, we may still consider that the edaphic characteristics were partly taken into account since we used 30 years averaged atmospheric variables, which form a good proxy for soil water dynamic over such long period. A second hypothesis lies on a hypothesis of hydraulics by Holtta et al., (2009), they showed thanks to an hydraulic model that cavitation events can release water during water stress that thus rehydrates living cells (capacitive effect). This mechanism could explain the fact that populations from dry provenance could benefit from being less cavitation resistant. Although theoretically plausible, it is hard to conceive the existence of such a mechanism at the intraspecific level and not across species (i.e. species less cavitation resistant are more drought tolerant). Finally, for us, the lack of correlation between cavitation resistance and climate of the provenance site should be simply due to the low genetic and phenotypic variation of cavitation resistance between populations.

Phenotypic plasticity of cavitation resistance is low compare to growth traits

Phenotypic plasticity of cavitation resistance seems to be a common subject in literature despite the fact that there are only two quantitative estimations of phenotypic plasticity for this trait (Corcuera et al., 2011; Wortemann et al., 2011). Many authors from both the fields of eco-physiology and ecology working on natural populations have speculate upon this issue (K.J. Kolb & Sperry, 1999; Maherali & DeLucia, 2000; Maherali et al., 2002; Martinez-Vilalta & Pinol, 2002; Jacobsen et al., 2007). Here, like (Corcuera et al., 2011; Wortemann et al., 2011), we provide a sound estimation of phenotypic plasticity of cavitation resistance. Our study enables to draw robust conclusions on phenotypic plasticity for cavitation resistance related-traits for the following reasons: (i) we measured a great number of genotypes, (ii) the statistical framework allowed a broad inference (mixed model versus fixed model) and (iii)

we provided a reference trait (growth height) because absolute numbers have no meaning *per se*. Growth related-traits are known to exhibit a high phenotypic plasticity in *Pinus pinaster* (Alia et al., 1997; González-Martínez et al., 2005). A strict comparison between cavitation resistance and growth traits show that cavitation resistance is less plastic (see *RDPI* value). Indeed, cavitation resistance traits do not have considerable phenotypic plasticity as phenology (Vitasse et al., 2010) or growth related-traits (Alía et al., 1997). *RDPI* values for cavitation resistance RDPI value are close to lowest values found in the literature for photosynthetic traits (Traveset et al., 2007; Baquedano et al., 2008). The other strong argument to assert that cavitation resistance phenotypic plasticity is low it is the same amount of phenotypic variance in provenance-progeny trial (CV_P^{ppt}) and in situ natural populations $CV_P^{in-situ}$.

Concluding remarks on drought tolerance in Pinus species

During drought episodes, *Pinus* species strongly regulate their stomatal conductance to reduce water loss by transpiration Delzon et al., (2004), and are also capable of adjusting the ratio of transpiring on conducting surfaces. This latter reaction is called hydraulic adjustment and it has been found in *Pinus ponderosa, Pinus palustris, Pinus sylvestris* and *Pinus halpensis* (Maherali & DeLucia, 2000; Addington et al., 2006; Martinez-Vilalta et al., 2009). For instance, Martinez-Vilalta et al., (2009) showed a negative relationship between needle area (A_L) on xylem area (A_S) and the climate dryness for *in situ* populations. This relationship was closed to what we found here between *h* and aridity index for populations growing in provenance-progeny trial. If we make the reasonable assumption that *h* is positively and more correlated to A_L compare to A_S (Porté et al., 2000), then hydraulic adjustment has a mixed determinism, the major part being due to environmental variation (70%), the other part being due to population genetic variation (10%). In other words, for *Pinus* species adaptation to

drought is done (mediated by genetic adaptation and phenotypic plasticity) by the modification of the ratio between conducting and transpiring surface or related hydraulic variables (leaf specific hydraulic conductivity) rather than a modification of wood related-trait like cavitation resistance. Despite the hydraulic adjustment, *Pinus* species have not able to sustain long drought period, because they have a reduced safety margin (difference between P_{50} and the leaf water potential at which 99% of the stomata are closed, (Martinez-Vilalta et al., 2004)) and they quickly closed their stomata to avoid runaway embolism. Consequently they are prone to carbon starvation (McDowell et al., 2006, 2008). Cavitation resistance is a major constraint on *Pinus* species physiology.

Acknowledgements

We thank Francois Luro for harvesting branches in Corsican mountains, Abdellah Kaji and all the reseach team from INRA (Meknes-Morroco) for their hospitality and helpfulness, Leyre Corcuera and Santiago González-Martínez from INIA (Zaragoza and Madrid-Spain) for the access to Calcena provenance-progeny trial. This research was supported by grants from : i/ INRA ecology division (innovative project 2010) and ii/ the European Union Provenance-progeny trials were set up in 2003 and 2004 by the INRA (Cestas-France) and INIA (Zaragoza-Spain) experimental units, as part of the TREESNIP-QLK3-CT2002-01973 project. JBL was supported by a doctoral fellowship from INRA and Auvergne Region, and a mobility grant from EGIDE. The funders had no role in study design, data collection and analysis, decision to publish, or preparation of the manuscript.

Bibliography

Addington RN, Donovan L a., Mitchell RJ, Vose JM, Pecot SD, Jack SB, Hacke UG, Sperry JS, Oren R. 2006. Adjustments in hydraulic architecture of Pinus palustris maintain

similar stomatal conductance in xeric and mesic habitats. *Plant, Cell and Environment* **29**: 535-545.

Alia R, Moro J., Denis J. B. 1997. Performance of Pinus pinaster provenances in Spain: interpretation of the genotype by environment interaction. *Canadian Journal of Forest Research-Revue Canadienne De Recherche Forestiere* **27**: 1548-1559.

Allen CD. **2009**. Climate-induced forest dieback: an escalating global phenomenon? *Unasylva* **60**: 43-49.

Allen CD, Breshears DD. **1998**. Drought-induced shift of a forest-woodland ecotone: rapid landscape response to climate variation. *Proceedings of the National Academy of Sciences of the United States of America* **95**: 14839-42.

Allen CD, Macalady AK, Chenchouni H, Bachelet D, McDowell NG, Vennetier M, Kitzberger T, Rigling A, Breshears DD, Hogg EH, et al. 2010. A global overview of drought and heat-induced tree mortality reveals emerging climate change risks for forests. *Forest Ecology and Management* **259**: 660-684.

Alía R, Moro Javier, Denis Jean Baptiste. **1997**. Performance of Pinus pinaster provenances in Spain□: interpretation of the genotype by environment interaction. *Main* **1559**: 1548-1559.

Arntz AM, Delph LF. **2001**. Pattern and process: evidence for the evolution of photosynthetic traits in natural populations. *Oecologia* **127**: 455-467.

Baquedano FJ, Valladares F, Castillo FJ. **2008**. Phenotypic plasticity blurs ecotypic divergence in the response of Quercus coccifera and Pinus halepensis to water stress. *European Journal of Forest Research* **127**: 495-506.

Beikircher B, Mayr S. **2009**. Intraspecific differences in drought tolerance and acclimation in hydraulics of Ligustrum vulgare and Viburnum lantana. *Tree physiology* **29**: 765-75.

Beniston M, Stephenson DB, Christensen OB, Ferro CAT, Frei C, Goyette S, Halsnaes K, Holt T, Jylha K, Koffi B, et al. 2007. Future extreme events in European climate: an exploration of regional climate model projections. *Climatic Change* **81**: 71-95.

Blum A. **2009a**. *Plant breeding for water-limited environments* (Springer, Ed.). Springer New York Dordrecht Haidelberg London.

Blum A. **2009b**. Effective use of water (EUW) and not water-use efficiency (WUE) is the target of crop yield improvement under drought stress. *Field Crops Research* **112**: 119-123.

Brendel O, Pot D, Plomion C, Rozenberg P, Guehl J-M. **2002**. Genetic parameters and QTL analysis of delta C-13 and ring width in maritime pine. *Plant Cell and Environment* **25**: 945-953.

Brendel O, Le Thiec D, Scotti-Saintagne C, Bodenes C, Kremer A, Guehl J-M. **2008**. Quantitative trait loci controlling water use efficiency and related traits in Quercus robur L. *Tree Genetics & Genomes* **4**: 263-278.

Breshears DD, Cobb NS, Rich PM, Price KP, Allen CD, Balice RG, Romme WH, Kastens JH, Floyd ML, Belnap J, et al. 2005. Regional vegetation die-off in response to global-change-type drought. *Proceedings of the National Academy of Sciences of the United States of America* **102**: 15144-15148.

Brodribb TJ, Cochard H. 2009. Hydraulic failure defines the recovery and point of death in water-stressed conifers. *Plant physiology* **149**: 575-84.

Brodribb TJ, Bowman DJMS, Nichols S, Delzon S, Burlett R. 2010. Xylem function and growth rate interact to determine recovery rates after exposure to extreme water deficit. *New Phytologist* **188**: 533-542.

Bréda N. 2006. Faut-il adapter la gestion de la forêt aux sécheresses et si oui, comment□? *Euroforest 2006*: 1-6.

Bréda N, Badeau V. 2008. Forest tree responses to extreme drought and some biotic events: Towards a selection according to hazard tolerance? *Comptes Rendus Geosciences* **340**: 651-662.

Bréda N, Huc R, Granier A, Dreyer E. 2006. Temperate forest trees and stands under severe drought: a review of ecophysiological responses, adaptation processes and long-term consequences. *Annals of Forest Science* **63**: 625-644.

Bucci Gabriele, González-Martínez SC, Le Provost G, Plomion C, Ribeiro Maria Margarida, Sebastiani F, Alía R, Vendramin GG. 2007. Range-wide phylogeography and gene zones in Pinus pinaster Ait. revealed by chloroplast microsatellite markers. *Molecular ecology* **16**: 2137-53.

Burban C, Petit RJ. 2003. Phylogeography of maritime pine inferred with organelle markers having contrasted inheritance. *Molecular Ecology* **12**: 1487-1495.

Cochard H. 2002. A technique for measuring xylem hydraulic conductance under high negative pressures. *Plant Cell and Environment* **25**: 815-819.

Cochard H, Damour G, Bodet C, Tharwat I, Poirier M, Ameglio T. 2005. Evaluation of a new centrifuge technique for rapid generation of xylem vulnerability curves. *Physiologia Plantarum* **124**: 410-418.

Corcuera L, Cochard H, Gil-Pelegrin E, Notivol E. 2011. Phenotypic plasticity in mesic populations of Pinus pinaster improves resistance to xylem embolism (P50) under severe drought. *Trees*.

Cumbie WP, Eckert A, Wegrzyn J, Whetten R, Neale DB, Goldfarb B. 2011. Association genetics of carbon isotope discrimination, height and foliar nitrogen in a natural population of Pinus taeda L. *Heredity* **107**: 105-114.

Debat V, David P. 2001. Mapping phenotypes: canalization, plasticity and developmental stability. *Trends in Ecology & Evolution* **16**: 555-561.

Della-Marta PM, Beniston M. 2008. Summer heat waves in western Europe, their past

247 change and future projections. In: Bronnimann S, Luterbacher J, Ewen T, Diaz HF, Stolarski
248 RS, Neu U, eds. Climate Variability and Extremes during the Past 100 Years.235-250.

249 **Delzon S, Douthe C, Sala A, Cochard H**. **2010**. Mechanism of water-stress induced
250 cavitation in conifers: bordered pit structure and function support the hypothesis of seal
251 capillary-seeding. *Plant, Cell & Environment* **32**: 1-11.

252 **Delzon S, Sartore M, Burlett R., Dewar R, Loustau D. 2004**. Hydraulic responses to height
253 growth in maritime pine trees. *Plant Cell and Environment* **27**: 1077-1087.

254 **Dhanda SS, Sethi GS, Behl RK**. **2004**. Indices of Drought Tolerance in Wheat Genotypes at
255 Early Stages of Plant Growth. *Journal Agronomy & Crop Science* **190**: 6-12.

256 **Dutkowski GW, Silva JCE, Gilmour AR, Lopez GA**. **2002**. Spatial analysis methods for
257 forest genetic trials. *Canadian Journal of Forest Research-Revue Canadienne De Recherche*
258 *Forestiere* **32**: 2201-2214.

259 **Dutkowski GW, Silva JCE, Gilmour AR, Wellendorf H, Aguiar A**. **2006**. Spatial analysis
260 enhances modelling of a wide variety of traits in forest genetic trials. *Canadian Journal of*
261 *Forest Research-Revue Canadienne De Recherche Forestiere* **36**: 1851-1870.

262 **Eveno E**. **2008**. L'adaptation à la sécheresse chez le pin maritime (Pinus pinaster Ait .)□:
263 patrons de diversité et différenciation nucléotidiques de gènes candidats et variabilité de
264 caractères phénotypiques. *Sciences-New York*: 1-390.

265 **Falconer DS, Mackay TFC**. **1996**. Introduction to quantitative genetics. *Introduction to*
266 *quantitative genetics.*: xv + 464 pp.

267 **Gilmour AR, Gogel BJ, Cullis BR, Thompson R**. **2009**. ASReml User Guide Release.

268 **González-Martínez SC, Gerber Sophie, Cervera MT, Martinez-Zapater JM, Alia R, Gil**
269 **L**. **2003**. Selfing and sibship structure in a two-cohort stand of maritime pine (Pinus pinaster
270 Ait.) using nuclear SSR markers. *Annals of Forest Science* **60**: 115-121.

271 **González-Martínez SC, Gil L, Alia R**. **2005**. Genetic diversity estimates of Pinus pinaster in
272 the Iberian Peninsula: a comparison of allozymes and quantitative traits. *Investigacion*
273 *Agraria, Sistemas y Recursos Forestales* **14**: 3-12.

274 **Granier A, Reichstein M, Bréda N, Janssens I, Falge E, Ciais P, Grunwald T, Aubinet**
275 **M, Berbigier P, Bernhofer C**. **2007**. Evidence for soil water control on carbon and water
276 dynamics in European forests during the extremely dry year: 2003. *Agricultural and Forest*
277 *Meteorology* **143**: 123-145.

278 **Herbette S, Wortemann R, Awad H, Huc R, Cochard H, Barigah T. S. 2010**. Insights into
279 xylem vulnerability to cavitation in Fagus sylvatica L.: phenotypic and environmental sources
280 of variability. *Tree Physiology*.

281 **Holtta T, Cochard H, Nikinmaa E, Mencuccini M**. **2009**. Capacitive effect of cavitation in
282 xylem conduits: results from a dynamic model. *Plant Cell and Environment* **32**: 10-21.

Houle D. **1992**. Comparing evolvabiliy and variability of quantitative traits. *Genetics* **130**: 195-204.

Houle D. **2009**. Numbering the hairs on our heads□: The shared challenge and promise of phenomics. *PNAS*: 1-7.

Houle D. **2010**. Numbering the hairs on our heads: The shared challenge and promise of phenomics. *Proceedings of the National Academy of Sciences of the United States of America* **107**: 1793-1799.

Jacobsen AL, Pratt RB, Ewers FW, Davis SD. **2007**. Cavitation resistance among 26 chaparral species of southern California. *Ecological Monographs* **77**: 99-115.

Jones HG. **1992**. *Plants and microclimate, a quantitative approach to environmental plant physiology - 2nd ed.* (U of Cambridge, Ed.). Cambridge, New York, USA: University of Cambridge.

Kolb KJ, Sperry JS. **1999**. Differences in drought adaptation between subspecies of sagebrush (Artemisia tridentata). *Ecology* **80**: 2373-2384.

Lamy J-B, Bouffier L, Burlett Régis, Plomion C, Cochard H, Delzon S. **2011**. Uniform selection as a primary force reducing population genetic differentiation of cavitation resistance across a species range. *Plos One* **6**: e23476.

Leinonen T, O'Hara RB, Cano JM, Merila J. **2008**. Comparative studies of quantitative trait and neutral marker divergence: a meta-analysis. *Journal of Evolutionary Biology* **21**: 1-17.

Lindner M, Maroschek M, Netherer S, Kremer A, Barbati A, Garcia-Gonzalo J, Seidl R, Delzon S, Corona P, Kolström M. **2010**. Climate change impacts, adaptive capacity, and vulnerability of European forest ecosystems. *Forest Ecology and Management* **259**: 698-709.

Lynch M, Walsh B. **1998**. Genetics and analysis of quantitative traits. *Genetics and analysis of quantitative traits.*: xvi + 980 pp.

Maherali H, DeLucia EH. **2000**. Xylem conductivity and vulnerability to cavitation of ponderosa pine growing in contrasting climates. *Tree Physiology* **20**: 859-867.

Maherali H, Pockman W T, Jackson RB. **2004**. Adaptive variation in the vulnerability of woody plants to xylem cavitation. *Ecology* **85**: 2184-2199.

Maherali H, Williams BL, Paige KN, Delucia EH. **2002**. Hydraulic differentiation of Ponderosa pine populations along a climate gradient is not associated with ecotypic divergence. *Functional Ecology* **16**: 510-521.

Martinez-Vilalta J, Pinol J. **2002**. Drought-induced mortality and hydraulic architecture in pine populations of the NE Iberian Peninsula. *Forest Ecology and Management* **161**: 247-256.

Martinez-Vilalta J, Cochard H, Mencuccini M, Sterck F, Herrero A, Korhonen JFJ, Llorens P, Nikinmaa E, Nole A, Poyatos R, et al. 2009. Hydraulic adjustment of Scots pine

319 across Europe. *New Phytologist* **184**: 353-364.

320 **Martinez-Vilalta J, Sala A, Pinol J**. **2004**. The hydraulic architecture of Pinaceae - a review.
321 *Plant Ecology* **171**: 3-13.

322 **McDowell NG, Adams HD, Bailey JD, Hess M, Kolb TE**. **2006**. Homeostatic maintenance
323 of ponderosa pine gas exchange in response to stand density changes. *Ecological Applications*
324 **16**: 1164-1182.

325 **McDowell NG, Pockman William T., Allen CD, Breshears DD, Cobb N, Kolb T, Plaut J,**
326 **Sperry JS, West A, Williams DG, et al. 2008**. Mechanisms of plant survival and mortality
327 during drought: why do some plants survive while others succumb to drought? *New*
328 *Phytologist* **178**: 719-739.

329 **New M, Hulme M, Jones PD**. **1999**. Representing twentieth-century space-time climate
330 variability. Part I: Development of a 1961-90 mean monthly terrestrial climatology. *Journal*
331 *of Climate* **12**: 829-856.

332 **New M, Hulme M, Jones PD**. **2000**. Representing twentieth-century space-time climate
333 variability. Part II: Development of 1901-96 monthly grids of terrestrial surface climate.
334 *Journal of Climate* **13**: 2217-2238.

335 **New M, Lister D, Hulme M, Makin I**. **2002**. A high-resolution data set of surface climate
336 over global land areas. *Climate Research* **21**: 1-25.

337 **Pammenter NW, Vander Willigen C**. **1998**. A mathematical and statistical analysis of the
338 curves illustrating vulnerability of xylem to cavitation. *Tree Physiology* **18**: 589-593.

339 **Pittermann J**. **2010**. The evolution of water transport in plants: an integrated approach.
340 *Geobiology* **8**: 112-139.

341 **Pittermann J, Sperry JS**. **2003**. Tracheid diameter is the key trait determining the extent of
342 freezing-induced embolism in conifers. *Tree Physiology* **23**: 907-914.

343 **Pittermann J, Sperry JS**. **2006**. Analysis of freeze-thaw embolism in conifers. The
344 interaction between cavitation pressure and tracheid size. *Plant Physiology* **140**: 374-382.

345 **Porté A, Bosc A, Champion I, Loustau Denis**. **2000**. Estimating the foliage area of
346 Maritime pine (Pinus pinaster Aït .) branches and crowns with application to modelling the
347 foliage area distribution in the crown. *October* **57**: 73-86.

348 **Ribeiro M. M., LeProvost G, Gerber S., Vendramin GG, Anzidei M, Decroocq S,**
349 **Marpeau A, Mariette S, Plomion C**. **2002**. Origin identification of maritime pine stands in
350 France using chloroplast simple-sequence repeats. *Annals of Forest Science* **59**: 53-62.

351 **Ribeiro M. M., Mariette S, Vendramin GG, Szmidt AE, Plomion C, Kremer A**. **2002**.
352 Comparison of genetic diversity estimates within and among populations of maritime pine
353 using chloroplast simple-sequence repeat and amplified fragment length polymorphism data.
354 *Molecular Ecology* **11**: 869-877.

Richardson DM. **1998**. Ecology and biogeography of Pinus. *Ecology and biogeography of /i Pinus/.*: xvii + 527 pp.

Riou-Nivert P, Landmann G, Dupouey JL, Badeau V, Lefevre Y, Bréda N, Nageleisen LM, Chuine I, Lebourgeois F, Gaudin S, et al. 2008. Climatic change - questions from silviculturists and replies from researchers. *Foret-Entreprise*: 11-45.

Rood SB, Patiño S, Coombs K, Tyree MT. **2000**. Branch sacrifice□: cavitation-associated drought adaptation of riparian cottonwoods. : 248-257.

SAS II. **2008**. *SAS/STAT® 9.2 User's Guide. Cary, NC: SAS Institute Inc.*

Scheiner SM, Lyman RF. **1989**. The Genetics of Phenotypic Plasticity .1. Heritability. *Journal of Evolutionary Biology* **2**: 95-107.

Scotti I. **2010**. Adaptive potential in forest tree populations: what is it, and how can we measure it? *Annals of Forest Science* **67**: 801.

Sperry JS. **2003**. Evolution of water transport and xylem structure. *International Journal of Plant Sciences* **164**: 115-127.

Spitze K. **1993**. Population structure in Daphnia obtusa: quantitative genetic and allozymic variation. *Genetics* **135**: 367-74.

Traveset A, Moragues E, Valladares F. **2007**. Spreading of the invasive Carpobrotus aff. acinaciformis in Mediterranean ecosystems: The advantage of performing in different light environments. *Applied Vegetation Science* **11**: 45-54.

Tyree MT, Kolb KJ, Rood SB, Patino S. **1994**. Vulnerability to drought-induced cavitation of riparian cottonwods in Alberta - A possible factor in the decline of the ecosystem. *Tree Physiology* **14**: 455-466.

Valladares F, Sanchez-Gomez D, Zavala MA. **2006**. Quantitative estimation of phenotypic plasticity: bridging the gap between the evolutionary concept and its ecological applications. *Journal of Ecology* **94**: 1103-1116.

Vendramin GG, Anzidei M, Madaghiele A, Bucci G. 1998. Distribution of genetic diversity in Pinus pinaster Ait. as revealed by chloroplast microsatellites. *Theoretical and Applied Genetics* **97**: 456-463.

Visscher PM, Hill WG, Wray NR. **2008**. Heritability in the genomics era--concepts and misconceptions. *Nature reviews. Genetics* **9**: 255-66.

Vitasse Y, Bresson CC, Kremer A, Michalet R, Delzon S. **2010**. Quantifying phenological plasticity to temperature in two temperate tree species. *Functional Ecology* **24**: 1211-1218.

Wilson AJ. **2008**. Why h^2 does not always equal VA/VP? *Journal of Evolutionary Biology* **21**: 647-650.

Wortemann R, Herbette S, Barigah Têtè Sévérien, Fumanal B, Alia R, Ducousso A,

Gomory D, Roeckel-Drevet P, Cochard H. **2011**. Genotypic variability and phenotypic plasticity of cavitation resistance in Fagus sylvatica L. across Europe. *Tree physiology*: 1-8.

Supplementary files

Q_{ST} and F_{ST} comparison

To assess whether differentiation of phenotypic traits were caused by either selection or drift, we compared the distribution of phenotypic differentiation (Q_{ST*}) with the distribution of genetic differentiation (F_{ST*}) obtained with molecular markers assumed to be neutral. The F_{ST}^{*} distribution was constructed using a dataset of 8 neutral nuclear microsatellites previously genotyped on the same populations (Eveno et al., 2008; Alberto et al., 2011; Lamy et al., 2011). To simulate the neutral expectation, we randomly resampled 10^3 times with replacement between loci to estimate the sampling variance of F_{ST}. Each F_{ST} replicate value was multiplied by a random number drawn from the Lewontin-Krahauer distribution (Lewontin & Krakauer, 1973), which accounts for deviations from the neutral model because of demography (Whitlock, 2008; Whitlock & Guillaume, 2009). The Q_{ST}^{*} distributions were constructed by performing a parametric bootstrap resampling procedure 10^3 times (O'Hara & Merilä, 2005) allowing estimation of the distribution of each variance component ($\sigma_A^2, \sigma_{pop}^2$) using the Satterthwaite's approximation (Satterthwaite, 1946). Finally, the two resulting distributions were compared using a non parametric test on 2.5 and 97.5 quantiles. All the analyses were performed with SAS version 9.2 (SAS, 2008). Codes are available on request.

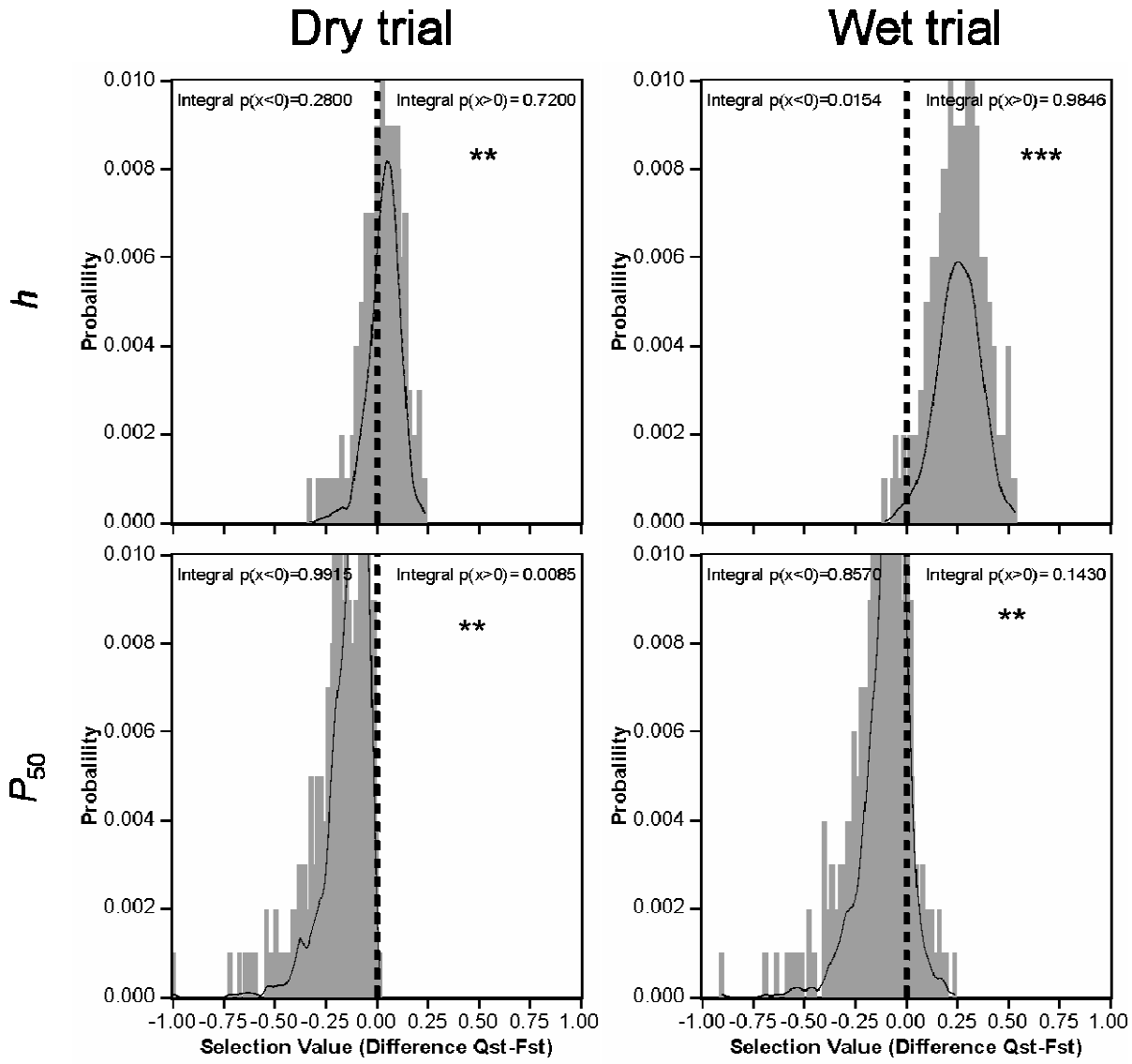

Fig. S5 The observed distribution (gray histogram) and the kernel density (black curves) of the Q_{ST}-F_{ST} difference are represented for each trait in each trial. ^{ns} $P > 0.05$, * $P < 0.05$, ** $P< 0.01$, *** $P < 0.001$, P-values are from non-parametric test on 2.5 and 97.5 quantile (Kosorok's test with a Bonferroni correction). On the top of each panel, we also show the integral probability of the distribution (using the kernel density estimator) above (see "Integral p(x>0)" on the left panel) and below (see "Integral p(x<0)" on the left panel) zero (marked with the thick and dotted line).

Table S6. Variance components estimation for the full model for both provenance-progeny trials.

	h		P_{50}	
Effects	**Variances**	***P*value**	**Variances**	***P*value**
Site*bloc (Dry trial)	17.61	na	0.0018	na
Site*bloc (Wet trial)	529.2	na	0.0014	na
Site*population (Dry trial)	8.819	<0.0001	0.00055	0.056
Site*population (Wet trial)	206.6	<0.0001	0.0028	0.056
Between populations across sites correlation	0.85	<0.0001	0.99	0.056
Site*Family(population) (Dry trial)	22.401	<0.0001	0.0084	0.0032
Site*Family(population) (Wet trial)	50.87	<0.0001	0.0089	0.0032
Between family across site correlation	0.22	<0.0001	-0.12	0.0032
Residuals (Dry trial)	126.2	na	0.045	na
Residuals (Wet trial)	450.4	na	0.058	na

Variance estimators are from full mixed model. This model assumes one variance for each site and each effect. In this case, phenotypic plasticity (at the family or population level) is given by estimating a genetic correlation between trait values in dry and wet trials. *P*-values are from a log-likelihood ratio test.

Table S7. Geographical coordinates of populations growing in wet and dry trials sorted by code number.

Populations	Code	Latitude (°)	Longitude (°)
Restonica	2.00	42.27	9.12
Aullène	10.00	41.67	9.05
Pineta	11.00	41.97	9.03
Pinia	15.00	42.02	9.48
Cenicientos	20.00	40.27	-3.52
Arenas de San Pedro	21.00	40.21	-4.91
Coca	22.00	41.23	-3.49
Cuellar	23.00	41.40	-3.68
Valdemaqueda	24.00	40.51	-3.70
Valdemaqueda	24.00	40.51	-3.70
San Leonardo de Yagüe	25.00	41.82	-2.93
Bayubas de Abajo	26.00	41.52	-1.13
San cipriano de Ribaterme	27.00	42.10	-7.59
Oria	29.00	37.53	-1.64
Tamrabta	30.00	34.00	-5.00
Punta cires	31.00	35.92	-5.47
Koudiat Erramla	32.00	35.47	-5.38
Tadiwine	36.00	34.93	-4.53
Tamjout	37.00	33.83	-3.98
Talaghine	38.00	32.45	-5.23
Sidi Meskour	39.00	31.47	-6.83
Petrock	40.00	44.05	-0.68
Mimizan	41.00	44.13	-0.70
Hourtin	42.00	45.17	-0.87
Le Verdon	43.00	45.57	-0.78

Olonne sur mer	44.00	46.57	-0.92
St Jean de Monts	45.00	46.77	-1.98
Pleucadec	46.00	47.78	-1.67
Erdeven	47.00	47.65	-2.87
Tabarka	50.00	37.08	7.10
Competa	60.00	36.84	-2.05
Boniches	61.00	39.99	-0.38
La Spezia	62.00	44.10	9.83
Montagna Grande	63.00	36.80	12.00
Monte Pino	64.00	40.92	9.42
Poggio Adorno/Pisa	65.00	43.75	10.73

Quand les arbres pleurent ou quand la sève surfe sur les lois de la thermodynamique.

Quand la reine organise une rave…

Royal Botanic Gardens of Kew, Jardins botaniques royaux de Kew, l'été cogne fort sur la banlieue londonienne, des écouteurs tombent des arbres, les fils s'entortillent autour des ramures, des grosses caisses sont arrimées aux troncs, de loin les arbres paraissent sous perfusion. Les gens s'arrêtent et mettent les écouteurs sur les oreilles, ils entendent des clics ! Clic, clic, clic, silence, clic, clic… Serait-ce les restes d'une rave sauvage qui aurait mal tournée… Non, l'institution royale se targue d'abriter une espèce sur huit existant sur la terre, elle ne mégote pas avec sa réputation. En plus des écouteurs, d'autres visiteurs scrutent les moindres bruits du tronc avec un cornet géant ! Oulala…

C'est grave docteur ?

Oui et non réponds l'artiste à l'origine de la performance, ce qu'on entend ne sont que les pleurs de l'arbre ! Qu'un saule puisse être pleureur ne surprend personne mais que tous les arbres soient en pleurs !... Les clics ne sont pas audibles dans le spectre de l'oreille humaine, il s'agit d'ultrasons que les appareils de l'artiste convertissent en sons dans l'audible… Quant à l'origine des ces clics, il faut se tourner vers la mécanique des fluides. Les clics dans les ultrasons sont des phénomènes connus en physique, il s'agit d'une des conséquences de la cavitation. Ca…vi… quoi ! Cavitation, c'est-à-dire la formation d'une cavité au sein d'un fluide. La cavitation est la bête noire ou le saint graal des ingénieurs navales, l'hélice du Charles de Gaulle s'est rompue à cause de ce phénomène et le sous marin Russe Koursk a coulé pendant des essais de nouvelles torpides à supercavitation (Ashley, 2001). Comment de tels phénomènes surviennent dans les arbres, qui pourtant ne sont pas des machines à propulsion nucléaires ?
Pour saisir comment les arbres « pleurent », il faut comprendre comment l'eau ou la sève est mise en mouvement dans l'arbre et comment cette dernière peut « caviter ».

Ne mettez pas de déo sur votre bégonia !

Non que votre bégonia soit allergique aux parfums de synthèses mais simplement que c'est grâce à l'évaporation de l'eau au niveau des feuilles que l'eau est extraite du sol par les racines. Le mécanisme physique de la circulation de la sève brute (l'eau et les minéraux extraits du sol) a longtemps était un mystère et un sujet polémique. Les plantes fonctionnent comme une pompe aspirante. Une molécule d'eau s'évapore au niveau des stomates (interruption microscopique dans les feuilles au travers desquelles les échanges de gaz et d'eau se font), une autre molécule d'eau va prendre sa place en entraînant sa voisine grâce à des liaisons chimiques particulières que l'on appelle les liaisons hydrogènes. De proche en proche, la dépression crée par l'évaporation au niveau des feuilles va se propager jusqu'au racine, c'est grâce à cette force aspirante que l'eau va être extraite du sol. La sève dans l'arbre est donc tirée par le haut, elle est sous tension (pression négative) et non poussé par le bas (pression positive)(Tyree & Zimmermann, 2002).

La circulation de la sèvre brute ou l'hydrodynamique de l'extrême.

Pourtant cette histoire de pression négative dans la sève a longtemps été une barrière à la compréhension… En effet si nous consultons un grimoire de physicien… Eh si ! Le

diagramme de phase de l'eau… Il s'agit d'un graphique qui représente les états de l'eau en fonction de la pression et de la température. Si l'on regarde l'état de l'eau en pression négative (Caupin & Herbert, 2006) ! Oh… Surprise ! L'eau est forcement sous forme de gaz ! Donc *a priori*, la circulation de la sève est impossible car elle viole les lois thermodynamiques.

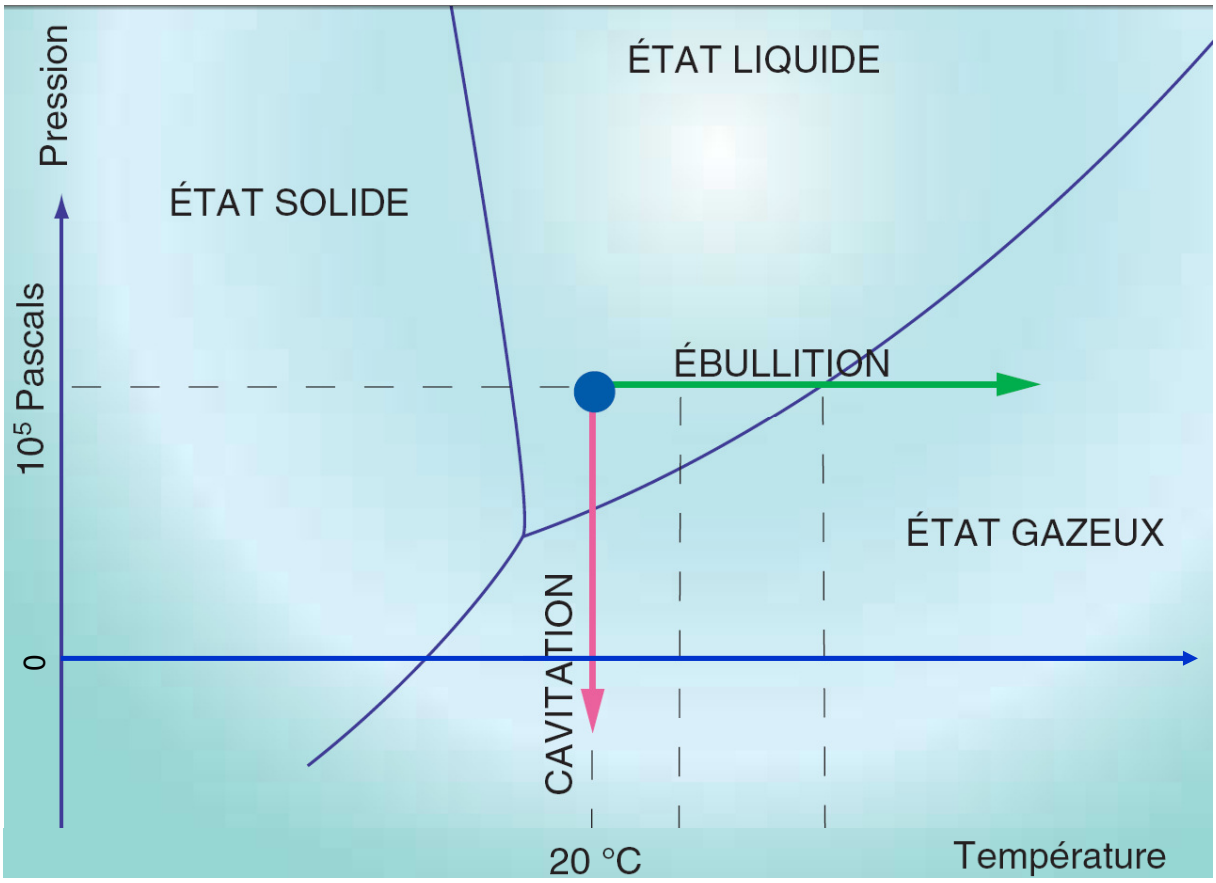

Si l'on considère un volume d'eau liquide à température constante (trajet en rose) et qu'on abaisse la pression, l'eau va se transformer en gaz comme l'indique ce diagramme, et ce jusqu'aux pressions négatives, que l'on trouve dans la sève.

La sève, c'est du jus ou du gaz ?

Heureusement l'eau est un fluide tout sauf normal, les liaisons hydrogènes entre les molécules d'eau peuvent maintenir un état liquide (eau en surfusion ou équilibre métastable) malgré les pressions négatives. Mais quand ces pressions négatives deviennent trop importantes, durant les étés lorsque les sols sont secs et que la transpiration est maximale, alors l'eau de la sève se vaporise par endroit et crée des bulles de vapeur d'eau, il y a cavitation (Cochard, 2006).

Ne perfusez pas votre bonzaï !

Ne transfusez jamais votre bonzaï anémique avec du Perrier ou avec votre bière belge favorite ! Il en mourrait… de soif ! En effet, les bulles de vapeur d'eau et d'air, issu de la cavitation (ou de votre transfusion) remplissent les vaisseaux du xylème qui sont chargés en temps normal d'acheminer l'eau liquide aux feuilles et aux bourgeons. Une fois les vaisseaux de la branche, ou pis du tronc, complément embolisés (remplie de vapeur d'eau issue de la cavitation), les tissus vivants situés au dessus de ce bouchon vont mourir par manque d'eau.

Les limites biophysiques des plantes ou les méfaits des bulles !

La circulation des sèves est rendue possible seulement grâce aux propriétés physico-chimiques très particulières de la molécule d'eau. Les contraintes biophysiques issues de la cavitation sont à l'origine de la limitation en hauteur des arbres. Les tissus végétaux sont virtuellement éternels tant qu'ils peuvent croître, cependant la hauteur des arbres actuels et fossiles est limitée à 130 m maximum à cause des raisons biophysiques évoquées ci-dessus (Koch *et al.*, 2004). Il est désormais prouvé que les préférences écologiques des arbres sont concordantes avec leur aptitude à résister à la cavitation, par exemple un Cyprès du Tassili (un dur à cuire du désert Algérien de Tassili) a une résistance à la cavitation beaucoup plus importante qu'un peuplier (Maherali *et al.*, 2004). Il existe une grande variation de ce caractère entre les espèces. La sélection naturelle a pu s'exercer sur ce caractère (Willson *et al.*, 2008). Beaucoup de travaux en cours tentent de comprendre la dynamique evolutive de la résistance à la cavitation. Non, non la recherche en physiologie végétale ne bulle pas !

Gibet Lamy

Reference

Ashley S. 2001. Propulsion sous-marine par supercavitation. *Pour la science* **285**(1): 68-72.

Caupin F, Herbert E. 2006. Cavitation in water: a review. *Comptes Rendus Physique* **7**(9-10): 1000-1017.

Cochard H. 2006. Cavitation in trees. *Comptes Rendus Physique* **7**(9-10): 1018-1026.

Koch GW, Sillett SC, Jennings GM, Davis SD. 2004. The limits to tree height. *Nature* **428**(6985): 851-854.

Maherali H, Pockman WT, Jackson RB. 2004. Adaptive variation in the vulnerability of woody plants to xylem cavitation. *Ecology* **85**(8): 2184-2199.

Tyree MT, Zimmermann MH. 2002. *Xylem structure and the ascent of sap*. Berlin Heidelberg New York: Springer.

Willson CJ, Manos PS, Jackson RB. 2008. Hydraulic traits are influenced by phylogenetic history in the drought-resistant, invasive genus Juniperus (Cupressaceae). *American Journal of Botany* **95**(3): 299-314.

Résumé

Force est de constater que les dépérissements forestiers augmentent. Ces observations vont de pairs avec l'accroissement des événements climatiques extrêmes. Aussi dans ce contexte, il est nécessaire d'identifier de nouveaux caractères de resistance à la sécheresse. La résistance à la cavitation est actuellement le meilleur marqueur de la survie d'une espèce à la sécheresse.

Cette thèse avait deux objectifs : (i) comprendre le mécanisme de propagation de la cavitation dans le xylème chez les gymnospermes. (ii) Quantifier la variation phénotypique intraspécifique de ce caractère chez *Pinus pinaster* La variation intraspécifique peut être décomposé en de la variation en variation génétique, de la variation environnemental et de l'interaction des deux (plasticité phénotypique).

La démarché a été la suivante (i) une étude interspécifique de la résistance à la cavitation a été couplé à des mesures micro-anatomiques. (ii) Pour le volet intraspécifique, nous avons phénotypé 6 populations dans deux test de populations-descendances, ainsi qu'en population naturelles *in situ*.

La propagation de l'embolie chez les *Pinaceae* et les ex-*Taxodiaceae* pourrait être due au passage du germe d'air (rupture capillaire) à travers des nanopores dans le torus. En effet, la pression de rupture d'un ménisque air-sève est corrélée à l'entrée de l'air dans le xylème. Alors que la variation interspécifique est grande, la résistance à la cavitation varie faiblement au sein d'une espèce. Ainsi les populations provenant de climat contrasté ne présentent pas ou peu de différence génétique (en test de provenance) ou en populations naturelles *in situ*. Ce caractère présente une plasticité phénotypique mais faible comparée à celle de la croissance en hauteur par exemple. La comparaison entre la variation génétique entre populations et la variation des marqueurs neutres entre ces mêmes populations montrent que la variation de ce caractère semble réduite par l'architecture génétique sous-jacente. La resistance à la cavitation est vraisemblablement un trait canalisé.

Several review reported global forest die-back that are caused, directly or indirectly, by extreme climatic events (like heat waves or prolonged drought). In this context, there is an urgent need to identify new traits to trace drought tolerance. Resistance to cavitation is one of the best proxy for survival during extreme drought.

The aim of this work was (i) to understand how spreads cavitation in the vascular pathway in the gymnosperms (ii) to quantify the phenotypic variation of resistance to cavitation for *Pinus pinaster* species, (iii) to quantify the genetic variation and phenotypic plasticity available for this trait.

A micro-anatomy study was coupled with the measurement of resistance to cavitation for various species to found where air-seeding occurs. To quantify the variability of resistance to cavitation, we phenotyped 506 genotypes using to replicated provenance-progeny trials and on natural *in situ* populations.

The spread of embolism for *Pinaceae* and ex-*Taxodiaceae* could be due to minute pore in tori, which are remains of secondary plasmodesmata. We found that the pressure needed to break a water/air meniscus in these minute pores is correlated with the xylem air entry (P_{12}). Despite the great variability of resistance to cavitation between species, we found low variability within species. Most of the variability is within population, rather than between populations. The phenotypic plasticity of resistance to cavitation is low compare to growth traits. Comparison between Q_{ST} and F_{ST} shows that populations exhibit less variation compare to what it is expected under genetic drift. The variation of resistance to cavitation seems to be narrowed by the genetic architecture, which is the sign of canalisation.